

NOV 4 1996

SANDIA REPORT

SAND96-0591 • UC-400
Unlimited Release
Printed October 1996

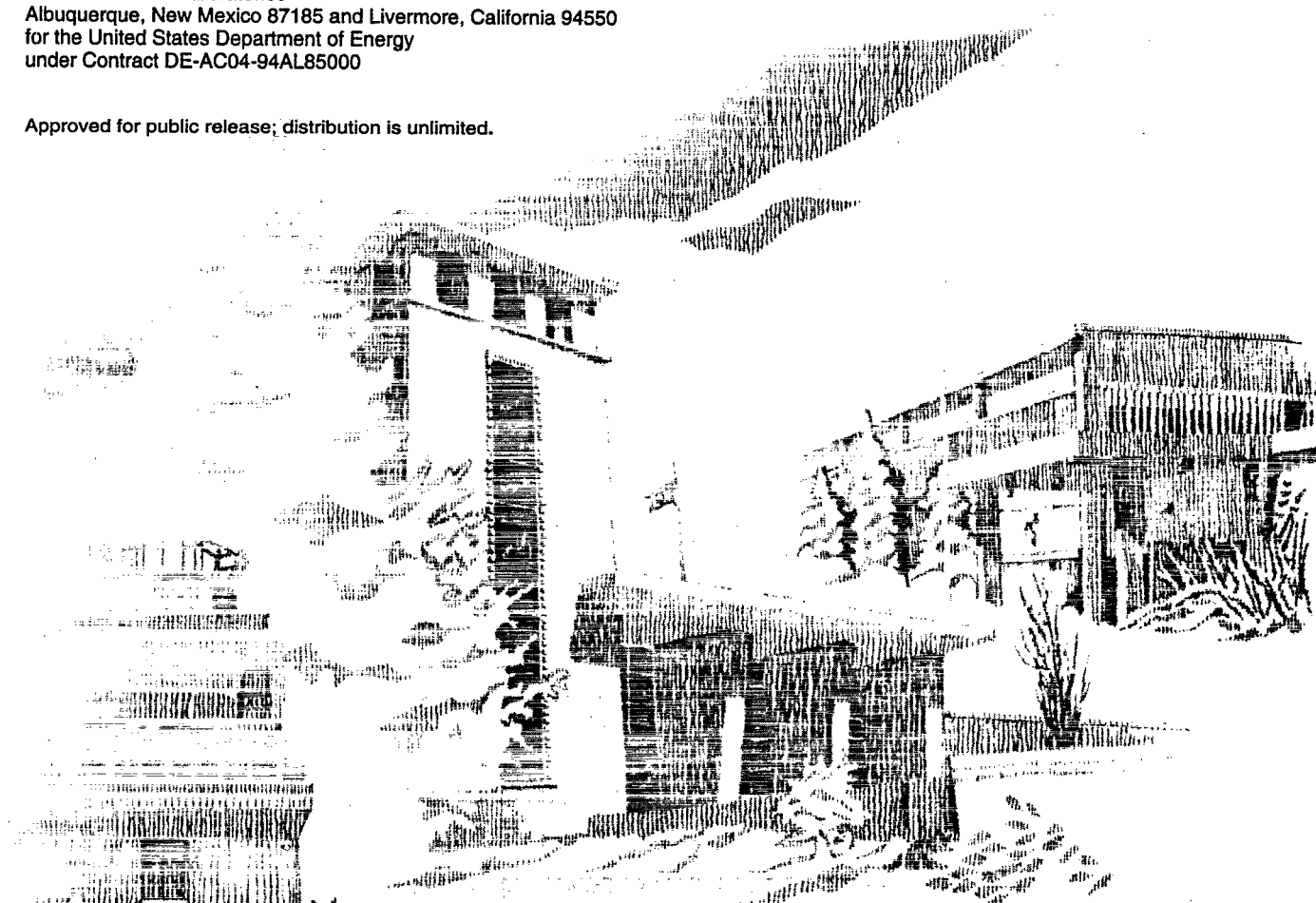
RECEIVED
NOV 12 1996
OSTI

Icarus: A 2D Direct Simulation Monte Carlo (DSMC) Code for Parallel Computers User's Manual - V.3.0

Tim Bartel, Steve Plimpton, Justine Johannes, Jeff Payne

Prepared by
Sandia National Laboratories
Albuquerque, New Mexico 87185 and Livermore, California 94550
for the United States Department of Energy
under Contract DE-AC04-94AL85000

Approved for public release; distribution is unlimited.



SF2900Q(8-81)

DISTRIBUTION OF THIS DOCUMENT IS UNLIMITED

DLC

MASTER

Issued by Sandia National Laboratories, operated for the United States Department of Energy by Sandia Corporation.

NOTICE: This report was prepared as an account of work sponsored by an agency of the United States Government. Neither the United States Government nor any agency thereof, nor any of their employees, nor any of their contractors, subcontractors, or their employees, makes any warranty, express or implied, or assumes any legal liability or responsibility for the accuracy, completeness, or usefulness of any information, apparatus, product, or process disclosed, or represents that its use would not infringe privately owned rights. Reference herein to any specific commercial product, process, or service by trade name, trademark, manufacturer, or otherwise, does not necessarily constitute or imply its endorsement, recommendation, or favoring by the United States Government, any agency thereof or any of their contractors or subcontractors. The views and opinions expressed herein do not necessarily state or reflect those of the United States Government, any agency thereof or any of their contractors.

Printed in the United States of America. This report has been reproduced directly from the best available copy.

Available to DOE and DOE contractors from
Office of Scientific and Technical Information
PO Box 62
Oak Ridge, TN 37831

Prices available from (615) 576-8401, FTS 626-8401

Available to the public from
National Technical Information Service
US Department of Commerce
5285 Port Royal Rd
Springfield, VA 22161

NTIS price codes
Printed copy: A11
Microfiche copy: A01

Icarus: A 2D Direct Simulation Monte Carlo (DSMC) Code for Parallel Computers

User's Manual - V. 3.0

Tim Bartel*, Steve Plimpton**, Justine Johannes***, and Jeff Payne

Plasma & Aerosol Sciences Department

**Parallel Computational Sciences Department

Sandia National Laboratories
Albuquerque, NM 87185

ABSTRACT

Icarus is a 2D Direct Simulation Monte Carlo (DSMC) code which has been optimized for the parallel computing environment. The code is based on the DSMC method of Bird[1] and models from free-molecular to continuum flowfields in either cartesian (x, y) or axisymmetric (z, r) coordinates. Computational particles, representing a given number of molecules or atoms, are tracked as they have collisions with other particles or surfaces. Multiple species, internal energy modes (rotation and vibration), chemistry, and ion transport are modelled. A new trace species methodology for collisions and chemistry is used to obtain statistics for small species concentrations. Gas phase chemistry is modelled using steric factors derived from Arrhenius reaction rates. Surface chemistry is modelled with surface reaction probabilities. The electron number density is either a fixed external generated field or determined using a local charge neutrality assumption. Ion chemistry is modelled with electron impact chemistry rates and charge exchange reactions. Coulomb collision cross-sections are used instead of Variable Hard Sphere values for ion-ion interactions. The electro-static fields can either be externally input or internally generated using a Langmuir-Tonks model.

The Icarus software package includes the grid generation, parallel processor decomposition, postprocessing, and restart software. The commercial graphics package, Tecplot, is used for graphics display. The majority of the software packages are written in standard Fortran.

*tjbarte@cfd.sandia.gov, (505)844-0124

**sjplimp@cs.sandia.gov

***jejohan@cfd.sandia.gov, (505)844-1994

MASTER

Acknowledgments:

The authors would like to thank several people who contributed to this work, either by their direct technical input, as 'friendly' users, or by their funding support. We first would like to thank Wahid Hermina, Sandia National Labs, for both his technical insight and his support of this project, George Davidson, Sandia National Labs, for early discussions on parallelizing the DSMC technique, and Mary Hudson, Sandia National Labs, for reviewing this manual. The support from Sudip Dosanjh for the extensive use of the parallel computing facilities at Sandia is greatly appreciated. We also thank the following people at Sandia National Labs who provided feedback in the early stages of the code development: Don Potter, David Sears, Todd Sterk, and Yvette Castro. Professor Demetre Economou, University of Houston, did his sabbatical leave at Sandia and contributed to the plasma modelling portion of the code. Nadeem Alvi, SEMATECH, provided both project support and precipitated our interactions with microelectronics equipment suppliers or end users. We thank Paul Shufflebotham and Vikram Singh, Lam Research Corporation, for struggling through early versions of Icarus and for taking experimental data on their system to validate the code. We thank Tom Furlanni (SUNY-Buffalo) for his work on species weighting and VSS modelling and Penny Marriott for her work on the Maximum Entropy Model for post-collision internal energy partitioning and chemical reactions. We finally thank Graeme Bird, the developer of the DSMC method, for his insight during the early development of this code.

DISCLAIMER

**Portions of this document may be illegible
in electronic image products. Images are
produced from the best available original
document.**

DISCLAIMER

This report was prepared as an account of work sponsored by an agency of the United States Government. Neither the United States Government nor any agency thereof, nor any of their employees, makes any warranty, express or implied, or assumes any legal liability or responsibility for the accuracy, completeness, or usefulness of any information, apparatus, product, or process disclosed, or represents that its use would not infringe privately owned rights. Reference herein to any specific commercial product, process, or service by trade name, trademark, manufacturer, or otherwise does not necessarily constitute or imply its endorsement, recommendation, or favoring by the United States Government or any agency thereof. The views and opinions of authors expressed herein do not necessarily state or reflect those of the United States Government or any agency thereof.

Table of Contents

1. Direct Simulation Monte Carlo (DSMC) Background	5
1.1 Method	5
1.2 Grid Characteristics	6
1.3 Cell and Species Weighting	7
1.4 Elastic Scattering Cross Sections	8
1.5 Code Validation	8
1.6 MP Features	8
2. Overall Code Structure	9
3. init2d - Icarus Preprocessor Program Description	11
3.1 init2d Code Description	12
3.2 Grid Characteristics	12
3.3. Input File Description (<i>geometry.inp</i>)	13
3.4. Species File Description (<i>spec</i>)	25
3.5. Inlet File Description (<i>inlet</i>)	26
3.6. Surface Chemistry File (<i>surf_chem</i>)	28
3.7. Cross Section File (<i>cross_section</i>)	31
3.8. Gas Phase Chemistry File (<i>chem</i>)	32
3.9 Diagnostic Messages	38
4. decomp2d - Decomposition Code Description	39
5. icarus - Code & Command File(<i>dsmc.in</i>) Description	40
5.1. icarus Command List (<i>dsmc.in</i>)	41
5.2 icarus Command Description	43
5.3 Example <i>dsmc.in</i> Files	55
5.4 Diagnostic Messages	56
6. restart2d - Code Description	58
7. regrid2d - Code Description	59
8. Postprocessing Codes	69
8.1 Macroscopic Cell Information (post2d)	70
8.2 Surface Information (surface2d)	72
8.3 Wafer Information (waferxy2d)	73
8.4 Cell Convergence Statistics (stat2d)	74

9. Install/Compile Software	75
9.1 Make files	75
9.2 param.h and icarus.h files	76
9.3 shell scripts	78
9.4 PVM	78
10. Miscellaneous Information	79
10.1 Important relationships	79
10.2 Chemical species database	80
Appendix	84
Appendix A: References	
Appendix B: Sample Problems	
-Prob1: Metal Etch	
-Prob2: Chlorine Plasma in GEC Cell	
-Prob3: ESA Test Case: LENS geometry	
-Prob4: MBF Expansion Chamber	
-Prob5: Sputter Deposition	
-Prob6: Si Etch by Chlorine Plasma in UH geometry	
-Prob7: NO Nozzle Expansion and Data Comparison	
-Prob8: NO Vibrational Relaxation (Time Dependent)	

1. Direct Simulation Monte Carlo (DSMC) Background

1.1 Method

DSMC is a method for the direct simulation of rarefied gas flows[1]. The method assumes that the gas is a dilute gas; that is, binary collisions dominate the molecular interactions. The flow domain is first divided into a number of cells. The cell size is determined by the local mean free path, λ ; a cell size $\sim \lambda/3$ is typically recommended. Unlike CFD grids with mesh orthogonality and one-to-one cell side correspondence constraints, the DSMC grid system serves only to identify a volume for choosing collision partners and for obtaining sampling statistics. The flow field is simulated using a number of computational particles (some 10^7 particles are not atypical for runs on massively parallel supercomputers). Particles consist of all kinds of species such as radicals, ions, and molecules. The species type, spatial coordinates, velocity components, internal energy partitioning, and weight factor of each computational particle are stored. As the particles move through the domain, they collide with one another and with surfaces. New particles may be added at specified inlet port locations, and particles may be removed from the simulation due to chemical reactions or through the pumping ports. Since this is a statistical method in which the system evolves in a time-like manner, a steady-state solution is then an ensemble average of a number of solution time steps (snapshots of the system) after the flow field has reached a steady-state. *Icarus* can also be run in a *time accurate mode* to model unsteady problems.

The basic premise of DSMC is that the motion of simulated particles can be decoupled from their collisions over a time step. The size of the time step is selected to be a small fraction of the mean collision time, or a fraction of the transit time of a molecule through a cell (similar to an explicit CFL constraint). During the motion phase, particles move in free molecular motion according to their starting velocity and any forces acting on the particles (for example the Lorentz force on charged species). During this phase, particles may cross cell boundaries, collide with walls, or exit the flow field. During the collision phase, random collision pairs are selected from within each cell *regardless of the position* of the particles within the cell. The no-time-counter (NTC) technique [3], is used to determine the computational particle collision frequency. The number of pairs to be selected from a given cell at a time step is

$$\# \text{ pairs} = 1/2 N \bar{N} F_n (\sigma_T C_r)_{\max} \Delta t / V$$

where N is the number of computational particles in the cell, F_n the number of real particles per simulated one, $(\sigma_T C_r)_{\max}$ is the maximum of the product of the total cross-section and relative velocity for the pairs in the cell and V the cell volume. The pair collision is then computed with a probability $(\sigma_T C_r) / (\sigma_T C_r)_{\max}$. This technique does not have the disadvantages of the older time counter (TC) method while maintaining computational efficiency, i.e., the simulation time is proportional to the number of molecules. This is a great advantage of DSMC as compared to other particle simulation methods such as molecular dynamics. Also, the NTC method allows

for unsteady flows to be simulated in a time accurate manner. A collision limiter model is used to improve computational performance at high pressures. The model simply limits the number of collisions in a cell to a multiple of the number of actual collisions. This model has been shown to reproduce inviscid flow fields and has been used to model high pressure (2 atm) nozzle expansions into a vacuum.

Although only two position coordinates (r, z) of each simulated particle are stored, collisions are handled as three dimensional events to correctly conserve momentum transfer. The molecular model used for collision cross sections is the variable hard sphere (VHS) model [1]. According to this model, the collision cross section σ_{ij} depends on the relative speed (energy) of the colliding partners E_c as

$$\sigma_{ij} = A_{ij} E_c^{-\omega}$$

where A_{ij} is a constant and $\omega = s - 0.5$, with s the exponent of the dependence of the coefficient of viscosity on temperature. The chief advantage of the VHS model is that, although the collision diameter is allowed to vary with the relative speed (unlike the constant cross section hard sphere model), when a collision does occur, the post-collision velocity components are computed as if it were a hard sphere collision; that is, isotropic scattering in the center of mass frame of reference.

The DSMC technique can easily model internal energy modes: rotational and vibrational energies. The phenomenological Borgnakke and Larsen [2] model is used to determine the post-collision internal energy partitioning given the number of internal degrees of freedom of each species. This is a harmonic oscillator model which drives the post-collision energy distribution towards equilibrium. Recently, Marriott[4] has applied the Maximum Entropy strategy for particle systems to obtain this energy distribution; unfortunately, the complex chemical species in typical manufacturing plasma etch systems are poorly characterized so typically only translational nonequilibrium is modelled.

Gas phase chemistry consists of four models: elastic gas reaction, charge exchange with constant cross sections, charge exchange using the model of Rapp and Frances, and electron impact reactions. Elastic collision gas phase chemistry is modelled using steric factors derived from Arrhenius reaction rates. That is, the chemical reaction probability given a particle collision is determined assuming a local Maxwellian distribution to convert the rate to a energy dependent probability. Charge exchange reactions model the exchange of both energy and momentum between neutral and charged species. Electron chemistry models electron impact chemistry using energy dependent rates and local electron number density and temperature. These rates are converted into a total reaction probability. That is, a probability which includes both collision and reaction. Surface chemistry is modelled with surface reaction probabilities; a coverage dependent model is being implemented.

1.2 Grid Characteristics

Icarus uses a multi-block system of algebraic meshes to define the computational domain. The grid is generated using the input processor program, *init2d*. This simple grid system allows great flexibility for capturing local high gradient regions without excessively gridding the entire domain because there is no requirement for side correspondence between regions. See the paper by Bartel and Plimpton in Appendix A for more details.

As mentioned before, the key assumption in DSMC is that particle transport is de-coupled from particle-particle interaction. Therefore particles move without collisions for a specified time step, and then collision partners are chosen probabilistically from within a defined grid cell. Implementation of this method requires that the cell sizes and the time step be chosen carefully; particles should not travel longer than the mean free path(λ) in a time step and the unit cell should be sized approximately less than λ . The Knudsen number (Kn) and the Courant number (CFL) are quality metrics for the cell size and the time step:

$$(Kn > 1) = \lambda / \text{cell length}$$

$$(CFL < 1) = \text{particle velocity} / (\text{cell length} / \text{time step})$$

The cell Kn and CFL numbers are output from the DSMC code in the *cell.** file and are used to verify that the particle transport assumptions were obtained.

1.3 Cell and Species Weighting

Icarus uses several strategies to obtain sufficient statistics for both local regions of disparate densities and for 'trace' species which have a very small mole fraction. First, each grid cell has a 'weight' which is simply used to spatially adjust the global or input ratio of real-to-computational particles. This 'cell weight' is initially proportional to the cell volume; this results in an equal number of computational particles per cell for a uniform initial density. As the simulation progresses, the number of particles in a given cell can become extremely large due to either chemical events or mass injection into the system. The 'cell adaption' logic of Icarus dynamically 'adjusts' the cell weight to maintain an upper bound on the number of computational particles per cell. Thus the user can be assured of sufficient statistics without a few cells with an unreasonable number of particles. This feature is transparent to the user.

Species weighting is another method which is used to increase the sampling statistics for the simulation. In this strategy, species which occur in small, trace amounts have a lower 'computational worth' than do other species. For example, in low density plasma systems, the ionization fraction is very small: < 0.1%. Thus, the neutral species will have a single weight of 10^{10} molecules or atoms per computational particle while the ions which occur in trace amounts will have a weight of 10^6 ions per computational particle. The code is limited to two species weight multipliers: 1.0 for the base or full case and a number less than 1.0 for all the trace species.

1.4 Elastic Scattering Cross Section

The Variable Hard Sphere (VHS) model treats each molecule as a fixed diameter sphere with isotropic scattering. The VHS model employs the simple isotropic scattering law of the hard sphere model but accounts for the temperature dependence of the collision cross section by use of a single parameter which may be determined

from the viscosity temperature dependence

$$\sigma = \sigma_{\text{ref}} \left(\frac{T}{T_{\text{ref}}} \right)^{-\omega}$$

where σ_{ref} is the collision cross section at the reference temperature, T_{ref} , and T is the kinetic temperature of the collision partners. The VHS parameter, ω is related to the temperature exponent of viscosity, s

$$\eta = \eta_0 \left(\frac{T}{T_0} \right)^s$$

as $s = \omega + \frac{1}{2}$; where η is the viscosity and subscript 0 denotes the reference temperature and viscosity (see ref. [1])

A database of viscosity index, ω , and molecular diameters at the reference temperature for approximately 150 species has been compiled and given in Chapter 10.2. Curve fits to viscosity of species not listed can be used to obtain s (the slope) and therefore ω .

Icarus contains a method to extend the computationally efficient pressure range to higher pressures. A collision limiter model is used: the number of computational collisions per computational particle in a time step is constrained. This method has been shown to reproduce inviscid flow systems. The enclosed AIAA in appendix A paper by Bartel, Sterk, Payne, et.al. contains the details and method comparisons.

1.5 Code Validation

Icarus has been validated over a wide range of problems. The papers in Appendix A contain some of these. The pressure range has varied from very low pressure applications of space orbital conditions which are free-molecular flow to two atmosphere pressure systems which are highly collisional.

1.6 MP Features

Icarus is a 2D DSMC code which can model systems in either cartesian or axisymmetric coordinate systems. This code was written to take advantage of parallel computer systems; either massively parallel system or workstations with a few processors. The enclosed AIAA paper by Bartel and Plimpton in Appendix A describes the basic strategy used for the parallel method. This strategy is directly extendable to 3D and allows timely computation of large problems which were previously unsolvable

2. Overall Code Structure

The **Icarus** code requires pre- and post-processor programs. Table 1 is a summary of the individual program names, program descriptions, and the files that each program uses and creates. Throughout this manual, program names are indicated by bold type and file names are identified by italics. Underlined filenames indicate that the file name is determined by the user, otherwise filenames are hardwired.

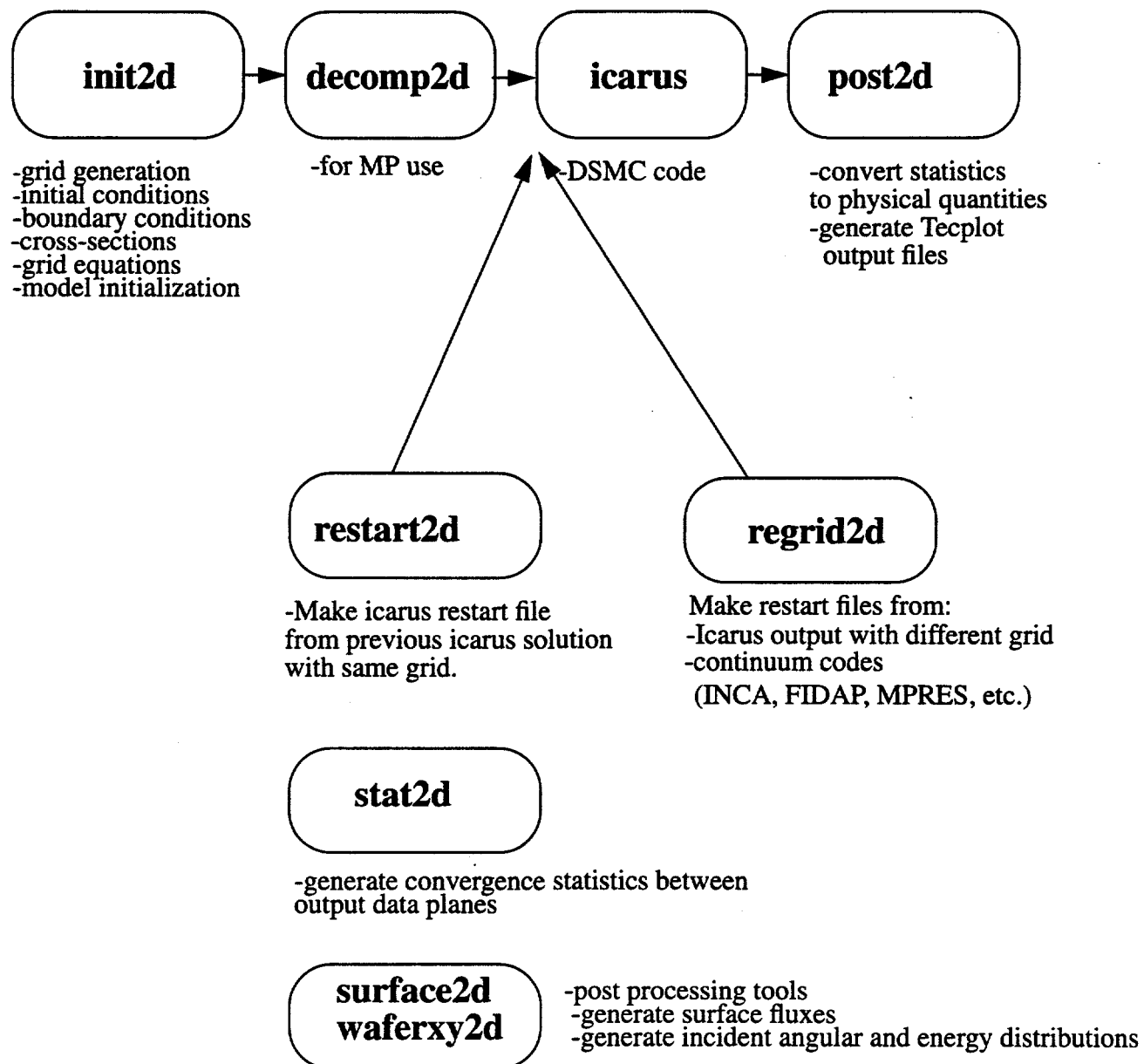


Table 1: DSMC 2D Code Descriptions

Code	Description	Input Files	Output Files
init2d	Grid generation and problem description. Converts geometry and chemistry information to icarus format.	<i>geometry.inp, spec, <inlet>, <surf_chem>, <chem>, <cross_section></i>	<i>datap, grid</i>
decomp2d	Decomposes problem for parallel environment. This code is not necessary for single processor use.	<i>datap</i>	<i>dsmc.node, dsmc.in2</i>
icarus	Performs DSMC calculation and gathers statistics. Typically run in parallel environment.	<i>dsmc.in, dsmc.in2(MP), datap(1P), <dsmc.restart>, <dsmc.node>, <dsmc.em>, <dsmc.plasma></i>	<i>cell.* surf.* wafer.* chem.* plasma.* particle.* dsmc.log, dsmc.pump</i>
restart2d	Converts previous DSMC simulations with same grid for initial guess for starting a new DSMC calculation.	<i>cell.* dsmc.in2, dsmc.node</i>	<i>dsmc.restart</i>
regrid2d	Converts previous fluid simulation or DSMC simulation with a different grid to an initial guess for starting a new DSMC calculation.	<i>cell.* dsmc.in2, dsmc.node, btecplot</i>	<i>dsmc.restart</i>
post2d	Converts cell information (particle statistics) to macroscopic quantities(i.e., pressure, density, species concentrations, velocities, etc.)	<i>cell.* (or chem.* plasma.*) post2d.vlist, datap</i>	<i>cellout</i>
surface2d	Converts surface element information to incident flux, reflected flux (etchant), surface coverage, surface pressure, shear stress and heat flux.	<i>surf.* datap</i>	<i>surfout</i>
waferxy2d	Converts wafer information to angular and energy distribution of incident particles by species. Only for material specified as a wafer in <i>geometry.inp</i> .	<i>wafer.* datap</i>	<i>waferout</i>
stat2d	Determines convergence between two different icarus <i>cell.*</i> files.	<i>cell.* cell.**</i>	<i>stat.out, stat.tec</i>

where:< > optional files, * - time step stamp

3. init2d - Icarus Preprocessor Program Description

In this section, the input files for the preprocessor **init2d** will be presented. This program converts the geometry, chemistry and DSMC parameters input by the user, into the format required by **icarus**. All input is in MKS units. The files used in **init2d** contain the following information:

- geometry.inp* Grid information and DSMC parameters (file name is determined by user, but typically has *.inp extension.)
- spec* Chemical species information.
- chem* Gas phase reactions, rate constants and heat of reaction.
- surf_chem* Surface reactions, reaction probabilities, creation probabilities and permeability.
- inlet* Specifies flowrate and location for gas injection into the domain; a point source injection or an outgassing surface are examples of inlet options.
- cross_section* Input collision cross sections used instead of the variable hard sphere(VHS) model for elastic collisions.

3.1 init2d Code Description

Goal: -generate a graphical file to display grid
 -generate an input file for the **icarus** code

Usage: **init2d <geometry.inp**

Input files:

geometry.inp - input data file for problem definition: grid, boundary conditions, etc.
spec - species definition file
chem - gas phase chemistry input (optional)
surf_chem - surface chemistry input (optional)
inlet - inlet boundary file (optional)
cross_section - elastic cross sections (optional)

Output files:

datap - input file for **icarus** or **decomp2d** for MP simulations
grid - Tecplot formatted file of grid description

3.2 Grid Characteristics

See the papers in Appendix A for examples of the multi-blocked algebraic grid strategy which is used in **init2d**. Also, numerous examples are found in Appendix B.

3.3 Input File Description (*geometry.inp*)

An example *geometry.inp* file is given below, followed by a description of the numbered input lines. An asterisk, *, in column 1 indicates a comment card; blank lines are not allowed. The order of the input is important--do not leave out input even if it will not be used for the current simulation.

Input Index:

```
*-----  
1 GEC/ICP -- 6 species chemistry  
*  
* point injection model for inlet  
*  
*-----  
*  
2 1 control: -1 -- plot grid only;  
* 1 -- initialization & plot file  
3 1 0/1 for X-Y or Z-R flow  
*-----  
* Initial Conditions  
*-----  
4 1 0/1 for vacuum/freestream  
5 0. x-component of velocity, m/sec (ft/sec x 0.3048)  
6 0. y-component of velocity, m/sec  
7 3.0e19 number density, molecules/m**3 (mol./ft**3 x 35.315)  
8 300.00 temperature, deg K (deg R/1.8)  
*-----  
* Specie Information  
*-----  
9 6 Number of molecular species  
*-----  
* Cl Cl+ Cl- Cl2 Cl2+ SiCl2  
10 0.9 0.0 0.0 0.1 0.0 0.0  
*-----  
*-----  
11 3 internal structure of most complex molecule:  
* 3-monatomic(translational), 4-rotation, 5-rotat. + vibrat.  
12 10 # of chem. rx. (from file chem)  
*-----  
* Weighting Information (particles and time step)  
*-----  
13 1.0e10 base # of real mols. per simulation one  
14 1.E-06 base time step, sec  
15 4 cell weighting option
```

```

*-----
*          Collision Model Input
*-----
16      300.0      ref. temp. for VHS model, deg K
17      1.0       temperature exponent of viscosity coeffs.
*-----
*          Surface Modelling Information
*-----
18      1.000      thacc: thermal accomodation coefficient
*-----
*          Misc input Section
*-----
19      4          vacuum pump region #
20      0          ic region distribution
21      1          wafer material type
22      11         pressure iteration control pt.
23      0          volume Multiplier
24      0.0000     minimum expansion radius
25      1.          external e-field multiplier
26      0.          not used at the present
27      0.          gravity orientation
28      0.0         use external cross-sections
*-----
*          Region Definition
*-----
29      4          number of regions (must be .le. 30)
30      11         number of global points (must be.le.120)
*-----
*          Global corner pt. coordinates
*          Pt.      z (m)      r (m)
*-----
31      1          0.0        0.0
      2          -0.0300    0.0
      3          -0.0405    0.0
      4          0.0        0.0826
      5          -0.0341    0.05715
      6          -0.0405    0.05715
      7          0.0        0.1152
      8          -0.0341    0.1152
      9          0.0        0.12520
     10          -0.0341    0.1252
     11          -0.0190    0.0823

```

* Individual Region Definitions Follow
 * --REGION NUMBERS MUST BE SEQUENTIAL--
 *
 *
 32 1 <----- Inputs specific to this region follow
 *
 33 1.0 base number multiplier
 34 1.0 dtm multiplier
 35 3 global point - 1
 6 - 2
 5 - 3
 2 - 4
 36 35 number of cells along sides 1 and 3
 37 60 number of cells along sides 2 and 4
 38 0 sides 1 and 3 curvature: 0/1 for line/circular arc
 39 0 sides 1 and 3 cell spacing:
 40 3 sides 2 and 4 cell spacing:
 41 1.03
 42 100.
 43 1 boundary type code for sides 1 - 4, resp.
 5 side 2
 51 side 3
 7 side 4
 44 2 number of surface input lines to follow
 *
 * Side Cell1 Cell2 Spec. refl. Temp. K Material# Value
 *
 45 2 1 100 0.000 300.00 2 0.
 3 1 100 0.000 300.00 2 0.
 *
 * Region interface/matching
 * Reg. side reg. sides Adj. sidel Adj. reg.
 *
 46 1 0
 2 0
 3 0
 4 1 2 2
 *
 2 <----- Inputs specific to this region follow
 *
 .
 .
 .
 *
 * END OF INPUT FILE
 *

Line description:

Input lines 1 thru 30 are required in the order shown.

- 1) The first line processed from the file is the title. Lines that begin with an asterisks, *, are comments.
- 2) The control flag determines if only the mesh file, *grid*, should be generated (indicated by -1) or if a *datap* file should also be created (indicated by 1). The -1 option is helpful when first setting up a problem to resolve gridding issues and executes much faster.
- 3) Coordinate system definition;
If 0 is specified, the problem will be 2-Dimensional with coordinates (X,Y).
(Note, Y must be ≥ 0.0 , depth of 1 meter is assumed.)
If 1 is specified, the problem will be 2-D axisymmetric with coordinates (Z,R).
(Note, Z is the first coordinate and R the second)
- 4) Initial conditions;
If input = 0 all cells in computational domain will have initial conditions of vacuum.
If input = 1 all cells in computational domain will have initial conditions of freestream or constant values.
Even if input = 0 option is chosen, the velocities, number density, and temperature of a freestream condition need to be specified.
- 5) Initial x-component of velocity, m/sec (Vx or Vz)
- 6) Initial y-component of velocity, m/sec (Vy or Vr)
- 7) Initial number density (molecules/m³)
- 8) Initial freestream temperature (K).
- 9) Number of species defined in the *spec* file.
- 10) Initial free stream species distribution in mole fractions, must be given in the same order as the species in the *spec* file.
- 11) Internal structure of the most complex molecule,
3 - monatomic - translational energy exchange
4 - rotation - translational and rotational energy exchange
5- rotation and vibration - translational, rotational and vibrational energy exchange
- 12) Number of gas phase chemical reactions defined in the *chem* file.

- 13) Base number of real particles per simulation particle. A typical number is 1e10 real particles per simulated particle. Screen output from **init2d** indicates the number of computational particles assuming the constant freestream initial density. Typically for a 5,000 cell problem, approximately 100,000 particles should be simulated (~20 particles/cell).
- 14) Base time step, should be defined to generate a cell CFL number less than 1.
Note: this value can be modified later in the input file for the **icarus** code (*dsmc.in*). A suggested base value is 1.0e-6 s (1 μ s). Cell CFL # is output in *cell.** file.
- 15) The last value in this section defines the cell weighting option; this refers to the strategy used to optimize the number of computational particles per cell in regions of large density variations (for example, inlet ports and vacuum pump entrance.) The most often used cell weighting strategy is defined by the number 4, although all possible options are defined below:

Cell Weighting options:

- 0 region number and dt based on base number and base dt with a input region ratio (definition of base number and dt refer to variables 13 and 14)
- 1 local cell weights based on volume, region dt from base dt and region ratio
- 2 local cell weights based on volume and option 0
- 3 local cell weights based on volume, region ratio, and region dt base value (constant dt for all cells)
- 4 local cell weights based on volume and region ratio, with region dt based on base value of dt
- 2 uses option 2 with radial expansion assumption from origin. This varies the cell weights in a $1/r^2$ manner--typically used for nozzle exit flow expansions.
 $x > 0.0$
 $r > rmin$
 $wt = wt / (r/rmin)^2$
- 3 similar to option 3 but with radial expansion model
- 4 similar to option 4 but with radial expansion model
- 16) Reference temperature used in VHS collision model (T_{ref}). (Chapter 1.0)
- 17) Viscosity exponent(ω) in VHS collision model. (Chapter 1.0)

A database of viscosity index, ω , and molecular diameters at the reference temperature for approximately 150 species has been compiled and given in Chapter 10. Curve fits to viscosity of species not listed can be used to obtain s and therefore ω .
- 18) A thermal accommodation coefficient for computing surface heat transfer. A value of 1.0 means fully accommodated with the surface temperature and a value of 0.0 means adiabatic wall boundary condition (no accommodation).

- 19) Region number for the vacuum pump, if a vacuum pump is not needed use a 0.
- 20) This option allows the initial number density to vary from region to region. If this option is turned on, a multiplier must be specified in each region description after the dtm multiplier.
0 - option off
1 - option on
- 21) Material number used to indicate the wafer. Identifies the surface where energy and angular distributions fluxs should be computed. The wafer material number will be used as a boundary condition material specification later in the region definition.
- 22) Global point number to use in the DSMC pressure control model to specify the physical location for pressure feedback. This model allows pump speed to vary to achieve a desired pressure at a specified point. The starting pump speed, pump speed limits, and desired pressure are specified in the input file (*dsmc.in*) for the **icarus** code. Do not use a region global point or specify a point exactly on the perimeter; computer round-off may be a problem.
- 23) Volume multiplier used to preserve actual volume to surface area ratios. For example, for a showerhead configuration where circumference is made up of many holes rather than a slit the volume multiplier is used to specify the fraction of volume along the radius. If this option is turned on with a 1, a volume multiplier is added after the dtm number for all region definitions.
- 24) Minimum expansion radius for radial expansion problems. See cell weighting line input 15.
- 25) Electron density multiplier when doing electron impact chemistry using Gemini.
- 26) Not used.
- 27) Gravity term is added to velocity vector if set to +1 or -1. Plus or minus indicates coordinate system convention, use +1 if wafer is zero and top of the reactor is positive z, -1 if top of the reactor is negative z for wafer at zero.

- 28) 0.0 - use cross sections computed using the VHS model
1.0 - use constant input collision cross_section from *cross_section* file, (for cross sections not defined in the file the VHS model is used.)
- 29) The total number of regions in the DSMC grid. The regions are specified by four global corner points. Each region contains four sides with each side usually having a single specified boundary condition.
- 30) Total number of global points. Not all global points must be used; extra values are allowed.

31) Global point definition given by global point number, and coordinates in meters.

NOTE: either Y (cartesian) or R (axisymmetric) MUST be > 0.0

for coordinate system X, Y (type 0):

point #, x y

for coordinate system Z, R (type 1):

point #, z r

The remainder of the init2d input lines, 32 - 46, are duplicated for each region.

32) Region number.

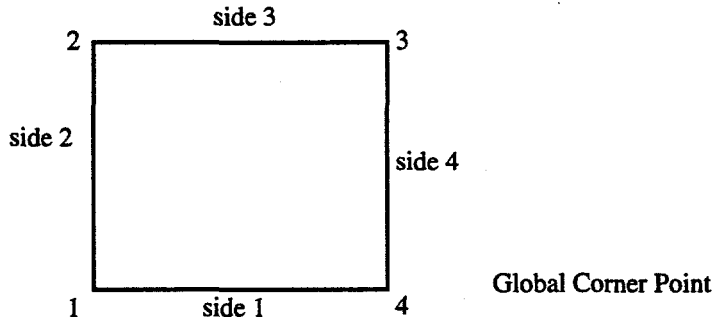
33) Region weighting multiplier which is used to change the number of molecules per cell in a specific region to obtain approximately 20 to 30 computational particles per cell. This feature is used for regions of large density variations: high pressure stagnation regions and low pressure wake or pump regions. This value can be set to 1.0 for initial simulations and later changed to increase the resolution in regions with lower densities. Note that a value greater than 1.0 will result in fewer computational particles and a value less than 1.0 will increase the number of computational particles in that region; this value simply multiplies the base value (input #13).

34) Region time step multiplier, dtm, which changes the region time step. Used to increase or decrease the time steps in regions where high and low gradients exist. This value is typically set to 1.0 for all regions.

(Include ic region distribution (20) or volume multiplier (23) next if they are specified.)

35) Four global corner points define the region. A region is a general quadrilateral and not required to be rectangular. A diagram describing the layout of a region with regards to side and global corner point definition is shown below. Definition of the region sides and corner points is by a clockwise rule. In general the first corner point defining the region will be the lower left hand point (1) followed by points 2,3, and 4 respectively (clockwise direction). Sides 1 will always be defined as the side between global corner points 1 and 4 respectively. The other sides are defined in a similar fashion. Side 1 and 3 should be nominally parallel to

the x or z axis. Sides 1 and 3 must not be vertical lines in the z-r or x-y plane.



- 36) Number of cells along sides 1 and 3. The same number of cells will be specified for the side pairs of (1,3) and (2,4). If you select 50 cells for side 1 of region 1 then there will also be 50 cells for side 3 of region 1.
- 37) Number of cells along sides 2 and 4.
- 38) A radius with its center along the centerline or some other radius of curvature can be defined for sides 1,3.
 - 0 - a straight line,
 - 1 - indicates curvature with the center of the radius along the centerline (z axis).
- 39) Cell Spacing along sides 1 and 3. Spacing of the cells either can be uniform or the cells can be clustered to one end.
 - 0 - Uniform spacing
 - 1 - Manually assign cell spacing via cell weights, 10 per line following this input line
 - 2 - Cluster cells toward the lower number of side. For example, clustering cells along sides 1 and 3 would cluster the cells toward side 2.
 - 3 - Cluster cells toward the higher number side.

for option 2 or 3, two additional input lines must follow immediately, before #40 --see #41 and #42 for input format.
- 40) Cell Spacing along sides 2 and 4. Spacing of the cells either can be uniform or the cells can be clustered to one end.
 - 0 - Uniform spacing
 - 1 - Manually assign cell spacing via cell weights, 10 per line
 - 2 - Cluster cells toward the lower number of side. For example, clustering cells along sides 1 and 3 would cluster the cells toward side 2.
 - 3 - Cluster cells toward the higher number side.

for option 2 or 3, two additional input lines must follow immediately--see #41 and #42

41) Optional input; required if cell spacing type 2 or 3.
Specifies size variation from cell to cell using a simple geometry ratio. For a value of 1.03, a 3% cell size variation will be obtained.

42) Optional input; required if cell spacing type 2 or 3.
Ratio of maximum to minimum cell size limit. This limits the smallest cell size.

43) Boundary conditions for sides 1 through 4 are specified. Each side must have a specific boundary condition type.

- 1 Line of symmetry (rz axis)
- 3 Freestream bc (constant value, see #5 - #10)
- +/-3x Freestream bc using an inlet table.
- 5 Solid surface
- +/-5x Solid surface with sources from an inlet table
- 7 Connection to another region or multiple regions
- +/-7x Region connection with sources from an inlet table
- 9 Porous wall (porosity specified in the variable, value, on surface info. #45)
or mixed boundary type (solid surface and region connectivity)
- +/-9x Porous wall or mixed boundary with sources from an inlet table
- 11 Outflow (non-reentrant, vacuum pump of infinite speed)
(note type 11 cannot be used for a region connection)

Boundary types +/-3x, +/-5x, +/-7x, and +/-9x require a table entry be specified for 'x'. This specifies the table number to refer to in the *inlet* file. The boundary condition type can be + or -; positive number indicates that coordinate specified in the *inlet* file is either x or z, a negative boundary condition indicates that the coordinate is either y or r. Examples are: -51, and 32.

44) Number of surface specification input lines (#45). Required for boundary conditions 5, 5x, 9 and 9x.

45) Surface specification input variables on each line are:

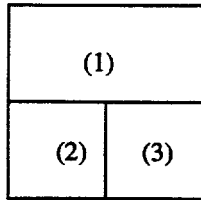
- 1 - Region side number
- 2 &3 - Define the starting and stopping cell number for this specification.
note: this feature can input piecewise property variations along a surface
--cells are numbered as:
 - side 1-- cell 1 adjoins side 1-2 intersection
 - side 2 -- cell 1 adjoins side 1-2 intersection
 - side 3 -- cell 1 adjoins side 2-3 intersection
 - side 4 -- cell 1 adjoins side 1-2 intersection
- 4 - Amount of specular reflection in Maxwell Model (0.0 for fully diffuse) (Chapter 1)
- 5 - Temperature of the surface (K).
- 6 - Material number associated with material number defined in the *surf_chem* file.
(input 0 if no surface chemistry). A number without a *surf_chem* input can be used to 'mark' a particular surface for postprocessing with **surface2d**.
- 7 - Porosity for boundary type 9 and 9x (value of 1.0 for freeflow, 0.0 for no flow)
(input 0.0 for boundary conditions other than type 9)

46) Region connectivity table. In most cases, multiple regions will need to be connected to define the specific geometry.

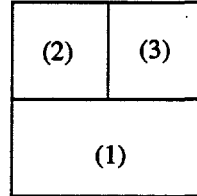
There are four rows in the region connectivity table, one for each side. The entries are:

- 1 - side number
- 2 - the number of connecting regions to this side. For example, if a side is a solid surface there are no connecting regions and the entry is 0.
- If 2nd value is non-zero, then there must be ((input 2)*2) numbers to follow, one pair for each connecting region.
- 3 - input pair which specify the connected region side number and region number in clockwise fashion for that side (see example below).

The diagram below shows two examples of region connectivity based on the clockwise rule.

EXAMPLE 1**Region 1: side 1**

Order will start with Region 3 and end with Region 2

EXAMPLE 2**Region 1: side 3**

Order will start with Region 2 and end with Region 3

In example 1, regions 2 and 3 are connected to side 1 of region 1. Applying the **clockwise rule** results in a region numbering sequence 3 and 2 on side 1 of region 1. Similarly, in example 2, regions 2 and 3 are connected to side 3 of region 1. In this case the connectivity order will be regions 2 and 3 to side 3 of region 1.

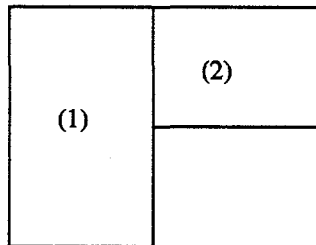
Example 1 - region 1 connectivity input for side 1:

1 2 3 3 3 2

Example 2 - region 1 connectivity input for side 3:

3 2 1 2 1 3

Boundary type 9 allows for multiple boundary type specification; for example side 4 of region 1 is connected to another region and is partly a solid surface:



boundary type for side 4 of region 1 == 9

surface specification (input #45) is required for side 4-- the porosity variable is used for the connecting side (1.0 for freeflow between the regions)

example: 4 1 50 0.0 300. 0 0.95

(the surface is defined to be at 300K and a porosity of 95% is used ONLY for the portion which connects to region 2. You do not have to have the region cell boundaries lineup on the region1-region 2 interface. The code logic will determine the correct particle trajectory. Also, the cell range of 1-50 simply needs to be inclusive of the actual number of cells.)

Example region connectivity for side 4 of region 1:

4 2 2 2 -1

Note: a pseudo-region, -1, is used to indicate where the solid surface is. Alternating regions and pseudo-regions can be used to build complex geometries.

3.4 Species File Description (*spec*)

Example file for chlorine etch of silicon:

```
*****
*   species data file      *
*****
*-----*
* ID
* Mwt   Mol. mass      Diam.   #Rot.Deg.   Rot.Rel.   Vib. Rel.   Vib.Temp.   specie wt.   charge
*   (kg)      (m)          Freedom      Coll. #      Coll. #      (K)
*-----*
Cl
35.45  0.59e-25  3.831e-10  0.0      0.0      0.0      0.0      1.0      0.0
Cl+
35.45  0.59e-25  3.831e-10  0.0      0.0      0.0      0.0      0.02     1.0
Cl-
35.45  0.59e-25  3.831e-10  0.0      0.0      0.0      0.0      0.02     -1.0
Cl2
70.91  1.18e-25  5.405e-10  2.       5.       0.0      0.0      1.0      0.0
Cl2+
70.91  1.18e-25  5.405e-10  2.       5.       0.0      0.0      0.02     1.0
SiCl2
98.99  1.647e-25 8.000e-10  2.       5.       0.0      0.0      1.0      0.0
```

All of the species information is contained in the *spec* file. **The order of the species in the *spec* file is very important; this order is assumed throughout the calculation.** For example, when specifying the initial conditions in the *geometry.inp* file, the order of the species is assumed to be the same as the order given here. An asterisk, *, in column 1 denotes a comment line.

Each species requires two lines of input.

- line 1: species chemical symbol (used in postprocessing files, 6 characters long)
- line 2: description of the species for transport and interactions:
molecular weight, molecular mass (kg), molecular diameter (m), # of rotational degrees of freedom, rotational relaxation collision number, vibrational relaxation collision number, vibrational temperature, species weight (described below) and charge. If either not modelling or have no information for rotational/vibrational interactions, enter 0.0.

Species weighting is a strategy used to increase statistics on species that exist in low concentrations. Only two different specie weights are allowed: 1.0 and a number < 1.0. In the example, you will see that either 1.0 or 0.02 are used for species weight. A species weight less than 1 multiplies the cell ratio of the # of real molecules per simulated one. For example, consider a mixture of 2 species: one with a mole fraction of 0.99 and the other 0.01. If the weights were equal to 1.0 for both species and there were 100 computational particles in the cell, 99 would be species 1 and 1 particles would be species 2. Thus, if there were only 20 particles in the cell, on the average, the 20 particles would all be species type 1! If the species weight was 0.02 for species 2, then on the average, the cell would have 14 particles of species 1 and 6 of species 2. **Species weight must be a number between 0.0 and 1.0!**

3.5 Inlet File Description (*inlet*)

Example *inlet* file:

```
*  
*-- 15sccm -- point source -- new grid2  
*  
2      number of tables  
*  
1 1 1      table number, number of entries, BC type  
*      #/s  
-0.038 6.7179e+18 0.00 -199.725 255.79 255.79 255.79 0. 0. 0. 1.0 0.0.  
*  
*-- 15sccm distributed over the outer-ring radius, outgassing boundary condition  
2 2 2      table number, number of entries  
* location #/m2s  Vz  Vr  Tt  Tr  Tv  Cl2  
-0.001 2.669e20 0.0 0.0 300. 300. 300. 0.0 0.0 0.0 1.0 0.0 0.0  
-0.033 2.669e20 0.0 0.0 300. 300. 300. 0.0 0.0 0.0 1.0 0.0 0.0
```

An *inlet* file is required if you specified an inlet as a boundary condition in the *geometry.inp* file (*inlet* file for BC types: +/-3x, +/-5x, +/-7x, +/-9x). An asterisk, *, in column 1 denotes a comment line.

line 1: Number of tables to be read (number of separate inlets).

for each table:

first line: Table number, number of entries, table type

Table Types: 1 -- point source, #/s (1 sccm = 4.48e17 #/s)

2 -- surface flux, #/m²-s

(note--a unit depth of 1m is assumed in cartesian (XY) coordinates)

3 -- volume source, #/m³

Note: order of the tables is not important

next lines: single input line for each table entry

-inlet location, BC type specifies coordinate (m)

-flow rate (units depend on the BC type)

-Vx or Vz average inlet velocity vector (m/s)

-Vy or Vr average inlet velocity vector (m/s)

-Translational Temperature (K)

-Rotational Temperature (K)

-Vibrational Temperature (K)

-species mole fractions in same order as *geometry.inp* and *spec* file

inlet location:

The inlet location can be either x or y (z or r in axisymmetric systems). A single coordinate is used since the inlet boundary conditions must be along a region boundary; the `init2d` code determines the second coordinate to machine accuracy. If the BC type code specified in `geometry.inp` is negative (i.e. -31, -52, -93, etc.) then the inlet location coordinate is assumed to be either y or r. If the BC type code is positive, the inlet coordinate is either x or z.

flow rate:

for any boundary type: 3x, 5x, 7x, or 9x, each can have either a 1, or 2, or 3 type boundary.

Notes:

- for a point source (+/-5x), $1\text{sccm} = 4.48\text{e}17 \text{#/s}$
- multiple point sources can exist along a boundary
- For BC 2 and 3, linear interpolation is used between input values; profiles are modelled as a series of line segments.
- BC type +/-3x is generally used for a 'line' inflow boundary condition
- BC type +/-5x if for a point source (small inlet nozzle - code 1) or for an outgassing surface (code 2).
- BC type +/-9x is for the special case where a region has both a surface and region connection on the *same side* or for a porous connection between regions.

velocities:

The input velocities are the average velocities; the translational temperature is used to obtain the velocity distribution which is sampled for the inlet particle velocity.

Notes:

- use standard sonic flow relationships (see Chapter 10) to obtain both orifice velocities and exit temperatures (V^* and T^*)
- make sure that the velocity vectors are into the computational domain!

3.6 Surface Chemistry File (*surf_chem*)

The surface chemistry file contains a separate table for each type of material specified in the *geometry.inp* file. An asterisks, *, in column 1 denotes a comment line.

Line 1: Number of material tables

For each table:

first line: Table number, number of reactions, site density(#/m²).

Note: order of the tables is not important

Following Input (either one or two lines per material)

- One input line(A) required for simple surface reactions without surface temperature dependence or ion energy yield dependence (8 entries on first line)
- Optional line(B) for surface reactions with temperature dependence or ion energy dependence (6 entries on second line)

Surface reaction probability can be defined with a simple sticking coefficient or it it can be a function of site coverage. The surface coverage model is simple: sites are either occupied or vacant. Thus, only one type of surface species can be defined. Ion energy sputtering yield can also be described for a surface reaction using the expression $A(E_{ion}^a - E_{ion}^b)^b$ as defined by Gray et al. (*J. Vac. Sci. Technol. A*, vol. 12, pp. 354-364, 1994).

Line A: A positive reaction type indicates that the reaction reaction rate is not temperature dependent and no ion energy dependent yield information is required. Negative reaction types indicate an extra line is read in to allow for surface temperature dependence and ion energy dependent yield parameters.

- 1) reaction type:
 - +/-1 Simple model (no coverage dependence)
 - +/-2 Absorption rxn - takes open surface site.
 - +/-3 Etch reaction - vacates occupied surface site.
 - +/-4 Requires an open site but leaves the surface unchanged.

- 2) reacting species number (corresponding to *spec* and *geometry.inp* files)
- 3) reaction product species #1
- 4) reaction product species #2 (specify 0. if only one reaction product)
- 5) creation probability species #1
- 6) creation probability species #2
- 7) degree of surface specular reflection (0.0 for diffuse)
- 8) Surface reaction probability (A)

Line B:

- 1) B - surf. reaction temperature dependence (for Arrhenius fit $K = AT^B e^{(Ea/T)}$)
- 2) Ea (joules) - surf. reaction activation energy
- 3) A - energy dep. etch yield in the form of $A(E_{ion}^a - E_{th}^a)^b$
- 4) a - energy dep. etch yield parameter
- 5) b - energy dep. etch yield parameter
- 6) Eth (joules) - energy dep. etch yield threshold energy

The creation probability contains reaction stoichiometry information; for Cl etch to create $SiCl_2$ the creation probability is 0.5 because it will only form once for two Cl's that hit the surface. ($Cl \rightarrow 1/2 SiCl_2$ the 1/2 is the creation probability per incident particle).

examples:

• Cl recombination to Cl_2 can be described as either an overall reaction with a wall recombination coefficient of 0.1 for $Cl \rightarrow 1/2 Cl_2$ (fully diffuse reflected product):

1. 1. 4. 0. 0.5 0. 0. 0.1

Or, Cl recombination can be described as a two step process dependent on surface coverage:



2. 1. 0. 0. 0.0 0. 0. 1.0

3. 1. 4. 0. 1.0 0. 0. 0.05

An example of temperature dependent etching rate is given for C_2F_6 etch of SiO_2

* OMEGA C_2F_6 plasma simulations with 10 rnxs, 11 species

* C_2F_6 CF, CF+, F, F+, F-, F2, SiF4, O, O2, CO

* 1 2 3 4 5 6 7 8 9 10 11

1 number of material table types

*

* material 1 (wafer), wafer (SiO_2)

1. 3. 1.75e19

2. 4. 0. 0. 0.5 0. 0. 0.3 (Make SiF_2 Surface site)

3. 2. 8. 11. 0.5 1.0 0. 0.01

-3. 4. 8. 10. 0.5 0.5 0. 0.015823

0.0 16300.0.0 0.0 0.0 0.0

Example *surf_chem* file:

```
*  
* this file contain surface chemistry information for the  
* UH - GEOM1 Problem Cl2 chemistry  
* Cl, Cl+, Cl-, Cl2, Cl2+, SiCl2  
* 1 2 3 4 5 6  
*  
2 number of material table types etch of Si --> SiCl2  
*  
* material 1 (wafer), wafer  
1. 7. 1.75e19 table number, number of entries(reactions), site density(#/m2)  
* Following input defines surface reactions on material type #1  
*First two reactions are Cl recombination to Cl2 with surface coverage dependence (see explanation below)  
2. 1. 0. 0. 0. 0. 1.0  
3. 1. 4. 0. 1.0 0. 0. 0.05  
* Next reaction is Cl- reflecting at wall fully specular due to sheath.  
1. 3. 3. 0. 1.0 0.0 1. 1.0  
* Cl+ and Cl2+ ion etching (doesn't include values for energy dependent etch yield)  
3. 2. 6.0 0. 1.0 0. 0. 1.0  
1. 5. 6.0 0. 1.0 0. 0. 1.0  
*  
* material 2, upper head  
2. 4. 1.75e19  
1. 1. 4. 0. 0.5 0. 0. 1.0  
1. 2. 1. 0. 1.0 0.0 0. 1.0  
1. 3. 3. 0. 1. 0.0 1. 1.0  
1. 5. 4. 0. 1.0 0.0 0. 1.0
```

3.7 Cross Section File (*cross_section*)

This file is used to specify a constant cross section for a particle-particle interaction instead of the default VHS model. For cross sections not specified in this file the VHS model will be used.

Example *cross_section* file:

```
* cross section input file - overwrite the VHS based values
* file for charged particles and neutral
*
9
2 1
100.e-20
2 4
100.e-20
2 6
100.e-20
3 1
100.e-20
3 4
100.e-20
3 6
100.e-20
5 1
100.e-20
5 4
100.e-20
5 6
100.e-20
```

line 1: number of entries

for each entry

first line: pair of species numbers as defined by the order in the *spec* file.
second line: collision cross section (m^2)

3.8 Gas Phase Chemistry File (*chem*)

The number of reactions defined in the *chem* file must match the number of gas phase reactions specified in the *geometry.inp* file. Formats for different types of reactions (elastic gas, charge exchange and electron impact) are slightly different however, all reactions follow the same basic input structure:

Each reaction requires the following input:

- line 1: Character string (comment line) - same for all reaction types
- line 2: MUST have 8 integers - defines reaction type and stoichiometry
- line 3 for type 0, -1, & -2 MUST have 5 real numbers
- line 3 for type -3 MUST have 2 integers and 1 real number -
- line 4 for type -3 MUST have 6 real numbers - electron impact fit parameters

Second line: for reaction type 0 to -2:

- (Rxn type) a b (# in first product group) (#. in second group) c d e
- for reaction type -3 or -4:
- (type) a b (stoichiometric coeff. first group) (stioch. coef. second group) c d e

Reaction types:

- 0 elastic gas rxn - kinetic treatment
- 1 charge exchange rxn, using VHS model
- 2 charge exchange rxn using Rapp and Francis relationship
- 3 electron impact rxn
- 4 elastic gas rxn - continuum treatment (for trace-trace chemistry)

reaction stoichiometry format:

- a + b --> (c + d) + (e), note: species are identified by order in *spec* file
- note: (c + d) denotes the first product group
- use a + b --> c + e for a simple binary chemistry exchange

Third line:

Reaction type 0 or -4: Elastic gas reaction

Arrhenius collisional chemistry reaction rate expression: $k = A T^B \exp(-E_a/kT)$

Requires 5 real numbers:

- 1 -- number of internal degrees of freedom
- 2 -- E_a
- 3 -- A
- 4 -- B
- 5 -- heat of rx (+ for exothermic) - joules

Reaction type -1: Charge exchange with constant cross-section, σ

Requires 5 real numbers:

- 1 -- probability
- 2 -- σ (m^2)

3 -- 0.00
4 -- 0.00
5 -- 0.00

Reaction type -2: Charge exchange using model from Rapp & Frances(1962)
 $\sigma = (k_1 - k_2 \cdot \log(v_r))^2$

Requires 5 real numbers:

1 -- k_1 for elastic collision
2 -- k_2 for elastic collision
3 -- k_1 for charge exchange
4 -- k_2 for charge exchange
5 -- 0.0

For example, this format was used by Kilgore, Wu and Graves (J. Vac. Sci. Technol. B 12(1)) for an Ar plasma for MKS units on velocity. The following parameter values are given:

1 = 7.746x10-10
2 = 4.493x10-11
3 = 1.288x10-9
4 = 7.436x10-11

Reaction type -3: Electron Impact reactions

Requires 2 integer numbers and 1 real number
second line variables:

1 -- Reaction rate equation # (if <0, T in K instead of eV), defined below
2 -- number of products (1 or 2)
3 -- heat of formation (e.g., Franck-Condon)- joules

Fourth Line: Only Required for Electron impact reactions

Requires 6 real numbers:

Variables 1-6 are for electron impact reaction fits as described below
(note: when using fits that have less than six variables use 0.0 as a place holder)

Electron impact reactions rate equation forms:

Several different forms of equations can be used to express electron impact rate constants as a function of electron temperature (either in eV or K).

The first parameter on the third line determines the form of the equation to be used.

Fit 1: $K = k_1 * (T_e^{k_2}) * \exp(-k_3 / T_e)$
Fit 2: $K = k_1 * (T_e^{k_2}) * \exp(-k_3 * T_e)$
Fit 3: $K = k_1 * ((k_2 / T_e)^{k_3})$
Fit 4: $K = k_1 * (T_e^{k_2}) * \exp((k_3 / T_e) + (k_4 / T_e^{k_2}) + (k_5 / T_e^{k_3}) + (k_6 / T_e^{k_4}))$
Fit 5: $K = k_1 + (T_e^{k_2}) + (k_3 * T_e^{k_2}) + (k_4 * T_e^{k_3}) + (k_5 * T_e^{k_4}) + (k_6 * T_e^{k_5})$
***the sign of the fit specifies the units for the electron temperature:

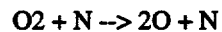
- (negative fit #) - Te is in K.
- + (positive fit #) - Te is in eV.

Variables k1-k6 for the fits are given in the fourth line.

Two example *chem* files follow:

Example 1: A 23 equation set of elastic gas reactions for air chemistry with 5 species: O2, N2, O, N, and NO. Species 1 == O2, 2==N2, etc.

*



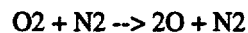
0 1 4 2 1 3 3 4
1. 8.197E-19 5.993E-12 -1. -8.197E-19

*



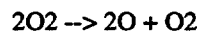
0 1 5 2 1 3 3 5
1. 8.197E-19 5.993E-12 -1. -8.197E-19

*



0 1 2 2 1 3 3 2
1.5 8.197E-19 1.198E-11 -1. -8.197E-19

*



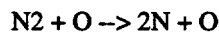
0 1 1 2 1 3 3 1
1.5 8.197E-19 5.393E-11 -1. -8.197E-19

*



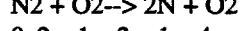
0 1 3 2 1 3 3 3
1. 8.197E-19 1.498E-10 -1. -8.197E-19

*



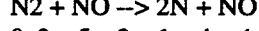
0 2 3 2 1 4 4 3
0.5 1.561E-18 3.187E-13 -0.5 -1.561E-18

*



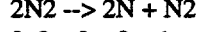
0 2 1 2 1 4 4 1
0.5 1.561E-18 3.187E-13 -0.5 -1.561E-18

*



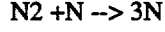
0 2 5 2 1 4 4 5
0.5 1.561E-18 3.187E-13 -0.5 -1.561E-18

*



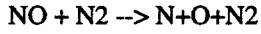
0 2 2 2 1 4 4 2
1. 1.561E-18 7.968E-13 -0.5 -1.561E-18

*



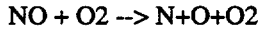
0 2 4 2 1 4 4 4
1. 1.561E-18 6.9E-8 -1.5 -1.561E-18

*



0 5 2 2 1 4 3 2
1. 1.043E-18 6.59E-10 -1.5 -1.043E-18

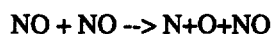
*



0 5 1 2 1 4 3 1

1. 1.043E-18 6.59E-10 -1.5 -1.043E-18

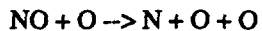
*



0 5 5 2 1 4 3 5

1. 1.043E-18 1.318E-8 -1.5 -1.043E-18

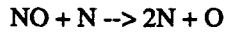
*



0 5 3 2 1 4 3 3

1. 1.043E-18 1.318E-8 -1.5 -1.043E-18

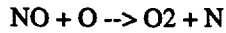
*



0 5 4 2 1 4 3 4

1. 1.043E-18 1.318E-8 -1.5 -1.043E-18

*



0 5 3 1 1 1 0 4

0. 2.719E-19 5.279E-21 1. -2.719E-19

*



0 2 3 1 1 5 0 4

0. 5.175E-19 1.120E-16 0. -5.175E-19

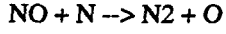
*



0 1 4 1 1 5 0 3

0. 4.968E-20 1.598E-18 0.5 2.719E-19

*



0 5 4 1 1 2 0 3

0. 0. 2.49E-17 0. 5.175E-19

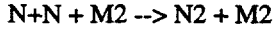
*

O+O + M1 --> O2 + M1 (note M1 denotes a third body partner -- the entry of -1 indicates the table index

0 3 3 1 0 1 0 -1

0. 0. 8.297E-45 -0.5 8.197E-19

*

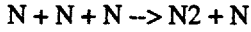


*

0 4 4 1 0 2 0 -2

0. 0. 3.0051E-44 -0.5 1.561E-18

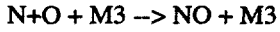
*



0 4 4 1 0 2 0 -3

0. 0. 6.3962E-40 -1.5 1.5637E-18

*



0 4 3 1 0 5 0 -4

0. 0. 2.7846E-40 -1.5 1.043E-18

Example 2: Chlorine plasma with charge exchange and electron impact chemistry

*

* Cl, Cl+, Cl-, Cl2, Cl2+, SiCl2

* 1 2 3 4 5 6

*

Cl+ + Cl -> Cl + Cl+ (charge exchange)

-1 2 1 1 1 1 0 2
0.75 120.e-20 0. 0. 0.

*

Cl2+ + Cl2 -> Cl2 + Cl2+ (charge exchange)

-1 5 4 1 1 4 0 5
0.75 120.e-20 0. 0. 0.

*

Cl- + Cl -> Cl + Cl- (charge exchange)

-1 3 1 1 1 1 0 3
0.90 240.e-20 0. 0. 0.

*

Cl+ + Cl- -> Cl + Cl (recombination)

0 2 3 1 1 1 0 1
0.0 0.0 5.e-14 0.0 1.5e-18

*

Cl2+ + Cl- -> 2Cl + Cl (recombination)

0 5 3 2 1 1 1 1
0.0 0.0 5.e-14 0.0 1.26e-18

*

Cl- detachment to Cl (electron impact)

-3 3 3 1 0 1 0 0
1 1 0.0
2.94e-14 0.680 3.7994 0.0 0.0 0.0

*

Cl2 attachment to Cl + Cl- (electron impact)

-3 4 4 1 1 1 0 3
2 2 5.78e-19
2.21e-16 0.485 -0.174 0.0 0.0 0.0

*

Cl2 dissociation to 2Cl (electron impact)

-3 4 4 1 1 1 0 1
1 2 0.96e-19
3.99e-14 0.115 4.43 0.0 0.0 0.0

*

Cl2 ionization to Cl2+ (electron impact)

-3 4 4 1 0 5 0 0
1 1 0.0
2.13e-14 0.771 11.7 0.0 0.0 0.0

*

Cl ionization to Cl+ (electron impact)

-3 1 1 1 0 2 0 0

1 1 0.0

2.96e-14 0.554 13.1 0.0 0.0 0.0

*

Cl2+ attachment to 2Cl (electron impact)

-3 5 5 1 1 1 0 1

3 2 1.84e-18

9.0e-13 0.0258526 0.61 0.0 0.0 0.0

*

3.9 Diagnostic Messages

The init2d code checks for several types of problem areas:

- 1- length of program arrays
-see section 9.2 for adjusting the parameters in init2d.h
- 2- region side connectivity
-the code will check the region side connectivity consistency. An error will occur if the region connectivity section is not consistent between two regions
- 3- files
-the code will provide screen output when an input file is opened and closed to facilitate debugging
- 4- the final screen output from the init2d code contains problem size definition information. This can be used to determine parameters for the param.h file (section 9.2)

4. **decomp2d** - Decomposition Code Description

Goal: Decomposes the problem for parallel computing environment.

Usage: **decomp2d** *param1 param2*

param1 and *param2* can be entered either on the command line, as shown, or in response to interactive questions.

param1: number of processors to decompose the input file, *datap*, into

param2: decomposition strategy (1 for sequential and 2 for block)
(recommend 1 for massively parallel and 2 for few processors)

Input files:

datap: geometry and boundary definition file from **init2d**

Output files:

dsmc.in2: decomposed data file -- specific to # of processors

dsmc.node: link list file to associate cell information with a processor.
used by **restart2d** and coupled plasma capability (**GEMINI**)

Notes:

decomp2d does NOT need to be used if a single processor simulation is being done. The output file from **init2d**, *datap*, can be used directly by **icarus**.

We use decomposition strategy 1 for $> \sim 16$ nodes and 2 for $< \sim 16$ processors. For example, use 2 for a network of workstations, a Sun Dragon or SGI Power Challenge and use 1 for a Paragon or nCUBE.

5. icarus - Code and Command File (*dsmc.in*) Description

Goals: Performs DSMC calculation and gathers statics.

Usage: **icarus <***dsmc.in* &

dsmc.in is a command line syntax file

Input Files: *dsmc.in2(MP)*, *datap(1P)*
dsmc.node, *dsmc.restart* (for restart calculation)
dsmc.em and *dsmc.plasma* (for plasma application)

Output Files: Output filenames are defined in the ***dsmc.in***
typical names are: *cell.**, *surf.** and *wafer.**
* denotes the time step when file was written.

File Descriptions:

<i>cell.*</i>	Contains macroscopic quantities of pressure, temperature, density, species concentrations and velocities. Local Cell Knudsen number, CFL number and λ are also contained in this file.
<i>surface.*</i>	Contains surface element information such as incident flux by species, reflected flux(etchant), surface coverage, surface pressure, shear stress and heat flux.
<i>wafer.*</i>	Contains wafer element information of angular and energy distribution functions by species.
<i>chem.*</i>	Contains statistics of the number of times each chemical reaction occurred per cell.
<i>plasma.*</i>	Contains electron number density and temperature for each cell.
<i>particle.*</i>	Contains information on ALL computational particles: position, velocity, species, and kinetic energy
<i>dsmc.log</i>	Contains log information of icarus run such as number of time steps, number of particles, number of collisions, number of surface collisions, etc.
<i>dsmc.pump</i>	Contains pump and pressure information when using the pressure feedback loop. Output includes old pressure at control point, new pump speed and current pressure at control point.

5.1 icarus Command List

This is a complete list of valid DSMC commands found in the *dsmc.in* file, their defaults, and the "type" of parameters that should be used (i=integer,r=real,c=character string). The type (integer, real, character string) of the parameters is important since the input parser expects certain kinds of values. All of the input commands take one or more parameters. The keyword for each command must begin in the left most column and all characters in the command should be in lower-case. Parameters can be separated by arbitrary numbers of spaces and/or tabs.

Note: a '#' as the first character denotes a comment line

i/o files

log file	dsmc.log	(c)
id string	character string	(c)
cell file	cell	(c)
surface file	surface	(c)
wafer file	wafer	(c)
movie file	movie	(c)
gemini files	DSMC.OUT GD.COUNT	(cc)
special file	50 dsmc.nbari	(ic)
plot file	dsmc.plot	(c)
chemistry file	chem	(c)
particle file	particle	(c)

input

read definition	1.0 dsmc.def	(rc)
read restart	1.0 1.0 dsmc.def dsmc.restart	(rrcc)
read efield	dsmc.em dsmc.plasma	(cc)
load particles	1.0	(r)
loadn cutoff	0	(i)
loadv cutoff	0	(i)

output control

output screen	100	(i)
output cells	0	(i)
output surface	0	(i)
output wafer	0	(i)
output movie	0 0.1	(i)
output chemistry	0	(i)
output plot	0	(i)
output flag	0	(i)
output plasma	0	(i)
output particles	0	(i)
ion energy	30.0	(r)
neutral energy	1.0	(r)
species energy	3 20.0	(ir)

misc run param.

limit flag	0	1000.0	(ir)
debug flag	0		(i)
random seed	48729873		(i)

dsmc params

collision flag	1		(i)
vr-sigma flag	1		(i)
chemistry flag	0		(i)
exchange flag	0		(i)
adapt flag	50	0.5	(ir)
stat flag	1		(i)
zero flag	100		(i)
coverage	500		(i)
collision limit	5		(i)

run params

time factor	1.0		(i)	
pump speed	1.0		(r)	
pump control	100	1.0 0.5 2.0	dsmc.pump	(irrc)
run	1000	0	(ii)	

plasma option

gemini flag	0		(i)
ne flag	0		(i)
ne limit	1.e12	1.e19	(rr)
efield flag	1		(i)
efield subcycle	1	1	(ii)
field mult	1.0		(r)
ne mult	1.0		(r)
nion collide	0		(i)
no ionchem	99999		(i)

5.2 icarus Command Descriptions

comments

blank lines are ignored. Everything on a line after last parameter is ignored. Lines starting with a '#' are comments and are echoed into the log file.

-----i/o files-----

log file

All info from this point on will dump into this file. Any previous file is closed. New file name can exist, will be overwritten. Anything in input file before the first "log file" command will not be echoed into a log file..

default = none

id string

following character string will be printed at top of output files

default = none

cell file

name of cell file to dump to; timestep # is appended to name; file can exist, will be overwritten.

default = cell

surface file

name of surface file to dump to; timestep # is appended to name file can exist; will be overwritten

default = surf

wafer file

name of wafer file to dump to; timestep # is appended to name file can exist; will be overwritten

default = wafer

movie file

name of movie file to dump to; timestep # is appended to name file can exist; will be overwritten

default = movie

gemini files

control coupling to the Glow Discharge code(MPRES) for Plasma-DSMC (GEMINI) simulations
1st file is the file to write cell data file name

2nd file is the counter file updated by the GD code--if counter changed, then read dsmc.rate and
dsmc.em_1 files

default = DSMC.OUT & GD.COUNT

special file

1st parameter = output user-defined statistics every this many steps

2nd parameter = filename to record statistics in

dump user-defined statistics to a file every this many timesteps; user can edit output_special rou-
tine to change what stats are written out; value of 0 for 1st parameter means never write out; 2nd
parameter not needed if 1st parameter is 0; file can exist, will be overwritten

default = 0

plot file

name of plot file to dump timestep info to

file can exist, will be overwritten; only columns of numbers (no text) are written into this file to
make it suitable for post-processing by plotting programs; if this command is not specified, no
plot file is created

default = none

chemistry file

name of chemistry file to dump to, timestep # is appended to name file can exist, will be overwrit-
ten

default = chem

particle file

name of the file to write information on ALL computational particles: position, velocity, species,
and kinetic energy.

default = particle

-----input-----

read definition

1st parameter = problem size scale factor

2nd parameter = data file

read problem definition from filename

use 1st parameter to scale problem size (divides scale base input value #13 in init2d input by this value---i.e. >1 increases the number of computational particles)

reading a new definition file clears all info from previous runs

read restart

1st parameter = problem size scale factor

2nd parameter = multiplier for initial density

3rd parameter = def data file

4th parameter = restart file

read problem definition from filename and restart info from restart file restart file is created by running previously generated cell output files thru a serial restart program use 1st parameter to scale problem size (divides scale base input value #13 in init2d input by this value---i.e. >1 increases the number of computational particles) reading a data and restart file clears all info from previous runs this command causes loading of particles at the cell densities specified in the restart file

read xrestart

1st parameter = problem size scale factor

2nd parameter = multiplier for initial density

3rd parameter = def data file

4th parameter = restart file

same basic definition as 'read restart' except that the cell weights are the values from the definition file (dsmc.in2) rather from the restart file (dsmc.restart). This is useful for subsonic simulations.

read efield

1st parameter = efield filename

2nd parameter = plasma filename

read efield definition on grid from efield and plasma files uses efield file as prefix for zone files, appends "_N" to efield filename to generate zone filename for zone N next "run" following this command must be unsteady. The efield file includes E_r and E_z the plasma file includes n_e and T_e .

load particles

initialize cells with particles at freestream density and velocity scaled (multiplied) by specified parameter
parameter shouldn't specify this command when "read restart" command is used, since is done automatically

loadv cutoff

region with id number <= this number get loaded with particles with thermal and freestream component of velocity; othersie only get thermal component of velocity. if = 0, particles in all regions get both freestream and thermal components

useful for loading particles in wake region of high-speed flow
default = 0

loadn cutoff

region with id number <= this number get loaded with particles at 'freestream' density
if = 0, all regions loaded with freestream density
default = 0

-----output control-----

output screen

current timestep info displayed to screen and logfile every this many steps value of 0 means never display
default = 100

output cells

cell stats dumped to file every this many steps always dumped at the end of each run value of 0 means never dump except at end of run
default = 0

output surface

surface stats dumped to file every this many steps always dumped at the end of each run value of 0 means never dump except at end of run
default = 0

output wafer

wafer stats dumped to file every this many steps always dumped at the end of each run if wafer is defined value of 0 means never dump except at end of run
default = 0

output movie

1st parameter = every this many steps
2nd parameter = probability of tagging a particle

particle stats dumped to movie file every this many steps also dumped at the end of each run 2nd param determines what fraction of particles are dumped, not needed if 1st parameter = 0 currently this command only works if are running on 1 processor value of 0 means never dump
default = 0

output chemistry

chemical reaction stats dumped to file every this many steps always dumped at the end of each run if chemistry is defined value of 0 means never dump except at end of run
default = 0

output flag

flag to invoke writing cell output file name into file dsmcfile see gemini flag to set dsmcfile name (default filename = DSMC.OUT). This feature is useful to trigger a script to compress the output files or run the post2d script.
default = 0

output plasma

plasma parameters are dumped to file every this many steps, contains ne and Te. Values are either initial values or updated ne based on local charge neutrality assumption. Used to verify plasma parameters used for computing electron impact chemistry rates.

default = 0

output plot

flag to invoke writing screen output to a file suitable for direct plotting (column format)

let flag=1 to write file.

default = 0

output particles

computational particle information (position, velocity, species type, kinetic energy) are dumped to a file every this many steps.

default = 0

ion energy

maximum value (in eV) to scale incoming wafer ion particle energies to see “species energy” command for how to override this

default = 30.0

neutral energy

maximum value (in eV) to scale incoming wafer neutral particle energies to see “species energy” command for how to override this

default = 1.0

species energy

1st parameter = species id number

2nd parameter = energy value (eV)

set incoming wafer particle energy for this species to this energy value these energies are set to values specified by “ion/neutral energy” commands every time a “run” command is performed this command overrides those defaults for a specific species specifying energy value of 0.0 unsets a previous setting -- use the default “ion/neutral energy” value

-----misc run params-----

limit flag

1st parameter = # of timesteps

2nd parameter = # of CPU seconds

check every this many timesteps to see if total run time has exceeded this many CPU seconds
value of 0 for 1st parameter means never check if it has, stop the program immediately units of
seconds for 2nd parameter, only needed if 1st parameter $\neq 0$

default = 0 for 1st parameter

debug flag

flag for whether to print verbose messages to screen

0 = none,

-1 = definition file printout checkpoints

1 = some (hung particles in move),

2 = debug info during move

3 = module debug info (in dsmc)

default = 0

random seed

initial seed for random number generator seed only used 1st time the generator is called after
this command is specified if not specified, program will initialize generator with default seed

default = 12345678

dsmc params

collision flag

flag for whether or not to perform collisions 0 = do not, 1 = do collisions
default = 1

vr-sigma flag

flag to control resetting the max. Vr•sigma product during the unsteady phase for the no-time counter collision logic
default = 1 (reset product and force a collision in every cell)

chemistry flag

flag for whether or not to perform chemistry 0 = no chemistry, 1 = B/L chemistry, 2 = maximum-entropy chemistry
default = 0

exchange flag

flag for kind of energy exchange in collisions
0 = Borgnakke-Larsen, 1 = maximum entropy
default = 0

adapt flag

adjusts cell weight to reduce # of computational particles/cell; *mass is conserved*
1st parameter = number of particles per cell to limit to
2nd parameter = tolerance factor

determines whether or not to limit maximum particles in a cell

1st parameter = 0 -> no limit (2nd parameter not needed)

1st parameter = n -> delete particles if more than $n*(1+\text{tolerance})$ in a cell
for efficiency of adapt routine, tolerance should be set ≥ 0.25
default = 50 for 1st parameter, 0.5 for 2nd parameter

stat flag

accumulate cell statistics every this many timesteps 0 = never accumulate
default = 1 (every step)

zero flag

zero out accumulation quantities every this many timesteps used to run unsteady flow, is ignored
when running steady flow 0 = never zero out quantities
default = 100

coverage

Number of time steps between coverage calculation during unsteady portion--Note: coverage chemistry activated by input files from **init2d**
default=500

collision limit

max number of collisions allowed for any one particle
default = 5

-----run params-----

time factor

time scale factor to multiply timestep by in all regions this parameter is NOT cumulative, should be set explicitly to the desired scale factor to dilate or compress time for each stage of a run
default = 1.0

pump speed

pumping speed (in m^3/sec) of region defined as vacuum pump value of 0.0 turns off pump other pump parameters (region, pump volume) must be defined in “read definition” file
default = 0.0

pump control

1st parameter = adjust pump speed every this many steps
2nd parameter = target pressure in specified cell (Pascals)
3rd parameter = minimum allowed pump speed
4th parameter = maximum allowed pump speed
5th parameter = data file to record pump parameters in

control pump speed so as to achieve target pressure in one simulation cell; this command only applies to the next “run”, which must be unsteady; cell # for target pressure is specified in “read definition” file; initial pump speed will be whatever is specified by “pump speed” command; pump speed will be kept between min and max values; data filename can exist, will be overwritten

run

1st parameter = # of timesteps
2nd parameter = 0 (unsteady). 1 (steady)

run or continue DSMC for this many timesteps.

unsteady mode: zeroes out cell, surface, and collision statistics at the beginning of the “run” command and every so many steps (see “zero flag” command). Also resets the maximum σV_r per cell used by the NTC collision model.

steady mode: all statistical quantities continuously accumulate

-----plasma option-----

gemini flag

flag to enable plasma coupling with the MPRES plasma code running on a separate workstation. Value of flag is the time step frequency during the steady phase in which the DSMC code will check the MPRES.COUNT (default file) for a change which will signal new dsmc.rate and dsmc.em files to be read. Program control will exit current steady logic and continue to next command entry.

default = 0

ne flag

flag to invoke local charge neutrality for calculation of ne (electron number density). Perform averaging every neflag time steps in steady phase.

default = 0

ne limit

minimum and maximum values for electron number density (ne) based on local charge neutrality

default = 1.e12 and 1.e19 #/m³

efield flag

determines use of efields during a "run"

0 = no fields (turn them off if used previously)

1 = apply fields during particle move

2 = apply fields during particle move and do ion chemistry

if 1 or 2 is specified then must do a "read efield" before unsteady "run"

default = 0

efield subcycle

1st parameter = # of timestep subcycles in bulk interior region

2nd parameter = # of timestep subcycles in sheath region

number of timestep subcycle to perform in particle move of charged ions only useful when "efield flag" is set so as to turn on efields

default = 1 for both parameters

field mult

multiply the electrostatic fields by this value; must occur BEFORE the 'read efield' command to alter the input values.

default = 1.0

ne mult

multiplier for the input electron number density - must occur BEFORE the 'read efield' command
default = 1.0

nion collide

option to turn off elastic collisions for the negative ions (if = 0); recombination chemistry will still
occur if chemistry option '-4' is used
default = 1 (collisions)

no ionchem

option to turn off Lorentz force transport and electron impact chemistry for regions greater than or
equal to this value
default = 99999 (operate in all regions)

5.3 Example *dsmc.in* Files

Example 1: Using Initial Freestream Conditions

Neutral flow reactor *dsmc.in* file

```
log file      dsmc.log
output screen 100
zero flag     100
pump control  100 0.75 0.003 0.3 dsmc.pump
pump speed    0.03
read definition 0.2 dsmc.in2
load particles 6.0
adapt flag    500 0.25
time factor   1.0
run           20000 0
output cells   5000
output surface  5000
adapt flag    1000 0.25
time factor   1.0
run           400000 1
```

Example 2: Using Restart File

#shield calculations with shorter length

```
log file      dsmc.log
output screen 100
zero flag     100
pump control  100 0.75 0.01 1.0 dsmc.pump
pump speed    0.05
read restart   1.0 0.3 dsmc.in2 dsmc.restart
adapt flag    500 0.25
time factor   1.0
run           20000 0
output cells   5000
output surface  5000
output wafer   5000
adapt flag    1000 0.25
time factor   1.0
run           400000 1
```

5.4 Diagnostic Messages

- 1- code parameters are checked with input values...see section 9.2 for changing param.h
- 2- if the 'debug flag' is set to -1, input diagnostic as the file is read will be performed
- 3- messages: 'Too many in reacta' or 'Too many in create' indicate that the max. number of particles per processor has been exceeded (lmmo in param.h). Either increase lmmo and recompile or use the adapt flag to limit the number of computational particles per cell.
- 4- a message: 'Too many in self-communicate' indicates that the communication buffer array is too small (gbuf in param.h). Either increase gbuf and recompile, decrease the time step, or limit the number of particles in the simulation by using the adapt limit or the global scale factor on the *read def* (*read restart*) input.
- 5- 'Stop - Comm buffer overflow' indicates that the buffer is too small...code hangs in a MP environment. Either increase the buffer size, gbuf, and recompile or reduce the number of simulation particles by using adapt or the global scale factor on the *read def* (*read restart*) input.
- 6- Icarus checks for consistency between the input files (dsmc.in2 and dsmc.restart) and the number of processors requested. That is, you cannot run a 2 processor simulation if either the input file, dsmc.in2, or the restart file, dsmc.restart, were created for a different number of processors or load balancing schemes. Rerun either (or both) *init2d* or *decomp2d* as necessary.
- 7- a message in "which surface" indicates that a computational particle is *hung*. That is, round-off error has caused a particle position to be undefined in the computational domain. This error is only a problem if it occurs many times per time step; check the output after a run step (unsteady or steady) where the #-hung particles per time step are computed.
- 8- Check the output after each run step (unsteady or steady) for global statistics to determine if the simulation is running satisfactory. For example, for statistical reasons, there should be at least ~10 particles per cell.
- 9- Load balancing information is printed at the of each run step (unsteady or steady). This information includes a 10 group histogram of the computational time during specific code blocks.

10- messages: 'Too many in init' or 'Too many in create' indicate that the max. number of particles per processor has been exceeded (lmmo in param.h). Either increase lmmo and recompile or use the adapt flag to limit the number of computational particles per cell. NOTE: when this message occurs, no more computational particles are loaded into the cells for that processor. For example, during problem initiation, if the message: 'Too many in init' occurs, then the remainder of the cells for that processor will not have any particles -- a vacuum condition.

6. restart2d - Code Description

Goal: Generate starting solution for a icarus calculation with the same grid.

Usage: **restart2d** *cell.* value*

*cell.**: icarus cell data file (default *cell.1000*, *cell.2000*, etc.)

value: optional input: 2 for a mp restart case and 1 for a single processor case

Note: if *dsmc.node* file (mp file) does not exist, single processor assumed
interactive response to creation of a mp(2) or single processor(1) restart file

Additional Input files:

if single processor file, none

if mp restart file, *dsmc.node* (from **decomp2d**)

Output files:

dsmc.restart: file for icarus

Notes:

mp to mp

The *dsmc.node* file has to be decomposed for the restart calculation (*dsmc.in2*). You can change the number of processors between restart runs(i.e. start with 256 and then restart with 128).

1p to mp

Just use the *dsmc.node* file of the decomposed input file.

mp to 1p

Just select the option, 1, to decompose into a *dsmc.restart* file for a 1p simulation.

misc:

restart2d only requires the number of grid cells and region distribution to remain the same as well as the number of chemical species; boundary conditions, reaction rates, vacuum pump flows, etc. can be changed during the restart simulation.

NOTE: *restart2d* uses only the macroscopic properties (cell density, velocity, temperature, etc) and assumes a Boltzmann distribution to restart a simulation. Therefore, several unsteady time steps are required to obtain non-equilibrium conditions before the steady ensemble phase should begin.

7. regrid2d - Code Description

Goal: The **regrid2d** program serves three basic functions:

1. Allows the **icarus** program to be started from a continuum code.
2. Allows an **icarus** solution to be restarted on a different grid or a different MP configuration.
3. To couple the **icarus** code with the **MPRES** code. This coupling includes both **icarus->MPRES** and **MPRES->icarus**.

Each of the different restart types will be discussed below in some detail.

1. To start **icarus** from a continuum code.

At the present time the only supported format is 2D Tecplot binary (point or block). Future plans include the addition of other formats.

Usage: **regrid2d -btecplot -mp *file1***

-btecplot: Command line input to set the input type of *file1*

-mp: Command line input to set MP restart

file1: 2d tecplot binary in block or point format

Required input files:

dsmc.in2: Provides grid point location for the inverse distance interpolation

dsmc.node: Provides processor mapping.

btecplot.map: Provides the variable mapping (similar to *post2d.vlist*)

Output file:

dsmc.restart - A restart file for **icarus**

2. To restart **icarus** from a prior **icarus** solution.

At present this restart type requires the same number of species for the old and new simultaneous.

Usage: **regrid2d -dsmc -mp *file1***

-dsmc: Command line input to set the input type of *file1*

-mp: Command line input to set MP restart

file1: Data file from **icarus** code -- for example *cell.40000*

Required input files:

dsmc.in2: Provides grid point location for the inverse distance interpolation

dsmc.node: Provides processor mapping.

dsmc.in2_old: Provides original grid point location

dsmc.node_old: Provides original processor mapping.

Output file:

dsmc.restart - A restart file for **icarus**
3a. To restart icarus from MPRES code.

Usage: **regrid2d -glow -mp file1**

-glow: Command line input to set the input type of *file1*
-mp: Command line input to set MP restart
file1: A MPRES ASCII output file

Required input files:

dsmc.in2: Provides grid point location for the inverse distance interpolation
dsmc.node: Provides processor mapping.
glow.map: Provides the variable mapping (similar to *post2d.vlist*)
Sheath: Provides em-field at domain boundaries

Output files:

dsmc.restart - A restart file for **icarus**
dsmc.plasma - Provides electron densities and temperatures for **icarus**
dsmc.em - Provides em-field for **icarus**

3b. To restart MPRES from icarus

Usage: **regrid2d -glow -mp file1 file2**

-glow: Command line input to set the input type of *file1*
-mp: Command line input to set MP restart
file1: A MPRES ASCII output file
file2: Data file from **icarus** code -- for example *cell.40000*

Required input files:

dsmc.in2: Provides grid point location for the inverse distance interpolation
dsmc.node: Provides processor mapping.
dsmc.map: Provides the variable mapping (similar to *post2d.vlist*)

Output file:

glow.restart - A restart file for **MPRES**

Given a Tecplot binary File with a variable list as follows:

variable 1 = Physical coordinate Z(m)
variable 2 = Physical coordinate R(m)
variable 3 = Velocity Component Vz(m/s)
variable 4 = Velocity Component Vr(m/s)
variable 5 = Pressure P(pa)
variable 6 = Translational Temperature Tt(k)
variable 7 = Density ρ (kg/m³)
variable 8 = Mach Number M
variable 9 = Vibrational Temperature Tv(k)
variable 10 = Diatomic Nitrogen N₂(kg/m³)
variable 11 = Atomic Nitrogen N(kg/m³)

An example of a btecplot.map file

* This is an example of a two species mapping from a btecplot output file to icarus.
* This is the btecplot mapping file. The star in the first line is a comment statement.
* The btecplot index is the order the var. appears in the btecplot output file.
*
* Z/R are defined and the direction is reversed on Z.
* The dsmc var 1 defines Z and dsmc var 2 defines R
* the first 10 spaces are defined for char. use only...
*
* var. name dsmc var btecplot default/mult
z 1 1 1.0
r 2 2 1.0
* the dsmc var 51 through 100 define the species number density. The order is given by
* adding the icarus species number to 50. i.e. species 1 is indexed as 51, 2 as 52, etc.
* The mass density is converted to a number density by the column 4 multiplier.
*
* var. name dsmc var btecplot default/mult
n2 51 10 2.1507e25
n 52 11 4.3014e25

* The dsmc var 100 through 200 defines the species V x/z velocity. The order is given by adding
 * the icarus species number to 100.
 *
 * var. name dsmc var btecplot default/mult
 Vz_n2 101 3 1.0
 Vz_n 102 3 1.0
 * The dsmc var 200 through 300 defines the species V y/r velocity. The order is given by adding
 * the icarus species number to 200.
 *
 * var. name dsmc var btecplot default/mult
 Vr_n2 201 4 1.0
 Vr_n 202 4 1.0
 * The dsmc var 300 through 400 defines the species translational temperature.
 * The order is given by adding the icarus species number to 300.
 *
 * var. name dsmc var btecplot default/mult
 tt_n2 301 6 1.0
 tt_n 302 6 1.0
 * The dsmc var 400 through 500 defines the species rotational temperature.
 * The order is given by adding the icarus species number to 400.
 *
 * var. name dsmc var btecplot default/mult
 tr_n2 401 6 1.0
 tr_n 402 6 1.0
 * The dsmc var 500 through 600 defines the species vibrational temperature.
 * The order is given by adding the icarus species number to 500.
 *
 * var. name dsmc var btecplot default/mult
 tv_n2 501 9 1.0
 tv_n 502 9 1.0
 * The dsmc var 600 through 700 defines the species weights cxy. The order is given by adding
 * the icarus species number to 600.
 * NOTE: as the code is set up the cxy are over-written by the values in the dsmc.in2 file.
 *
 * var. name dsmc var btecplot default/mult
 cxy_n2 601 -1 1.0
 cxy_n 602 -1 1.0

An example of a glow.map file

* This is an example of a six species mapping from a MPRES output file to icarus.
* This is the glow mapping file. The star in the first line is a comment statement.
* The glow index is the order the var. appears in the MPRES output file.
*
* Z/R are defined and the direction is reversed on Z.
* The dsmc var 1 defines Z and dsmc var 2 defines R
* the first 10 spaces are defined for char. use only...
*
* var. name dsmc var MPRES default/mult
z 1 2 -1.0
r 2 1 1.0
* the dsmc var 51 through 100 define the species number density. The order is given by
* adding the icarus species number to 50. i.e. species 1 is indexed as 51, 2 as 52, etc.
*
* var. name dsmc var MPRES default/mult
n_cl 51 7 1.0
n_cl+ 52 5 1.0
n_cl- 53 6 1.0
n_cl2 54 9 1.0
n_cl2+ 55 4 1.0
n_Sicl2 56 8 1.0
* The dsmc var 100 through 200 defines the species V x/z velocity. The order is given by adding
* the icarus species number to 100. The MPRES output provides no velocity data so a value of -1
* in the glow col., tells the mapping code to apply the constant value in col. 4 over the
* entire domain.
*
* var. name dsmc var MPRES default/mult
Vz_cl 101 -1 0.0
Vz_cl+ 102 -1 0.0
Vz_cl- 103 -1 0.0
Vz_cl2 104 -1 0.0
Vz_cl2+ 105 -1 0.0
Vz_Sicl2 106 -1 0.0
* The dsmc var 200 through 300 defines the species V y/r velocity. The order is given by adding
* the icarus species number to 200. The glow output provides no velocity data so a value of -1
* in the glow col., tells the mapping code to apply the constant value in col. 4 over the
* entire domain.
*
*

* var. name	dsmc var	MPRES	default/mult
Vr_cl	201	-1	0.0
Vr_cl+	202	-1	0.0
Vr_cl-	203	-1	0.0
Vr_cl2	204	-1	0.0
Vr_cl2+	205	-1	0.0
Vr_Sicl2	206	-1	0.0

* The dsmc var 300 through 400 defines the species translational temperature.

* The order is given by adding the icarus species number to 300. The MPRES output

* provides no temperature data so a value of -1 in the glow col., tells the mapping code

* to apply the constant value in col. 4 over the entire domain.

*

* var. name	dsmc var	MPRES	default/mult
tt_cl	301	-1	500.0
tt_cl+	302	-1	500.0
tt_cl-	303	-1	500.0
tt_cl2	304	-1	500.0
tt_cl2+	305	-1	500.0
tt_Sicl2	306	-1	500.0

* The dsmc var 400 through 500 defines the species rotational temperature.

* The order is given by adding the icarus species number to 400. The MPRES output

* provides no temperature data so a value of -1 in the glow col., tells the mapping

* code to apply the constant value in col. 4 over the entire domain.

*

* var. name	dsmc var	MPRES	default/mult
tr_cl	401	-1	500.0
tr_cl+	402	-1	500.0
tr_cl-	403	-1	500.0
tr_cl2	404	-1	500.0
tr_cl2+	405	-1	500.0
tr_Sicl2	406	-1	500.0

* The dsmc var 500 through 600 defines the species vibrational temperature.

* The order is given by adding the icarus species number to 500. The MPRES output

* provides no temperature data so a value of -1 in the glow col., tells the mapping

* code to apply the constant value in col. 4 over the entire domain.

*

* var. name	dsmc var	MPRES	default/mult
tv_cl	501	-1	500.0
tv_cl+	502	-1	500.0
tv_cl-	503	-1	500.0

tv_cl2	504	-1	500.0
tv_cl2+	505	-1	500.0
tv_Sicl2	506	-1	500.0

* The dsmc var 600 through 700 defines the species weights cxy. The order is given by adding
 * the icarus species number to 600. The MPRES output provides no weight. data so a value of -1
 * in the glow col., tells the mapping code to apply the constant value in col. 4 over the
 * entire domain.

* NOTE: as the code is set up the cxy are over-written by the values in the dsmc.in2 file.

*

* var. name	dsmc var	MPRES	default/mult
cxy_cl	601	-1	1.0
cxy_cl+	602	-1	1.0
cxy_cl-	603	-1	1.0
cxy_cl2	604	-1	1.0
cxy_cl2+	605	-1	1.0
cxy_Sicl2	606	-1	1.0

*

* The dsmc var 1000 through 2000 defines the plasma. The dsmc var 1001 is the
 * electron temperature and 1002 is the electron density.

*

* var. name	dsmc var	MPRES	default/mult
Te	1001	10	1.0
ne	1002	3	1.0

* The dsmc var 2000 through 3000 defines the em-field mapping Ex/z is defined as 2001 and
 * Ey/r is defined as 2002

*

* var. name	dsmc var	MPRES	default/mult
Ez	2001	13	-1.00
Er	2002	12	1.00

*

* If a mapping is not provided in the file the constant
 * default values defined in the code are used.....

An example of a dsmc.map file

* This is an example of a six species mapping from a icarus output file to MPRES.
* This is the dsmc mapping file. The star in the first line is a comment statement.
* The glow index is the order the var. appears in the MPRES output file.
* If a -1 appears in the 3 column the that MPRES variable is not over-written and value in
* the MPRES output file are used. If a valid variable index appears in column 3 then the
* value is over-written with the icarus value.
*
* Z/R are defined and the direction is reversed on Z.
* The dsmc var 1 defines Z and dsmc var 2 defines R
* the first 10 spaces are defined for char. use only...
* var. name dsmc var MPRES default/mult
z 1 2 -1.0
r 2 1 1.0
*
* the dsmc var 51 through 100 define the species number density. The order is given by
* adding the icarus species number to 50. i.e. species 1 is indexed as 51, 2 as 52, etc.
* Variables 19, 22, 21 are over-written with the icarus values, while the other species retain
* there original values.
*
* var. name dsmc var MPRES default/mult
n_cl 51 19 1.0
n_cl+ 52 -1 1.0
n_cl- 53 -1 1.0
n_cl2 54 22 1.0
n_cl2+ 55 -1 1.0
n_Sicl2 56 21 1.0
* The dsmc var 100 through 200 defines the species V x/z velocity. The order is given by adding
* the icarus species number to 100. No velocity data is provided to MPRES so a value of -1
* in the MPRES col., in the mapping file causes the variable to be skipped.
*
* var. name dsmc var MPRES default/mult
Vz_cl 101 -1 0.0
Vz_cl+ 102 -1 0.0
Vz_cl- 103 -1 0.0
Vz_cl2 104 -1 0.0
Vz_cl2+ 105 -1 0.0
Vz_Sicl2 106 -1 0.0
* The dsmc var 200 through 300 defines the species V y/r velocity. The order is given by adding
* the icarus species number to 200. The order is give by adding

* the icarus species number to 100. No velocity data is provided to MPRES so a value of -1
* in the MPRES col., in the mapping file causes the variable to be skipped.

*

* var. name	dsmc var	MPRES	default/mult
Vr_cl	201	-1	0.0
Vr_cl+	202	-1	0.0
Vr_cl-	203	-1	0.0
Vr_cl2	204	-1	0.0
Vr_cl2+	205	-1	0.0
Vr_Sicl2	206	-1	0.0

* The dsmc var 300 through 400 defines the species translational temperature.

* The order is given by adding the icarus species number to 300. No temperature data is provided to MPRES so a value of -1

* in the MPRES col., in the mapping file causes the variable to be skipped.

*

* var. name	dsmc var	MPRES	default/mult
tt_cl	301	-1	500.0
tt_cl+	302	-1	500.0
tt_cl-	303	-1	500.0
tt_cl2	304	-1	500.0
tt_cl2+	305	-1	500.0
tt_Sicl2	306	-1	500.0

* The dsmc var 400 through 500 defines the species rotational temperature.

* The order is given by adding the icarus species number to 400. No temperature

* data is provided to MPRES so a value of -1 in the MPRES col., in the

* mapping file causes the variable to be skipped.

*

* var. name	dsmc var	MPRES	default/mult
tr_cl	401	-1	500.0
tr_cl+	402	-1	500.0
tr_cl-	403	-1	500.0
tr_cl2	404	-1	500.0
tr_cl2+	405	-1	500.0
tr_Sicl2	406	-1	500.0

* The dsmc var 500 through 600 defines the species vibrational temperature.

* The order is given by adding the icarus species number to 500. No temperature

* data is provided to MPRES so a value of -1 in the MPRES col., in the

* mapping file causes the variable to be skipped.

*

* var. name	dsmc var	MPRES	default/mult
tv_cl	501	-1	500.0
tv_cl+	502	-1	500.0
tv_cl-	503	-1	500.0
tv_cl2	504	-1	500.0
tv_cl2+	505	-1	500.0
tv_Sicl2	506	-1	500.0

* The dsmc var 600 through 700 defines the species weights cxy. The order is given by adding

* the icarus species number to 600. No species weights data is provided to MPRES

* so a value of -1 in the MPRES col., in the mapping file causes the variable to be skipped.

*

* var. name	dsmc var	MPRES	default/mult
cxy_cl	601	-1	1.0
cxy_cl+	602	-1	1.0
cxy_cl-	603	-1	1.0
cxy_cl2	604	-1	1.0
cxy_cl2+	605	-1	1.0
cxy_Sicl2	606	-1	1.0

*

* The dsmc var 1000 through 2000 defines the plasma. The dsmc var 1001

* is the electron density. A new ne is given to the MPRES code in the variable

* three location.

*

* var. name	dsmc var	MPRES	default/mult
ne	1001	3	1.0

8. Postprocessing Codes

post2d:

- cellwise information
- converts particle statistics into macroscopic quantities:
pressure, density, velocities, temperatures, species concentrations, etc.
- use cell data files from icarus

surface2d:

- information for surface elements (sides of cells which are boundaries):
surface pressure, shear stress, & heat flux
- incident flux by species
- reflected flux from surface reactions (i.e. etch products)
- use surface cell files from icarus

waferxy2d:

- angular and energy distribution of incident particles (by species)
- information only for designated surfaces (storage limitations)
- output format is in pseudo-2D format
- use wafer files from icarus

stat2d:

- generate statistics between two output files (different iteration steps)
- quantify the rate of change of specific variables to indicate whether a converged solution has been attained.

example usage:

post2d cell.10000 file2
(file *cell.10000* from icarus, file *file2* created by post2d)

preplot file2

(Tecplot supplied file to create binary input file *file2.plt*)

tecplot file2.plt

(Tecplot graphics package for *file2.plt* data set)

Default output file format is Tecplot (commercial plotting package)

8.1 Macroscopic Cell Information (post2d)

Goal: -specify the output variables from the cell data file
 -re-order spatial coordinates
 -units conversion (i.e. pascals to mtorr, K to C, meters to cm or inches)

Usage: **post2d cell.* cellout**
 or **post2d chem.* chemout**
 or **post2d plasma.* plasmaout**

cell.:* output data file from **icarus** code -- for example *cell.40000*
*cellout:*output file in Tecplot format (requires preplot)

Other input files:

post2d.vlist (optional - will use default output variable list)
datap

Variables: -variables 1 - 14 are default in the *cell.** file (hardwired Variable Index number)
-'*' in column 1 signifies a comment

Variable Type	Variable Name
1	X or Z (first dimension-m)
2	Y or R (second dimension-m)
3	#/cell (average number of computational particles per cell)
4	number density (#/m ³)
5	pressure (pascals)
6	cell weight (icarus parameter)
7	velocity, first direction - V _x or V _z (m/s)
8	velocity, second direction - V _y or V _r (m/s)
9	Maxwellian translation temperature (K)
10	Maxwellian rotational temperature (K)
11	Maxwellian vibrational temperature (K)
12	average temperature (K)
13	cell Knudsen number (mfp / characteristic cell length)
14	cell CFL number (avg. velocity / cell length/dt)
15	Mean Free Path MFP (m)
5x	species x mole fraction
10x	species x velocity for first dimension (m/s)
20x	species x velocity for second dimension (m/s)
30x	species x average temperature (K)

Note: use the string, 'END', as the last variable name to avoid problems with extra lines at the end of the file.

Example *post2d.vlist* file

```
*  
* * in col 1 for comment or to comment out a line  
* specie number fractions are 5x where x is the specie #  
* specie velocities are in pairs of 10x and 20x for Vz and Vr  
*  
*Var. name(10 Char MAX) multi. factor Var. index  
X(m) 1. 1  
Y(m) 1. 2  
n 1. 4  
p(mtorr) 7.50075 5 convert Pa to mtorr  
Vx(m/s) 1. 7  
Vy(m/s) 1. 8  
Tt(k) 1. 9  
Kn 1. 13  
CFL 1. 14  
Ar 1. 51 species mole fract. inputs  
N2 1. 52  
Ti 1. 53  
*N 1. 54  
*Ar+ 1. 55  
*Sih4 1. 55  
Vx_Ar 1. 101 species Velocities  
Vy_Ar 1. 201  
Vx_N2 1. 102  
Vy_N2 1. 202  
*Vx_Ti 1. 103  
*Vy_Ti 1. 203  
*Vx_N 1. 104  
*Vy_N 1. 204  
*Vx_Ar+ 1. 105  
*Vy_Ar+ 1. 205  
t Ar 1.0 301 species temps.  
t N2 1.0 302 species temps.  
t Ti 1.0 303 species temps.  
END
```

8.2 Surface Information (surface2d)

Goal: Converts boundary cell information to surface fluxes and reactant fluxes (etchant flux).

Usage: **surface2d** *surf.* surfout*

interactive responses to region #, material #

(note: region #'s to plot and material #'s from *geometry.inp* file)

Other Input Files:

datap

Output Files:

surfout - Output file is in Tecplot format

Variables:			
1	X or Z	first dimension, X or Z (m)	
2	Y or R	second dimension, Y or R (m)	
3	P	surface pressure (pascals)	
4	shear	surface shear stress (N/m ²)	
5	qwall	surface heat flux (W/m ²)	
6	avg. hits	average number of particle-surface collisions per time step	
7	tot. hits	total number of particle-surface collision in sample	
7+1	I spec1	incident flux for species 1 (#/m ² -s)	
7+2	I spec2	incident flux for species 2 (#/m ² -s)	
7+i+1	R spec1	surface reaction flux for species 1 (#/m ² -s)	
7+i+2	R spec2	surface reaction flux for species 2 (#/m ² -s)	

Note: spec1 and spec2 will be replaced with their respective character strings from the *spec* file.

8.3 Wafer Information (waferxy2d)

Goal: Convert boundary wafer cell stats to incident angular and energy distributions.

Usage: **waferxy2d *wafer.** *waferout***

*wafer.** from **icarus** code (i.e. wafer.1000)

waferout in Tecplot format

(the surface cells designated as 'wafer' are defined in the **geometry.inp** file.)

Other Input Files:

datap

Variables:

1	first dimension, X or Z (m)
2	second dimension, Y or R (m)
3	delta angle increment, dAng (deg)
4	normalized angular distribution function for species 1 (A spec1)
5	normalized angular distribution function for species 2 (A spec2)
.	.
3+i	normalized angular distribution function for species i (A speci)
3+i+1	delta energy increment for species 1, del1 (eV) (dE spec1)
3+i+2	normalized energy distribution function for species i, eng1 (E spec1)

note: spec1, spec2, and speci will be replaced with their respective character strings from *spec* file

to plot normalized angular distributions:

select variable 3 for the x plot variable

select variable 4 - 3+i for the y plot variable

to plot normalized energy distributions:

select variable 3+i+1 for the x plot variable for species 1

select variable 3+i+2 for the y plot variable for species 1

Note: The reason for this data structure is that all species have the same angular increment for the angular distribution function (1 degree for axisymmetric systems and 2 degrees or cartesian). However, each species can have its own range of energy distribution function: 0 to X ev.

The output data is normalized by species for both the angular and energy distributions.

8.4 Cell Convergence Statistics (stat2d)

Usage: **stat2d** *cell.* cell.***

*cell.**: 2d tecplot binary of dsmc solution at time 1

*cell.***: 2d tecplot binary of dsmc solution at time 2

the order of file1 and file2 is not important.

Other input files:

post2d.vlist: for each variable in column 3 (third variable after variable name)

0- skip variable

1- obtain statistics for variable

note: if standard default *post2d.vlist* is used, no variables are marked

Output files:

stat.out - A text file with following info for each region and globally.

$\text{min}(\%)$ = percent change in the min value of a variable between solution planes.

$\text{max}(\%)$ = percent change in the max value of a variable between solution planes.

$\text{mean}(\%)$ = mean percent change in a variable between solution planes.

standard deviation = the standard deviation of the change in a variable between solution time planes.

stat.tec - A text file which can be read into tecplot. The *stat.tec* file allows the $\text{min}(\%)$, $\text{max}(\%)$, $\text{mean}(\%)$ and standard deviation of a variable to be plotted versus region number.

9. Install/Compile Software

9.1 Makefiles

The Icarus code and the utilities are in a directory structure under the directory, icarus.

./icarus/code	source code for Icarus (DSMC)
./icarus/util	source codes for utility programs: init2d, post2d,....
./icarus/bin	location of executables which makefiles create
./icarus/etc	shell scripts for running utility programs in a heterogeneous environment
./icarus/samples	sample problem files (see appendix B)
./icarus/documentation	postscript file of this document

To install the Icarus (DSMC) code:

cd ./icarus/code

make dsmc_sun (for SUN systems)

or

make dsmc_sgi (for SGI systems)

or

make dsmc_hp (for HP systems)

or

..... other systems found in the Makefile in ./icarus/code

the executable, icarus_sun (for Sun systems) will be found in ./icarus/bin.

To install the utility codes:

cd ./icarus/util

make sunV (for SUN Solaris)

or

make sunos (for SUN SUNOS)

or

make sgi (for SGI)

or

make hp (for HP -- requires ANSI C compiler for stat2d and some features of regrid)

All the executables, init2d_sunos, post2d_sunos, restart2d_sunos, ... will be found in ./icarus/bin

Supported Platforms:

Icarus: SUN, SGI, HP, IBMR6k, nCUBE, Paragon(OSF), Paragon(SUNMOS),
PVM for SUN and SGI

utils: SUN (SUNOS & Solaris), SGI, HP, IBMR6k

9.2 param.h and init2d.h files

Icarus does not use dynamic memory allocation for its arrays since parallel computers typically have defined memory resources per processor; a single program executable can be compiled for any number of processor configurations. The particular problem memory requirements are implemented via two parameter statement blocks: param.h for Icarus and most of the utility programs and init2d.h for the init2d code.

Note: Icarus and the utility programs will check for program limits write and respond with diagnostic messages.

param.h

example mp version of param.h

```
integer gmre,gcon,gmce,ggrd,gmob,gmse,gmss,gmmo,gpro,gbuf
integer gmnre,gmrea,gmpcm,gmtbp,gstat,gmwaf,gmtab
integer gmrx,movie,gmemrx,gmcp

parameter (gmre=10,ggrd=1000,gmse=500)
parameter (gmob=200,gmce=5000,gmcp=4000,gcon=500)
parameter (gmss=6,gmmo=40000)
parameter (gpro=1024,gbuf=800000)
parameter (gmnre=2,gmrea=23,gmpcm=2,gmtbp=4,gstat=9)
parameter (gmwaf=50,gmtab=5,gmrx=20)
parameter (movie=2,memrx=10)

integer lmce,lmmo,lmob

c  parameter (lmce=3510,lmmo=50000,lmob=250)
c  parameter (lmce=10000,lmmo=500000,lmob=200)

parameter (pi=3.1415926,eps=1.0E-5,maxk=5)
```

The parameters which start with 'g' are global and apply to all processors; those which start with an 'l' apply only to a single processor. For a single processor executable, the quantities with the 'l' are the total program limits and for a MP executable, the local cell requirements are dictated by the number of processors which are used (see the output from decomp2d).

typical values which may require adjustment (init2d output contains many of these quantities):

gmre	-max. number of grid regions
gmse	-max. number of surface elements
gmob	-max. number of outer boundary elements

gmce	-max. number of cells (for plasma option only -- for electrostatic fields)
gmcp	-max. number of grid corner points
gmss	-max. number of chemical species
gmrea	-max. number of chemical reactions
gmwaf	-max. number of 'wafer' surface elements
gmtab	-max. number of surface reaction tables
lmce	-max. number of local (or single processor) number of cells
lmmo	-max. number of local (or single processor) number of particles

init2d.h

example init2d.h (parameter section)

```

c
c   include for program init2d  version 6.0
c
parameter ( m13 = 201, m24 = 201, mnc = 500000,
1      mas = 100, mie = 5000, mntab = 4, mnrx=20,
2      mmi = 50, mnvt = 1, mdsp = 10,
3      mnre= 2, mob = 1300,
4      mpcm= 2, mrea = 23, msd = m13*2+m24*2,
5      mse = 5500, msp = 10, mtbp = 4,
6      mnr = 100, mac = 50,
7      meb = 2*(m13+m24-1)*mnr, mcpt = mnr * 4,
8      mcp = 2*mnc,          msce = mse,
9      mmp = 3, mccc = 2*mnc, mnb = 5000,
a      mng = (m13+m24+2), eps=1.e-6 )

```

character*130 title

typical values which may require adjustment:

m13	-max. number of grid lines along region side 1 or side 3 (number of cells + 1)
m24	-max. number of grid lines along region side 2 or side 4 (number of cells + 1)
mnc	-max. number of computational cells
mrea	-max. number of chemical reactions
mse	-max. number of surface elements
msp	-max. number of chemical species
mnr	-max. number of grid regions

9.3 shell scripts

Shell scripts for the various utility programs are found in `./icarus/etc`. There are three functions for these scripts:

- 1-script will check for particular platform in a heterogeneous system and execute the appropriate executable (i.e. `post2d file1 fileout` will automatically use `post2d_hp` for a HP system or `post2d_sunos` for a SUN system running SUNOS)
- 2-allow for multiple functions to be performed. For example, the `post2d` script executes both the `post2d` code and the graphics preprocessor, `preplot`.
- 3-to make all the user interfaces to the utility programs identical

9.4 PVM

Icarus was written for native data parallel communication calls for the nCUBE and Paragon systems. Icarus also uses the PVM interface for the IBM SP2, Cray, and workstation based parallel systems.

installation:

the files are distributed in a directory structure starting at `./pvm`---see the `pvm.doc` file

- 1- add these three env. variables to your `.cshrc` file
`PVM_ROOT` (i.e. `/local/pvm`)
`PVMBUFSIZE` (typically 4000000)
`PVM_ARCH` (i.e. SUN or SGI)
- 2- `cd ./pvm/pvm_utils`
`make` (to make the `xpvm` executable -- check `Makefile` for site specific routines)
- 3- `cd ./icarus/code`
`make icarus_sunpvm`, or `make icarus_sigpvm`, etc.....
- 4- `cd` application directory
-decompose the datap file from `init2d` using the number of processors and the option 2 decomposition scheme
-the input file for icarus MUST be called `icarus.inp` (PVM oddity)
-`cp` the `conf.pvm` file from `./pvm/pvm_utils` to the application directory
-`$PVM_ROOT/lib/pvmd conf.pvm & -----` start the PVM daemon
-`xpvm -d # filename & -----` start Icarus where # is the number of processors and filename is the icarus executable
- 5- type 'pvm' to check status of jobs
- 6- screen output will be written to `/tmp`

10. Miscellaneous Information

10.1 Important Relationships

Conversions:

$$1 \text{ Pascal (N/m}^2\text{)} = 7.50075 \text{ mtorr}$$

$$1 \text{ sccm} = 4.48 \cdot 10^{17} \text{ # molecules/s}$$

$$1 \text{ bar} = 10^5 \text{ Pa} = 0.9869 \text{ atm}$$

Sonic Orifice:

$$T^* = (2 / (\gamma + 1)) T_0$$

$$V^* = (\gamma R T^*)^{1/2}$$

where: T^* = temperature at sonic plane

V^* = velocity at sonic plane

T_0 = stagnation temperature

γ = ratio of specific heats (1.4 for air)

R = ideal gas constant

$$R = R/m$$

$$R = 8.3144 \text{ N-m/gmole-K}$$

m = molecular wt

(note: multiply by 1000 for MKS units, kg)

10.2 Chemical Species Database.

*Values from transport chemkin, origin of transport properties not clear

*Values include those from Bird's DSMC Book

*effective diameter calculated at 300 K.

*viscosity coefficient fit from (default @ 273-500 K). -- mu ~ T^s, where s =visc.index

* file created 19 Dec. 1994 -- J. E. Johannes - SNL

*Species	Charge	Atomic wt(Kg)	Molecular wt	Diameter (m)	visc index	Rot. Rel. Coll. #	# Rot.Deg. Freedom	Vib. Rel. Coll. #	Vib. Temp. (K)
AR	0.0	.6633E-25	39.95	.3555E-09	0.8100	5.0	0.0	0.0	0.
AS	0.0	.1244E-24	74.92	.7777E-09	0.8968	5.0	0.0	0.0	0.
AS2	0.0	.2488E-24	149.84	.9356E-09	0.8968	5.0	2.0	0.0	0.
ASH	0.0	.1261E-24	75.93	.4831E-09	0.8734	5.0	0.0	0.0	0.
ASH2	0.0	.1277E-24	76.94	.4945E-09	0.9107	5.0	0.0	0.0	0.
ASH3	0.0	.1294E-24	77.95	.5051E-09	0.9433	5.0	0.0	0.0	0.
C	0.0	.1994E-25	12.01	.3232E-09	0.6902	5.0	0.0	0.0	0.
C2	0.0	.3988E-25	24.02	.3678E-09	0.7246	5.0	2.0	0.0	0.
C2H	0.0	.4156E-25	25.03	.4748E-09	0.8855	5.0	0.0	0.0	0.
C2H2	0.0	.4323E-25	26.04	.4748E-09	0.8856	5.0	0.0	0.0	0.
C2H3	0.0	.4490E-25	27.05	.4748E-09	0.8856	5.0	0.0	0.0	0.
C2H4	0.0	.4658E-25	28.05	.4934E-09	0.9631	5.0	0.0	0.0	0.
C2H5	0.0	.4825E-25	29.06	.5204E-09	0.9349	5.0	0.0	0.0	0.
C2H6	0.0	.4993E-25	30.07	.5204E-09	0.9349	5.0	0.0	0.0	0.
C2N	0.0	.6314E-25	38.03	.4541E-09	0.9138	5.0	0.0	0.0	0.
C2N2	0.0	.8639E-25	52.04	.5733E-09	1.0077	5.0	0.0	0.0	0.
C2O	0.0	.6645E-25	40.02	.4541E-09	0.9137	5.0	0.0	0.0	0.
C3H2	0.0	.6317E-25	38.05	.4748E-09	0.8855	5.0	0.0	0.0	0.
C3H2(S)	0.0	.6317E-25	38.05	.4748E-09	0.8855	5.0	0.0	0.0	0.
C3H4	0.0	.6652E-25	40.07	.5756E-09	0.9346	5.0	0.0	0.0	0.
C3H4P	0.0	.6652E-25	40.07	.5756E-09	0.9346	5.0	0.0	0.0	0.
C3H6	0.0	.6987E-25	42.08	.6111E-09	0.9500	5.0	0.0	0.0	0.
C3H8	0.0	.7321E-25	44.10	.6108E-09	0.9469	5.0	0.0	0.0	0.
C4H	0.0	.8144E-25	49.05	.6858E-09	1.0234	5.0	0.0	0.0	0.
C4H2	0.0	.8312E-25	50.06	.6858E-09	1.0235	5.0	0.0	0.0	0.
C4H6	0.0	.8981E-25	54.09	.6851E-09	1.0118	5.0	0.0	0.0	0.
C4H8	0.0	.9316E-25	56.11	.6852E-09	1.0234	5.0	0.0	0.0	0.
C5H2	0.0	.1031E-24	62.07	.6858E-09	1.0235	5.0	0.0	0.0	0.
C5H5	0.0	.1081E-24	65.10	.6858E-09	1.0235	5.0	0.0	0.0	0.
C6H2	0.0	.1230E-24	74.08	.6858E-09	1.0235	5.0	0.0	0.0	0.
C6H5	0.0	.1280E-24	77.11	.7367E-09	1.0526	5.0	0.0	0.0	0.
C6H5(L)	0.0	.1280E-24	77.11	.7367E-09	1.0526	5.0	0.0	0.0	0.
C6H5O	0.0	.1546E-24	93.11	.7760E-09	1.0658	5.0	0.0	0.0	0.
C6H6	0.0	.1297E-24	78.11	.7367E-09	1.0526	5.0	0.0	0.0	0.
C6H7	0.0	.1314E-24	79.12	.7367E-09	1.0525	5.0	0.0	0.0	0.
CH	0.0	.2162E-25	13.02	.2726E-09	0.6933	5.0	2.0	0.0	0.
CH2	0.0	.2329E-25	14.03	.4087E-09	0.7845	5.0	0.0	0.0	0.
CH2(S)	0.0	.2329E-25	14.03	.4087E-09	0.7845	5.0	0.0	0.	0.0
CH2CHCCH	0.0	.8646E-25	52.08	.6858E-09	1.0235	5.0	0.0	0.0	0.

CH2CHCCH2	0.0	.8814E-25	53.08	.6858E-09	1.0235	5.0	0.0	0.0	0.
CH2CHCH2	0.0	.6819E-25	41.07	.5907E-09	0.9392	5.0	0.0	0.0	0.
CH2CHCHCH	0.0	.8814E-25	53.08	.6858E-09	1.0235	5.0	0.0	0.0	0.
CH2(CH)2CH2	0.0	.8981E-25	54.09	.6858E-09	1.0235	5.0	0.0	0.0	0.
CH2CO	0.0	.6980E-25	42.04	.5553E-09	1.0614	5.0	0.0	0.0	0.
CH2O	0.0	.4985E-25	30.03	.5206E-09	1.0747	5.0	0.0	0.0	0.
CH2OH	0.0	.5153E-25	31.03	.5164E-09	1.0386	5.0	0.0	0.0	0.
CH3	0.0	.2496E-25	15.04	.4093E-09	0.7969	5.0	0.0	0.0	0.
CH3CC	0.0	.6485E-25	39.06	.5756E-09	0.9345	5.0	0.0	0.0	0.
CH3CCCH2	0.0	.8814E-25	53.08	.6851E-09	1.0118	5.0	0.0	0.0	0.
CH3CCCH3	0.0	.8981E-25	54.09	.6851E-09	1.0118	5.0	0.0	0.0	0.
CH3CCH2	0.0	.6819E-25	41.07	.5911E-09	0.9435	5.0	0.0	0.0	0.
CH3CH2CCH	0.0	.8981E-25	54.09	.6851E-09	1.0118	5.0	0.0	0.0	0.
CH3CHCH	0.0	.6819E-25	41.07	.5911E-09	0.9435	5.0	0.0	0.0	0.
CH3CO	0.0	.7147E-25	43.05	.5539E-09	1.0353	5.0	0.0	0.0	0.
CH3O	0.0	.5153E-25	31.03	.5150E-09	1.0120	5.0	0.0	0.0	0.
CH3OH	0.0	.5320E-25	32.04	.5194E-09	1.0386	5.0	0.0	0.0	0.
CH4	0.0	.2664E-25	16.04	.4022E-09	0.8400	5.0	0.0	0.0	0.
CL	0.0	.5886E-25	35.45	.3831E-09	0.7762	5.0	0.0	0.0	0.
CL+	1.0	.5886E-25	35.45	.3831E-09	0.7762	5.0	0.0	0.0	0.
CL-	-1.0	.5886E-25	35.45	.3831E-09	0.7762	5.0	0.0	0.0	0.
CL2+	1.0	.1177E-25	70.91	.5405E-09	1.0100	5.0	2.0	0.0	0.
CL2	0.0	.1177E-24	70.91	.5405E-09	1.0100	5.0	2.0	0.0	0.
CN	0.0	.4320E-25	26.02	.3798E-09	0.6942	5.0	2.0	0.0	0.
CNN	0.0	.6645E-25	40.02	.4541E-09	0.9138	5.0	0.0	0.0	0.
CO	0.0	.4651E-25	28.01	.3710E-09	0.7254	5.0	2.0	0.0	0.
CO2	0.0	.7307E-25	44.01	.4516E-09	0.9264	5.0	0.0	0.0	0.
E	0.0	.9049E-30	0.00	.6941E-07	0.9523	5.0	0.0	0.0	0.
F	0.0	.3154E-25	19.00	.2728E-09	0.7005	5.0	0.0	0.0	0.
F2	0.0	.6309E-25	38.00	.3477E-09	0.7680	5.0	2.0	0.0	0.
GA	0.0	.1158E-24	69.72	.9372E-09	0.8264	5.0	0.0	0.0	0.
GAH	0.0	.1174E-24	70.73	.5515E-09	1.0002	5.0	2.0	0.0	0.
GAME	0.0	.1407E-24	84.76	.8246E-09	0.9151	5.0	0.0	0.0	0.
GAME2	0.0	.1657E-24	99.79	.8123E-09	1.0043	5.0	0.0	0.0	0.
GAME3	0.0	.1906E-24	114.83	.7414E-09	1.0208	5.0	0.0	0.0	0.
H	0.0	.1674E-26	1.01	.2211E-09	0.7984	5.0	0.0	0.0	0.
H2	0.0	.3347E-26	2.02	.2701E-09	0.6700	5.0	2.0	0.0	0.
H2C4O	0.0	.1097E-24	66.06	.6851E-09	1.0118	5.0	0.0	0.0	0.
H2CCC	0.0	.6317E-25	38.05	.4748E-09	0.8855	5.0	0.0	0.0	0.
H2CCC(S)	0.0	.6317E-25	38.05	.4748E-09	0.8855	5.0	0.0	0.0	0.
H2CCCCH	0.0	.1047E-24	63.08	.6851E-09	1.0118	5.0	0.0	0.0	0.
H2CCCCH	0.0	.8479E-25	51.07	.6851E-09	1.0118	5.0	0.0	0.0	0.
H2CCCCH2	0.0	.8646E-25	52.08	.6851E-09	1.0119	5.0	0.0	0.0	0.
H2CCCH	0.0	.6485E-25	39.06	.5756E-09	0.9345	5.0	0.0	0.0	0.
H2CN	0.0	.4654E-25	28.03	.5424E-09	1.0303	5.0	0.0	0.0	0.
H2NO	0.0	.5317E-25	32.02	.3636E-09	0.7535	5.0	0.0	0.0	0.
H2O	0.0	.2991E-25	18.02	.4387E-09	1.0855	5.0	0.0	0.0	0.
H2O2	0.0	.5647E-25	34.01	.3555E-09	0.7310	5.0	0.0	0.0	0.
H2S	0.0	.5658E-25	34.08	.4551E-09	0.9799	5.0	0.0	0.0	0.
H2SISIH2	0.0	.9996E-25	60.20	.5875E-09	0.9862	5.0	0.0	0.0	0.

H3SISIH	0.0	.9996E-25	60.20	.5875E-09	0.9862	5.0	0.0	0.0	0.
HCCCHCCH	0.0	.1047E-24	63.08	.6858E-09	1.0235	5.0	0.0	0.0	0.
HCCHCC	0.0	.8479E-25	51.07	.6858E-09	1.0235	5.0	0.0	0.0	0.
HCCO	0.0	.6812E-25	41.03	.2707E-09	0.7924	5.0	0.0	0.0	0.
HCCOH	0.0	.6980E-25	42.04	.5553E-09	1.0614	5.0	0.0	0.0	0.
HCL	0.0	.6054E-25	36.46	.4396E-09	0.9953	5.0	2.0	0.0	0.
HCN	0.0	.4487E-25	27.03	.5452E-09	1.0774	5.0	0.0	0.0	0.
HCNO	0.0	.7143E-25	43.03	.4537E-09	0.9067	5.0	0.0	0.0	0.
HCO	0.0	.4818E-25	29.02	.5206E-09	1.0747	5.0	0.0	0.0	0.
HCO+	1.0	.4818E-25	29.02	.5206E-09	1.0748	5.0	0.0	0.0	0.
HE	0.0	.6646E-26	4.00	.2157E-09	0.6330	5.0	0.0	0.0	0.
HF	0.0	.3322E-25	20.01	.4598E-09	1.0871	5.0	2.0	0.0	0.
HNCO	0.0	.7143E-25	43.03	.4537E-09	0.9067	5.0	0.0	0.0	0.
HNNO	0.0	.7475E-25	45.02	.4537E-09	0.9067	5.0	0.0	0.0	0.
HNO	0.0	.5149E-25	31.01	.3632E-09	0.7437	5.0	0.0	0.0	0.
HNOH	0.0	.5317E-25	32.02	.3632E-09	0.7437	5.0	0.0	0.0	0.
HO2	0.0	.5480E-25	33.01	.3555E-09	0.7311	5.0	0.0	0.0	0.
HOCHN	0.0	.7143E-25	43.03	.4537E-09	0.9067	5.0	0.0	0.0	0.
He	0.0	.3340E-26	4.02	.2333E-09	0.6600	5.0	0.0	0.0	0.
I*C3H7	0.0	.7154E-25	43.09	.6111E-09	0.9500	5.0	0.0	0.0	0.
K	0.0	.6492E-25	39.10	.6944E-09	0.9523	5.0	0.0	0.0	0.
K+	1.0	.6492E-25	39.10	.6944E-09	0.9523	5.0	0.0	0.0	0.
KCL	0.0	.1238E-24	74.56	.7964E-09	0.8441	5.0	2.0	0.0	0.
KH	0.0	.6659E-25	40.11	.3578E-09	0.7186	5.0	2.0	0.0	0.
KO	0.0	.9148E-25	55.10	.5137E-09	1.0227	5.0	2.0	0.0	0.
KOH	0.0	.9316E-25	56.11	.7879E-09	0.8647	5.0	2.0	0.0	0.
Kr	0.0	.1391E-24	83.80	.4760E-09	0.8000	5.0	0.0	0.0	0.
N	0.0	.2326E-25	14.01	.3229E-09	0.6825	5.0	0.0	0.0	0.
N*C3H7	0.0	.7154E-25	43.09	.6108E-09	0.9469	5.0	0.0	0.0	0.
N2	0.0	.4651E-25	28.01	.3675E-09	0.7400	5.0	2.0	0.0	0.
N2H2	0.0	.4986E-25	30.03	.3718E-09	0.6825	5.0	0.0	0.0	0.
N2H3	0.0	.5153E-25	31.04	.4469E-09	0.8645	5.0	0.0	0.0	0.
N2H4	0.0	.5320E-25	32.05	.4872E-09	0.8711	5.0	0.0	0.0	0.
N2O	0.0	.7307E-25	44.01	.4537E-09	0.9067	5.0	0.0	0.0	0.
NCN	0.0	.6645E-25	40.02	.4541E-09	0.9139	5.0	0.0	0.0	0.
NCO	0.0	.6976E-25	42.02	.4541E-09	0.9139	5.0	0.0	0.0	0.
NH	0.0	.2493E-25	15.01	.2628E-09	0.6989	5.0	2.0	0.0	0.
NH2	0.0	.2660E-25	16.02	.2628E-09	0.6988	5.0	0.0	0.0	0.
NH3	0.0	.2828E-25	17.03	.4290E-09	1.1000	5.0	0.0	0.0	0.
NNH	0.0	.4818E-25	29.02	.3721E-09	0.6886	5.0	0.0	0.0	0.
NO	0.0	.4982E-25	30.01	.3678E-09	0.7900	5.0	2.0	0.0	0.
NO2	0.0	.7638E-25	46.01	.4014E-09	0.8733	5.0	0.0	0.0	0.
Ne	0.0	.3350E-25	20.80	.2770E-09	0.6600	5.0	0.0	0.0	0.
O	0.0	.2656E-25	16.00	.2727E-09	0.6989	5.0	0.0	0.0	0.
O2	0.0	.5313E-25	32.00	.3558E-09	0.7700	5.0	2.0	0.0	0.
O3	0.0	.7969E-25	48.00	.4601E-09	0.8455	5.0	0.0	0.0	0.
OH	0.0	.2824E-25	17.01	.2727E-09	0.6988	5.0	2.0	0.0	0.
S	0.0	.5324E-25	32.06	.6273E-09	0.9600	5.0	0.0	0.0	0.
S2	0.0	.1065E-24	64.13	.6373E-09	0.9600	5.0	2.0	0.0	0.
SH	0.0	.5491E-25	33.07	.6373E-09	0.9600	5.0	2.0	0.0	0.

SI	0.0	.4663E-25	28.09	.5923E-09	0.8241	5.0	2.0	0.0	0.
SI2	0.0	.9326E-25	56.17	.6676E-09	0.8241	5.0	2.0	0.0	0.
SI2H2	0.0	.9661E-25	58.19	.5651E-09	0.9974	5.0	0.0	0.0	0.
SI2H3	0.0	.9828E-25	59.20	.5768E-09	0.9937	5.0	0.0	0.0	0.
SI2H5	0.0	.1016E-24	61.21	.5997E-09	0.9856	5.0	0.0	0.0	0.
SI2H6	0.0	.1033E-24	62.22	.6109E-09	0.9814	5.0	0.0	0.0	0.
SI3	0.0	.1399E-24	84.26	.7225E-09	0.8241	5.0	0.0	0.0	0.
SI3H8	0.0	.1533E-24	92.32	.7210E-09	0.9975	5.0	0.0	0.0	0.
SICL2	0.0	.1647E-24	98.00	.8000E-09	0.8386	5.0	2.0	0.0	0.
SICL4	0.0	.2821E-24	169.90	.5428E-09	0.8363	5.0	0.0	0.0	0.
SIF3	0.0	.1413E-24	85.08	.5554E-09	0.9876	5.0	0.0	0.0	0.
SIF3NH2	0.0	.1679E-24	101.10	.5894E-09	0.9122	5.0	0.0	0.0	0.
SIF4	0.0	.1728E-24	104.08	.5428E-09	0.8363	5.0	0.0	0.0	0.
SIH	0.0	.4830E-25	29.09	.3711E-09	0.7206	5.0	0.0	0.0	0.
SIH2	0.0	.4998E-25	30.10	.4041E-09	0.7776	5.0	0.0	0.0	0.
SIH3	0.0	.5165E-25	31.11	.4377E-09	0.8320	5.0	0.0	0.0	0.
SIH4	0.0	.5333E-25	32.12	.4722E-09	0.8826	5.0	0.0	0.0	0.
SIHF3	0.0	.1429E-24	86.09	.5258E-09	0.8485	5.0	0.0	0.0	0.
SO	0.0	.7980E-25	48.06	.5051E-09	0.9811	5.0	2.0	0.0	0.
SO2	0.0	.1064E-24	64.06	.5188E-09	1.0500	5.0	0.0	0.0	0.
SO3	0.0	.1329E-24	80.06	.5611E-09	1.0261	5.0	0.0	0.0	0.
Xe	0.0	.2180E-24	131.29	.5740E-09	0.8500	5.0	0.0	0.0	0.

Appendices

A ---- Cited References & Papers

B ---- Sample Problems

A References

- 1 Bird, G. A., **Molecular Gas Dynamics and the Direct Simulation of Gas Flows**, Clarendon Press - Oxford, 1994.
- 2 Borgnakke, C. and P. S. Larsen, Statistical collision model for Monte Carlo simulation of polyatomic gas mixtures, *J. Comp. Phys.*, 18, 405-420 (1975).
- 3 Hermina, W. L., "Monte Carlo Simulation of Transitional Flow Around Simple Shaped Bodies", Proceedings of the 15th International Symp. on Rarefied Gas Dynamics, Vol. I, pp. 451-460 (1986).

Papers

Bartel, T.J. and Plimpton, S.J., "DSMC Simulation of Rarefied Gas Dynamics on a Large Hypercube Supercomputer", AIAA 92-2860, 1992.

Bartel, T.J. and Justiz, C.R., "DSMC Simulation of Ionized Rarefied Flows", AIAA 93-3095, 1993.

Bartel, T.J., Sterk, T.M., Payne, J.L., and Preppernau, B., "DSMC Simulation of Nozzle Expansion Flow Fields", AIAA 94-2047, 1994.

Bartel, T.J., "Low Density Gas Modelling in the Microelectronics Industry", 19th International Symp. on Rarefied Gas Dynamics-1994, Oxford University Press, 1995.

Bartel, T.J. and Economou, D.J., "Modelling of Plasma Etching Discharges", invited paper to AVS Conference, Denver 1994, in progress.

Shufflebotham, P.K., Bartel, T.J., Berney, B., "Experimental validation of a direct simulation by Monte Carlo molecular gas flow model, *J. Vac. Sci. Technol. B* 13(4), Jul/Aug 1995.



AIAA 92-2860

**DSMC Simulation of
Rarefied Gas Dynamics on a
Large Hypercube Supercomputer**

T. J. Bartel and S. J. Plimpton
Sandia National Labs.
Albuquerque, NM

AIAA 27th Thermophysics Conference
July 6-8, 1992 / Nashville, TN

DSMC Simulation of Rarefied Gas Dynamics on a Large Hypercube Supercomputer

Timothy J. Bartel* and Steven J. Plimpton

Sandia National Laboratories, Albuquerque NM, USA
(tjbarte@cfd.sandia.gov, sjplimp@cs.sandia.gov)

Abstract

Direct Simulation Monte Carlo is a well-established technique for modeling low density fluid flows. The parallel implementation of a general simulation tool which allows for body-fitted grids, particle weighting, and a variety of surface and flow chemistry models is described. We compare its performance on a 1024-node nCUBE 2 to a serial version for the CRAY Y/MP with two test geometries and a range of Knudsen number from near continuum to free molecular. Speedups compared to a single processor of the Y/MP range from 5x to 30x. Experience with several static load-balancing strategies are also discussed. This is a critical issue since density fluctuations can create orders-of-magnitude differences in computational loads as the simulation progresses.

1. Introduction

When modeling flow in a simulation geometry, the transport terms in the Navier-Stokes equations for continuum flow begin to break down at very low densities. The physical reason is that the linear transport relationships for mass diffusion, viscosity, and thermal conductivity are no longer valid when the distance particles move between collisions is comparable to length scales of interest. This is a characteristic of flows with a Knudsen number (ratio of mean-free path to a length scale) on the order of 0.2. A commonly used method for modeling such flows is via particle simulation on a grid - a technique known as Direct Simulation Monte Carlo (DSMC), pioneered by Bird¹. It has utility in aerospace applications (upper-atmosphere flows for hypersonic cruise vehicles, re-entry vehicles, rocket plumes, etc.) and in vacuum-related technologies for the semiconductor industry (modeling plasma etching or chemical vapor deposition).

The key concept in DSMC is that particle motion is decoupled from particle collisions. That is, during a time step particles move through the grid independent of each other. At the end of the time step, the particles in the grid cell are sampled to obtain collision partners which are collided with probabilistic techniques to ob-

tain the velocity and species distributions. An attractive feature of DSMC is that complex gas and surface chemistry can be done straightforwardly as particles of different species collide with each other and with objects in the simulation geometry.

Large-scale DSMC computations on current supercomputers can easily be in the 10^6 particles, 10^4 grid cells, and thousands of time step range. However, the large computational resources required has limited the use of DSMC for many applications. The method lends itself to a code which is heavily scalar. This is evident in the timing comparisons obtained from several different computer platforms for the method as shown in Table 1. The relatively poor performance of the advanced workstations is due to the fact that the method is not easily amenable to superscalar or piped computer architectures. The Intel, Sparc2 and nCUBE cpu chips (see Table 1) are the basic building blocks for several MIMD parallel computer systems.

Table 1: Scalar DSMC Benchmarks

Computer	normalized time
Cray Y/MP (1 p)	1.0
IBM 6000/520	1.5
Sun Sparc10 (40 Mhz)	1.8
HP 9000/720	2.2
Sun Sparc2	3.0
Intel i860 (40 Mhz)	3.6
SGI 330 (1 p)	4.2
Sun Sparc1	10.
nCUBE-2 (1 p)	12.

Researchers have made efforts to speed these computations for vector supercomputers.^{2,3} Typically, the codes have been very complex and have lacked some of the collision physics found in the scalar versions. However, the DSMC method in principle is a good match for MIMD parallel computers because many of the computations associated with finding particles on a complex grid and performing probabilistic chemistry and collisions, which do not vectorize well, can be distributed among several processors since the particle motion is

* Senior Member AIAA

decoupled from collisions. Several investigators have developed parallel implementations of the DSMC method.^{4,5,6,15} Reference [5] is particularly notable because it showed scalable speed-up can be obtained on a parallel machine and also incorporated a dynamic load-balancing scheme whereby grid cells are reapportioned between processors. Reference [6] also incorporated an adaptive load-balancing scheme for a regular 2-D grid. All of these methods were for simulations performed on a regular mesh which greatly simplifies the problem of moving and locating particles on the grid and (for the parallel case) also simplifies the dynamic load balancing problem.

In this work, we describe our parallel implementation of the DSMC technique with very general capabilities. Specifically the code has a flexible gridding algorithm and includes the general multiple-specie chemistry model found in previous scalar implementations. In the next sections we discuss the features of our DSMC code, its performance on the nCUBE 2 parallel supercomputer, and the issues of static and dynamic load balancing using different grid-partitioning algorithms.

2. nCUBE MIMD Computer

The nCUBE 2 parallel supercomputer has 1024 nodes, each with a 1-2 megaflop floating point processor and 4 MB of memory (4 GB total). The nodes are interconnected in a hypercube topology with each node directly connected to 10 other nodes ($2^{10} = 1024$) in the hypercube. The nCUBE is a multiple-instruction/multiple-data (MIMD) parallel machine; that is, each processor stores its own copy of the executable program and can operate on its local data independently of all the other processors. This is important for the DSMC simulation described here since completely different physics routines may be executed for different molecules depending on where they are in the simulation geometry and their interactions with other molecules. The nCUBE is programmed in standard F77 (or C) and calls are made to message passing libraries to exchange information between processors (e.g. send molecules to another cell).

3. DSMC-MP Code

A. Grid Characteristics

Our implementation of the DSMC technique employs body-fitted, multi-region grids such as that illustrated in Figure 1. The grid is composed of adjoining regions; figure 1 has seven such regions. Each region is constructed of curved and/or straight lines of variable spacing which may be body-fitted to a surface. Therefore the surface is uniquely determined. A singular correspondence between cell faces of adjoining regions is not required. The cells in region 1 in the figure have both

curved and straight sides; the code retains this cell description in determining the particle position and does not simply use line segments. This has greatly minimized the problem of *losing* particles at curved region boundaries when the opposite cell faces do not share the same corner points.

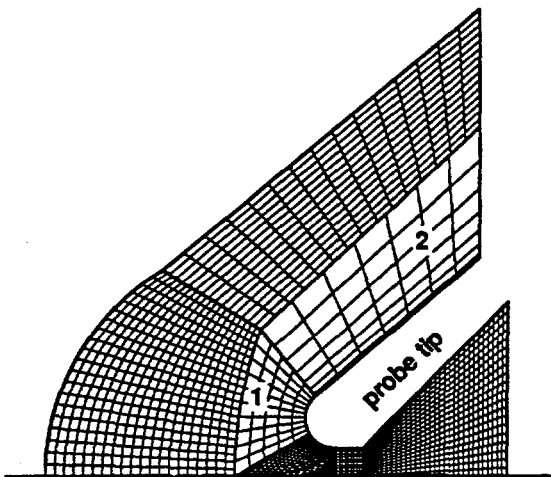


Figure 1-Multi-region grid for a 2-D, axisymmetric probe tip. Coarse cell spacing in regions 1 and 2 for purposes of illustration only.

There are trade-offs when using this type of mesh as compared with either an analytical description of the grid or an orthogonal mesh system. The first reason we adopted this strategy was to uniquely define the body surface irrespective of the number of mesh cells. Methods which use localized refinement based on orthogonal meshes tend to alter the surface description when the mesh is refined further. The next reason was to allow each processor to have the complete geometry description. This allowed the processor to be able to determine the cell number after a molecule move, irrespective of whether the processor *owned* that final cell. Figure 2 illustrates a possible particle-surface interaction: the entire trajectory of the particle during the time step including the surface interaction and movement through the different regions is performed by the processor which *owned* the initial cell. This greatly reduced the communication overhead during the molecule move portion of the algorithm. The final reason was to allow complex geometries to be easily gridded; the multi-block approach easily allows for grids to be quickly obtained for complex shapes as shown in figure 1 and as used in numerous continuum CFD applications. Clustering of the mesh lines in a region, as illustrated by region 2 in figure 1, allows the local grid size to be less than the local mean-free-path so that the computational domain is efficiently subdivided.

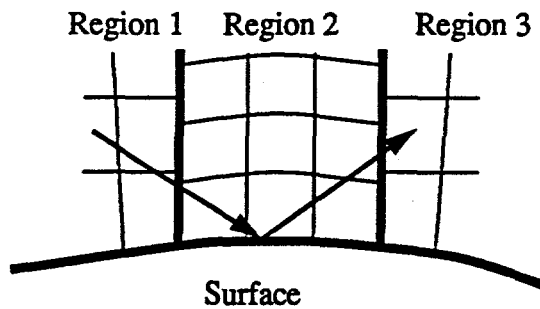


Figure 2-Possible particle move and surface interaction during a time step.

Since each processor of the nCUBE-2 has only 4MB of memory, memory management of the grid description is a critical issue when each processor is required to have the complete grid description. Since this simulation tool will be extended to 3-D, we have developed a novel, compact, grid algorithm. Our approach stores the equations which determine the mesh lines/curves on a region basis rather than the cell coordinates. For example, the grid description for region 2 in figure 1 is composed of 16 lines; a typical region would have many more cells as illustrated in this figure. This compact technique for storing the grid information also allows for a very fast move algorithm since determining which *side* of the line a particle is on is a simple operation. This new method can be easily extended to 3-D by using the equations for a plane rather than for a 2-D curve. No restrictions are placed on the cell boundaries at a region interface allowing several cells on one side of the interface to share the same cell face on the other side. A ray tracing algorithm is used to determine into which cell the particle moves when entering a new region. This computationally expensive operation is required only for those particles moving between regions.

B. Particle Weights and Time Steps

Spatial particle weighting, either by cell or region is used in our DSMC code. That is, all simulation particles in a cell have the same value of the weight function. This simplifies the chemistry physics since each particle represents the same number of actual molecules for all species. We have found that using a cell weight which is proportional to its normalized volume has been a good initial value. An algorithm is used to modify the cell weight as the solution progresses limiting the number of particles in a cell; molecules are probabilistically deleted such that the species distribution is preserved. This method allows high density areas of the simulation domain to be modelled with a reasonable number of particles. This is important for both the efficiency of the simulation and also to ensure that the local memory of a processor is not exceeded during the simulation.

A single time step is used for all the cells in a given region; a no-time-counter (NTC) method developed by Hermina⁷ is used to determine the number of collisions based on a given time step. This strategy either allows for time accurate simulations where all regions have the same time step or for accelerated convergence where each region's time step meets the local CFL condition. This condition limits the time step to be less than the transient time of the particle through the cell.

C. Collision and Chemistry Models

The Larsen-Borgnakke model⁸ is used to model the energy transfer between translation and rotational energy modes during an inelastic collision. Presently, this code is restricted to modelling neutral particles and uses the standard 23 chemical reaction model for air¹⁴. The chemistry has been modelled such that when a disassociation event occurs, the resultant third particle is immediately available as a potential collision partner during the remainder of the time step.

D. Load Balancing

DSMC simulations are typically of steady-state flows which may have density variations of many orders of magnitude; additionally, in the transient phase of the simulation, density fluctuations are large since the calculation begins with an uniform freestream density distribution. Since it is often difficult to predict *a priori* which cells will have a high computational load even for the steady-state regime, load-balancing is a serious problem for a parallel implementation if high efficiency is desired. Several static cell-wise decomposition strategies have been evaluated in the current work. These schemes distribute the cells in the computational domain to the processors at the start of the simulation; the processor *owns* them for the entire calculation.

We have had the best success thus far with a static scattered decomposition scheme, where each processor is assigned an equal number cells which are scattered across the simulation domain. On average, each processor will own some cells with many particles and some with few, so that a rough load balancing is achieved for even the dynamically changing balance of work among the cells. This decomposition scheme has proven to work better (by a factor of 1.5-2x) than schemes that allocate a *block* of cells to a processor. This is because a *block* in the wake or free stream regions of a vehicle will have much less work to do than a *block* near the stagnation region. The drawback of the scattered decomposition method is that it maximizes communication since the processor will not typically own any of the cells adjacent to one of its owned cells and hence many particles will have to be exchanged at every time step.

In contrast, the advantage of a load-balancing scheme that assigns *blocks* of cells to each processor is that it

does, in fact, minimize the communication for this simulation (by minimizing the surface/volume ratio). Examples of such load-balancers that we have tried include the heuristic Kernighan/Lin graph bisectioner⁹ and the newly developed spectral techniques^{10,11,12}. The spectral methods, which partition the cells by finding an eigenvalue of a matrix associated with the mesh topology, are particularly attractive for this problem because they can be readily parallelized (because the computational kernel in the Lanczos eigenvalue calculation is a sparse matrix-vector multiply). However, we have not yet been able to use the spectral technique for the DSMC problem because it does not provide for a *weighted* decomposition (by particle numbers or computational load in a cell) so that a smaller *block* of computationally-intense cells can be given to some processors and a larger *block* of few-particle cells to others. Research on such an enhancement to the spectral technique is being worked on at Sandia¹³ and we plan to eventually use it in our DSMC simulation to achieve both a computational load-balance and to minimize the communication of particles between processors.

However, it is clear that whichever scheme is used to determine the initial decomposition, an adaptive method based on the local processor load will be needed to achieve optimal load balancing. Periodically during the simulation, the processor computational load would be equalized by adjusting which processor *owns* a certain cell. Since the grid geometry is global to all processors, only information unique to a cell needs to be communicated. The multi-block, general grid structure used in the current code makes this a more difficult problem than methods used for a regular grid structure^{5,6}.

4. Results

Two geometries were used to compare the results from the nCUBE and Cray computers: a sphere and a sphere-cone re-entry vehicle. Various freestream and grid parameters for these calculations are given in Table 2. Three cases were considered for the sphere-cone to evaluate the load balancing as a function of the flow

Table 2: Test Conditions for Sample Calculations

	sphere	sphere-cone_80a	sphere-cone_80b	sphere-cone_100
# cells	2500	4711	4011	4011
# particles	35,000	255,000	80,000	250,000
freestream V_∞ (m/s)	7500.	7500.	7500.	7500.
freestream n_∞ (#/ m^3)	4.2e+20	4.16e+20	4.16e+20	1.2e+19
equivalent alt. (km)	80	80	80	100
Knudsen Number (λ/D)	0.0044	0.173	0.173	5.6

physics and number of simulation particles. All calculations were run axisymmetric-2D with 5 species, 23 chemical reactions, and inelastic collisions with rotation and vibration energy modes. Also, only a static decomposition was used for these calculation: there was no adaptive load balancing.

The new move algorithm was approximately 50% faster than the previous method based on tracking a particle on a cell-by-cell basis and had a much smaller storage requirement.

A. Sphere

A sphere of radius 0.5 m was used to test the speedup characteristics as a function on number of processors on the nCUBE. Figure 3 shows the grid for this series of cases as well as a contour plot of the relative number density for the input conditions. Of importance is that the shock is quite narrow; this means that relatively few cells will be performing the bulk of the work. A single region composed of curved and straight lines was used.

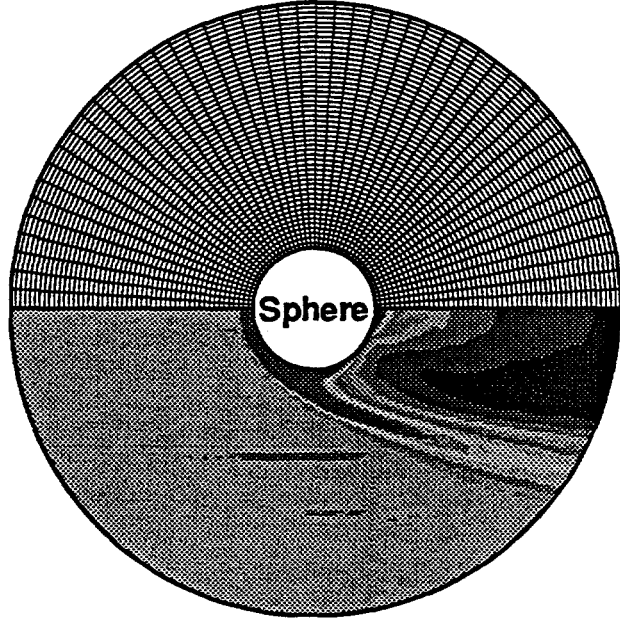


Fig. 3 - Grid and number density contour for the sphere.

Figure 4. shows the speedup ratios, to a single processor Cray Y/MP, for 32, 64, 128, and 256 processors of the nCUBE. The speedup is linearly increasing with the smaller hypercube configuration and rolls over at the larger one. This is because the sphere problem is relatively small in the number of cells and simulation particles. Communication overhead and load imbalance caused the turn over for this problem. Again, from figure 3, most of the cells are either freestream ones with little collisions or chemistry or in the wake with few particles; there are only a few cells with many particles, many collisions, and chemistry.

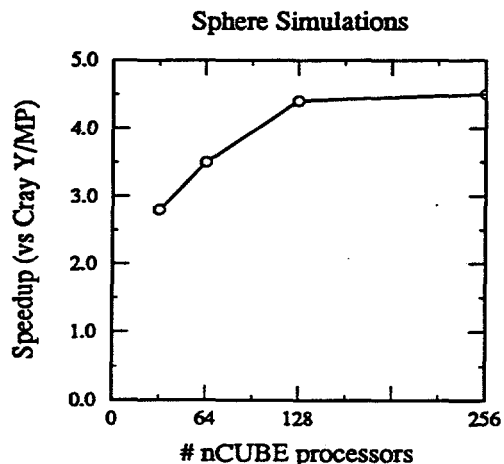


Figure 4 - Speedup ratios for sphere calculations

B. Sphere-Cone

Several calculations were performed for 2 freestream conditions corresponding to an altitude of 80 and 100 km for a sphere-cone re-entry vehicle geometry with a nose diameter of 0.0254m. Table 2 tabulates the conditions. Figure 5 shows a typical grid for these calculations as well as a contour plot for the relative number density for the 80b calculation. The grid contained 16 regions. One will note that many more cells are in the bow shock region in this calculation than were in the previous sphere calculation; therefore, more efficient load balancing would be expected.

Table 3 shows the relative speedup results for these calculations compared to a single processor of a Cray Y/MP. The actual cpu time for the 100-512 run on the nCUBE was 2140 s. The first three results were for a 256 node nCUBE configuration and the last for a 512 node configuration. The speedups for these calculation are much higher than for the sphere results. This is in part because of better load balancing due to more cells with high computational load. Also, these sphere-cone calculations were much larger with approximately twice the number of cells and many more simulation molecules. Large problems are required to efficiently utilize massively parallel computers. This problem size trend is also illustrated by the sphere-cone results for the 80a and 80b calculations. Calculation 80a has 3.2 times the number of simulation particles than calculation 80b; this reduced the load imbalance since all processors had more work to perform.

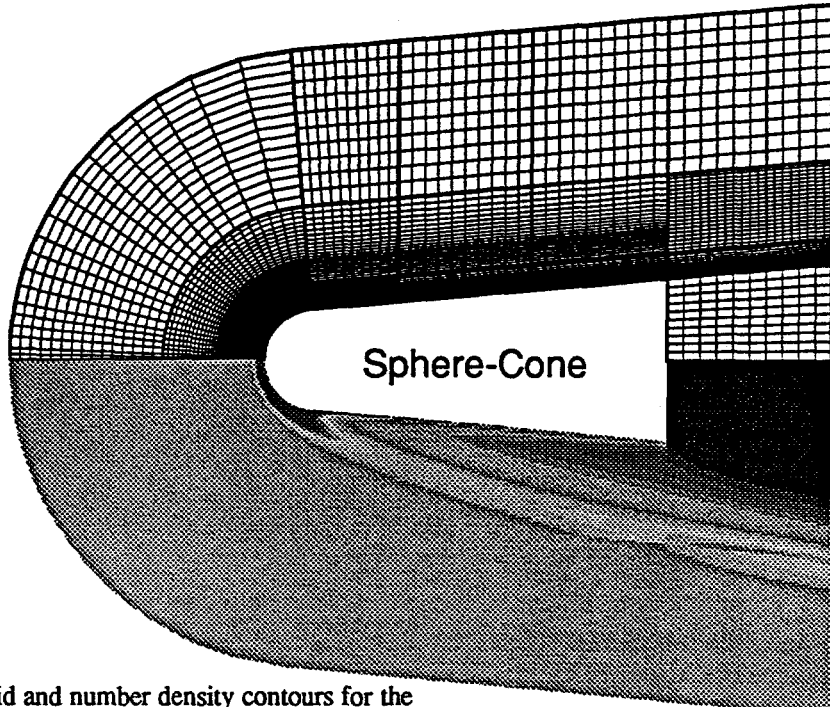


Figure 5 - Grid and number density contours for the 80 km sphere-cone calculation

Table 3: Speedup Ratios for Sphere-Cone Runs

calculation	# processors	speedup ratio
80a	256	19.7
80b	256	14.5
100	256	20.6
100	512	30.8

Table 3 shows that doubling the number of processors from 256 to 512 for the 100km calculation only increased the speedup 50%, from 20.6 to 30.8. Again, the culprit is increased load imbalance as more processors have less than the average work load. It is difficult to ascertain an exact efficiency since the large problems do not fit on a single nCUBE processor. Table 1 notes that the speed of an individual processor is approximately 1/12 that of a single Cray Y/MP processor. Therefore, using 256 processors, this would indicate that the maximum speedup would be 21.3. The speedup for the 100-256 case was 20.8 with a 33% load imbalance. The discrepancy is due to the fact that this sphere-cone problem is very large and i/o time represents a small fraction of the total time while this was not the case for the small test problem used to obtain the results in Table 1. Also, the 256 node calculation represents an average efficiency for all 256 nodes: some ran at 1 Mflop and some closer to 2 Mflop depending on whether their work is dominated by collisions or moves.

Table 4 shows the percentage of computational time spent for several portions of the code logic for the sphere-cone calculations. The terms are defined as follows:

move-work required to determine the particle's location at the end of the time step, including any surface interactions,

comm-time spent in message passing the information on particles which have moved out of the cells owned by a processor and also the work required to create or clone new particles after the move,

coll-the time spent on the collision algorithm and the chemistry logic,

load-the average time spent by a processor waiting until all the processors are ready to perform the communicate function--a synchronization effect,

other-the remaining time spent in creating new particles on the boundaries, the adaption logic, storing the statistics, etc.

Several trends are evident from this table. The first is that the larger the problem, the less load imbalance. This is obvious from the load results of the 80a and 80b calculations. The second observation is that more time is spent in the move routine as the Kn increases. This is

Table 4: Processor Time Distribution (%)

	80a	80b	100-256	100-512
move	26	17	42	30
comm	13	11	16	21
coll	21	14	3	2
load	37	55	33	42
other	3	3	6	5

due to the reduced number of collisions and chemistry. If one performs many calculations in the very rarefied conditions, an analytical expression for the grid would greatly reduce the execution time. The final observation is that the number of processors is increased, the load imbalance increases and the speedup is no longer linear.

Figure 6 shows the distribution of the move and load times as a function from their minimum to maximum values for the two 100 km calculations. Recall that the average move processor times decreased from 42% to 30% when the number of processors doubled; similarly, the load imbalance percentage increased from 33% to 42%. In the calculation was perfectly balanced, there would be no load imbalance time and the processors would have similar times spent in the work routines for this high Kn case. Figure 6 shows that the move time for the 256 node configuration was peaked at approximately 40% of the maximum difference and that the spread of the distribution increased for the 512 node configuration. Therefore, the wider range of difference between the move times for the larger configuration translated to an increased load imbalance. The static decomposition used for this calculation was not as efficient as for the 256 node configuration.

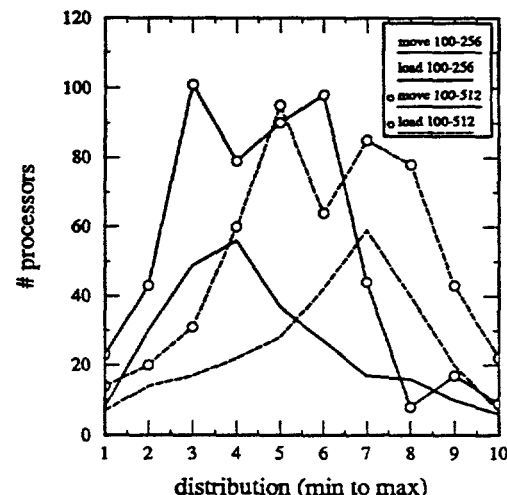


Figure 6 - nCUBE performance histogram for 100 km sphere-cone calculations.

5. Summary

We have described a DSMC model which uses general body-fitted irregular grids and particle weighting factors to minimize the numbers of cells and particles that must be used to simulate a particular problem. MIMD parallel computers provide the flexibility needed to efficiently parallelize such a code and allow each processor to independently compute trajectories and probabilistically determine the collision and chemistry interactions for its particles. The MIMD paradigm is critical because the computations can be completely different for each particle.

Several issues have been discussed through comparison of two geometries and different free stream conditions. The load-balancing issue was the dominate one for this parallel implementation. Presently, we are using a static scattered decomposition scheme to distribute the cells at the initial phase of the calculation. With this algorithm, we achieved a speedup ration of 30.8 for a 512 node configuration compared to a single Cray Y/MP processor. An adaptive load scheme is required to further reduce the load imbalance and increase the speedup ratios. Fortunately, the current implementation based on the computational cell would allow cells to be distributed to different processors during the calculation. This will be the focus of future work. Also, for simple geometries, an analytical expression for the grid will greatly reduce the time spent in the move logic as well as further reduce the storage requirements. This will allow more storage to be allocated to particles.

It should be noted that we have used the speedup comparison to a Cray Y/MP as the comparison metric for our current work. The massively parallel computers not only have a cpu performance benefit, but they also have a much larger system memory, albeit in a distributed configuration. For example, the nCUBE computer used in the present work has 10^9 words (32 bit) while the total memory of the Cray Y/MP is 64×10^6 words (64 bit); however, operational constraints limit the maximum allocation on our Cray to 20×10^6 words per processor. Therefore, the parallel supercomputers are not only faster than the Cray, but have the potential of performing much larger calculations.

Acknowledgments

We thank Bruce Hendrickson and Rob Leland at Sandia for many useful discussions concerning load-balancing algorithms and strategies. This work was partially supported by the Applied Mathematical Science Program, U. S. Department of Energy, Office of Energy Research, and was performed at Sandia National Laboratories which is operated for the DOE under contract number DE-AC04-76DP00789.

References

- [1] Bird, G. A., Molecular Gas Dynamics, Clarendon Press, Oxford (1976).
- [2] Baganoff, D. and McDonald, J. D., "A Collision-Selection Rule for a Particle Simulation Method Suited to Vector Computers", *Phys Fluids A*, 2, (1990) 1248.
- [3] Prisco, G., "Optimization of DMSC Codes for Vector Processing", *J of Comp Phys*, 94, (1991) 454.
- [4] Furlani, T. R. and Lordi, J. A., "Implementation of the DSMC Method for an Exhaust Plume Flowfield in a Parallel Computing Environment", *Computers & Fluids*, 18, (1990) 217.
- [5] McDonald, J. D., "Particle Simulation in a Multicore Processor Environment", AIAA 91-1366, AIAA Thermophysics Conference, Honolulu, 1991.
- [6] Wilmeth, R. G., "Adaptive Domain Decomposition for Monte Carlo Simulations", in Rarefied Gas Dynamics, A. E. Beylich, Ed., VCH, 1991.
- [7] Hermina, W. L., "Monte-Carlo Simulation of Transitional Flow Around Simple Shaped Bodies", in Rarefied Gas Dynamics, Boffi and Cercignani, eds., B. G. Teubner Stuttgart 1986.
- [8] Borgnakke, C. and Larsen, P. S., "Statistical Collision Model for Monte Carlo Simulation of Polyatomic Gas Mixture", *Journal of Computational Physics*, 18, P. 405, 1975.
- [9] Kernighan, B. and Lin, S., "An Efficient Heuristic Procedure for Partitioning Graphs", *Bell System Technical Journal*, 29, (1970) 291.
- [10] Bopana, R., "Eigenvalues and Graph Bisection: An Average Case Analysis", proceedings of 28th Annual Symposium on Foundations of Computer Science", published by IEEE, (1987), p. 280.
- [11] Pothen, A., Simon, H. and Liou, K., "Partitioning Sparse Matrices with Eigenvectors of Graphs", *SIAM J. Matrix Anal*, 11, (July 1980) 430.
- [12] Simon, H., "Partitioning of Unstructured Problems for Parallel Processing", proceedings of Conference on Parallel Methods on Large Scale Structural Analysis and Physics Applications, published by Pergamon Press, 1991.
- [13] Hendrickson, B. and Leland, R., "Spectral Load Balancing for Hypercubes", in preparation.
- [14] Bird, G. A., "The G2 Program System Users Manual", September, 1987.
- [15] Dagum, L., "Three Dimensional Direct Particle Simulation on the Connection Machine", AIAA 91-1365, June 1991.



AIAA 93-3095

DSMC Simulation of

Ionized Rarefied Flows

Timothy. J. Bartel
Sandia National Labs.
Albuquerque, NM

Charles R. Justiz
NASA-Johnson Space Center
Houston, TX

AIAA 24th

Fluid Dynamics Conference

July 6-9, 1993 / Orlando, FL

DSMC Simulation of Ionized Rarefied Flows

Timothy J. Bartel* and Charles R. Justiz^{**}

*Sandia National Laboratories, Albuquerque NM, USA

**NASA-Johnson Space Center, Houston, TX, USA

(tjbarter@cfd.sandia.gov, justiz@ecfa.jsc.nasa.gov)

Abstract

Recently a renewed interest has been exhibited in understanding contamination and space environmental effect in the Low Earth Orbit range of 200 to 600 km as well as low density microelectronics manufacturing technologies. Realistic simulations must model the physics of the highly coupled effects of neutral and charged particle flows, thermodynamic non-equilibrium, surface charging, and electromagnetic field effects. The computational requirements are enormous for this level of modelling and are almost impossible on current single processor supercomputers. An effort has been initiated to develop this capability on a massively parallel MIMD supercomputers. The Wake Shield Facility experiment will be used for test case calculations. Preliminary results indicate that parallel supercomputers may be the only computers capable of simulating the required level of physics and spatial resolution. Calculations which contain from 1 to 8 million simulation particles are presented.

Introduction

The transport terms in the Navier-Stokes equations begin to break down for very low density flows. The physical reason is that the linear relationships for mass diffusion, viscosity, and thermal conductivity are no longer valid when the distance particles move between collisions is comparable to length scales of interest. This is a characteristic of flows with a Knudsen number (ratio of mean-free path to a length scale) on the order of 0.2. A commonly used method for modeling such flows is via particle simulation on a grid - a technique known as Direct Simulation Monte Carlo (DSMC), pioneered by Bird¹. It has utility in a variety of low density applications. The focus of this work is on low density applications which require modelling neutral and charged

particles and their transport due to collision kinetics and induced or applied electromagnetic fields. These include space related applications such as contamination effects on the Space Station Freedom², the flow field on the Long Duration Exposure Facility(LDEF)³, and the epitaxial thin film experiment using the Wake Shield Facility(WSF)^{4,5}. Important non-space related applications include low pressure technologies for the semiconductor industry such as plasma etching of silicon wafers⁶.

The key concept in the DSMC technique is that particle motion is decoupled from particle collisions. That is, during a time step particles move through the grid independent of each other. At the end of the time step, the particles in each grid cell are sampled to obtain collision partners which are collided with probabilistic techniques to obtain the velocity and species distributions. An attractive feature of DSMC is that complex gas and surface chemistry can be done straight forwardly as particles of different species collide with each other and with objects in the simulation geometry.

Typically, the DSMC technique has been used to model flow fields with neutral particles; that is, for air, the 5 major species used are: N₂, O₂, N, O, and NO. The applications of current interest require the inclusion of charged species such as N⁺, O⁺, NO⁺, and e⁻ and the modelling of their coupled interactions with surfaces of interest. Bird⁷ approximated this interaction by 'tagging' the neutral particles with their degree of ionization; this implies local charge neutrality and essentially a zero Debye length. Carlson⁸ modeled the effects of ambipolar diffusion in a localized sense while still maintaining charge neutrality over a domain composed of several computational cells. Again, a very small Debye length assumption was employed. Justiz^{9,10} modelled these problems by solving for a separate E-field from the distribution of the charge density. He could now incorporate the effects of a charged surface on the motion of charged parti-

*,** Senior Members AIAA

cles in a near wake region. This coupled solution strategy greatly increased the computational requirements of an already inefficient DSMC algorithm on a vector supercomputer to the point of having limited functionality.

The goal of the present work is to efficiently implement a coupled EM field - DSMC neutral particle solver in the massively parallel distributed memory computing environment. The solution strategy is to solve the particle collision and transport with the standard DSMC algorithm and directly solve the E-field from the local charge distribution, including charged surfaces, to determine the Lorentz forces for charged particle transport. The MIMD (multiple-instruction/multiple-data) parallel computers will be utilized for both computational efficiency and their increased memory compared to typical vector supercomputers.

Parallel Processing

The nCUBE 2 parallel supercomputer used in the present study has 1024 nodes, each with a 1-2 megaflop floating point processor and 4 MB of memory (4 GB total). The nodes are interconnected in a hypercube topology with each node directly connected to 10 other nodes ($2^{10} = 1024$) in the hypercube. The nCUBE is a MIMD parallel machine; that is, each processor stores its own copy of the executable program and can operate on its local data independently of all the other processors. This is important for the DSMC simulation described here since completely different physics routines may be executed for different molecules depending on where they are in the simulation geometry and their interactions with other molecules.

Bartel and Plimpton¹¹ have recently demonstrated a factor of 30 speedup compared with a single processor of a Cray Y/MP using only a 512 node nCUBE configuration on a simple sphere-cone geometry with 250,000 neutral simulation particles. The basic strategy for our MIMD parallel DSMC technique, DSMC-MP, is to divide the computational domain between the processors; each processor then 'owns' the physical space for the duration of the calculation and the particle information is communicated between processors as they move through the domain. This is in contrast to a strategy where the processor 'owns' a fixed number of particles and then tracks them throughout the domain. We use the prior technique to minimize the communication overhead for computing the representa-

tive collisions and chemistry in a cell. Figure 1 shows the speedup of the current DSMC-MP code on a larger problem: with 17,000 cells and 1.5 million particles. Also included are results from the Intel Delta computer at Caltech. Both MP computers show a reasonable scaling behavior between 64 and 128 nodes; that is, doubling the number of processors will ideally half the computer time. However, as the number of processors are increased, the communication overhead increased and the speedup rate slowed. For comparison, this calculation required 254 CPU hours on a Sun Sparc2 and approximately 85 CPU hours on a single processor Cray YMP. This computational capability available on the MIMD parallel supercomputers is a requirement for attempting to perform the coupled EM-rarefied gas simulations discussed in this work.

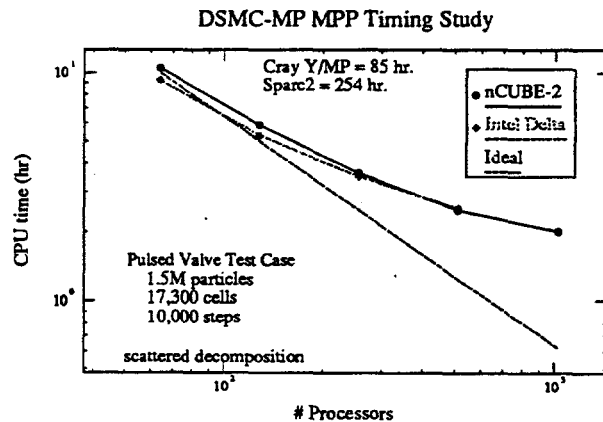


Figure 1. MPP speedup comparisons for DSMC-MP

Coupled EM-DSMC Technique

Neutral DSMC

The implementation of the DSMC algorithm for neutral particle motion used in the present study is described in ref. [11]. Several features were added to the code for this work. First, the addition of a global species weighting factor to the existing spatially varying factors was deemed necessary due to the orders of magnitude difference between neutral and charged particle species fractions; typically, neutral species weights of 1.0 and charged species weights of 0.01 were used. Issues related to recombination reactions and momentum exchange between particles of different weights, although a real concern, were not important in the present study due to the small collision frequencies. Second, a

cell adaptive algorithm was used to adjust the cell weight to limit the number of simulation particles in the cell. Thus, local regions of high density, e.g. stagnation points, will have their cell weights automatically increased relative to areas of low density. However, as described in ref. 11, we use a multi-blocked grid scheme for convince where each block has its own time step so with this adaption scheme the ratio of local particle weight to time step varies throughout the computational domain. It would be impracticable to use a boundary element strategy as Bird has done in his G2¹⁹ code to satisfy microscopic detailed balancing since each cell side would require an element. We chose to probabilistically create or destroy particles as them move between cells based on the weight-time step ratio and satisfy detailed balancing in the macro limit. The advantage of using the present scheme is that problems of disparate densities and velocities can be readily simulated since the cell weights and region time steps are totally decoupled.

This technique was validated by comparing the simulations to the pulsed-valve orifice expansion experiment performed at the USAF Phillips Lab^{17,18}. Figure 2 shows the schematic of the geometry. The gas, NO, enters radially into the orifice region at a pressure of approximately 20 torr and then expands into the vacuum chamber; rotational temperature measurements were made in the expansion region. This is a difficult problem to simulate with the Bird G2 strategy since the density varies several orders of magnitude in the flowfield and areas of low density require a larger time step than areas of high density; a constant cell weight-time step ratio is going in the opposite direction. This experiment is very useful for the present work since it exhibits similar expansion physics as will required to model the wake shield.

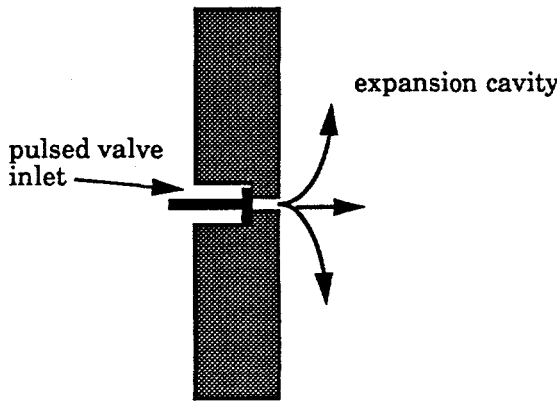


Figure 2. Orifice expansion experiment geometry

Campbell performed simulations using a Navier-Stokes solver in the orifice and then starting the DSMC G2 code at the orifice exit plane¹⁸. With the increased computational power of the nCUBE computer, were able to extend the DSMC technique to the orifice region to avoid the N-S solver. The present problem was modelled using 34,000 grid cells and 1.7 million simulation particles; the calculation took 14.5 hr using 256 nodes of the nCUBE to obtain 35,000 time steps. Figure 3 shows density contours of the DSMC-MP simulation. Note that the logarithm of the density is plotted. The flow region in the orifice is essentially continuum: the orifice radius was 0.5 mm and 11,500 cells were simulated in the orifice region alone. The cell dimensions in the orifice were kept less than the local mean free path. The local region time step was limited to a pseudo CFL time step: the particle transient time through a cell was less than the time step. Thus, the particle could undergo representative collisions in each cell along its trajectory.

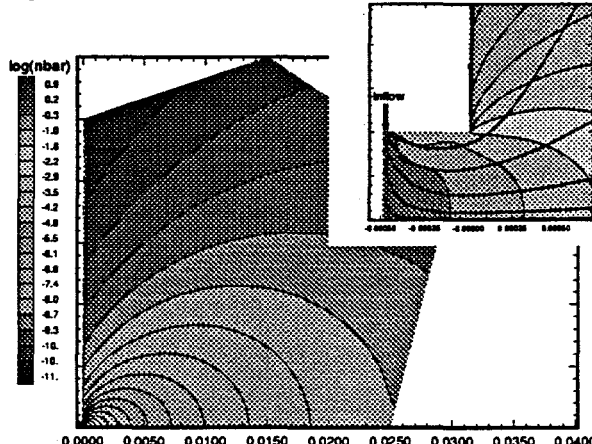


Figure 3. Density contours (log(nbar))

Figure 4 compares the experimentally measured rotational temperature with the DSMC simulations for two radial locations: $z/d=3$ and 5 (d is the orifice diameter and z is measured from the orifice exit plane). The comparison between the data and the DSMC-MP results are quite good. Figure 5 compares the data to the simulations along the centerline of the expansion. Again, the DSMC-MP results agree well with the data. Of note in this figure is the smooth nature of the DSMC-MP results; the results are the actual cell averaged quantities and have not been smoothed. This behavior is due to the increased number of particles and cells in the DSMC-MP simulation, the locally

varying cell weights technique and the large ensemble sample step. Since rotational temperature is more difficult to predict than density, we feel that this comparison is a good test of our present technique.

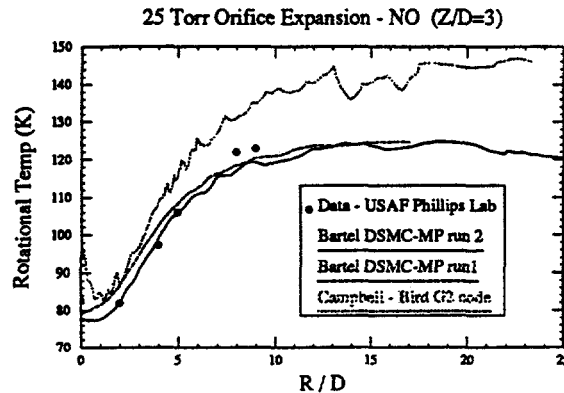


Figure 4a. Rotational Temp. along $Z/D=3$

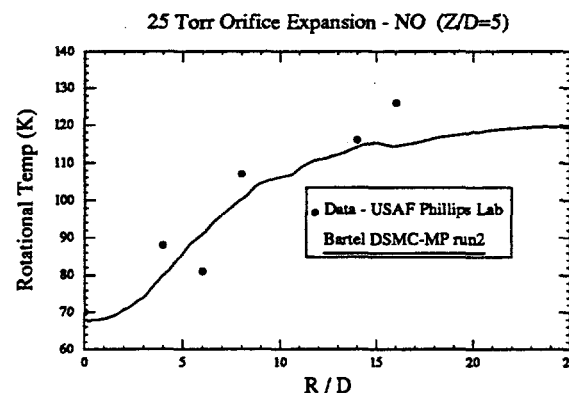


Figure 4b. Rotational Temp. along $Z/D=5$

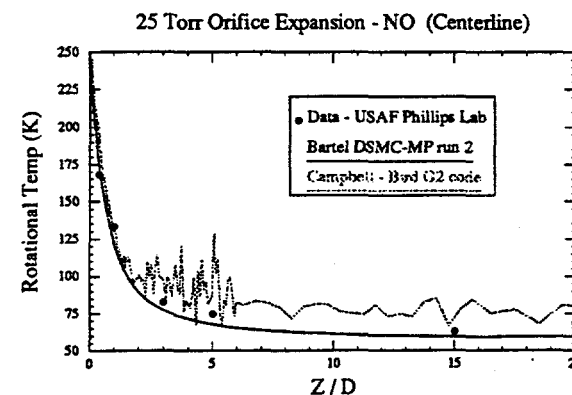


Figure 5. Rotational Temp. comparisons along centerline

EM-Fields

The motion of particles due to their electrical charge is determined from the Lorentz force composed of electric and magnetic field contributions:

$$\mathbf{F} = \mathbf{F}_{\text{electric}} + \mathbf{F}_{\text{magnetic}} = q \mathbf{E} + q (\mathbf{v} \times \mathbf{B}),$$

where \mathbf{F} is the total electromagnetic force on the particle, q is the particle charge (1.6022×10^{-19} Coulomb/electron), \mathbf{E} is the electric field (Volt/m), \mathbf{v} is the particle velocity (m/s), and \mathbf{B} is the magnetic field. Presently, the magnetic field is not modeled and assumed zero. The Debye length is a length scale used to determine whether an ionized gas exhibits a collective behavior and is called a plasma or is simply a collection of charged particles. It is defined as $\lambda_D = 69(T_e/n_e)^{1/2}$, where T_e is the electron temperature in K and n_e is the electron number density in $\#/m^3$. Since the length scales of interest for the current test problem are of the order or greater than the Debye length, charge separation can occur so the electrostatic plasma approximation can be used to reduce Maxwell's equations to:

$$\nabla \cdot \mathbf{E} = \rho/\epsilon_0$$

$$\nabla \cdot \mathbf{B} = 0$$

$$\nabla \times \mathbf{B} = \nabla \times \mathbf{E} = 0$$

where ρ is the volumetric charge density and ϵ_0 is the permittivity of free space (8.8542×10^{-12} F/m). If the electrostatic potential ϕ (volts) is defined such that $\mathbf{E} = -\nabla \phi$, then $\nabla^2 \phi = -\rho/\epsilon_0$. Therefore, the sequence of events for the electric field solution algorithm is to first obtain a volume charge density on a grid, solve the Poisson equation for the potential and finally obtain the electric field from the gradient of the potential. The surface charge on any structure is computed assuming full charge accommodation and is directly incorporated into the grid charge density, ρ . The additional force on a charged particle (with no magnetic field) is then $q\mathbf{E}$; the new spatial particle position after a time step, Δt , is:

$$\mathbf{X}_{\text{new}} = \mathbf{X}_{\text{old}} + \mathbf{V}_{\text{collision}} \Delta t + 1/2 (q/m) \mathbf{E} \Delta t^2,$$

where \mathbf{X} is the position vector, \mathbf{V} is the velocity due to particle collisions, and m is the particle mass.

An important issue for the present work is the strategy for solving the Poisson equation and the grid structure in the MIMD parallel computing environment. There are two grid options: use the same mesh for both the particle algorithm and the E-field or use separate meshes. Justiz⁹ used separate grids for a vector super computer; he required a uniform mesh for the EM grid since he used a fast spectral solver (FFT). A uniform mesh would be unacceptable as a DSMC (particle move) mesh since regions of high densities could not meet the mean free path con-

straint without the use of an prohibitive number of cells. Recent work on field solvers for plasma particle-in-cell (PIC) codes¹² for hypercube computer architectures have used a single, uniform grid and also a FFT solver. The problem with these uniform grids is that the charge potential varies exponentially away from charged surfaces; again, a prohibitive number of cells may be required to adequately model the field. The FFT solvers are direct solvers; that is, they invert the potential function matrix each time step. Since the spatial charge density changes only slightly at each time step, an iterative scheme which used the previous potential function solution will be more efficient.

The use of a single grid presents problems in a parallel computing environment. While the DSMC is a decoupled technique and performs very well in a parallel environment, the Poisson equation is elliptic and requires coupling with all the cells during the solution process. This problem is aggravated for the present model problem: approximately 5000 cells with thousands of particles per cell are used for the DSMC simulation of the 1024 node nCUBE. With approximately 5 cells/processor, inverting a coupled matrix over 1024 nodes would result in a high communication overhead and also decrease the convergence rate if a blocked-matrix decomposition scheme were used.

To balance the efficiencies of the DSMC method and a Poisson solver, we have chosen in the present work to use a dual mesh concept: a multi-blocked grid for the DSMC particle technique and a nonuniform, analytical grid for the EM grid. An analytical grid is a grid which can be described completely with an analytical function. For example, we use a function of the form:

$$x_j = x_{\max} (\exp(j B / N) - 1) / (\exp(B) - 1)$$

where x_{\max} is the position of the last grid line in the domain, N is the number of grid lines (number of grid cells + 1) and B is a grid clustering parameter¹⁵. The clustering feature allows the grid to resolve the EM fields near surfaces. This is an embedded grid strategy, that is, the EM grid can be contained in the DSMC grid or its domain larger than the DSMC domain to capture other EM features. Figure 6 illustrates this grid strategy applied to the Wake Shield Test Problem. The grid density has been thinned for illustrative purposes. For this example, the embedded EM grid's domain is from ± 10 m in z and 10 m in r while the DSMC grid's domain is from -30 to +20m in z and 15m in r . The Wake Shield is located at the origin.

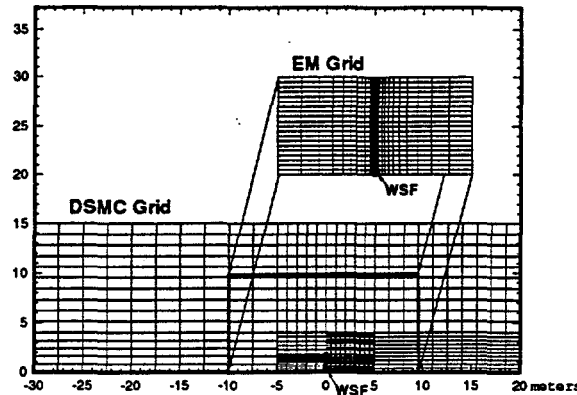


Figure 6. Composite grid strategy for DSMC and EM grids

The important issues of load balancing the computational effort among the processors to achieve maximum performance and convergence rate for the elliptical problem was resolved by assigning a single processor to compute the E-field. For example, for a 1024 node calculation on the nCUBE, up to 1023 nodes will be used for the DSMC technique and 1 node will be dedicated as the EM solver. Since the EM mesh may be contained within the DSMC mesh (as in the Wake Shield), only those processors with cells in the EM domain need communicate their charge density to the EM processor and conversely, the EM processor only has to communicate the solved Lorentz forces back to those processors. This dual grid technique allows the DSMC grid to be decomposed for optimum performance independent of the EM grid. Since the Poisson equation is solved on a single grid, a point SOR technique with Chebyshev acceleration is used¹⁶, a cell averaged value is used for the spectral radius of the Jacobi iteration since the grid is nonuniform.

This embedded grid strategy does not involve any interpolation: the charged particles in the DSMC grid are directly mapped onto the EM grid via the analytical grid function and the resultant Lorentz force field is directly indexed by the charged particle during the move operation. Therefore, only the charged particle density and EM grid location are communicated to the EM solver node and only the complete Lorentz field grid communicated to those nodes who 'own' cells in the EM domain.

Test Problem

The test problem for this new code, DSMCEM-MP, was to model the complete flow field around the Wake Shield Facility exper-

iment^{4,5}. Figure 7 shows the geometry of the shield. In this experiment, a stainless steel disk, 3.7 meters in diameter, will be placed in Low Earth Orbit (LEO) at approximately 380 km altitude. The facility will be positioned a

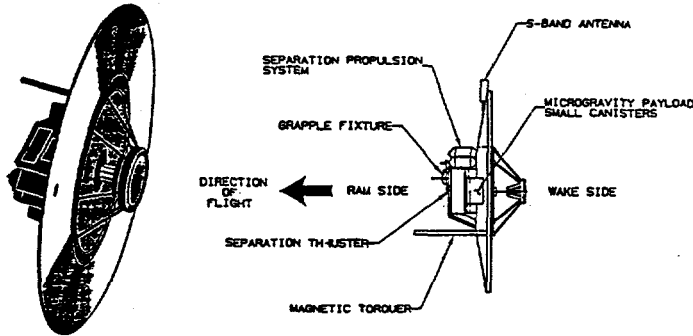


Figure 7. Wake Shield Geometry

distance from the Space Shuttle to minimize any contamination from it. Instrumentation will measure both the ram and wake neutral and charged particle environment for the duration of the test (~40 hours). The potential use of this facility is to obtain a very low density environment in which one would grow high purity crystals (e.g. superconductive thin films). The low density equates to a low impurity or defect level. An addition to this experiment are several higher range density transducers to measure the plume from the attitude control rockets of the Space Shuttle when it maneuvers to retrieve the experiment. Therefore, simulations of the near-wake region and also a higher density plume impingement region will be required for this experiment.

Numerical Simulations

The WSF was modelled as a zero-thickness disk of diameter 3.7 m. Several large 2-D axisymmetric simulations were run on the nCUBE using the DSMCEM-MP code. All calculations used an axisymmetric, multi-block grid of approximately 5000 - 7500 particle cells. Table 1 shows the different calculation combinations and their respective cpu times. The freestream conditions for the disk at 380 km are given in Table 2^{13,14}. The surface of the disk was

Table 2. Freestream Conditions

Number Density (#/m ³)	1.906×10 ¹³
Velocity (m/s)	7800.
Neutral Temp. (K)	1055
Ion Temp. (K)	1055
<u>Species Fraction</u>	
O ₂	0.000136
N ₂	0.253
O	0.7282
N	0.0
NO	0.0
O ⁺	0.0001576
N ⁺	0.0001576
NO ⁺	0.0
e ⁻	0.0
He	0.018

assumed fully diffuse with complete energy accommodation. At the present time a surface charging model has not been included; the surface was assumed to be uniformly charged to -2 volts for runs 4 and 4c and -10 volts for run 4b.

The Debye lengths are approximately 0.0009 m and 0.3 m for the ram and wake sides of the shield for the conditions in Table 2. Therefore, the ram side would be charge neutral on

Table 1. DSMCEM-MP Calculation Matrix

simulation	# particles	species	fields	# nCUBE processors	CPU time (hr)	# time steps
1	8,000,000	O ₂ ,N ₂ ,O,N,NO	none	1024	5.5	10,000
1b	2,050,000	5 species	none	256	26.	50,000
2	800,00	O ₂ ,N ₂ ,O,N,NO, O ⁺ ,N ⁺ ,NO ⁺ ,e ⁻ ,He	none	256	2.6	10,000
4	3,800,000	O ₂ ,N ₂ ,O,N,NO, O ⁺ ,N ⁺ ,NO ⁺ ,e ⁻ ,He	e-field	512	8.1	10,000
4b	1,200,000	10 species	e-field	256	8.4	10,000
4c	1,550,000	10 species	e-field	256	7.2	10,000

the length scale of interest while large charge separations would be expected in the wake region. The Lorentz Force fields were typically updated every 50-100 DSMC step.

Results

Figure 8 shows the relative number density (to freestream) contours of the flowfield around the Wake Shield from calculation 1b. The maximum density in the ram region of the shield was approximately 22 times freestream. Although this calculation was for neutral particles, the addition of the E-field did not alter the appearance of the density contours. The inset portion of the figure for the wake region shows the logarithm of the density ratio to visualize differences in the contours.

Figure 9 shows the relative densities along the centerline for three neutral particles calculations: the freestream number densities were varied about the nominal value of $1.38 \times 10^{14} \text{ #/m}^3$. The density in the near wake region is calculated to be approximately 10^{-4} to 10^{-5} smaller than the freestream density. These values are very difficult to achieve in an Earth-based man-

ufacturing environment.

Figure 10 shows the similar centerline number density profiles for the coupled charged particle/E-field calculations for both surface charge assumption. A surface charge of -10 volts is several times the expected value; it was included to bound the results. Aside from the obvious increase in statistical noise in the results for the charged case, there is no difference between the near wake behavior due to charged particle transport. The momentum of the particles is too high and the collision frequency too low for the particles to be migrate to the near wake region. The surface charge is insufficient to attract the positively charged particles (O^+ , N^+ , and NO^+) into this region.

Concluding Remarks

A technique to treat coupled neutral/charged and electromagnetic fields in problems with large Debye lengths has been demonstrated. We feel that the compute power of a massively parallel supercomputer is a necessity for this class of problems. The DSMC algorithm is well suited for parallel processing so that special techniques

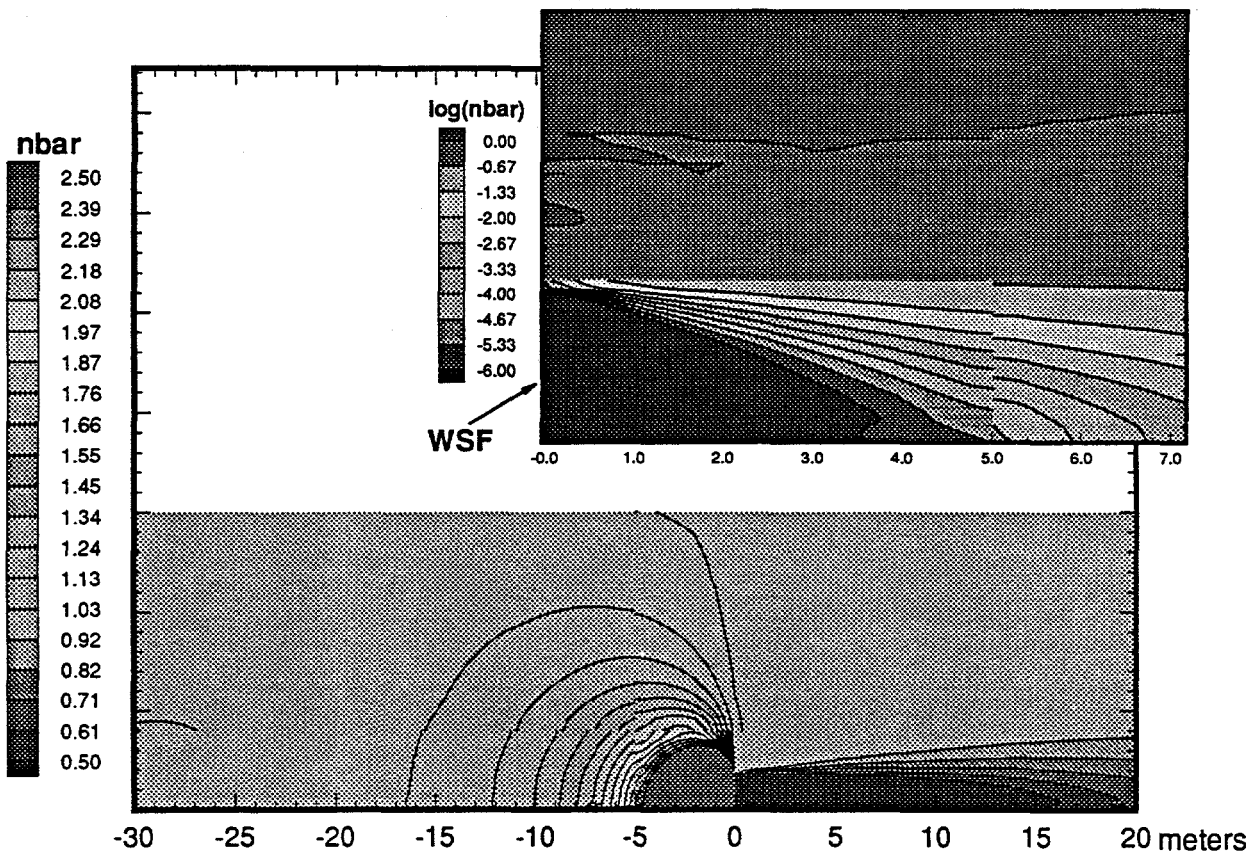


Figure 8. Relative number density contours around the Shield

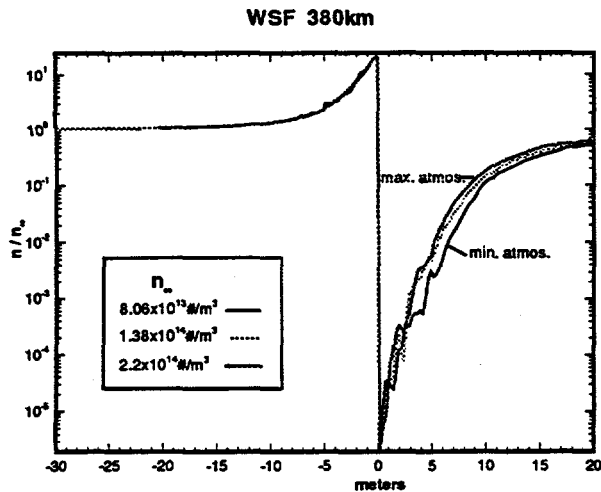


Figure 9. Relative number densities along centerline for the neutral particle calculations.

do not have to be employed to obtain a vector processing paradigm. Full flow calculations with 10 million particles are easily achieved with the nCUBE. Problems such as the Wake Shield Facility and plasma etch reactors may now be addressed with these large parallel supercomputers. When available, the data from the Wake Shield Facility experiment will help to further validate the coupled DSMC and EM solution algorithms.

Acknowledgments

We thank Wahid Hermina at Sandia for many useful discussions concerning the DSMC algorithm and charged particle interactions, David Campbell and Ingrid Wysong at the USAF Phillips Lab for providing and interpreting their experimental data, and Steve Taylor and Sharon Brunett at Caltech for performing the Delta simulations. This work was funded by a DOE Laboratory Directed Research & Development grant and performed at Sandia National Laboratories which is operated for the DOE under contract number DE-AC04-76DP00789.

References

- 1 Bird, G. A., Molecular Gas Dynamics, Clarendon Press, Oxford (1976).
- 2 "Space Station External Contamination Control Requirements," NASA/JSC 30426, 1986.
- 3 Kinard, W., LDEF Environmental Effects Newsletter, Vol II, No. 5, 1991.
- 4 Sega, R. M. and Ignatiev, A., "A Space Ultra-Vacuum Experiment - Application to Material Processing." Proceedings of the AIAA/IKI Microgravity Science Symposium, 1991.
- 5 Bering III, E. A. and Ignatiev, A., "Particle Radiation Near the Orbit of the Vacuum Wake Shield", *J. Spacecraft*, Vol. 27, No. 1, pp38-42.
- 6 Sommerer, T. J., "Models of Low Pressure Plasma-Aided Materials Processing," AIAA 92-3017, AIAA 23rd Plasmadynamics & Lasers Conf., Nashville, TN, 1992.
- 7 Bird, G. A., "Computation of Electron Density in High Altitude Re-Entry Flows", AIAA 89-1882, AIAA 20th Fluid Dynamics Conference, Buffalo, N.Y., 1989.
- 8 Carlson, A., and Hassan, H., "Direct Simulation of Reentry Flows With Ionization", AIAA 90-0144, 28th Aerospace Sciences Mtg., Reno Nevada, 1990.
- 9 Justiz, C. R., "Wake Characterization: Full Flow Simulation of Space Structures in Low Earth Orbit", Ph.D. Dissertation, University of Houston, 1991.
- 10 Justiz, C. R., Sega, R. M., and Dalton, C., "A Hybrid Flow Model for Charged and Neutral Particles Around Spacecraft in Low Earth Orbit", AIAA 92-2935, AIAA 27th Thermophysics Conf., Nashville, TN, 1992.
- 11 Bartel, T. J. and Plimpton, S. J., "DSMC Simulation of Rarefied Gas Dynamics on a Large Hypercube Supercomputer", AIAA 92-2860, AIAA 27th Thermophysics Conference, Nashville, TN, 1992.

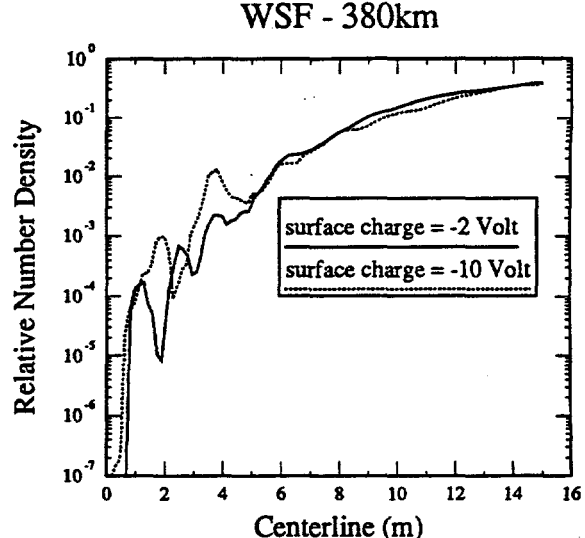


Figure 10. Relative number densities along centerline for the charged particle runs:4 & 4b

-8-

- 12 Liewer, P. C. and Decyk, V. K., "A General Concurrent Algorithm for Plasma Particle-in-Cell Simulation Codes", *J. of Comp. Physics*, Vol. 85, No. 2, Dec. 1989, pp302-322.
- 13 U. S. Standard Atmosphere, N.O.A.A. (1976).
- 14 Rawer, K., International Reference Ionosphere - IRI 79, Report UAG-82, 1981.
- 15 Elgin, J. B. and Sundberg, R. L., Model Description for the Socrates Contamination Code, AFGL-TR-88-xxxx(Draft), October 1988.
- 16 Press, W.H, Flannery, B. P., Teukolsky, S. A., and Vetterling, W. T., Numerical Recipes-The Art of Scientific Computing, 1986, Cambridge University Press.
- 17 Wysong, I.J. and Campbell, D. H., "LIF Measurements of Supersonic Expansion Flow and Comparisons with DSMC Calculations", in proceedings of the 18th Rarefied Gas Dynamics, July 1992.
- 18 Campbell, D. H., Wysong, I. J., Weaver, D. P., and Muntz, E. P., "Flowfield Characteristics in Free Jets of Monatomic and Diatomic Gases", in proceedings of the 18th Rarefied Gas Dynamics, July 1992.
- 19 Bird, G. A., "The G2 Program System Users Manual", Sept. 1987.



AIAA 94-2047

**DSMC Simulation of
Nozzle Expansion Flow Fields**

Timothy. J. Bartel, Todd M. Sterk, Jeff L. Payne, and
Bryan Preppernau

Sandia National Labs.
Albuquerque, NM

**6th AIAA/ASME Joint Thermophysics
and Heat Transfer Conference**
June 20-23, 1994 / Colorado Springs, CO

DSMC Simulation of Nozzle Expansion Flow Fields

Timothy J. Bartel*, Todd M. Sterk*, Jeff Payne **, and Bryan Preppernau⁺

Sandia National Laboratories, Albuquerque NM, USA
(tjbarde@cfd.sandia.gov)

Abstract

Detection of trace chemical species is a difficult and time consuming process. A new area of interest for acquiring this capability is in environmental monitoring and nuclear treaty verification. An effective alternative to current techniques may be expanding a gas mixture through a nozzle and employing beam diagnostic techniques to monitor signal time of arrival and strength. The differences in the inertial of the species alters the signal strength and possibly the arrival time in a rapidly expanding flowfield. In this investigation, the DSMC method of Bird¹ has been used to predict species mass and concentration ratios and to evaluate two chamber designs. The flowfield of interest varies from approximately atmospheric pressure at the nozzle throat to essentially vacuum in the chamber. A approximate technique to allow the DSMC method to be efficiently applied in the high density nozzle region has been implemented and compared with continuum simulations: Couette and nozzle flow. DSMC simulations of the complete expansion of a gas mixture from 0.2 MPa into a vacuum are presented.

Introduction

Sandia has developed an ultra-sensitive ultraviolet (UV) technique to detect and identify airborne volatile compounds. This technique has been developed to reduce the complexity of UV absorption spectra and to increase the sharpness of individual absorption lines, thereby providing lower detection limits and increased specificity in identifying ultra-low concentrations of volatile compounds in a sampled air stream. Sandia's molecular beam fluorometer technology uses a

free-jet expansion to cool molecules entrained in an incoming air stream. Temperatures below 10 K are achieved by expanding the air stream into a vacuum chamber through a pulsed valve. The cooled molecules have a simplified absorption spectrum with sharp molecular features which improve the detection and identification of specific compounds in chemical mixtures. Measurements made under vacuum conditions allow both ionization and fluorescence spectra to be measured. Using a high accuracy mixing system, calibrated samples can be produced to determine the sensitivity of measurements made with the pulsed molecular beam laser fluorometer. The apparatus shown in Figure 1. uses a mass spectrometer to monitor the concentration of volatile vapors in helium and dry air carrier gases. Calibrated concentrations down to about 10 parts-per-billion can be prepared with the mixing system.

Molecular beam laser fluorometer measurements are expected to improve the capability of airborne air-sampling measurements by providing real-time feedback on the detection of volatile compounds in sampled air masses. Incorporation of signal analysis software and all-solid-state tunable UV laser technology will further improve the capabilities of the molecular beam laser fluorometer in detecting and identifying volatile compounds.

Methodology

When modeling flow in the present simulation geometry, a high pressure expansion, the transport terms in the Navier-Stokes equations for continuum flow begin to break down at the low densities in the expansion plume. The physical reason is that the linear transport relationships for mass diffusion, viscosity, and thermal conductivity are no longer valid when the distance molecules move between collisions is comparable to length scales of interest. This is a characteristic of flows with a Knudsen number (ratio of mean-free path to a length scale) on the order of 0.2. A commonly used method for modeling such flows is via particle simulation on a grid

* Thermophysics Department
Senior Member AIAA

** Aerodynamics Department
Senior Member AIAA

+ Laser, Optics, and Remote Sensing Dept.

This paper is declared a work of the U.S. Government and is not subject to copyright protection in the United States.

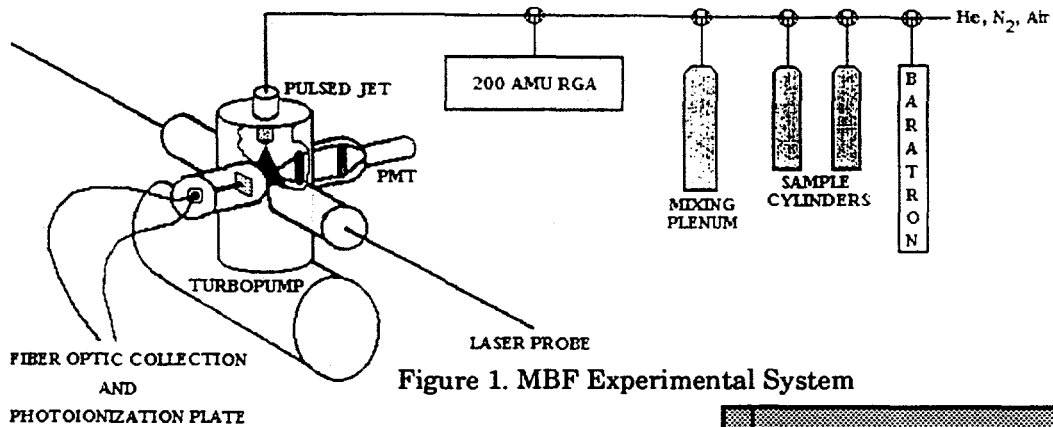


Figure 1. MBF Experimental System

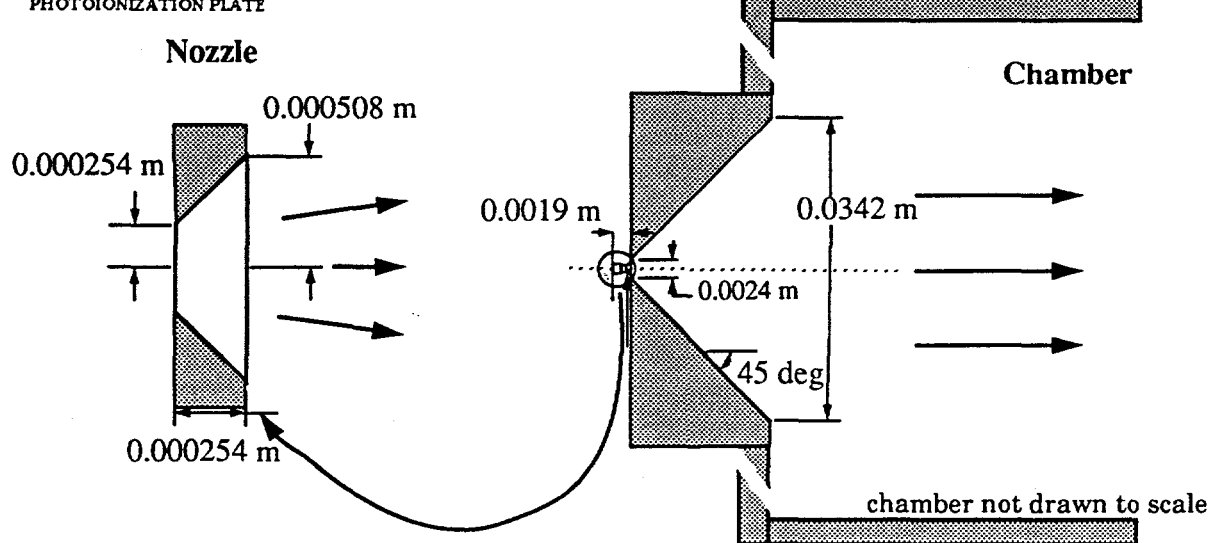


Figure 2. Nozzle and Expansion Chamber Geometry

- a technique known as Direct Simulation Monte Carlo (DSMC), pioneered by Bird¹. It has utility in aerospace applications (upper-atmosphere flows for hypersonic cruise vehicles, re-entry vehicles, rocket plumes, etc.) and in vacuum-related technologies for the semiconductor industry (modeling plasma etching or chemical vapor deposition). We have used a 2-D DSMC² code which has been optimized for the massively parallel computer environment. All of the 2-D simulations were performed on a 1024 node nCUBE-2 parallel supercomputer.

The DSMC method, with a simple collision limiter technique to allow it to be applied to a restricted set of very high density flow situations, was used to model the entire gas expansion from the nozzle to the sampling chamber. This geometry is shown in figure 2. Gas, at essentially atmospheric pressure, is pulsed into the chamber from the nozzle. Since the inlet nozzle conditions are high pressure, the Navier-Stokes equations are valid and results from a continuum code have been used to verify the DSMC simulations. The INCA³ continuum code

was used to obtain the flowfield results from the nozzle inlet into the first expansion region in the present study. The INCA code solves the Navier-Stokes equations which account for multi-chemical species and energy modes with thermochemical nonequilibrium. An LU-SGS^{4,5} (lower-upper symmetric Gauss-Seidel) implicit finite-volume method was used to solve the conservative form of the governing equations.

The questions for this investigation include whether the DSMC technique can accurately and efficiently model the expansion from the nozzle exit plane into the chamber and can determine an optimum chamber design to increase the signal sensitivity. Unfortunately, experimental measurements have not been finished with which to verify the numerical predictions. This paper will present comparison results which verify the simple collision model for these class of problems, compare the DSMC results in the nozzle with continuum results and then discuss the chamber performance for two geometries.

Collision Limiter

There are at least two strategies which may be employed to address the very high density and subsequent very high collision frequency at the conditions of interest: the first would limit the number of computational collisions and the second would assume that the large collision frequency would result in a Boltzmann distribution and would simply sample from this distribution based on the cell average quantities for the particle energies. We choose the former in the present investigation.

We implement a very simple method to limit the number of computational collisions:

- calculate the number of collisions per time step, n_{sel} , using the No Time Counter (NTC) technique
- then limit the number of collisions to be attempted to a multiple of the number of computational particles in the cell, n_{avg} ,

$$n_{sel} = \text{amin0}(n_{sel}, 5*n_{avg}).$$

This model is based on physical arguments that suggest that after a finite number of collisions, the computational particles would achieve a gaussian or Boltzmann distribution. Further collisions will simply re-distribute the collision partners in this distribution. We evaluated a limiter of 5, 10, and 15 and found that for the present problem, a limiter of 5 was in good agreement with solutions obtained from a Navier-Stokes based CFD code. Thus this model implies that on the average, a computational particle will undergo at most 5 collisions per time step. Effects of chemical reactions were not investigated in the present work; the limiter value would have to be much larger than 5 to capture the correct chemical kinetics. Two test cases were used to evaluate this method: Couette Flow and a supersonic expansion in a nozzle.

Couette Flow

The problem is the flow of a compressible fluid between infinite parallel plates of separation h , the lower one fixed and the upper plate moving at a velocity, U_e . Both plates are at the same temperature, T_s , with fully diffuse surfaces. There are zero axial gradients; the flow is generated entirely by the moving upper plate. Therefore, this is a 1-D problem; the DSMC code in ref. 1 was used for this study. The test case conditions, characteristic of those in the nozzle of the MBF chamber, were:

$$\begin{aligned} T_s &= 273K \\ n_\infty &= 6.1027 \cdot 10^{25} \text{ #/m}^3 & (0.202 \text{ MPa}) \\ U_e &= 1000 \text{ m/s} \\ h &= 0.5 \cdot 10^{-3} \text{ m} \\ \text{Argon (diameter} &= 4.17 \cdot 10^{-10} \text{ m).} \end{aligned}$$

Based on these conditions, the following can be calculated:

$$\begin{aligned} \lambda \text{ (mean free path)} &= 2.1 \cdot 10^{-8} \text{ m} \\ Kn_h &= 4.2 \cdot 10^{-5} \\ \delta \text{ (molecular spacing)} &= 2.5 \cdot 10^{-9} \text{ m.} \\ v \text{ (collision frequency)} &= 1.3 \cdot 10^{10} \text{ s}^{-1} \\ N_c &= 4 \cdot 10^{35} \text{ #/s-m}^3 \end{aligned}$$

This flow is highly collisional and continuum: since the molecular spacing is only 20 times larger than the molecular diameter, the fundamental assumption in the DSMC method of a dilute gas and therefore a flow dominated by binary collisions may even be approaching the limits of validity.

The fundamental problem with attempting this problem with DSMC is illustrated in determining the number of potential collisions per time step, $N_c \cdot \Delta t \cdot V$. Assuming a uniform grid of 100 cells and a time step of 10^{-8} s, one calculates that you will have to perform approximately 10^{25} collisions per cell per time step! This is an impossible task! Using a collision limiter of 5 and assuming approximately 40 computational or test particles per cell, the maximum number of collisions per cell per time step is now only 200, a tractable amount. The test of this simple method is whether it matches results from the Navier-Stokes equations.

Three different uniform grids were used: 50, 100, and 500 cells. The cell spacing corresponds to approximately 50λ , 25λ , and 5λ and are consistent with the grid spacing used in the 2-D study which was performed on the MBF inlet nozzle. The 1-D DSMC simulations typically used a time step of $5 \cdot 10^{-8}$ s and were executed with 6,000 unsteady and 6,000 steady time steps. Figure 3 shows the velocity profiles for these three grids using a collision limiter of 5. The profiles are in excellent agreement and exhibit the expected linear behavior. The velocity offset at the edges is attributed to the large mesh size used: the gradient from the wall velocity to the fluid is very steep in this region.

Figure 4 shows the fluid temperature distribution for these simulations. Since the DSMC technique treats the fluid as fully compressible, a simple comparison with incompressible theory is inappropriate¹. Using the curves for the tem-

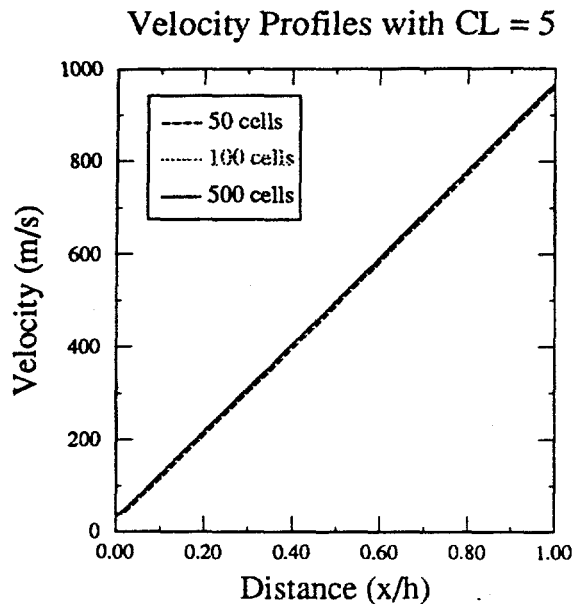


Fig. 3 Couette Flow with CL = 5

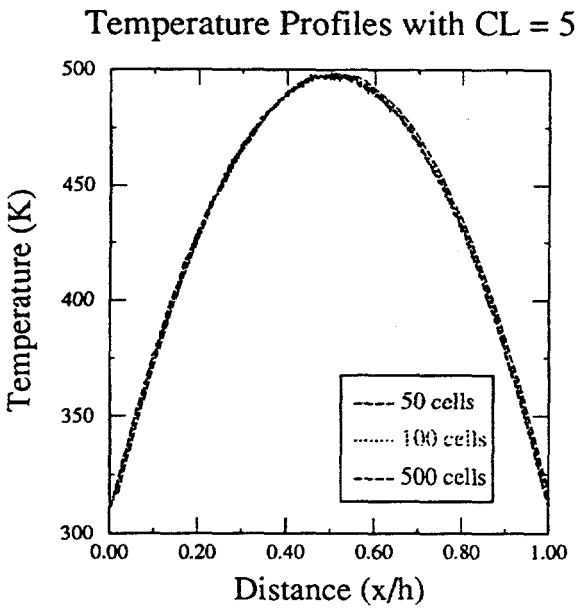


Fig.4 Couette Flow with CL = 5

perature distribution for compressible Couette flow from White⁶ with $\text{Pr } \text{Ec} (\mu C_p/k \cdot U_e^2/C_p T_e) = 7.3$ for argon at these conditions, the peak-to-wall temperature ratio is predicted to be approximately 1.9; the peak-to-wall temperature ratio from figure 4 is 1.83 and in good agreement considering that the $\text{Pr } \text{Ec}$ number was calculated with transport properties which may be inconsistent with the VHS values used in the DSMC simulation. This figure also exhibits the same surface jump conditions as in figure 3. Again, it is expected that the very large cell size and large time step are the cause for this.

Figure 5 compares the temperature profiles for a uniform grid of 50 cells with a collision limiter of 5 and 1. The peak temperatures are remarkably similar and the edge temperature jump is absent from the simulation with CL = 1. Although the CL = 1 simulation appears to better predict both the center and edge temperature distributions, we believe that this is a false conclusion and simply attributed to the large cell size. On the average, 1 collision per computational particle is made per time step so the effect of the surface temperature will be propagated further into the grid.

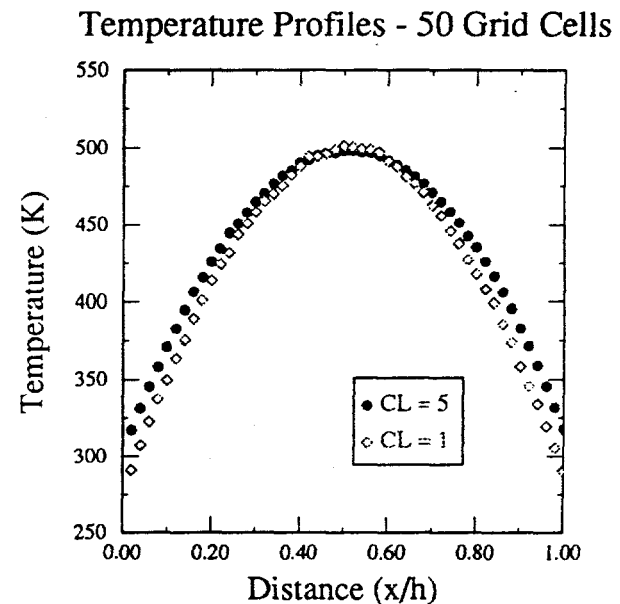


Fig. 5 Couette Flow with CL = 1 & 5

The conclusion from this test problem is that the use of a simple collision limiter method with a value of 5 and a grid with 50 cells adequately simulates the flow physics in this particular problem. Again the effects of chemically reacting flows were not studied.

MBF

The MBF expansion problem can be logically broken up into two regions: the nozzle and the expansion cavity (see Figure 2). Since a N-S code would not be valid for the entire expansion chamber, we have only used it to verify the DSMC solutions with the collision limiter in the nozzle section. Once that was established, we performed complete axisymmetric simulations from the nozzle to the expansion cavity with the DSMC code.

A. DSMC and N-S Nozzle Comparisons

The DSMC2D-MP and INCA codes were used to predict the flow field from the nozzle into the first expansion region. A 60×70 grid in the nozzle was used in the continuum solutions; a grid refinement study was performed to ensure a grid independent solution. The first expansion region was gridded to minimize the effect of the downstream boundary condition in the continuum solutions. Three grids were used in this region for the DSMC simulations: 50×60 , 100×125 , and 200×250 . A collision limiter of 5 was used for all of the DSMC simulations. Typically from 4 to 10 hours on a 256 node nCUBE were required for the DSMC simulations.

We investigated two sets of inlet nozzle boundary conditions, on either side of the sonic conditions:

Case 1

Mach = 1.05
Gas = He
 $U = 941$ m/s
 $P = 0.196$ MPa
 $T = 232.3$ K

Case 2

Mach = 0.906
Gas = He
 $U = 822$ m/s
 $P = 0.196$ MPa
 $T = 232.3$ K

Two different inlet boundary conditions were used for the DSMC simulation: a constant radial line and a radial profile extracted from the INCA solution a few grid cells from the inlet boundary. Results are presented for a constant profile for the Case 2 conditions and using an extracted profile for Case 1 conditions.

Figure 6a and 6b compares the DSMC and INCA axial velocities one mesh cell in from the inlet plane for both the constant and extracted profile cases respectively. The profiles differ at the wall boundary; a flat inlet profile for the DSMC simulation results in non-physical behavior for the first few cells along the surface since a large tangential velocity has been imposed on a fully diffuse boundary. The collision frequency in this area is unphysically high. The use of the extracted profile has included the no-slip N-S boundary condition which forces the axial velocity to zero at the surface. Figure 7a and 7b shows the temperature comparison for the same simulations. Here the effect of using the extracted initial profile to obtain a consistent set of starting conditions is more pronounced.

The primary goal of the comparison between the DSMC and N-S simulations is to determine whether the simple collision limiter method can adequately allow the DSMC technique to be applied in this high density region. Figures 8

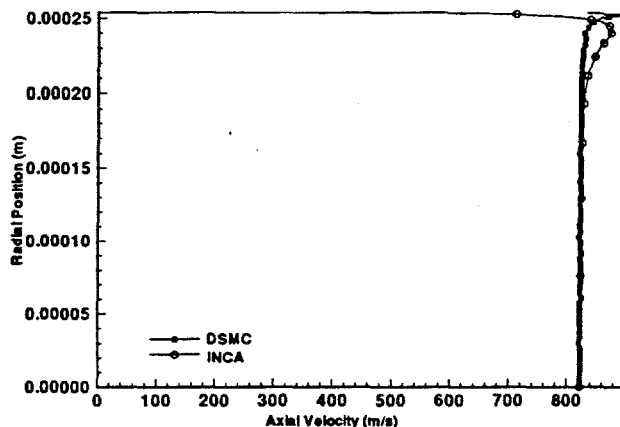


Fig. 6a Near inlet velocity profiles for flat initial profile for DSMC

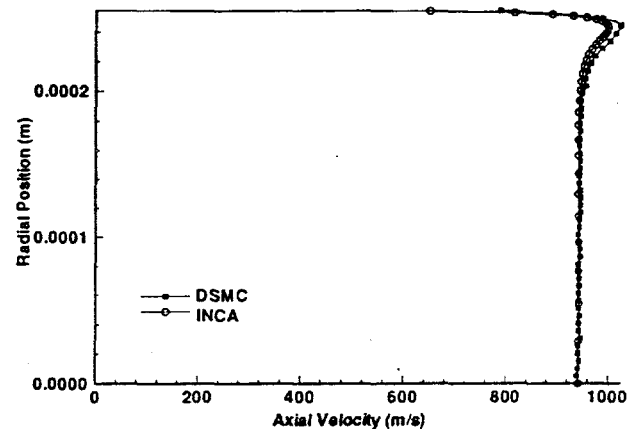


Fig. 6b Near inlet velocity profiles for extracted initial profile for DSMC

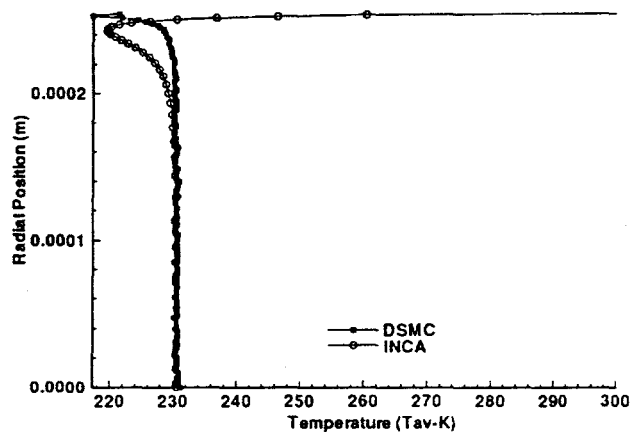


Fig. 7a Near inlet temperature profiles for flat initial profile for DSMC

thru 10 compares the DSMC and INCA nozzle exit radial profiles of axial velocity, temperature, and pressure, respectively. Both the flat and the extracted inlet profiles are included. The effect of using the flat profile is clearly seen in the devia-

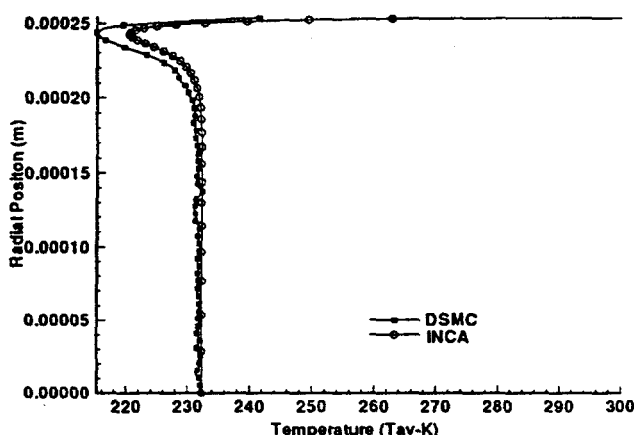


Fig. 7b Near inlet temperature profiles for extracted initial profile for DSMC

tion of the profiles at the surface; the DSMC simulations are evolving the flat inlet profile to one which is consistent with the no-slip boundary conditions. The comparisons between the DSMC simulations using the extracted inlet profile and the N-S code are extremely good. We conclude that for this problem class, the use of the collision limiter allows the DSMC method to both accurately and efficiently simulate the high density flow physics. This has given us a new tool to compute the complete expansion flow in a single numerical simulation.

B. Cavity Results

Two different gas mixtures were used for the cavity simulations:

Case A: 0.99 He & 0.01 $(CH_3)_2CO$ (acetone) and conditions of Case 2, and

Case B: 0.999 He & 0.001 $(CH_3)_2CO$ and conditions of Case 1.

The viscosity for the INCA code was calculated by using Blottner's formula⁷ for individual species and then Wilke's mixing formula³ to obtain the mixture viscosity. The conductivity was calculated by using Eucken's formula³ to calculate the species conductivity from the species viscosity and then determine the mixture conductivity using Wilke's formula. The specific heat at constant pressure, the enthalpy, and the entropy for each species was obtained from a curve fit as a function of temperature. The VHS model was used in the DSMC simulations with a single mixture viscosity index. The VSS model is currently being implemented with species dependent coefficients.

Steady-State Flow

Figures 11a and 11b show contours of axial velocity for the N-S and DSMC simulations for Case A. The anomaly along the exit plane of the N-S simulation is due to the particular exit BC being used. This comparison is made only to confirm the need to use the DSMC method for these expansion flows. Figure 12 shows a contour of the Bird Continuum Breakdown Parameter¹:

$$B = \frac{V \cdot \nabla \ln(\rho)}{V}$$

Note that for a value of 0.05, the region of validity of the N-S equations is limited to approximately 5 mm from the nozzle exit plane. Based on this, there is qualitative agreement between the N-S and DSMC simulations within this region as shown in Figure 11.

Figure 13 shows the DSMC grid for the complete measurement cavity configuration. The upper surfaces are assumed to be fully diffuse; the right hand boundary is a non-reentrant condition. The grid consisted of approximately 40,000 cells and 7.4 million computational particles were used; the simulation took 10 hours on a 512 node nCUBE-2 MPP computer for 20,000 time steps. We have found that the use of the divergent grid structure for expanding flows results in a better choice of collision partners than a simple rectangular cartesian grid. Figure 14 shows contours of the relative molar fraction of acetone for the Case B set of conditions. A thin concentration "shock" of acetone is evident in the results. Its angle is qualitatively equal to the nozzle angle of 45°; this angle is much smaller than the Prandtl-Meyer angle for a free expansion. The high concentration region at the chamber wall is due to the diffuse reflection of the incident acetone molecules. Figure 15 shows the radial profiles of the species concentration at the 0.04 m. axial location; experimental measurements will be taken along this plane. The DSMC simulations indicate that the optimum location for increased sensitivity in the steady-state would be at a radial location of 0.022 m.

Transient Behavior

The addition of the collision limiter has enabled the DSMC method to calculate the flow transient; this would be quite time consuming if a composite N-S & DSMC method were used. Figure 16 shows the contours of the local mole fraction of acetone 26 μ s into the expansion. One

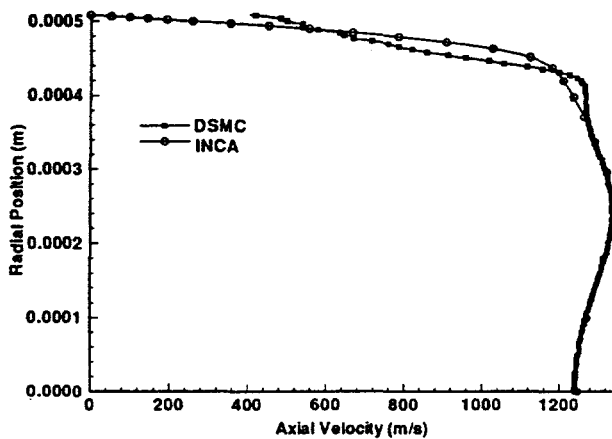


Fig. 8a Radial profile at nozzle exit - flat profile DSMC

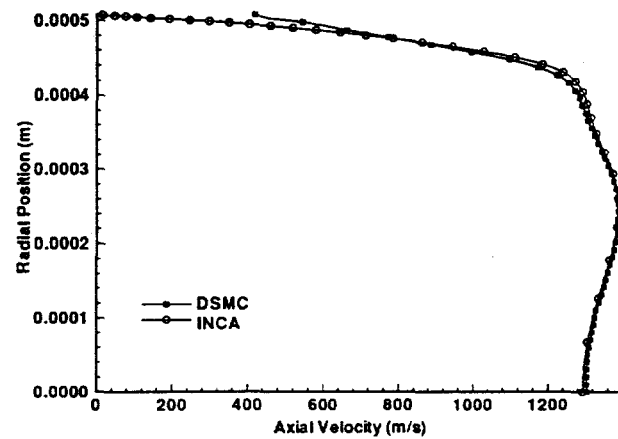


Fig. 8b Radial profile at nozzle exit - extracted profile DSMC

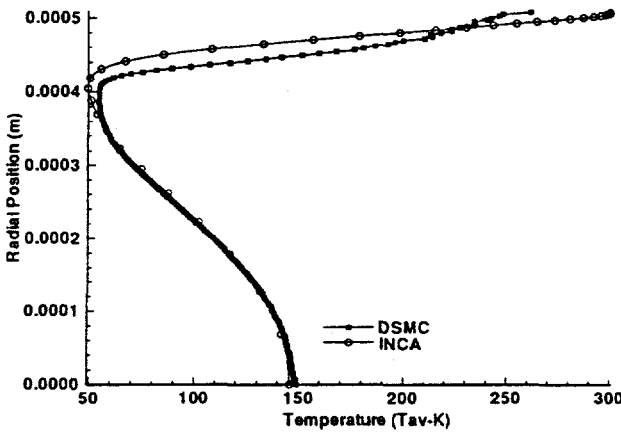


Fig. 9a Radial profile at nozzle exit - flat profile DSMC

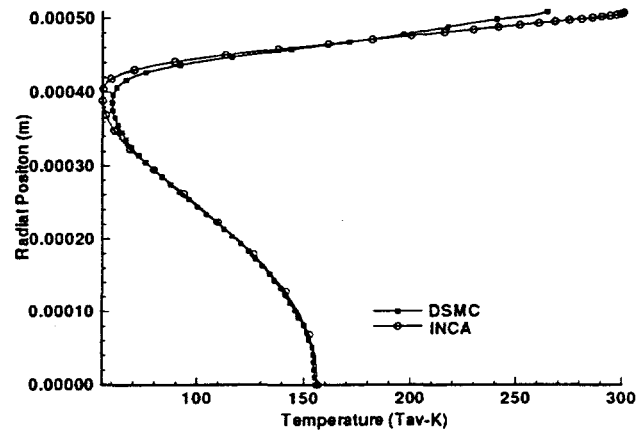


Fig. 9b Radial profile at nozzle exit - extracted profile DSMC

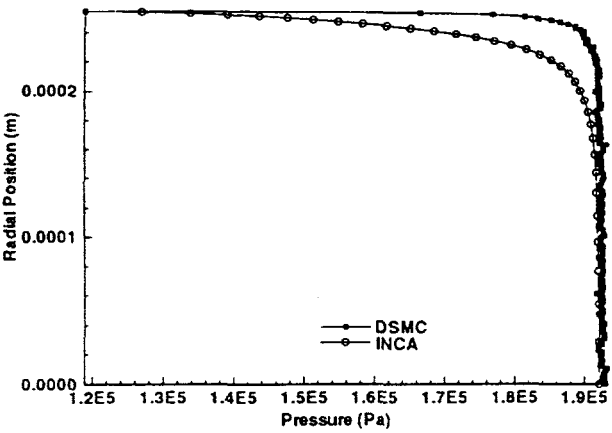


Fig. 10a Radial profile at nozzle exit - flat profile DSMC

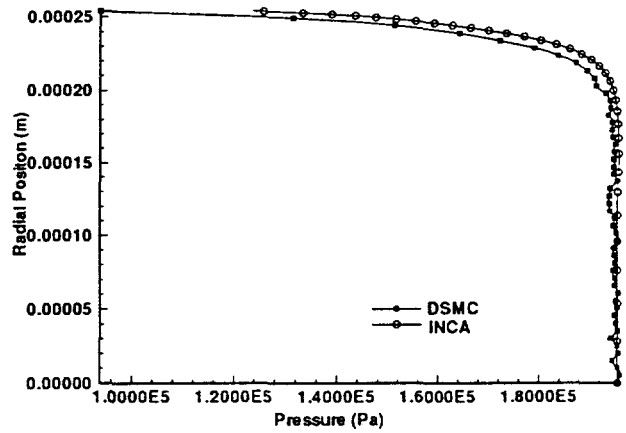


Fig. 10b Radial profile at nozzle exit - extracted profile DSMC

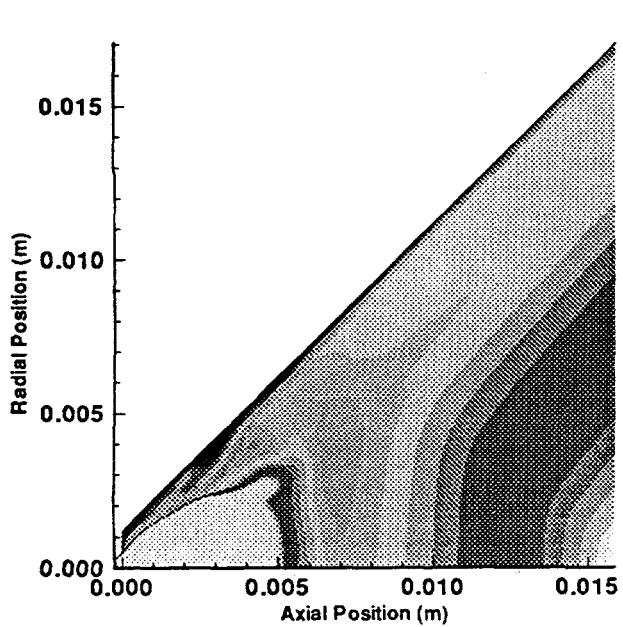


Fig. 11a Contour plot of axial velocity for N-S simulation

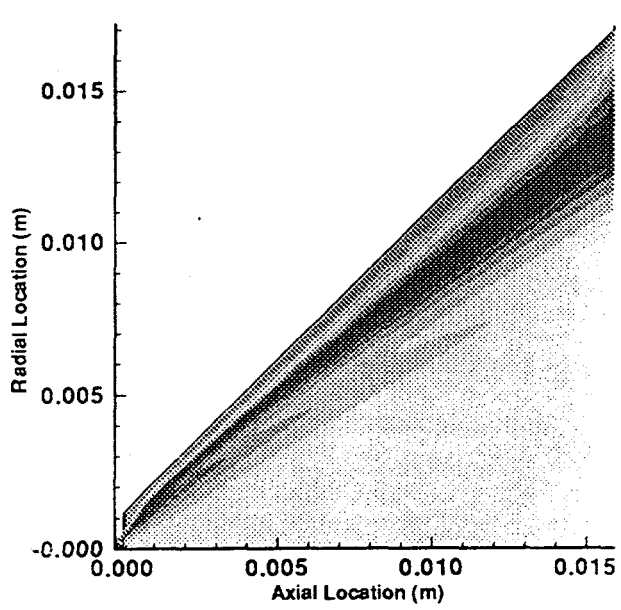


Fig. 11b Contour plot of axial velocity for DSMC simulation

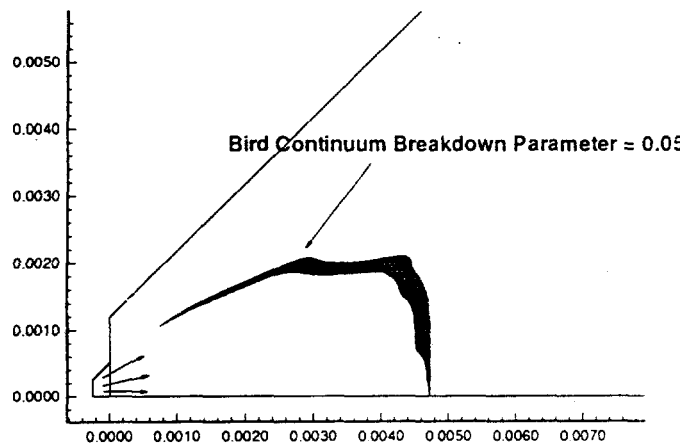


Fig. 12 Contour plot of Breakdown Parameter

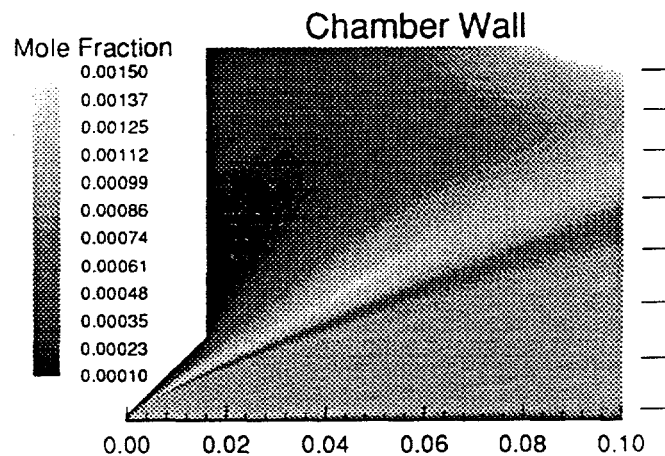


Fig. 14 Contour plot of acetone mole fraction

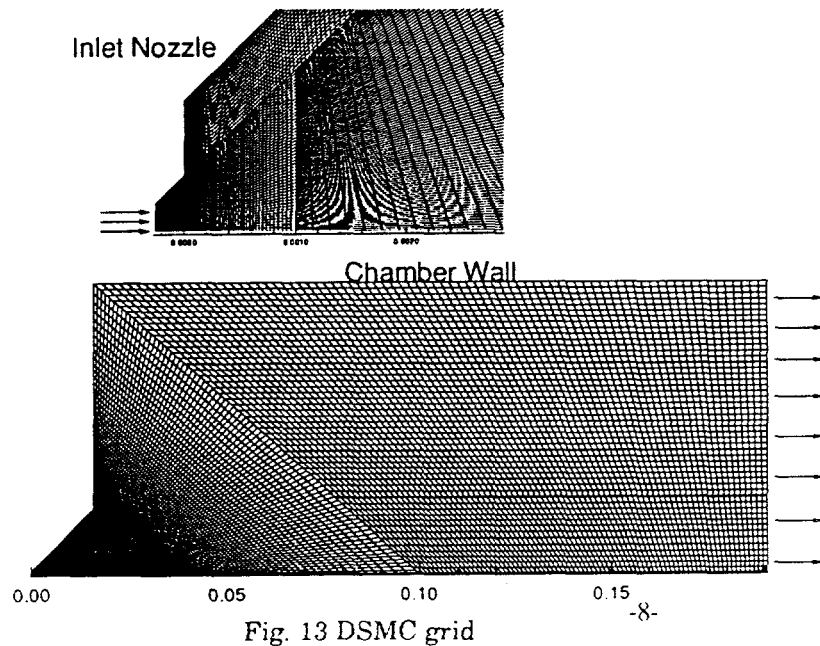


Fig. 13 DSMC grid

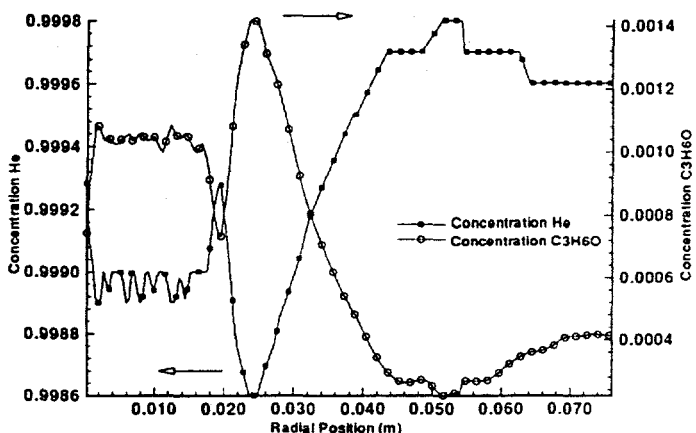


Fig. 15 Radial profiles of species mole fractions at 0.04 m

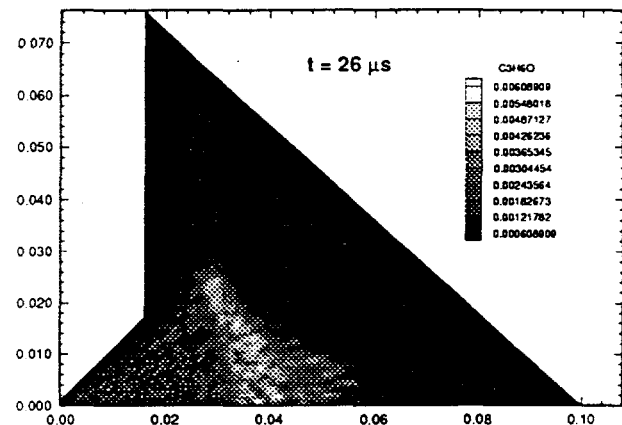


Fig. 16 Contours of acetone mole fraction at 26 μ s (case B)

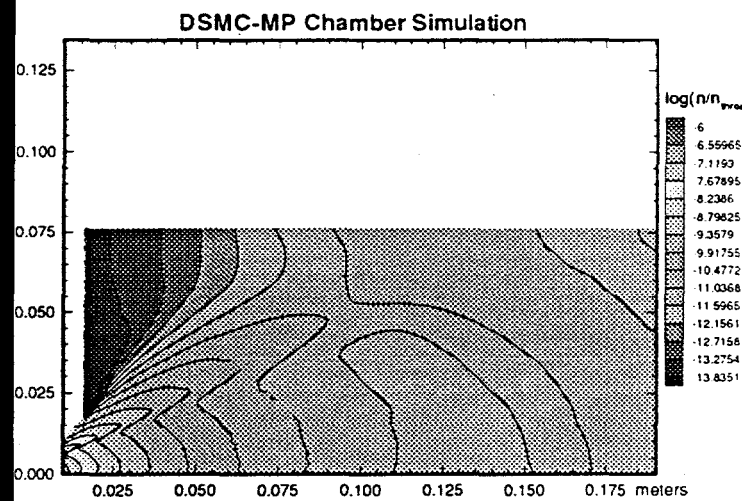


Fig. 17a Relative number density for chamber expansion

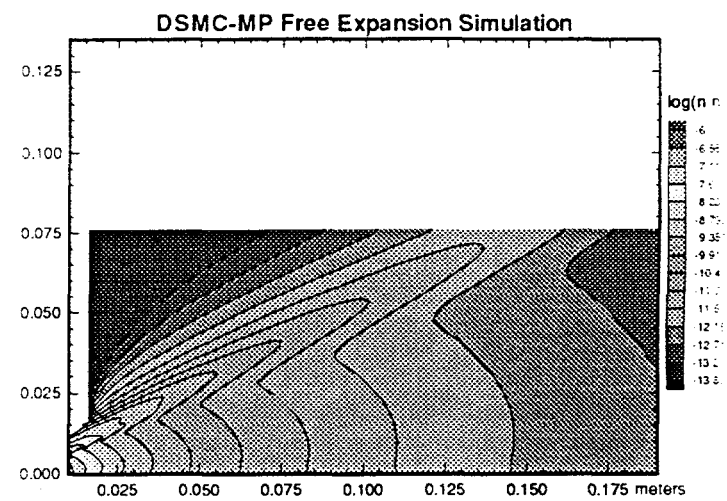


Fig. 17b Relative number density for free expansion

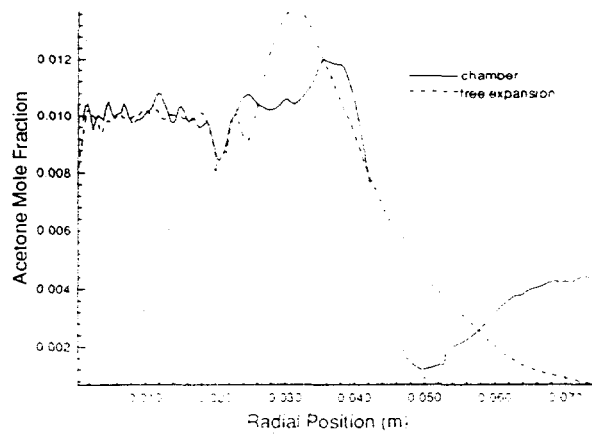


Fig. 18 Radial profiles of acetone mole fractions at 0.04 m

will note that there is a steep concentration gradient at the front of the expansion; the helium has expanded approx. twice as far at this time. The mass ratio of acetone to helium is approximately 15; therefore, the helium has a greater thermal velocity and can expand faster. This time dependent concentration enhancement of the heavier trace species will enhance the sensitivity of the MBF technique; this simulation indicates a concentration increase of approximately 6 from the inlet stream can be measured at the 0.04 m radial plane. Note that the steady-state mole fraction is 5 times smaller than the transient one. Experimental verification of this concentration shock will be done.

Chamber Design

A goal of this study was to be able to computationally evaluate various chamber designs to determine their effectiveness. Figures 17a and b shows the relative number densities for the test A conditions for a chamber with a solid boundary for the upper surface and a chamber in which the flow is allowed to expand freely. The effect of the contained expansion is to depress the expansion. This can also be seen in Figure 18 which shows the radial profile of the relative concentration ratios of the species for these two configurations; a free expansion would increase the trace gas sensitivity.

Summary & Conclusions

- The DSMC method has been used to simulate the expansion of a gas mixture from the nozzle throat to the free expansion. These simulations spanned pressures from approximately 0.2 MPa. (2 atm.) to near vacuum.
- A simple technique, a collision limiter, was used to allow these simulations to be computationally tractable. This technique has been verified by comparisons with continuum solutions for the compressible Couette Flow and nozzle expansion problems. This method appears to be viable for neutral chemistry, high density flows. Further investigation needs to be done to determine its range of validity.
- DSMC simulations have been performed for the MBF measurement cavity and have shown areas with increased species mass separation which enhances the ability to perform trace species detection. The transient concentration shock shows particular promise for trace species detection.

- The DSMC2D-MP code, with the collision limiter, can be used to computationally evaluate nozzle/chamber designs to optimize sensitivity.
- The increased computationally performance provided by the massively parallel computer allows the DSMC method to be used as a design tool.
- Experimental data in this MBF chamber is being taken to verify the transient and steady-state DSMC results.

Acknowledgments

This work was funded by three DOE Laboratory Directed Research & Development grants: development of a MPP DSMC code, development of a MPP continuum capability, and the development of the MBF concept and data acquisition system. The work was performed at Sandia National Laboratories which is operated for the DOE under contract number DE-AC04-94AL85000.

References

- 1- Bird, G. A., Molecular Gas Dynamics and the Direct Simulation of Gas Flows, Clarendon Press - Oxford, 1994.
- 2- Bartel, T. J. and Plimpton, S. J., "DSMC Simulation of Rarefied Gas Dynamics on a Large Hypercube Supercomputer", AIAA 92-2860, AIAA 27th Thermophysics Conference, Nashville, TN, 1992.
- 3- *INCA: 3D Multi-Zone Navier-Stokes Flow Analysis with Finite-Rate Chemistry, User's Manual Part 1: Input Guide*, Amtec Engineering, Inc., Bellevue, Washington, January 1992.
- 4- Yoon, S., and Jameson, A., "An LU-SSOR Scheme for the Euler and Navier-Stokes Equations," AIAA 89-0600, 1987.
- 5- Yoon, S., and Kwak, D., "Artificial Dissipation Models for Hypersonic External Flow," AIAA 88-3708, 1988.
- 6- White, F. M., Viscous Fluid Flow, McGraw-Hill, 1974.
- 7- F.G. Blottner, M. Johnson, and M. Ellis, "Chemically Reacting Viscous Flow Program for Multi-component Gas Mixtures," Sandia Laboratories SC-RR-70-754, Dec. 1971

Low Density Gas Modelling in the Microelectronics Industry

T. J. Bartel

Sandia National Laboratories, USA

Abstract. The microelectronics industry is currently pursuing low pressure etch and deposition reactor systems to achieve the uniformity required to meet the demands of gigascale integrated circuits. These reactors operate at pressures $< 50 \text{ mTorr}$ and the high density plasma etch reactors have plasma densities $\sim 10^{17} - 10^{18} \text{ m}^{-3}$. In this paper, the basic concepts of deposition and etch reactors will be given with attention to current modelling problems. Another low density modelling area is macro-particle contamination. Particles, on the order of a few microns in diameter, can block the etch lines and result in a defective device. The Direct Simulation Monte Carlo technique is being used to model both the etch/deposition and the particle contamination systems. Although these flows are clearly rarefied, they present different computational modelling difficulties than the traditional hypersonic/space DSMC applications.

1 Introduction

The microelectronics industry is currently pursuing low pressure etch and deposition reactor systems to achieve the uniformity which is required to meet the demands of gigascale integrated circuits. These reactors operate at pressures $< 50 \text{ mTorr}$ and the high density plasma etch reactors have plasma densities $\sim 10^{17} - 10^{18} \text{ m}^{-3}$ in an effort to achieve an high etch rate and anisotropic etching.[1-5] Examples of the plasma systems are the inductively coupled plasma (ICP) and electron cyclotron resonance (ECR) systems. High plasma density provides high ion fluxes to surfaces, which assures processing rates that match or exceed those of conventional high pressure (20-100 mTorr) reactive-ion etch (RIE) systems. Low gas pressures are necessary to ensure collisionless ion transport through plasma sheaths, which provides anisotropy in the ion flux directed toward the surface. This

This work was performed at Sandia National Laboratories which is operated for the DOE under contract number DE-AC04-94AL85000. The work was funded by a DOE Sandia/SEMATECH CRADA for plasma etch modelling.

T. J. Bartel

enables etching of high aspect-ratio features. Etching uniformity over large area (> 200 mm diameter) wafers is of particular importance in these systems as the trend is towards large area, single-wafer processes. The minimum geometry for etching for 16Mbit DRAM memory chips is ~ 0.5 μm ; 256 Mbit chips will require 0.1 μm !

The transport of contaminants, macro particles, in these reactors before, during, and after the etch process is becoming an increasing area of concern since a 0.5 μm particle can block an etch channel and render the final product useless. The transient fluid behavior in the chamber during these processes occurs in the 1 to 20 mTorr pressure range and the role of thermophoretic forces on particles at these low pressures is not understood.

Currently, empirical/experimental data are used extensively to guide the development of new systems. The numerical simulation techniques which have been developed in traditional rarefied gas dynamic applications can have a role in guiding experimental efforts to identify etch reactor designs that deliver a uniform flux of radicals and ions to the wafer, thereby achieving etch uniformity or deposition reactor designs that deliver a uniform flux of the feed gas to the surface. The Direct Simulation Monte Carlo Technique [6] is ideally suited for these processes since it has the capability of correctly modeling the high density inlet, the complex gas phase chemistry, and the multi-species transport in system.[7,8] The mean-free-path at 1 mTorr is 20 mm and the diameter of the wafer is 200 mm; the Knudsen number would indicate that the flow is transitional. The focus of this paper will be on the modeling concerns of plasma etch systems; the application to deposition systems is similar.[9]

2 Plasma Etch Reactors

The purpose of plasma etch is to produce a permanent feature on a thin film. This is illustrated in Figure 1.

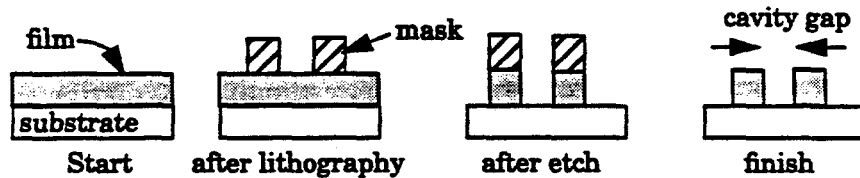


Figure 1- Pattern transfer using etch processes

The *feature scale* of the process refers to the minimum dimension of the process which is usually the gap width. There are three main characteristics or requirements of the process: anisotropy or directionality, selectivity, and damage. The anisotropy of the process is required to

T. J. Bartel

etch the bottom of the etch cavity and not the side walls to form vertical sides. The angle formed by the bottom and side walls is very critical in some applications: the allowable range is 88 - 91 degrees for one. The process selectivity refers to the ability to etch only the film material and not the mask or substrate. And minimizing damage of the substrate surface by high energy particles is required.

Plasma etching varies from chemical etching in that the charged particles have a much higher energy and their motion can be directed using electric or magnetic fields. In chemical etching, the neutrals (atoms, radicals, or molecules) will react with the film material and form volatile products which will be pumped away. This process does not have good anisotropy. In plasma and ion-enhanced etching, the ions will strike the surface and either physically remove material off due to momentum transfer (similar to sputtering) or will enhance the surface reaction between neutral atoms and the material. For example, in a chlorine etch system, the cavity will contain approximately 85 - 90% Cl atoms and 1 - 2% Cl⁺ ions. Therefore, the surface of the trench will be saturated with Cl; the incident Cl⁺ ions enhance the surface etch reaction of Si + 2Cl → SiCl₂ by an order-of-magnitude. If the substrate is negatively biased, the Cl⁺ ions will approach the surface in an orthogonal trajectory: preferentially etching the bottom of the trench. Thus, the ions enhance the etch rate and therefore the process speed as well as providing the required directionality.

Conditions typical of low pressure plasma etch systems are[10]:

pressure: 1 - 50 mTorr

neutral density: 10¹⁸ - 10²⁰ #/m³

degree of ionization: 1 - 10%

ion temperature: 300 - 600 K

electron temperature: 1 - 10 eV (hot electrons in cold plasma).

There are many candidate etch gases; most are compounds containing fluorine, chlorine and bromine: CF₄, SF₆, CCl₃F, CCl₄, Cl₂, CF₃Br, Br₂, HBr, HCl, CHCl₃, SiCl₄, SiF₄, etc. The etch products, SiF₄, SiCl₄ and SiBr₄ are the final products of etching silicon and are volatile-a requirement for removal from the system.

Chlorine etch of silicon is chosen to illustrate the general modeling requirements. Figure 2 shows an idealized geometry of such a system. The chamber is essentially cylindrical in shape. The chlorine is injected through a series of small diameter holes into the cavity either along the top or sides. External coils couple the power into the plasma to develop a region with a higher level of ionization than using biased electrodes. This is the region of the plasma *glow discharge*: the ionization of Cl₂ to Cl₂⁺, the dissociation of Cl₂ to 2Cl, and the excitation of Cl to Cl*. The discharge region will be larger with inductively coupled power addition than by charged electrodes; the resulting higher ionization will increase the etch rate.

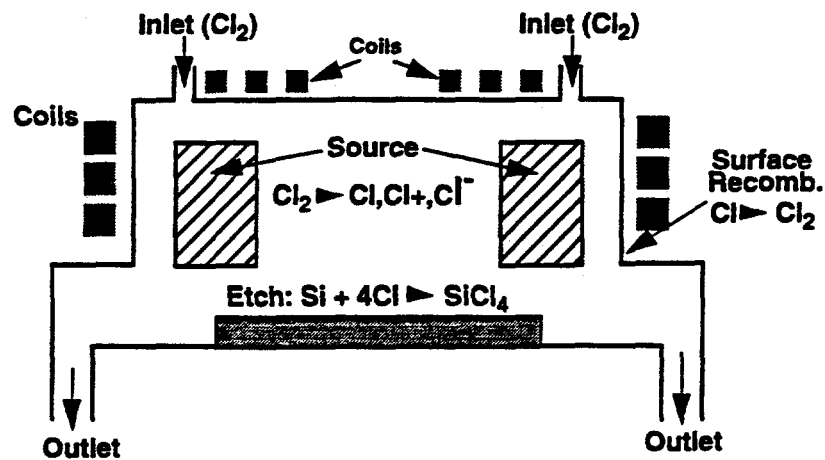


Figure 2- Typical Chlorine Plasma Etch Reactor Geometry

3 Process Modelling

The goal of process modelling is to be able to determine *a priori* the relative process/geometry figures of merit: growth/etch rates, uniformity, anisotropy, and selectivity. Various combinations of process parameters and system specifications can be combined to produce different electron and ion transport properties and fields which will result in different figures of merit. The process parameters include: external applied power, system gas pressure, gas flow rate and composition, and frequency of applied power. The system specifications include: cavity geometry, material types, and reaction scheme.

Historically, fluid or Navier-Stokes methods have been used to simulate these processes[11-13] even though their validity at these low pressures is questionable. The reason is simply that particle based techniques are computationally very intensive for these processes and PDE methods can be run in a reasonable time on advanced scientific workstations. Table 1 compares various modelling characteristics of the DSMC to fluid methods. It would appear obvious that the DSMC methods are superior to the fluid methods; the advent of the tremendous compute speedups available with massively parallel computer architectures has removed the serious cpu limitation. [14]

4 DSMC Modelling Issues

The traditional applications of the DSMC technique have been in hypersonic, low density flows; the present flows are very different and represent different modelling challenges.

Table 1: DSMC vs Fluid Models

DSMC	Fluid
Particle-based kinetic simulation	Solution of PDE equations of continuity
Provides species energy and angular distribution functions as output	Requires species energy distribution functions as input
More information about discharge (molecular level info.)	Less information about discharge (averages over dist. function)
Arbitrary 3-D geometries with complex boundary conditions	Boundary conditions may be difficult to specify
Robust (there is always a solution)	Convergence is not guaranteed
Computationally intensive	Workstation computing levels

First, the speed ratio for the material processing flows is very small; the mean gas velocities are ~ 2 m/s and the thermal velocities are ~ 300 m/s. This is in contrast to hypersonic flows where the speed ratios are very large with mean gas velocities of 1,000 - 10,000 m/s and thermal velocities of ~ 200 m/s. This difference is extremely important for computer time requirements. A typical characteristic time for a hypersonic simulation is 2 m / 6,000 m/s or approximately 10^{-4} s; a characteristic time for etch reactors, $\tau = PV/Q$ where $P = 0.002$ Torr, $V = 14$ l, and $Q = 70$ sccm is $\tau \sim 10^{-1}$ s. A typical time step for a hypersonic simulation is 10^{-6} - 10^{-7} s; a typical time step for the etch reactor is $5 \cdot 10^{-6}$ s due to the high energy ions and neutrals. Therefore, at least 10x more time steps are required for the etch simulations to resolve the subsonic nature of the flow; typical DSMC simulations performed at Sandia have from 50,000 to 200,000 time steps. This problem is analogous to using a compressible CFD code for an incompressible flow problem. To perform these kinds of simulations in the routine and frequent manner required for design loop simulation requires the performance of a massively parallel computer. We have achieved a speedup of 40x a single Cray Y/MP processor using a 1024 node nCUBE-2 and a speedup of 100x the Cray using a 512 node Intel Paragon. This compute performance has enabled design optimization simulations to be performed of etch systems.

Second, the boundary conditions are very different. Typically the hypersonic case has a defined freestream inflow and a non-reentrant

T. J. Bartel

outflow condition. The etch reactors are internal flow systems: the inflow is typically from discrete points of ~ 1 mm diameter and the outflow is defined by the pumping speed of a vacuum pump—an elliptic outflow boundary condition. The expansion flow from the injection points can be considered a sonic expansion due to the pressure ratios and modelled as a point source boundary in the DSMC grid. The vacuum pump presents some interesting modelling issues. Actually, at the low pressure and gas mixtures of interest, the vacuum pump speed is typically not well characterized; in operation the pump speed is adjusted to maintain a pressure somewhere in the system. Therefore, a outflow boundary feedback loop based on pressure in the system is needed to obtain the correct operating flows. Since this is a solution of the flowfield, this adds additional unsteady iteration steps for the DSMC simulation and increases the CPU requirements.

Third, gas-surface chemistry is very important and the etch rate distribution is one of the primary diagnostic results from the simulation. This chemistry is poorly understood. Present models base the etching on the ratio of the ion-to-neutral surface flux; therefore, the probability of surface chemistry depends on the flow field--yet another requirement for increased CPU performance.

Finally, 3-D simulations in traditional DSMC applications are performed because the geometry is 3-D. Most reactor system geometries are basically symmetric—to achieve an uniform etch rate. However, the boundary conditions are not; the injection ports are discrete and their plume expansion can lead to etch nonuniformity. Also, most pumping ports are located to the side of the wafer resulting in an asymmetric outflow. Therefore, cylindrical symmetry can be used to simplify the 3-D simulations.

5 Example DSMC Simulations

5.1 Neutral Flow

Figure 3 shows the geometry and results of a typical reactor geometry. This system is cylindrically symmetric with a symmetric outflow condition; two pressure gauges were modelled. The gas for this case was nitrogen; the calculation required approximately 7 hours of cpu time on a 256 node nCUBE-2 to obtain 100,000 time steps. Of interest in this case is the pressure gradient in the gauge. Also, due to the low pressures, there is a difference between the gas pressure approximated as nkT and the surface pressure computed as the normal momentum difference. Figure 4 shows the radial distribution of this difference for a geometry similar to that in Figure 3 but without the pressure gauges; the surface pressure from the particle impact is 2 - 5% higher than the equilibrium gas pressure near the surface.

outflow condition. The etch reactors are internal flow systems: the inflow is typically from discrete points of ~ 1 mm diameter and the outflow is defined by the pumping speed of a vacuum pump—an elliptic outflow boundary condition. The expansion flow from the injection points can be considered a sonic expansion due to the pressure ratios and modelled as a point source boundary in the DSMC grid. The vacuum pump presents some interesting modelling issues. Actually, at the low pressure and gas mixtures of interest, the vacuum pump speed is typically not well characterized; in operation the pump speed is adjusted to maintain a pressure somewhere in the system. Therefore, a outflow boundary feedback loop based on pressure in the system is needed to obtain the correct operating flows. Since this is a solution of the flowfield, this adds additional unsteady iteration steps for the DSMC simulation and increases the CPU requirements.

Third, gas-surface chemistry is very important and the etch rate distribution is one of the primary diagnostic results from the simulation. This chemistry is poorly understood. Present models base the etching on the ratio of the ion-to-neutral surface flux; therefore, the probability of surface chemistry depends on the flow field—yet another requirement for increased CPU performance.

Finally, 3-D simulations in traditional DSMC applications are performed because the geometry is 3-D. Most reactor system geometries are basically symmetric—to achieve an uniform etch rate. However, the boundary conditions are not; the injection ports are discrete and their plume expansion can lead to etch nonuniformity. Also, most pumping ports are located to the side of the wafer resulting in an asymmetric outflow. Therefore, cylindrical symmetry can be used to simplify the 3-D simulations.

5 Example DSMC Simulations

5.1 Neutral Flow

Figure 3 shows the geometry and results of a typical reactor geometry. This system is cylindrically symmetric with a symmetric outflow condition; two pressure gauges were modelled. The gas for this case was nitrogen; the calculation required approximately 7 hours of cpu time on a 256 node nCUBE-2 to obtain 100,000 time steps. Of interest in this case is the pressure gradient in the gauge. Also, due to the low pressures, there is a difference between the gas pressure approximated as nkT and the surface pressure computed as the normal momentum difference. Figure 4 shows the radial distribution of this difference for a geometry similar to that in Figure 3 but without the pressure gauges; the surface pressure from the particle impact is 2 - 5% higher than the equilibrium gas pressure near the surface.

T. J. Bartel

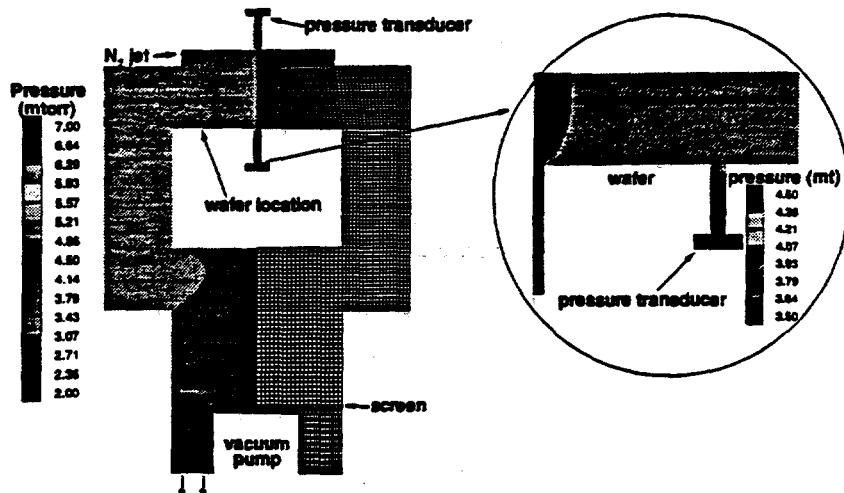


Figure 3- Pressure distribution in neutral flow

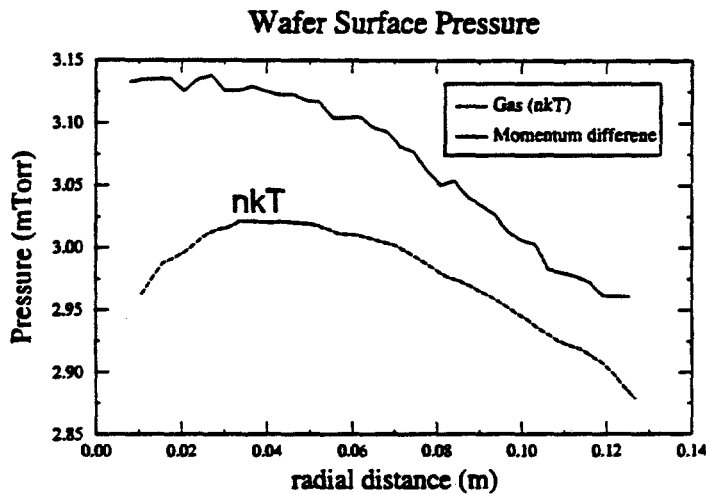


Figure 4 - Surface pressure profiles

5.2 Plasma Flow

Figure 5 shows the neutral Cl and Cl₂ mole fraction distribution in a sample plasma etch reactor configuration. The conditions were: 70 sccm Cl₂ injection, 3.4 kW RF power deposition, and 2 mTorr at the center of the pump inlet. This corresponds to an average power deposition of 0.2 w/cm³ and a peak value of 2.3 w/cm³. These results are for the RF cycle averaged conditions; the electron distribution was obtained by an external fluid model which was then used to determine

T. J. Bartel

the spatially varying ionization/dissociation rates and space charge fields. Six species were modelled in the DSMC simulation: Cl, C⁺, Cl⁻, Cl₂, Cl₂⁺, and SiCl₂. The large dissociation of Cl₂ is clearly seen; the system comes to equilibrium with a large fraction of neutral Cl.

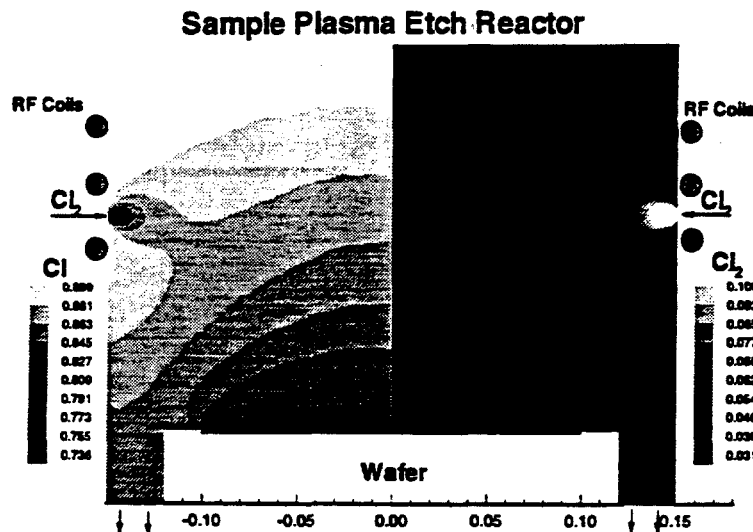


Figure 5 - Mole fraction distributions of neutral Cl and Cl₂.

Table 2 shows the 12 gas phase reactions which were modeled: 6 were due to heavy particle interactions and 6 due to electron impact chemistry. Effects such as the Franck-Condon energy of the Cl₂ dissociation is easily added to a particle simulation to determine the post dissociation energy distribution of the fragments.

Table 2: Gas phase reactions for the chlorine etch system

- 1- Cl⁺ + Cl \rightarrow Cl + Cl⁺
- 2- Cl⁺ + Cl₂ \rightarrow Cl + Cl₂⁺
- 3- Cl₂⁺ + Cl₂ \rightarrow Cl₂ + Cl₂⁺
- 4- Cl₂⁺ + Cl \rightarrow Cl₂ + Cl⁺
- 5- Cl⁺ + Cl⁻ \rightarrow Cl + Cl
- 6- Cl₂⁺ + Cl \rightarrow 2Cl + Cl
- 7- Cl₂ + e \rightarrow 2Cl + e
- 8- Cl₂ + e \rightarrow Cl₂⁺ + 2e
- 9- Cl + e \rightarrow Cl⁺ + 2e
- 10- Cl₂ + e \rightarrow Cl + Cl⁻
- 11- Cl⁻ + e \rightarrow Cl + 2e
- 12- Cl₂⁺ + e \rightarrow 2Cl

T. J. Bartel

Figure 7 shows the Cl^+ and SiCl_2 mole fraction distribution. The etch rate is primarily determined by the Cl^+ -ion enhanced etching. At these low pressures, the etch product, SiCl_2 , can diffuse into the chamber. Ionization of the etch product has not been included in this simulation. Finally, figure 8 shows the radial etch distribution for this simulation. For the given conditions and models, the etch rate is not very uniform.

Sample Plasma Etch Reactor

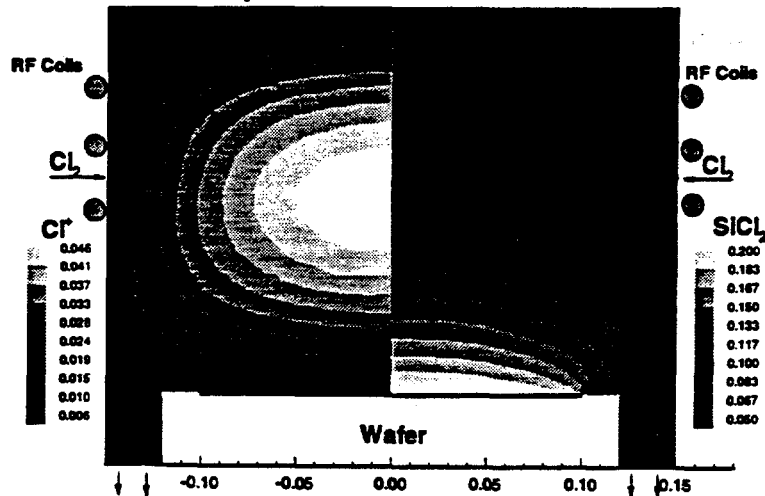


Figure 6 - Mole fraction distributions of Cl^+ and SiCl_2

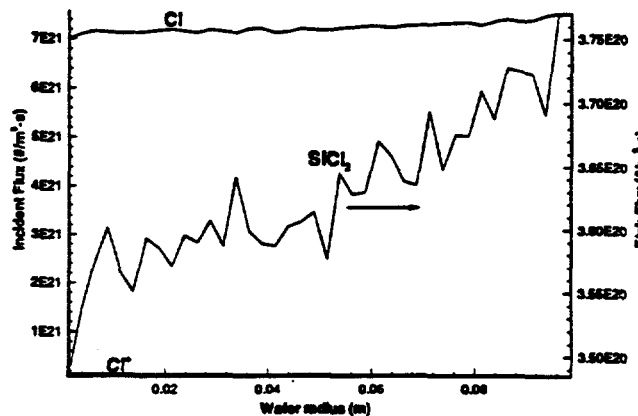


Figure 7 - Radial distribution of etch rate and incident Cl and Cl^+ flux.

6 Summary

The DSMC method is ideally suited to simulate material processing applications such as plasma etch/deposition systems at low pressure.

T. J. Bartel

Due to the nature of the flow, the computing requirements are much higher than for typical hypersonic applications. The massively parallel computers provide the enabling technology to apply the method as a design capability for future etch reactor design.

7 Acknowledgments

The work by Dr. Steve Plimpton at Sandia on the massively parallel version of DSMC has enabled this work to be done. Prof. Demetre Economou of the University of Houston has shared his extensive knowledge of chlorine plasma etch chemistry and is helping to implement it into the DSMC-MP code.

8 References

- 1 Lieberman, M. A. and Gottscho, R. A. "Design of High Density Plasma Sources for Materials Processing," *Physics of Thin Films*, Academic Press, New York, 1993.
- 2 McKillop, J. S., Forster, J. C., and Holber, W. M., *Appl. Phys. Lett.* **55**, 30, 1989.
- 3 Gorbatkin, S. M., Berry, L. A., and Roberto, J. B., *J. Vac. Sci. Technol. A* **8**, 2893, 1990.
- 4 Asmussen, J., *J. Vac. Sci. Tech. A* **7** 883, 1989.
- 5 Hopwood, J., "Electron cyclotron resonance microwave discharge for etching and thin-film deposition," *Plasma Sources Sci. Technol.*, **1** 109, 883-893, 1992.
- 6 Bird, G. A., *Molecular Gas Dynamics and the Direct Simulation of Gas Flows*, Clarendon Press - Oxford, 1994.
- 7 Nanbu, K, "Rarefied Gas Dynamics Problems on Fabrication Processes of Semiconductor Films", Proceeding of 15th RGD, Grado, Italy, 1986.
- 8 Igarashi, S., Nanbu, K., Mitamura, S., and Sugawara, T., "Growth Rate of Films in Low-Pressure CVD Reactors", Proceeding of 17th RGD, 1990.
- 9 Coronell, D. G. and Jensen, K. F., "Analysis of Transition Regime Flows in Low Pressure Chemical Vapor Deposition Reactors Using the Direct Simulation Monte Carlo Method", *J. Electrochem. Soc.*, Vol. 139, 8, 2264-2273, 1992.
- 10 Salimian, M., *Plasma Etching: Technologies and Processes*, University Consortium for Continuing Education, 1993.
- 11 Ventzek, P. L. G., Hoekstra, R. J. and Kushner, M. J. "2-Dimensional Modeling of High Plasma Density Inductively Coupled Sources for Materials Processing," *J. Vac. Sci. Tech. B*, **12** 461-477, 1994.
- 12 Stewart, R. A., Vitello, P., and Graves, D. B. "2-Dimensional Fluid Model of High Density Inductively Coupled Plasma Sources," *J. Vac. Sci. Tech. B*, **12** 478-485, 1994.
- 13 Park, S. and Economou, D. J. "Numerical Simulation of a Single-Wafer Isothermal Plasma Etching Reactor", *J. Electrochem. Soc.*, Vol. 137, 8, 2624-2634, 1990.
- 14 Bartel, T. and Plimpton, S. "DSMC Simulation of Rarefied Gas Dynamics on a Large Hypercube Supercomputer", AIAA 92-2860, 1992.

Modelling of Plasma Etching Discharges

T. J. Bartel* and **D. J. Economou****

**Sandia National Laboratories, USA*

tjbarte@cfd.sandia.gov

***University of Houston, USA*

economou@uh.edu

Abstract. The microelectronics industry is currently pursuing low pressure etch and deposition reactor systems to achieve the uniformity required to meet the demands of gigascale integrated circuits. These reactors operate at pressures < 50 mTorr and the high density plasma etch reactors have plasma densities $\sim 10^{17} - 10^{18} \text{ m}^{-3}$. In this paper, the basic concepts of the Direct Simulation Monte Carlo (DSMC) technique, a particle based simulation method, are presented and modeling issues pertinent to these reactor configurations described. These flows present different modelling difficulties than the traditional hypersonic/space DSMC applications. Example simulations for neutral and plasma flows will be presented to illustrate the simulation technique.

1 Introduction

The microelectronics industry is currently pursuing low pressure etch and deposition reactor systems to achieve the uniformity which is required to meet the demands of gigascale integrated circuits. These reactors operate at pressures < 50 mTorr and the high density plasma etch reactors have plasma densities $\sim 10^{17} - 10^{18} \text{ m}^{-3}$ in an effort to achieve an high etch rate and anisotropic etching. [1-5] Examples of the plasma systems are the inductively coupled plasma (ICP) and electron cyclotron resonance (ECR) systems. High plasma density provides high ion fluxes to surfaces, which assures processing rates that match or exceed those of conventional high pressure (20-100 mTorr) reactive-ion etch (RIE) systems. Low gas pressures are necessary to ensure collisionless ion transport through plasma sheaths, which provides anisotropy in the ion flux directed toward the surface. This enables etching of high aspect-ratio features. Etching uniformity over large area (> 200 mm diameter) wafers is of particular importance in these systems as the trend is towards large area, single-wafer processes.

Currently, empirical/experimental data are used extensively to guide the development of new systems. The numerical simulation techniques which have been developed in traditional rarefied gas dynamic applications can have a role in guiding experimental efforts to identify etch reactor designs that deliver a uniform flux of radicals and ions to the wafer, thereby achieving etch uniformity or deposition reactor designs that deliver a uniform flux of the feed gas to the surface. The Direct Simula-

tion Monte Carlo Technique [6] is ideally suited for these processes since it has the capability of correctly modelling the high density inlet, the complex gas phase chemistry, and the multi-species transport in system.[7,8] The mean-free-path at 1 mTorr is 100 mm and the diameter of the wafer is 200 mm; the Knudsen number, $Kn = \lambda/L$ where λ is the mean free path, would indicate that the flow is transitional. Simulations have been performed for the neutral flow in different etch systems[7,8,19,20,21,22] and for deposition systems[9]. However, the DSMC method was only used to predict the neutral flow in these applications. The focus of this paper will be on the modeling concerns of plasma etch systems and the application of the DSMC technique to predict the transport of neutral, ions, and electrons.

2 Direct Simulation Monte Carlo

A) Method

DSMC is a method for the direct simulation of rarefied gas flows[6]. The method assumes that the gas is a dilute gas; that is, binary collisions dominate the molecular interactions. The flow domain is first divided in a number of cells. The cell size is determined by the local mean free path λ ; a size $\sim \lambda/3$ is typically recommended. Unlike CFD grids with mesh orthogonality and one-to-one cell side correspondence constraints, the DSMC grid system serves only to identify a volume for choosing collision partners and for obtaining sampling statistics. The flow field is simulated using a number of computational particles (some 10^7 particles are not atypical for runs on massively parallel supercomputers). Particles consist of all kinds of species such as radicals, ions, and molecules. The species type, spatial coordinates, velocity components, internal energy partitioning, and weight factor of each computational particle are stored. As the particles move through the domain, they collide with one another and with surfaces. New particles may be added at specified inlet port locations, and particles may be removed from the simulation due to chemical reactions or through the pumping ports.

The basic premise of DSMC is that the motion of simulated particles can be decoupled from their collisions over a time step. The size of the time step is selected to be a small fraction of the mean collision time, or a fraction of the transit time of a molecule through a cell (similar to an explicit CFL constraint). During the motion phase, molecules move in free molecular motion according to their starting velocity and any forces acting on the molecules (for example the Lorentz force on charged species). During this phase, molecules may cross cell boundaries, collide with walls, or exit the flow field. During the collision phase, collision pairs are selected from within each cell *regardless of the position* of the molecules within the cell. The no-time-counter (NTC) technique [15], was used to determine the computational particle collision frequency. The number of pairs to be selected from a given cell at a time step is

$$\# \text{ pairs} = 1/2 N \bar{N} F_n (\sigma_T C_r)_{\max} \Delta t / V$$

where N is the number of computational particles in the cell, F_n the number of real particles per sim-

ulated one, $(\sigma_T C_r)_{\max}$ is the maximum of the product of the total cross-section and relative velocity for the pairs in the cell and V the cell volume. The pair collision is then computed with a probability $(\sigma_T C_r) / (\sigma_T C_r)_{\max}$. This technique does not have the disadvantages of the older time counter (TC) method while maintaining computational efficiency, i.e., the simulation time is proportional to the number of molecules. This is a great advantage of DSMC as compared to other particle simulation methods such as molecular dynamics. Also, the NTC method allows for unsteady flows to be simulated in a time accurate manner.

Because of the axisymmetric nature of the reactor problems only two position coordinates (r, z) of each simulated particle need be stored. However, collisions are handled as three dimensional events to correctly conserve momentum. The molecular model used was the variable hard sphere (VHS) model [6]. According to this model, the collision cross section σ_{ij} depends on the relative speed of the colliding partners E_c as

$$\sigma_{ij} = A_{ij} E_c^{-\omega} \quad (2)$$

where A_{ij} is a constant and $\omega = s - 0.5$, with s the exponent of the dependence of the coefficient of viscosity on temperature. The chief advantage of the VHS model is that, although the collision diameter is allowed to vary with the relative speed (unlike the constant cross section hard sphere model), when a collision does occur, the post-collision velocity components are computed as if it were a hard sphere collision; that is, isotropic scattering in the center of mass frame of reference.

A deficiency of the VHS model is that the ratio of the momentum to the viscosity cross-section follows the hard sphere value which differs from the real gas values; there is no coupling between the relative velocity and the post-collision deflection angle. In the variable soft sphere (VSS) model[17], the cross-section is a function of the Schmidt number, ratio of the viscosity to diffusion, as well as the viscosity. The deflection angle is now a function of the Schmidt number. The net effect is that species diffusion in reactor subsonic flow fields is better modelled.

The DSMC technique can easily model internal energy modes: rotational and vibrational energies. The phenomenological Borgnakke and Larsen [16] model is used to determine the post-collision internal energy partitioning given the number of internal degrees of freedom of each species. This is a harmonic oscillator model which drives the post-collision energy distribution toward equilibrium. Recently, Marriott[18] has applied the Maximum Entropy strategy for particle systems to obtain this energy distribution; unfortunately, the complex chemical species in typical etch systems are poorly characterized. Typically, only translational nonequilibrium is modelled.

B) Reactor Modelling Issues

The traditional applications of the DSMC technique have been in hypersonic, low density flows; the present flows are very different and represent different modelling challenges. Figure 1 shows a typical etch reactor using chlorine chemistry. This system is characterised as a subsonic, chemically reacting, internal flow.

1) Subsonic Flow

First, the speed ratio for the material processing flows is very small; the mean gas velocities are ~ 2 m/s and the thermal velocities are ~ 300 m/s. This is in contrast to hypersonic flows where the speed ratios are very large with mean gas velocities of 1,000 - 10,000 m/s and thermal velocities of ~ 200 m/s. This difference is extremely important for computer time requirements. A typical characteristic time for a hypersonic simulation is 2 m / 6,000 m/s or approximately 10^{-4} s; a characteristic time for etch reactors, $\tau = PV/Q$ where $P = 0.002$ Torr, $V = 14$ l, and $Q = 70$ sccm is $\tau \sim 10^{-1}$ s. A typical time step for a hypersonic simulation is 10^{-6} - 10^{-7} s; a typical time step for the etch reactor is $5 \cdot 10^{-6}$ s due to the high energy ions and neutrals. Therefore, at least 10x more time steps are required for the etch simulations to resolve the subsonic nature of the flow; typical DSMC simulations performed at Sandia have from 50,000 to 200,000 time steps. This problem is analogous to using a compressible CFD code for an incompressible flow problem. To perform these kinds of simulations in the routine and frequent manner required for design loop simulation requires the performance of a massively parallel computer[14]. As illustrated in Figure 2, we have achieved a speedup of 40x a single Cray Y/MP processor using a 1024 node nCUBE-2 and a speedup of 100x the Cray using a 512 node Intel Paragon for a detailed nozzle expansion problem. This compute performance has enabled design optimization simulations to be performed of etch systems.

2) Inflow/Outflow Boundary Conditions

The etch reactors are internal flow systems: the inflow is typically from discrete points of ~ 1 mm diameter and the outflow is defined by the pumping speed of a vacuum pump--an elliptic outflow boundary condition. The expansion flow from the injection points can be considered a sonic expansion due to the pressure ratios and modelled as a point source boundary in the DSMC grid. The inward component of the velocity is selected in proportion to the distribution function: $h(v) = (v + c_s) \{ \exp(-\alpha v)^2 \}$ where c_s is the local speed of sound, and $\alpha = [M_{Cl_2}/(2RT_{gi})]^{1/2}$, with M_{Cl_2} being the molecular weight of Cl_2 , R the universal gas constant, and T_{gi} the inlet gas temperature. The other two velocity components were selected from a Maxwellian at the choked flow temperature. The acceptance-rejection method[6] was used to sample $h(v)$; only velocities valid for incoming particles are accepted. The vacuum pump presents some interesting modelling issues. Actually, at the low pressure and gas mixtures of interest, the vacuum pump speed is typically not well characterized; in operation the pump speed is adjusted to maintain a pressure somewhere in the system. Therefore, a outflow boundary feedback loop based on pressure in the system is needed to obtain the correct operating flows. Since this is a solution of the flowfield, this adds additional unsteady iteration steps for the DSMC simulation and increases the CPU requirements.

3) Sheath

The sheath thickness in these systems is very small and typically much smaller than the DSMC mesh cell adjacent to surfaces. The computational particle transport in this cell is treated differently than in the interior of the domain. First we use a time step subcycling procedure for the charged par-

particle move portion of the time step. In this procedure, we subdivide the global time step from 30 to 45 times to *move* the charged particle in the sheath. This is done to correctly integrate the effect of the Lorentz force on the particle during the global time step and increase its velocity as it accelerates to the surface. We also do not allow particle collisions in these cells; since the DSMC method arbitrary obtains its collision partners from the cell, unrealistic collisions can result from the charged particle stream. This assumption is valid since the cell sizes are typically 1 - 2 mm and the mean-free-path is from 10 - 100 mm.

4) Electrons

The DSMC technique has been applied to combined systems of neutral, ions and electrons[23]; however, these were weakly coupled systems without external fields and only ambipolar diffusion for the charged particle transport. There is no conceptual reason why the method cannot be used to model all these particle types in a reactor system; the limitation may be simply a matter of computational resources required to capture the disparate time scales. In the present work, we have modelled the electrons as a fluid in a separate electron/Poisson solver[24]. In this hybrid strategy, the spatially varying electron impact chemistry rates and the fields from the glow discharge model are used in the DSMC code to model the charged particle sources and sinks and their transport.

5) Chemistry

Chemical reactions, both particle-particle and particle-surface are readily modelled. Particle-particle reactions are typically modelled using steric factors derived from Arrhenius reaction rates. Surface chemistry models can vary from a simple reaction probability model to a model which has both a threshold energy and is a function of available activation sites. The complexity of the model is limited only by the available data.

6) Computational Particle Weight Factors

Finally, spatial and species weights have to be used to account for the geometric variation in grid volumes as a function of radius and for trace species. These weights are used to optimize the number of computational particles in a grid cell. Typical simulations have approximately 50 - 200 computational particles per cell to capture the correct chemical composition.

C) DSMC vs Fluid Models

Historically, fluid or Navier-Stokes methods have been used to simulate these processes[11-13] even though their validity at these low pressures is questionable. The reason is simply that particle based techniques are computationally very intensive for these processes and PDE methods can be run in a reasonable time on advanced scientific workstations. Table 1 compares various modelling characteristics of the DSMC to fluid methods. It would appear obvious that the DSMC methods are superior to the fluid methods; the advent of the tremendous compute speedups available with massively parallel

computer architectures has removed the serious cpu limitation. [14]

Table 1: DSMC vs Fluid Models

DSMC	Fluid
Particle-based kinetic simulation	Solution of PDE equations of continuity
Provides species energy and angular distribution functions as output	Requires species energy distribution functions as input
More information about discharge (molecular level info.)	Less information about discharge (averages over dist. function)
Arbitrary 3-D geometries with complex boundary conditions	Boundary conditions may be difficult to specify
Robust (there is always a solution)	Convergence is not guaranteed
Computationally intensive	Workstation computing levels

3 Example DSMC Simulations

A) Neutral Flow

Figure 3 shows the geometry and results of a typical reactor geometry. This system is cylindrically symmetric with a symmetric outflow condition; two pressure gauges were modelled. The gas for this case was nitrogen; the calculation required approximately 7 hours of cpu time on a 256 node nCUBE-2 to obtain 100,000 time steps. Of interest in this case is the pressure gradient in the gauge. The measured pressure in the bottom of the gauge is different from the desired surface pressure. Also, due to the low pressures, there is a difference between the gas pressure approximated as nkT and the surface pressure computed as the normal momentum difference. Figure 4 shows the radial distribution of this difference for a geometry similar to that in Figure 3 but without the pressure gauges; the surface pressure from the particle impact is 2 - 5% higher than the equilibrium gas pressure near the surface.

The recent work of Shufflebotham[25] has validated the DSMC technique against experimental pressure measurements obtained from a nitrogen gas system. The DSMC code was run in a predictive manner; there was excellent agreement between the predicted and measured pressures.

B) Plasma Flow

Figure 5 shows the neutral Cl and Cl_2 mole fraction distribution in a sample plasma etch reactor configuration. The conditions were: 70 sccm Cl_2 injection, 3.4 kW RF power deposition, and 2 mTorr at

the center of the pump inlet. This corresponds to an average power deposition of 0.2 w/cm³ and a peak value of 2.3 w/cm³. These results are for the RF cycle averaged conditions; the electron distribution was obtained by an external fluid model which was then used to determine the spatially varying ionization/dissociation rates and space charge fields. Six species were modelled in the DSMC simulation: Cl, Cl⁺, Cl⁻, Cl₂, Cl₂⁺, and SiCl₂. The large dissociation of Cl₂ is clearly seen; the system comes to equilibrium with a large fraction of neutral Cl.

Table 2 shows the 12 gas phase reactions which were modeled: 6 were due to heavy particle interactions and 6 due to electron impact chemistry. Effects such as the Frank-Condon energy of the Cl₂ dissociation is easily added to a particle simulation to determine the post dissociation energy distribution of the fragments.

Table 2: Gas phase reactions for the chlorine etch system

- 1- Cl⁺ + Cl \rightarrow Cl + Cl⁺
- 2- Cl⁺ + Cl₂ \rightarrow Cl + Cl₂⁺
- 3- Cl₂⁺ + Cl₂ \rightarrow Cl₂ + Cl₂⁺
- 4- Cl₂⁺ + Cl \rightarrow Cl₂ + Cl⁺
- 5- Cl⁺ + Cl⁻ \rightarrow Cl + Cl
- 6- Cl₂⁺ + Cl⁻ \rightarrow 2Cl + Cl
- 7- Cl₂ + e \rightarrow 2Cl + e
- 8- Cl₂ + e \rightarrow Cl₂⁺ + 2e
- 9- Cl + e \rightarrow Cl⁺ + 2e
- 10- Cl₂ + e \rightarrow Cl + Cl⁻
- 11- Cl⁻ + e \rightarrow Cl + 2e
- 12- Cl₂⁺ + e \rightarrow 2Cl

Figure 7 shows the Cl⁺ and SiCl₂ mole fraction distribution. The etch rate is primarily determined by the Cl⁺-ion enhanced etching. At these low pressures, the etch product, SiCl₂, can diffuse into the chamber. Ionization of the etch product has not been included in this simulation. Finally, figure 8 shows the radial etch distribution for this simulation. For the given conditions and models, the etch rate is not very uniform.

Further discussion of the application of the DSMC technique to this geometry and chlorine chemistry can be found in ref. 26.

4 Summary

The DSMC method is ideally suited to simulate material processing applications such as plasma etch/deposition systems at low pressure. Due to the nature of the flow, the computing requirements are much higher than for the method's traditional hypersonic applications. Massively parallel computers provide the enabling technology to apply the method as a design capability for future etch reactor design. Current work has benchmarked the method for neutral flow in reactor systems and has shown its predictive capabilities. Further work is needed to implement the necessary physics to have a self-consistent numerical model for the plasma etch system.

5 Acknowledgments

The work by Dr. Steve Plimpton at Sandia on the massively parallel version of DSMC has enabled this work to be done. Also, the lively discussions with Dr. Wahid Hermina at Sandia on applying the DSMC technique to plasma etch systems is greatly appreciated. This work was performed at Sandia National Laboratories which is operated for the DOE under contract number DE-AC04-94AL85000. The work was funded by a Sandia LDRD, the Sandia/SEMATECH CRADA for plasma etch modelling and the National Science Foundation (CTS-9216023).

6 References

- 1 Lieberman, M. A. and Gottscho, R. A. "Design of High Density Plasma Sources for Materials Processing," **Physics of Thin Films**, Academic Press, New York, 1993.
- 2 McKillop, J. S., Forseter, J. C., and Holber, W. M., *Appl. Phys. Lett.* 55, 30, 1989.
- 3 Gorbatkin, S. M., Berry, L. A., and Roberto, J. B., *J. Vac. Sci. Technol. A* 8, 2893, 1990.
- 4 Asmusen, J., *J. Vac. Sci. Tech. A* 7 883, 1989.
- 5 Hopwood, J., "Electron cyclotron resonance microwave discharge for etching and thin-film deposition," *Plasma Sources Sci. Technol.*, 1 109, 883-893, 1992.
- 6 Bird, G. A., **Molecular Gas Dynamics and the Direct Simulation of Gas Flows**, Clarendon Press - Oxford, 1994.
- 7 Nanbu, K, "Rarefied Gas Dynamics Problems on Fabrication Processes of Semiconductor Films", Proceeding of 15th RGD, Grado, Italy, 1986.
- 8 Igarashi, S., Nanbu, K., Mitamura, S., and Sugawara, T., "Growth Rate of Films in Low-Pressure CVD Reactors", Proceeding of 17th RGD, 1990.
- 9 Coronell, D. G. and Jensen, K. F., "Analysis of Transition Regime Flows in Low Pressure Chemical Vapor Deposition Reactors Using the Direct Simulation Monte Carlo Method", *J. Electrochem. Soc.*, Vol. 139, 8, 2264-2273, 1992.
- 10 Salimian, M., **Plasma Etching: Technologies and Processes**, University Consortium for Continuing Education, 1993.
- 11 Ventzek, P. L. G., Hoekstra, R. J. and Kushner, M. J. "2-Dimensional Modeling of High Plasma Density Inductively Coupled Sources for Materials Processing," *J. Vac. Sci. Tech. B*, 12 461-477, 1994.
- 12 Stewart, R. A., Vitello, P., and Graves, D. B. "2-Dimensional Fluid Model of High Density Inductively Coupled Plasma Sources," *J. Vac. Sci. Tech. B*, 12 478-485, 1994.
- 13 Park, S. and Economou, D. J. "Numerical Simulation of a Single-Wafer Isothermal Plasma Etching Reactor", *J. Electrochem. Soc.*, Vol. 137, 8, 2624-2634, 1990.
- 14 Bartel, T. and Plimpton, S. "DSMC Simulation of Rarefied Gas Dynamics on a Large Hypercube Supercomputer", *AIAA 92-2860*, 1992.
- 15 Hermina, W. L., Monte Carlo simulation of transitional flow around simple shaped bodies, *Proceedings of the 15th International Symp. on Rarefied Gas Dynamics*, Volume I, pp. 451-460 (1986).

- 16 Borgnakke, C. and P. S. Larsen, Statistical collision model for Monte Carlo simulation of polyatomic gas mixtures, *J. Comp. Phys.*, 18, 405-420 (1975).
- 17 Koura, K. and Matsumoto, H., "Variable Soft Sphere Molecular Model for Inverse-Power-Law or Lennard-Jones Potential, *Phys. Fluids A* 3, 2459-2465 (1991).
- 18 Marriott, P., "Non-Equilibrium Chemical Reactins in the Simulation of Hypersonic Rarefied Flows", Ph.D. Thesis, Dept. of Aeronautics, Imperial College of Science, Tech. and Medicine, London (1994).
- 19 A. Kersch, W. Morokoff and Chr. Werner, Selfconsistent simulation of sputter deposition with the Monte Carlo method, *J. Appl. Phys.*, 75, 2278-2285 (1994).
- 20 A. M. Myers, J. R. Doyle, and D. N. Ruzic, Monte Carlo simulations of sputter atom transport in low-pressure sputtering: the effects of interaction potential, sputter distribution and system geometry, *J. Appl. Phys.*, 72, 3064-3071 (1992).
- 21 H. M. Urbassek and D. Sibold, Sputtered atom transport in high-current gas discharges: A self-consistent computer simulation study, *J. Vac. Sci. Technol. A*, 11, 676-681 (1993).
- 22 M. D. Kilgore, H. M. Wu and D. B. Graves, Neutral transport in high density reactors, *J. Vac. Sci. Technol. B*, 12, 494-506 (1994).
- 23 M. A. Gallis and J. K. Harvey, The Maximum Entropy Approach Applied to Energy Exchange, Chemical Rections and Ionisation in the DSMC Method for Rarefied Hypersonic Flows, ISSN 0308-7247, Imperial College of Science Technology & Medicine (1993).
- 24 D. P. Lymberopoulos and D. J. Economou, Modeling and simulation of glow discharge plasma reactors, *J. Vac. Sci. Technol. A*, 12, 1229-1236 (1994).
- 25 P. K. Shufflebotham, T. J. Bartel, and B. Berney, Experimental validation of a Direct Simulation by Monte Carlo Molecular Gas Model, presented at the 41st AVS meeting, Denver, CO (1994).
- 26 D. J. Economou, T. J. Bartel, R. S. Wise, and D. P. Lymberopoulos, Two-Dimensional Direct Simulation Monte Carlo (DSMC) of reactive neutral and ion flow in a high density plasma reactor, presented at the 41st AVS meeting, Denver, CO (1994).

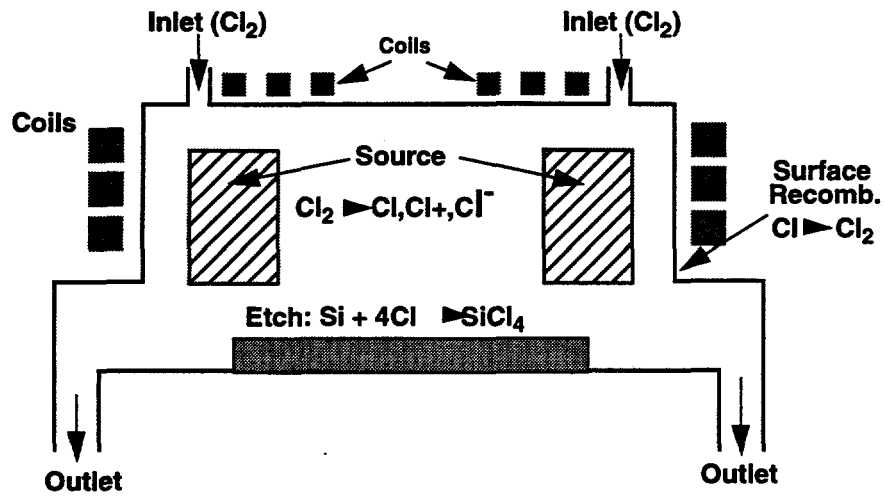


Figure 1- Typical Chlorine Plasma Etch Reactor Geometry

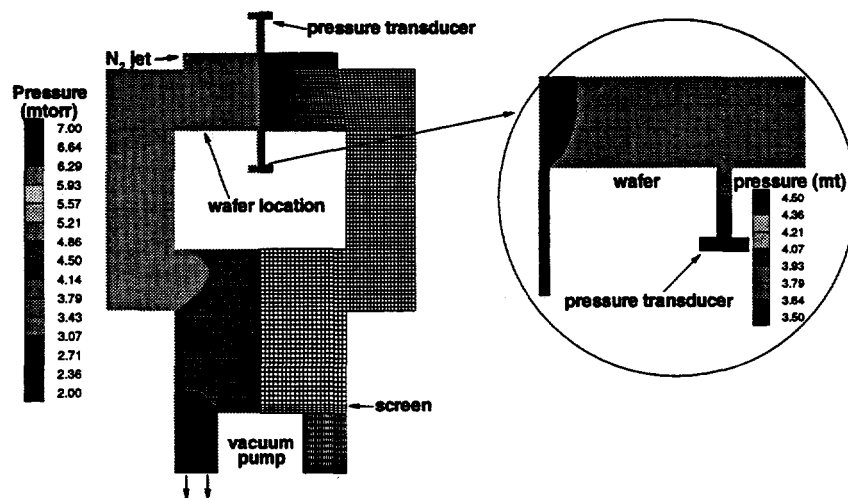


Figure 3 - Pressure distribution in neutral flow.

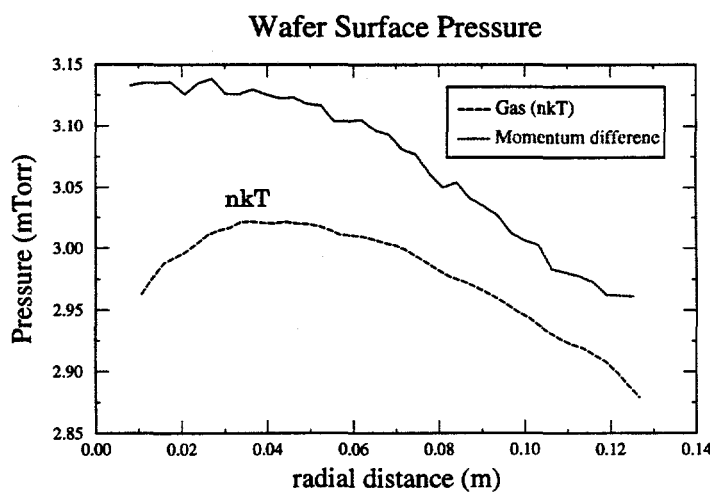


Figure 4 - Surface pressure profiles.

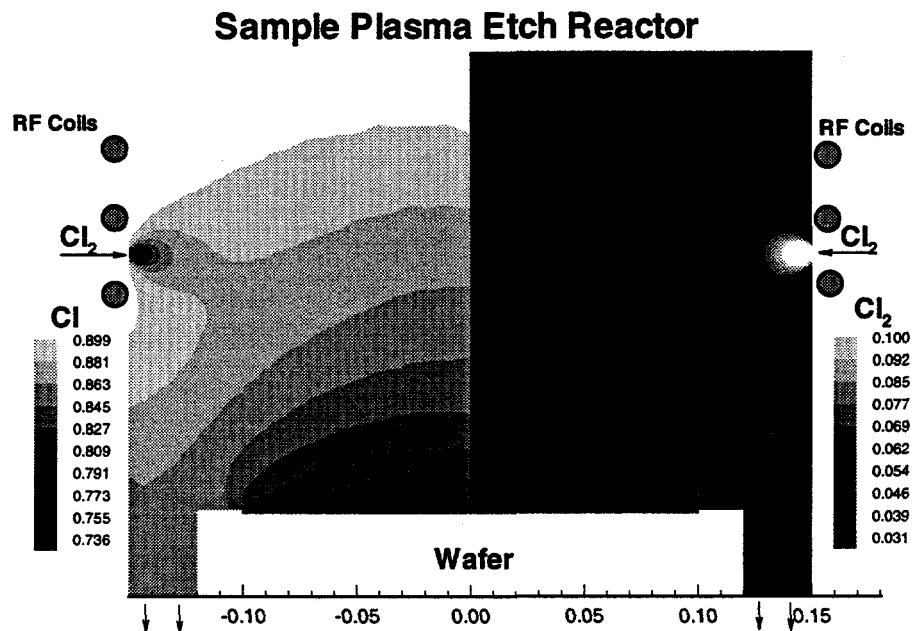


Figure 5 - Mole fraction distribution of neutral Cl and Cl₂

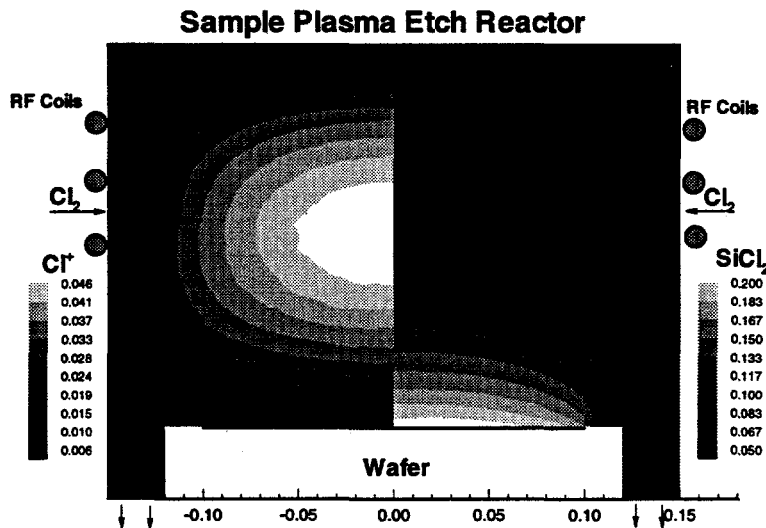


Figure 6 - Mole fraction distributions of Cl⁺ and SiCl₂

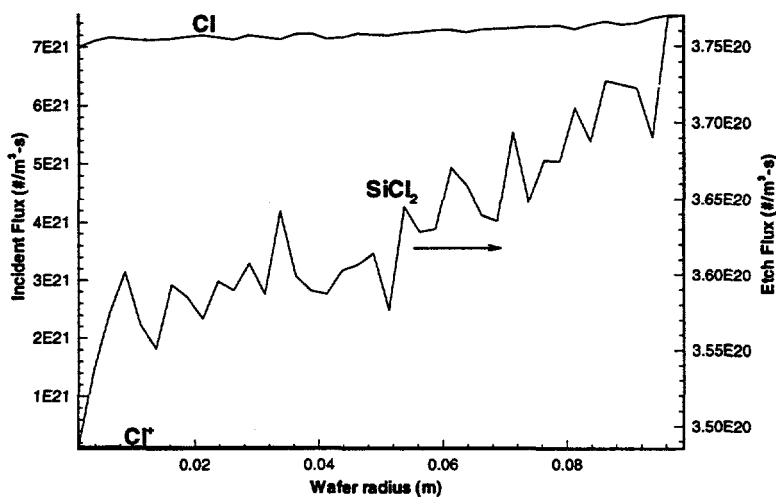


Figure 7 - Radial distribution of etch rate and incident Cl and Cl⁺ flux.

Experimental validation of a direct simulation by Monte Carlo molecular gas flow model

P. K. Shufflebotham^{a)}

Lam Research Corporation, Fremont, California 94538-6470

T. J. Bartel^{b)}

Sandia National Laboratories, Department 1514, Albuquerque, New Mexico 87185-5800

B. Berney^{c)}

Lam Research Corporation, Fremont, California 94538-6470

(Received 7 October 1994; accepted 16 January 1995)

The Sandia direct simulation Monte Carlo (DSMC) molecular/transition gas flow simulation code has significant potential as a computer-aided design tool for the design of vacuum systems in low pressure plasma processing equipment. The purpose of this work was to verify the accuracy of this code through direct comparison to experiment. To test the DSMC model, a fully instrumented, axisymmetric vacuum test cell was constructed, and spatially resolved pressure measurements made in N₂ at flows from 50 to 500 sccm. In a "blind" test, the DSMC code was used to model the experimental conditions directly, and the results compared to the measurements. It was found that the model predicted all the experimental findings to a high degree of accuracy. Only one modeling issue was uncovered. The axisymmetric model showed localized low pressure spots along the axis next to surfaces. Although this artifact did not significantly alter the accuracy of the results, it did add noise to the axial data. © 1995 American Vacuum Society.

I. INTRODUCTION

This article describes a collaboration between Lam Research and Sandia National Laboratories on supercomputer simulation of neutral gas flow in low pressure plasma processing equipment. The simulation software is a particle code based on the direct simulation Monte Carlo (DSMC) technique. The code is intended to provide physically correct, direct, dynamic simulations of gas flow in the transition (Knudsen) and molecular flow regimes.

Because of the direct way in which the DSMC code simulates nature, it has the potential to be an extremely powerful and useful computer-aided design (CAD) tool for the design of low-pressure vacuum systems. This assumes, of course, that the code is capable of *accurately predicting* the vacuum performance of real systems. The purpose of this article is to describe our experimental verification of the Sandia DSMC code.

II. VACUUM TEST CELL

The Vacuum Test Cell (VTC) was intended to be a directly modelable approximation of a low pressure plasma processing system. It consisted of an axisymmetric, bottom pumped, high vacuum chamber containing a centrally suspended cylindrical "electrode," as shown in Fig. 1. The chamber volume, with the gate valve closed, including the manometers and the roughing valve/port, was about 54 liters. The temperature of the VTC was 25 °C, with the electrode at 30 °C, due to heating by an internal capacitance manometer.

At the top of the cell was a gas ring containing 16 small, equally spaced holes. Since the pressure in the gas ring was

always at least 1000 times higher than the chamber pressure, the gas inlets were under conditions of *choked flow*. That is, the velocity of the gas leaving the inlet nozzles was sonic. This allowed the gas inlet conditions to be fully and uniquely specified in the DSMC model. The top of the VTC consisted of a plate containing manometers capable of axial and radial pressure measurements. Both manometers were mounted in this plate on a tube through a slide/rotate feedthrough. Axial pressure measurements were made by adjusting the depth of the centrally mounted tube into the chamber. An off-axis manometer was used to make radial measurements using a tubulation consisting of a short vertical section, followed by a horizontal section. Rotation of the off-center manometer caused the end of the tube to sweep out a 180° arc covering radii from 1.5 to 8.5 in. Due to the chamber symmetry, no azimuthal pressure gradients should have existed, so this was just a radial pressure measurement. The central electrode also contained a nonmovable axial capacitance manometer. A Penning gauge (Edwards CP25K) was used to measure the base pressure, which ranged from 8×10^{-7} to 3×10^{-6} Torr. The leakback rate was 0.045 mTorr/min (equivalent to 0.0032 sccm).

The VTC was evacuated through a 10 in. VAT gate valve by an Osaka Vacuum TG2003M (2000 liters/s at vacuum) compound magnetically levitated turbomolecular pump (TMP). This TMP was backed by an Edwards 40 mechanical pump equipped with an Edwards 250 Roots blower, through a 10 ft. long, 2 in. diameter foreline. A TMP isolation valve was used, and a separate roughing line and valve provided. A small N₂ purge flow into the bearing section of the TMP was used to keep it clean of backstreaming mechanical pump oils.

Dry N₂ was used in for all test conditions. The mass flow rate was controlled using a Unit 1200A 500 sccm N₂ MFC.

^{a)}Electronic mail: pkshuff@lamrc.com

^{b)}Electronic mail: tjbarte@cfd.sandia.gov

^{c)}Electronic mail: berney@lamrc.com

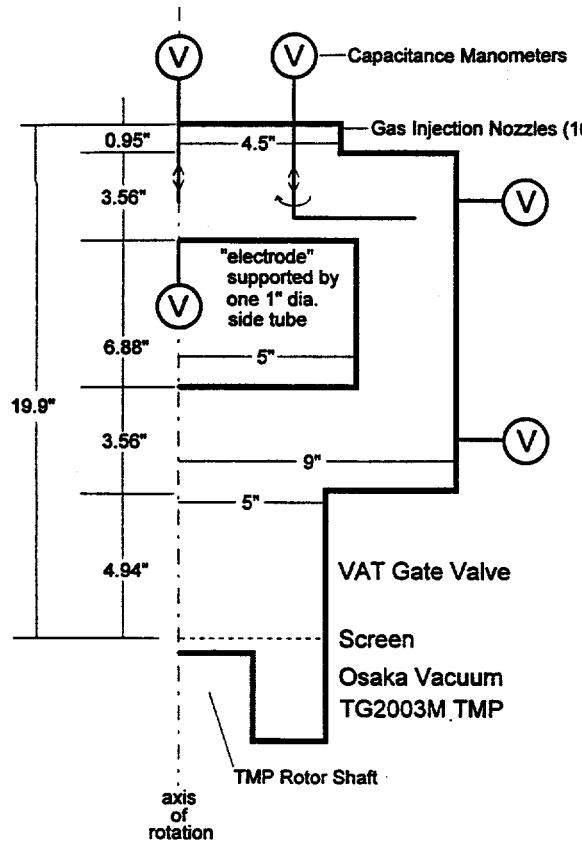


FIG. 1. Sketch of the Vacuum Test Cell. Except for some of the manometer locations and the electrode support (which consisted of a single 1 in. diameter tube from the side of the electrode to the wall) the chamber was fully axisymmetric.

An upstream shutoff valve was provided to prevent leakage through the MFC when gas flow was not desired. The accuracy of the MFC was checked using a standard rate-of-rise technique, and found to be correct to within the $\pm 4\%$ error of the measurement.

Capacitance manometers (Edwards 655, 20 mTorr, temperature controlled at 45 °C) were used for all pressure measurements. Mounting the manometers on extra tubulation (for the spatially resolved measurements) did not significantly affect the pressure readings.

All data was acquired using a computerized data acquisition system. The manometer readings were zeroed at base vacuum using both the potentiometers on the manometers and by collecting data at zero flow immediately before each set of measurements. Data collection at each point was entirely automated, and involved setting the mass flow rate, waiting for stabilization, and taking the average of 1500 readings from each manometer over 3 s.

III. DSMC CODE

This DSMC code was developed by Bartel of Sandia National Laboratories,¹⁻⁴ based on the methods of Bird.⁵ DSMC codes directly simulate nature by moving computational particles through space according to Newton's laws. At the end of each time step, collision partners are selected from within each grid cell and collided using probabilistic tech-

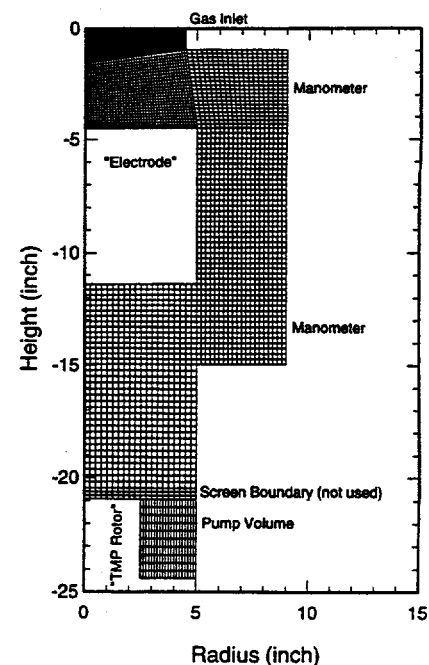


FIG. 2. Multiblocked computational grid used to simulate the Vacuum Test Cell.

niques, and the resultant statistics collected to obtain the local velocity and species distribution functions. From the distribution functions, the properties of the gas are then computed. In our case, parameters of interest include the N₂ number density, translational and rotational temperatures, radial and axial velocities and pressure. Collectively, this spatially resolved data set is referred to as the "flow field." Information concerning the fluxes and forces on selected surfaces are contained in separate files. The two-dimensional, axisymmetric version of the code was used in this work. Note that although the grid geometry is two-dimensional (2D), the code is physically three dimensional.

The temperature of all surfaces was 25 °C, except for the electrode which was 30 °C. All surfaces were assumed to be diffuse reflectors. No gas phase or surface chemical reactions were modeled. For simplicity, gas injection was modeled using an infinitely narrow slit. The equivalent gas inlet temperature, radial and axial velocities and molecular influx were calculated assuming choked flow conditions in the nozzles. The turbopump was simulated by a volume from which particles were randomly removed at a rate adjusted so as to produce the correct pump-speed at the pump inlet plane. The necessary pump speeds were obtained for each flow rate directly from the manufacturer's specification sheet.

The model geometry and grid pattern is shown in Figure 2. The very fine grids (which appear as black regions in the figure) were required to properly resolve the expansion of the high particle densities near the gas inlets. Since the VTC was axially symmetric (except for the very small electrode support), this was a very accurate model of the real chamber.

The code was run on a 1024 node n-CUBE 2 hypercube supercomputer. Five simulations were run for the model verification, one for each flow rate from 100 to 500 sccm at 100

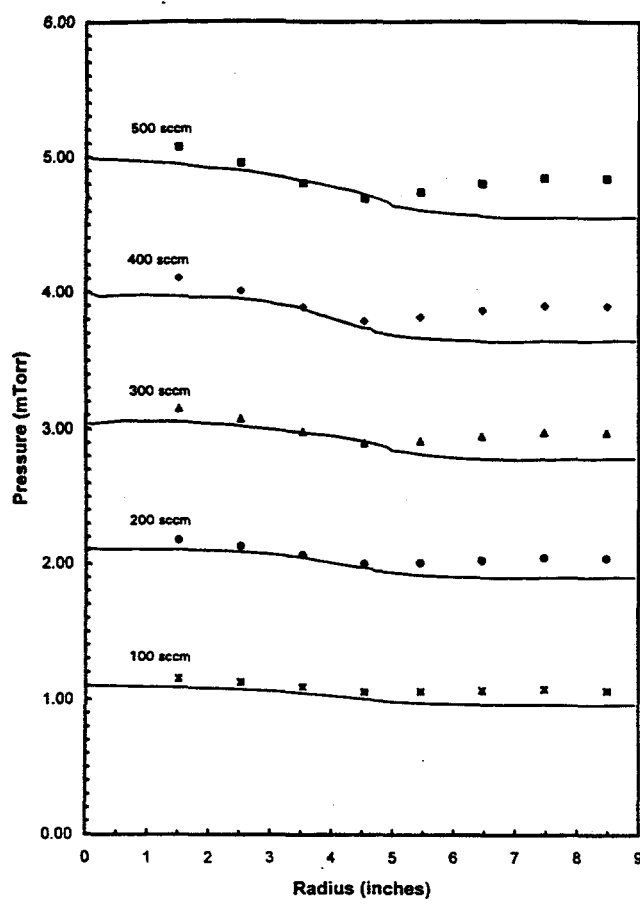


FIG. 3. Measured and simulated pressures vs radius as a function of flow 0.5 in. above the electrode. Points are measured data, lines are simulation results.

sccm intervals. Tens of thousands of computational particles were tracked for 150,000 to 250,000 time steps. The simulations were all run concurrently, each using 128 nodes of the n-CUBE, for 61 hours. Note that this is far, *far* longer than necessary for accuracy (1–3 h per condition is normal), but we wanted the smoothest possible converged flow fields. Please note that the simulations were performed “blind,” that is, *without knowledge of the experimental results*. There were no adjustable parameters.

IV. RESULTS AND DISCUSSIONS

A. Known sources of error

The measurement uncertainty/repeatability of the manometer and model data was generally less than $\pm 1\% 1 - \sigma$. In no case was the measurement error larger than the symbol size used in the graphs.

The single largest potential source of error was the pumping speed of the TMP. The values used in the simulation were obtained from the manufacturer’s specification sheet. Any difference between these values and the actual performance of the pump directly and adversely affects the predictive capability of the model. The TMP used in this work was chosen specifically for its especially tight conformance to specifications. Nonetheless, some small discrepancies be-

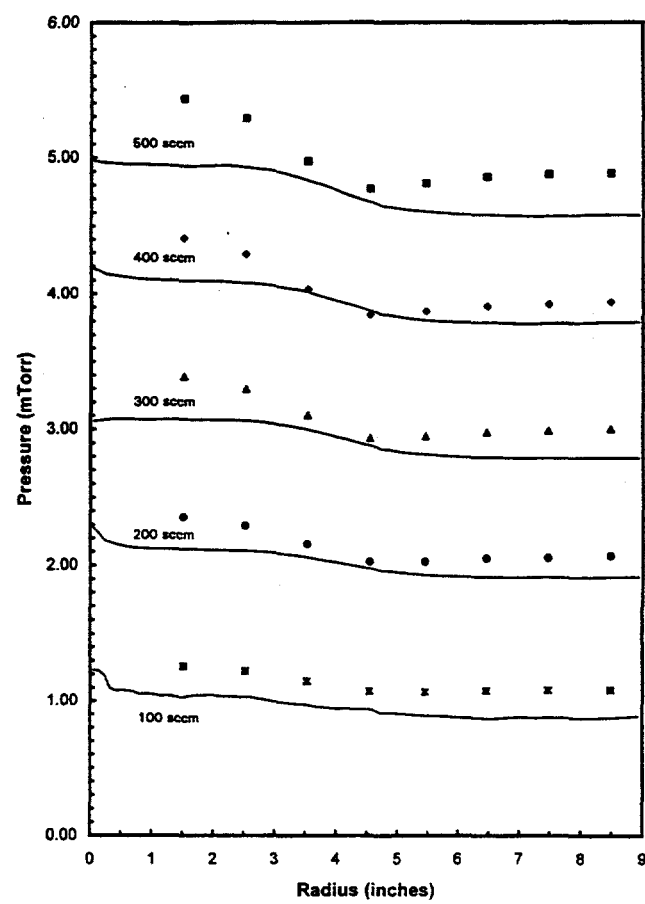


FIG. 4. Measured and simulated pressures vs radius as a function of flow 2.5 in. above the electrode. Points are measured data, lines are simulation results.

tween the measured and simulated pressures due to deviations of the real TMP from its specified performance must be expected.

A second source of systematic error was the screen protecting the TMP inlet. Unfortunately, due to schedule and resource constraints we did not get the opportunity to perform the full suite of spatial measurements with the screen removed. Due to the inability to get an accurate *a priori* statement of the conductance loss the screen produced, we decided to run the simulations without the screen (which could have been simulated by a partially permeable boundary had the screen conductance been known), and correct the measured data obtained with the screen in place, using data obtained in separate experiments. It was determined that in order to compensate for the effect of the screen, the measured pressures had to be reduced by 4.1%. This brought the test data closer to the simulation results. Note that the side manometer data used in Figure 6 was taken without the screen, and is therefore uncorrected.

Further error might have arisen from thermal transpiration in the capacitance manometers,⁶ although it appears that the manufacturer’s gauge calibration process corrects for this effect. This was not expected to produce a significant error.

Finally, there is the fact that both the simulated and experimental flow fields were not isotropic due to the sonic gas

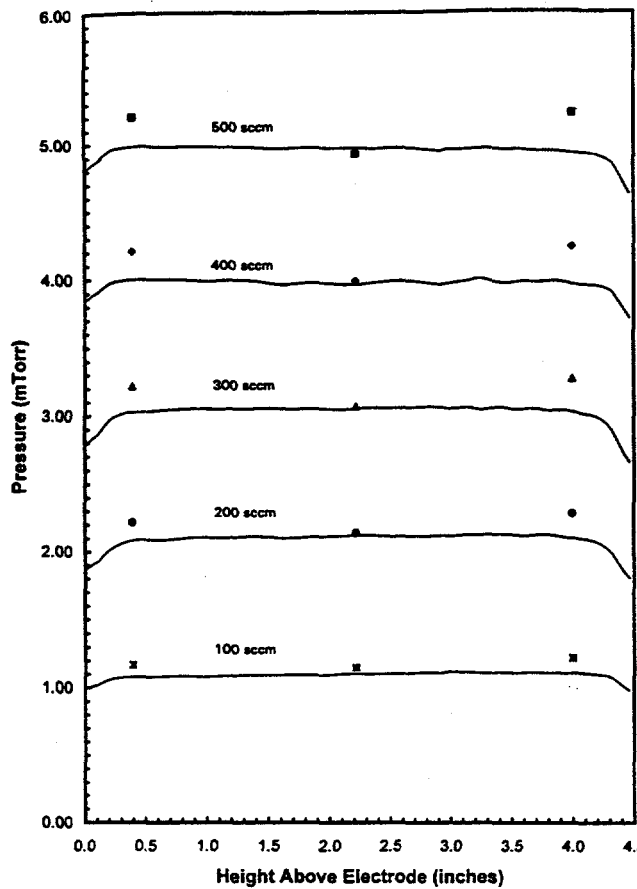


FIG. 5. Measured and simulated axial pressures as a function of flow above the electrode. Points are measured data, lines are simulation results. The glitches seen near 0 and 4.5 in. are artifacts due to the axisymmetric DSMC model (see the text for discussion).

injection and the net flow through the system. We feel that the combination of the geometry of the pressure measurement tube used in the radial measurements and gas anisotropy were probably responsible for the exaggerated radial gradients (and the unphysical minima at 4.5 in. in particular) in the experimental data relative to the simulation. Note that in the model, the volume equilibrium gas pressures (obtained from a Maxwellian assumption, nkT) are generally less than the equivalent surface pressures obtained from the net difference in momentum between adsorbing and desorbing molecules. For example, on the top of the "electrode" at 300 sccm, the surface pressures ranged from 0.05 to 0.10 mTorr higher than the Maxwellian gas pressures. Note that this brings the simulated pressures even closer to the measured values.

B. Comparison of simulation to experiment

Figures 3 through 6 compare the measured (corrected for the screen) and simulated data. Note the good agreement in both the absolute values and spatial gradients. Recall that there were no adjustable parameters in the model. The general form of the radial pressure gradients was correctly predicted. The features in the experimental radial data not fully predicted by the 2D axisymmetric model could probably

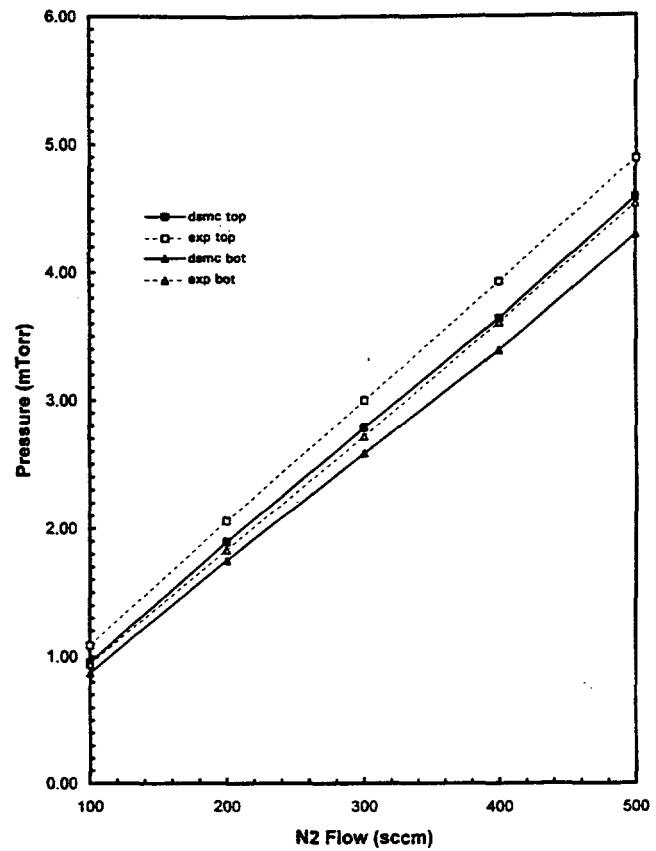


FIG. 6. Measured and simulated pressures vs flow for the side manometers.

have been captured by including the details of the pressure measurement device in a full 3D simulation (see previous discussion). The dependence on flow rate is also correctly predicted. Figure 7 shows the correlation between all simulated and measured values. A perfect correlation would follow the 45° line. Clearly, the correlation is excellent over all conditions and locations. The correlation coefficient (R^2 adjusted) between the measured and simulated data sets was 0.9951.

The only issue uncovered in the DSMC code were spurious pressure variations along the axis of symmetry near surfaces. This artifact is clearly seen in Figure 5; note the pressure glitches at either end of the graph (top plate and electrode surfaces). While cosmetically unappealing, the magnitude of the effect is actually quite small ($\pm 5\%$), highly localized and immediately recognizable. Also note that traditional DSMC applications, such as the simulation of space-based hypersonic flow fields, also exhibit this anomalous behavior. We therefore feel that, while efforts to resolve this issue should continue, it does not constitute a serious problem.

C. Application

The intended application of the DSMC code here is the design and analysis of low pressure, high density plasma processing equipment used in semiconductor wafer fabrication. While the VTC is an idealized design, intended solely for model verification, it does resemble several systems ei-

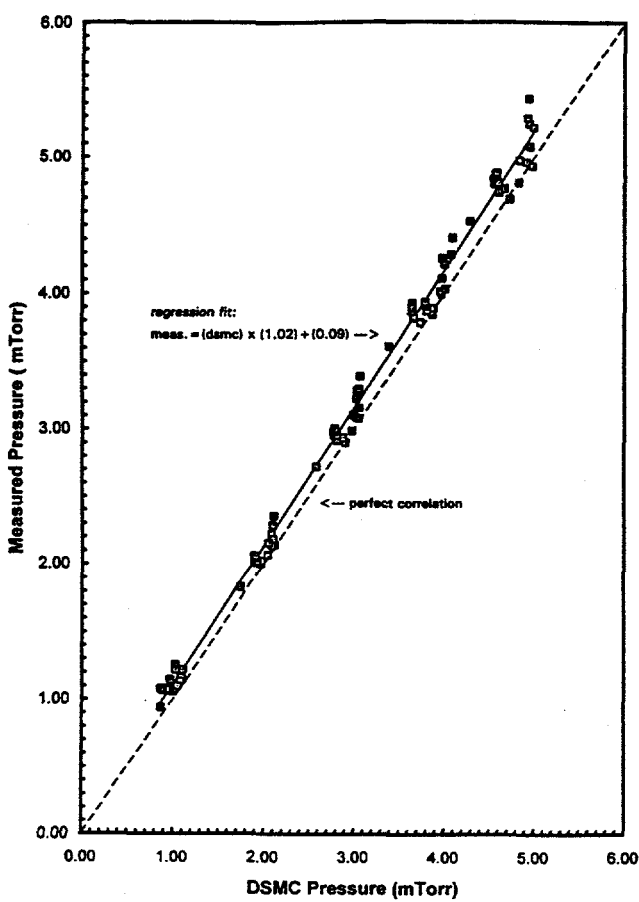


FIG. 7. Correlation between simulated and measured pressure values. A perfect correlation would follow the 45° line.

ther commercially available or in the design stage. For such systems, the 2D axisymmetric DSMC code is sufficient. In general, most semiconductor equipment is basically cylindrical, with side ports and manifolds breaking up the symmetry. This type of equipment can be modeled with the 3D version of the DSMC code, which is based on a "pie-section" gridding system. Arbitrary 3D simulations are currently not available. Since the only difference between the 2D and 3D codes is the grid complexity, the verification of the physics of the code performed in this work also applies to the 3D version.

Since the inputs to the DSMC model are known design parameters such as geometry, surface temperatures, gas flows in and pump speeds out, this makes the code useful as a CAD tool. The system is built on the computer, "virtual experiments" are run and the results examined. Thus the vacuum performance of the system can be fully designed and specified before hardware is built. In particular, critical is-

sues like neutral gas uniformity, residence time and stagnation effects can be worked out in advance. We expect that use of this code as a CAD tool could have numerous benefits. (1) Maximize the usefulness of the *concept design* stage by allowing many alternative designs to be *accurately* tested and compared via simulation. (2) Prevent surprises due to unsuspected design flaws, and overdesigning to try and compensate in advance for these flaws. (3) Minimize the number of hardware iterations required. In short, use of a DSMC CAD tool could significantly reduce the cost and duration of high vacuum and plasma processing equipment development cycles.

Obviously, the model is not restricted to pressure simulations. Any gas property can be obtained from the simulation. For example, the VTC simulations show a non-uniform pressure across the "electrode" (where the wafer would be in real equipment). This may or may not have an effect on real processes. Of greater interest are questions such as: "is the pressure gradient due to concentration or temperature gradients?", "what do the concentration gradients look like when multiple gas mixtures are used?", etc. The most useful properties that can be obtained from the model are the ones that cannot be measured readily.

V. CONCLUSIONS

The Sandia DSMC molecular/transition gas flow simulation code correctly and accurately predicted the pressures within the vacuum test cell, including their absolute values, spatial variations and dependencies on flow rate. This result, combined with the fact that hypothetical system designs can be modeled essentially the same way they are actually constructed and tested (specify geometry, flows in, pump speed out), demonstrates that the Sandia DSMC transition/molecular flow simulation code is extremely well suited for use as a vacuum system CAD tool.

ACKNOWLEDGMENTS

This work was supported by Lam Research Corporation, Sematech (Plasma Modeling Program), and the DOE (Contract No. DE-AC04-94AL85000).

¹S. Plimpton and T. Bartel, *Proceedings of the Scalable High Performance Computing Conference*, Williamsburg, VA, 1992 (IEEE, Washington, DC, 1992), p. 212.

²T. J. Bartel and S. J. Plimpton, AIAA 27th Thermophysics Conference, Nashville, TN, 1992 (unpublished), AIAA 92-2860.

³T. J. Bartel and C. R. Justiz, AIAA 24th Fluid Dynamics Conference, Orlando, FL, 1993 (unpublished), AIAA 93-3095.

⁴T. J. Bartel, T. M. Sterk, J. L. Payne, and B. Preppernau, 6th AIAA/ASME Joint Thermophysics & Heat Transfer Conference, Colorado Springs, CO, 1994 (unpublished), AIAA 94-2047.

⁵G. A. Bird, *Molecular Gas Dynamics and the Direct Simulation of Gas Flows* (Clarendon, Oxford, 1994).

⁶J. F. O'Hanlon, *A User's Guide to Vacuum Technology*, 2nd ed. (Wiley, New York, 1989), p. 22.

B**Sample Problems**

- Prob1: Metal Etch
- Prob2: Chlorine Plasma in GEC Cell
- Prob3: ESA Test Case: LENS geometry
- Prob4: MBF Expansion Chamber
- Prob5: Sputter Deposition
- Prob6: Si Etch by Chlorine Plasma in UH geometry
- Prob7: NO Nozzle Expansion and Data Comparison
- Prob8: NO Vibrational Relaxation (Time Dependent)

Prob1: Metal Etch

DSMC Workshop Test Problem 1

-Metal Etch Simulation

-Input Gases: BCl_3 & Cl_2 via symmetric ring injection

-Wafer Surface: Al

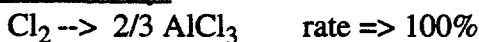
-Boundary conditions:

inlet: Ring 1- radius = 1.0 cm
 40 sccm BCl_3 & 60 sccm Cl_2
 Ring 2- radius = 4.0 cm
 50 sccm BCl_3 & 80 sccm Cl_2

use an inlet temperature of 255.92 K and a velocity of 200 m/s

outlet: symmetric pump
 1,500 l/s flow rate
 inlet screen blockage of 5%

-Surface Chemistry:



-Chemical Species:

BCl_3	117.16 gm/gmole	$1.9446 \cdot 10^{-25}$ kg	$6.538 \cdot 10^{-10}$ m
Cl_2	70.91 gm/gmole	$1.18 \cdot 10^{-25}$ kg	$5.53 \cdot 10^{-10}$ m
AlCl_3	133.33 gm/gmole	$2.213 \cdot 10^{-25}$ kg	$6.81 \cdot 10^{-10}$ m

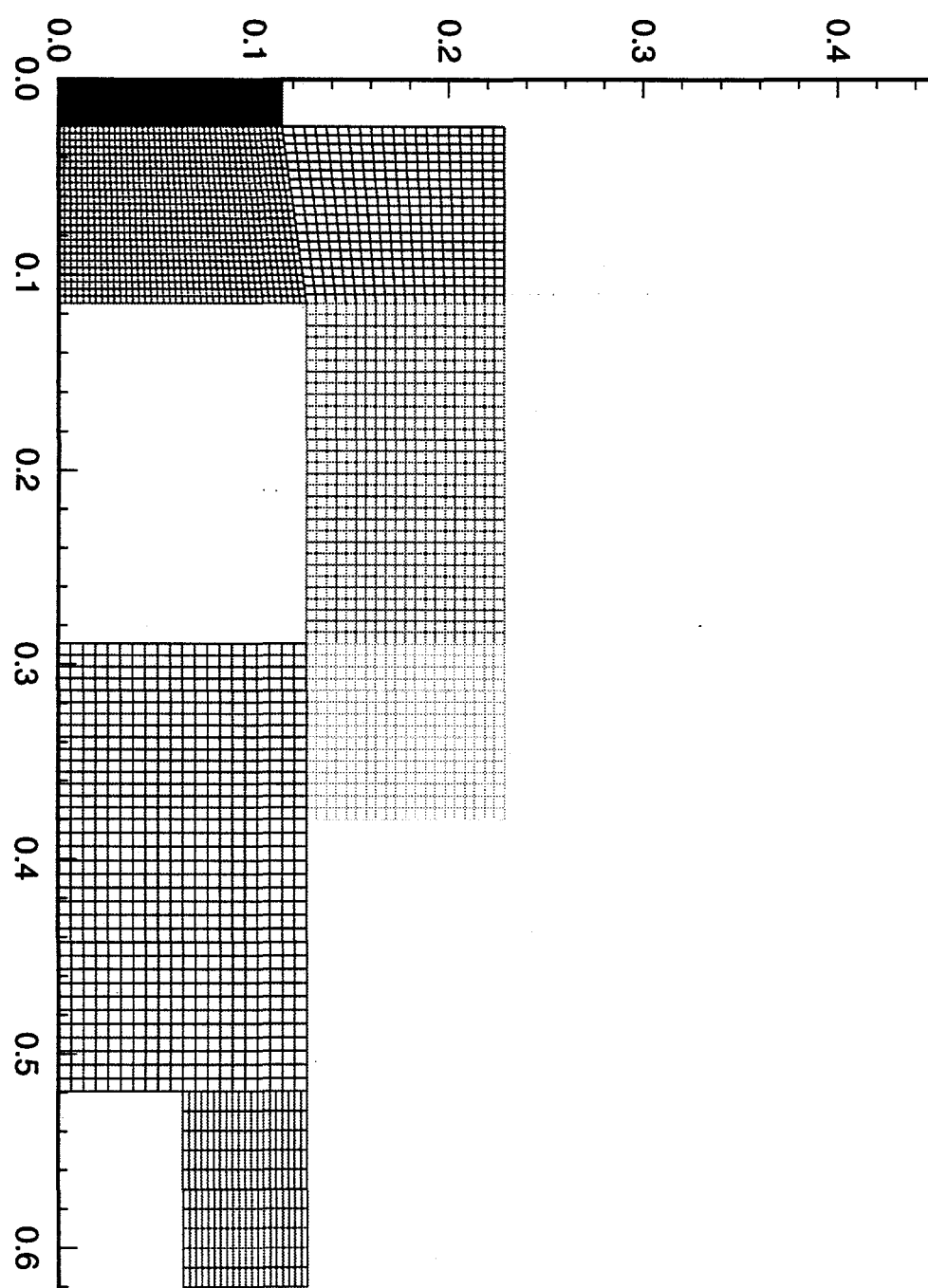
use a mixture viscosity coefficient of 0.9996 @ 273 K

-Surface Boundary Conditions:

100% thermal accommodation
100% diffuse surface reflection
temperature of all surfaces = 298.15 K

-Output:

- pressure and species distribution
- surface etch rate
- angular distribution of incident particles for wafer



prob1.inp

```

*----- Region interface/matching
*----- Only need if IVN > 0; then supply IVN pairs of (IVR, IVS)
*----- Number adj.          Adj. side      Adj. reg.
*----- reg. sides          (IVN)          no. (IVR)
*----- (IVS) no. (IVR)
*----- 1 0
*----- 2 1
*----- 3 0
*----- 4 0
*----- 4 7
*----- END OF EXPERT INPUT FILE

```

950920
14:04:57

inlet

* Table for DSMC Workshop problem 1
* 40sccm BC13, 60sccm Cl2 --- radial ring 1
* 50sccm BC13, 80sccm Cl2 --- radial ring 2

* 4.478e17 #/s == 1 sccm
total tables to read
1 2 1 table #, number of entries
0.01 447.e17 0. 200.0 255.92 255.92 255.92 0.4 0.6 0.0
0.04 581.e17 0. 200.0 255.92 255.92 255.92 0.3846 0.6154 0.0

1

surf_chem

* this file contain surface chemistry information for the
* DSMC workshop problem 1
* BC13 C12 AlCl3
* 1 2 3
*
* variable order for each reaction:
* number of material table types
1
* material 1 (wafer), number of reactions, site density
1 1.0
* (reaction type) (Species-i) (Species-r1) (Species-r2) (create prob1) (create prob2) (degree
e of specular) (Rx prob)
1. 2. 3. 0.0 0.6667 0.0 0.0 1.0
*

95/09/20
14:04:57

1

spec

* species data file

* number of species to input taken from problem description
* input --- they MUST be the same
* ---

ID	Mwt	Mol. mass	Diam.	#Rot.Deg.	Rot.Rel.	Vib.	Rel.	Vib.Temp.	specie	wt.	char
ge	(kg)	(m)		Freedom	Coll. #	Coll. #		(K)			
BC13	117.16	1.9446e-25	6.538e-10	2.	50.	00.		0000.	1.0		
CL2	0.0										
	70.91	1.18e-25	5.53e-10	2.	50.	00.		0000.	1.0		
	0.0										
AlC13	133.33	2.213e-25	6.81e-10	2.	50.	00.		0000.	1.0		
	0.0										

* the diameter of BC13 was based on the same density ratio as CL2
* same for AlC13
* ---

14:04:57

```
# DSMC Workshop Problem 1
log file          dsmc.log
output screen     100
zero flag         100
pump speed       1.5
read definition  1.0      dsmc.in2
load particles   1.0
adapt flag        40 0.25
time factor      5.0
run               15000 0
output cells     10000
output surface   10000
output wafer     10000
adapt flag        50 0.25
run               190000 1
```

Prob2: Chlorine Plasma in GEC Reference Cell

```
init2d prob1.inp
prob1.inp
    init2d for DSMC-MP -- version 6.00

starting region          1
starting region connectivity
begin initial processing of region info

opening inlet file, inlet, now
finished reading file--inlet

starting region          2
starting region connectivity
begin initial processing of region info

starting region          3
starting region connectivity
begin initial processing of region info

starting region          4
starting region connectivity
begin initial processing of region info

starting region          5
starting region connectivity
begin initial processing of region info

starting region          6
starting region connectivity
begin initial processing of region info

starting region          7
starting region connectivity
begin initial processing of region info

starting region          8
starting region connectivity
begin initial processing of region info

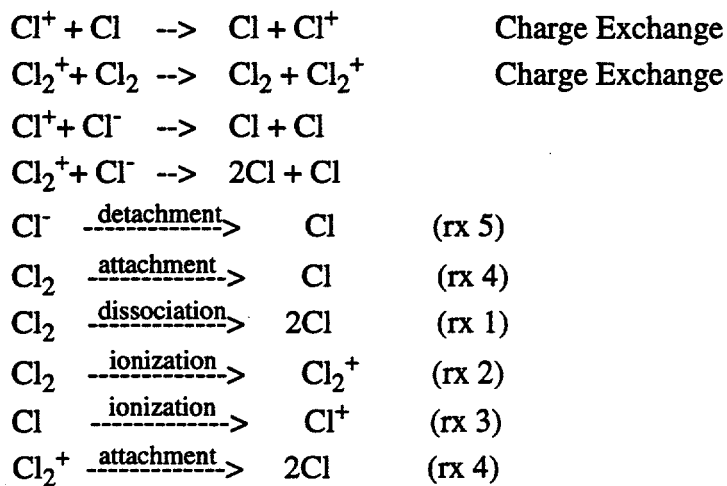
opening species file, spec, now
finished with file--spec

opening surface chemistry file, surf_chem, now
reading surface: material #          1 reaction #          1
finished with file--surf_chem

total cell volume(m^3) =  6.1428566E-02
210200 molecules in initial grid
    8 regions
    5200 computational cells
    3 chemical species

    78 region connections
    401 grid data size
    50 boundary elements
    365 surface elements
    5593 cell corner points
    2 inlet table boundary cells
```

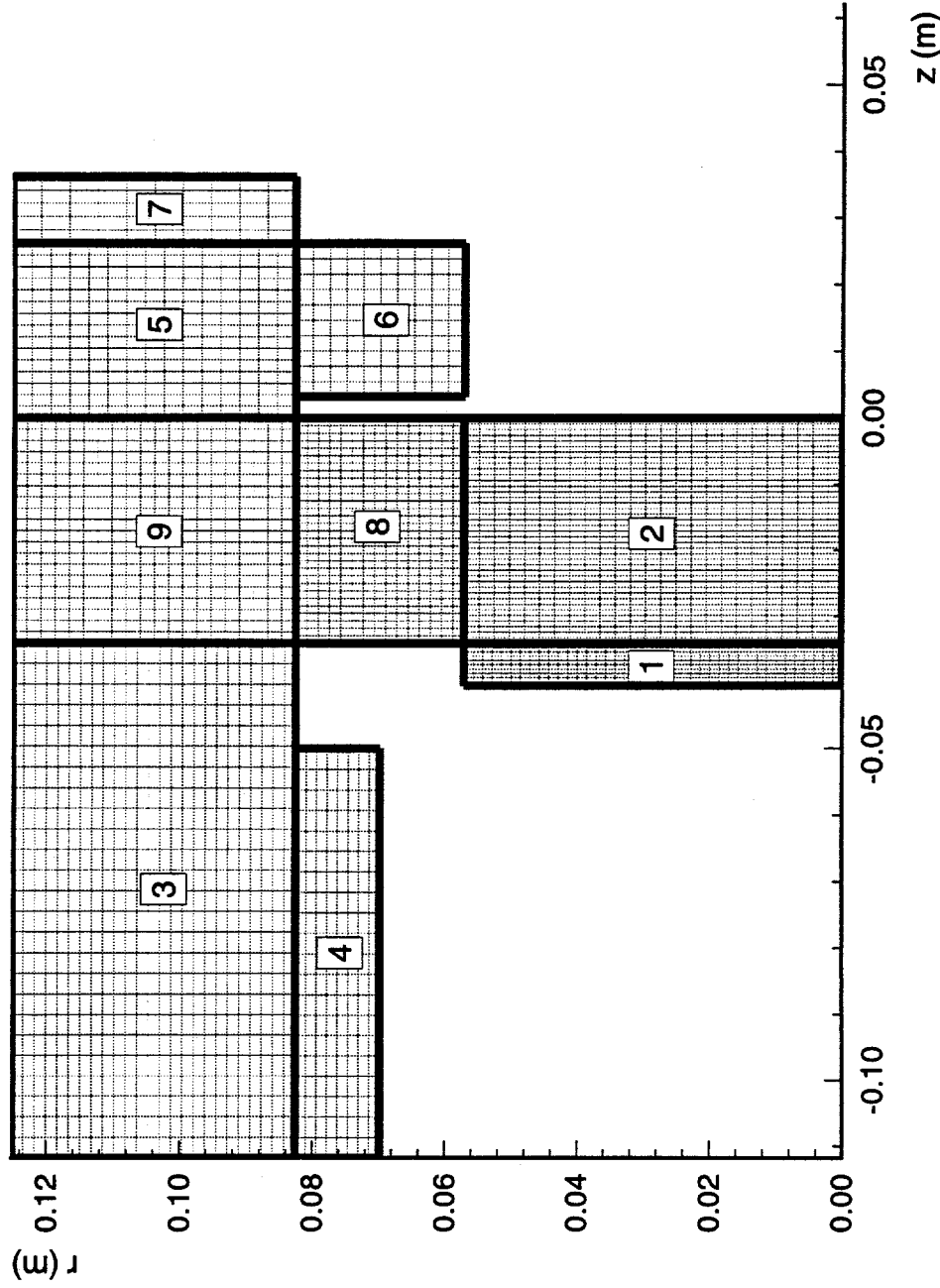
- Gas Phase Chemistry:



- Output:

- pressure, velocity, temperature and species distribution
- angular distribution of incident particles for wafer

Prob2: Chlorine Plasma in GEC Reference Cell



Side	Cell1	Cell12	Spec. refl.	Temp. K	Material#	Value
2	1	60	0.000	373.	3	1.
3	1	60	0.000	373.	3	0.
4	1	60	0.000	373.	1	1.

|-----> Only need if IVN > 0; then supply IVN pairs of (IVR, IVS)
 Number adj.
 Reg. side Adj. side
 reg. sides Adj. reg.
 (IVN) no. (IVS) | no. (IVR)

1 0
 2 1 4 1
 3 1 1 8
 4 0

3 <----- Inputs specific to this region follow

1.0
 1.0
 10
 11
 12
 6
 25
 0
 0
 10
 11
 12
 9

number of cells along sides 1 and 3
 number of cells along sides 2 and 4
 sides 1 and 3 curvature; 0/1 for line/circular arc
 sides 1 and 3 cell spacing;
 sides 2 and 4 cell spacing;
 boundary type code for sides 1 - 4, resp.

```

*----- Region interface/matching
*----- Only need if IVN > 0; then supply IVN pairs of (IVR, IVS)
*----- Number adj.
*----- Reg. side   reg. sides
*-----          (IVR)          (IVS) | no. (IVR)
*-----          1             2             3             4
*-----          2             0             3             -1
*-----          3             0             2             9
*-----          4             1             2             9
*----- 4 <----- Inputs specific to this region follow
*----- 1.0          enum multiplier
*----- 1.0          dtm multiplier
*----- 0.0          global routine

```

Prob2: Chlorine Plasma in GEC Reference Cell

- Input Gases: Chlorine (Cl₂)

- Wafer Surface: Stainless Steel (no etching)

- Chemical Species:

	<u>Mwt</u>	<u>Mass</u>	<u>VHS diameter</u>
Cl	35.45 gm/gmole	0.59 x 10 ⁻²⁵ kg	3.831 x 10 ⁻¹⁰ m
Cl ⁺	35.45 gm/gmole	0.59 x 10 ⁻²⁵ kg	3.831 x 10 ⁻¹⁰ m
Cl ⁻	35.45 gm/gmole	0.59 x 10 ⁻²⁵ kg	3.831 x 10 ⁻¹⁰ m
Cl ₂	70.91 gm/gmole	1.18 x 10 ⁻²⁵ kg	5.405 x 10 ⁻¹⁰ m
Cl ₂ ⁺	70.91 gm/gmole	1.18 x 10 ⁻²⁵ kg	5.405 x 10 ⁻¹⁰ m

use a mixture viscosity coefficient of 1.00 @ 300 K

- Boundary conditions:

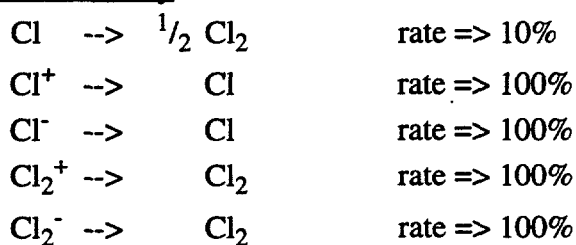
inlet: ring radius= 0.1252 m
 15 sccm distributed over outer ring radius
 use an inlet temperature of 255.79 K and a velocity of 200 m/s

outlet: anular pump
 3 1/4 s flow rate
 no inlet screen blockage
 pressure control to 20 mtorr.

- Surface Boundary Conditions:

- 100% thermal accommodation
- 100% diffuse surface reaction
- Temperature of all surfaces = 300 K

- Surface Chemistry:



```

7
5
7
2
*   *   Side Cell1 Cell12 Spec. refl. Temp. K Material# Value
*   1   1   20   0.000   350.00   3   1.
*   3   1   20   0.000   350.00   4   0.
*   *
*   *   Region interface/matching
*   *   |-----> Only need if IVN > 0; then supply IVN pairs of (IVR,IVS)
*   *   Number adj.
*   *   Reg. side reg. sides Adj. side Adj. reg.
*   *   (IVN) no. (IVS) no. (IVR)
*   *
*   1   2   3   6   3   -1
*   2   1   4   9
*   3   0
*   4   1   2   7
*   *
*   *   number of cells along sides 1 and 3
*   10  number of cells along sides 2 and 4
*   10  sides 1 and 3 curvature: 0/1 for line/circular arc
*   0   sides 1 and 3 cell spacing:
*   0   sides 2 and 4 cell spacing:
*   5   boundary type code for sides 1 - 4, resp.
*   5
*   5
*   3
*   *
*   *   Side Cell1 Cell12 Spec. refl. Temp. K Material# Value
*   *   1   1   40   0.000   350.00   3   0.
*   2   1   40   0.000   350.00   3   0.
*   4   1   40   0.000   350.00   3   0.
*   *
*   *   Region interface/matching
*   *   |-----> Only need if IVN > 0; then supply IVN pairs of (IVR,IVS)
*   *   Number adj.
*   *   Reg. side reg. sides Adj. side Adj. reg.
*   *   (IVN) no. (IVS) no. (IVR)
*   *
*   1   0
*   1.0
*   1.0
*   16  global points
*   15
*   15
*   18
*   17
*   10
*   10
*   10
*   0
*   0
*   0
*   0
*   5
*   5
*   5
*   5
*   3
*   *
*   *   Side Cell1 Cell12 Spec. refl. Temp. K Material# Value
*   *   1   1   40   0.000   350.00   3   0.
*   2   1   40   0.000   350.00   3   0.
*   4   1   40   0.000   350.00   3   0.
*   *
*   *   Region interface/matching
*   *   |-----> Only need if IVN > 0; then supply IVN pairs of (IVR,IVS)
*   *   Number adj.
*   *   Reg. side reg. sides Adj. side Adj. reg.
*   *   (IVN) no. (IVS) no. (IVR)
*   *
*   7   <---- Inputs specific to this region follow
*   *
*   7   <---- Inputs specific to this region follow
*   *
*   1.0
*   1.0
*   18
*   18
*   18

```

96/01/11
18:09:19

4 0
----- Inputs specific to this region follow -----
1.0 fnum multiplier
1.0 dnm multiplier
6 Global points
12
13
14
14 number of cells along sides 1 and 3
20 number of cells along sides 2 and 4
20 curvature: 0/1 for line/circular arc
0 sides 1 and 3 cell spacing:
0 sides 1 and 3 cell spacing:
0 sides 2 and 4 cell spacing:
0 boundary type code for sides 1 - 4, resp.
7
7
1
----- Side Cell1 Cell2 Spec. refl. Temp. K Material# Value -----
----- 3 1 60 0.000 350. 4 0. -----
*----- Region interface/matching
*----- Only need if IVN > 0; then supply IVN pairs of (IVR, IVS)
*----- Number adj.
*----- Reg. side reg. sides Adj. side Adj. reg.
----- (IVN) no. (IVS) no. (IVR) -----
*----- 1 1 3 8
2 1 4 3
3 0
4 1 2 5
*----- END OF EXPERT INPUT FILE
*-----

```

*   this file contain surface chemistry information for the
*   UH - GEOM1 Problem C12 chemistry
*   Cl, Cl+, Cl-, Cl2, Cl2+, SiCl2
*   1   2   3   4   5   6
*
*   variable order for each reaction:
*   (reaction type) (Species-r1) (Species-r2) (create prob1) (create prob2) (degree
*   of specular) (Rx prob1)
*
*   4   number of material table types
*
*   * material 1 (wafer), wafer
1 4 1.0
1. 1. 4. 0. 0.5 0. 0. 0.1
1. 2. 1. 0. 1.0 0. 0. 1.0
1. 3. 3. 0. 1.0 0. 1. 1.0
1. 5. 4. 0.. 1.0 0. 0. 1.0
*
*   * material 2, upper head
2 4 1.0
1. 1. 4. 0. 0.5 0. 0. 0.1
1. 2. 1. 0. 1.0 0. 0. 1.0
1. 3. 3. 0. 1.0 0. 1. 1.0
1. 5. 4. 0. 1.0 0. 0. 1.0
*
*   * material 3, chamber walls
3 4 1.0
1. 1. 4. 0. 0.5 0. 0. 0.1
1. 2. 1. 0. 1.0 0. 0. 1.0
1. 3. 3. 0. 1.0 0. 0. 1.0
1. 5. 4. 0. 1.0 0. 0. 1.0
*
*   * material 4, pump walls
4 4 1.0
1. 1. 4. 0. 0.1 0. 0. 0.5
1. 2. 1. 0. 1.0 0. 0. 1.0
1. 3. 1. 0. 1.0 0. 0. 1.0
1. 5. 4. 0. 1.0 0. 0. 1.0

```

1
960111
18:09:20
inlet

```
* new version of inlet file
* 2 number of tables
* 1 1 1 -- 15sccm -- point source -- new grid2
*      #/s
* 0.038 6.717899e+18 0.00 -199.725 255.79 255.79 255.79 0.0 0. 1.0 0. 0
*
* base case calc.
* 2 2 2 -- 10sccm distributed over the outer-ring radius
*      #/m2
* -0.033 1.967e20 0.0 0.0 300. 300. 300. 0.0 0.0 0.0 0.0 1.0
* 0.0 0.0 1.967e20 0.0 0.0 300. 300. 300. 0.0 0.0 0.0 0.0 1.0
* -0.004 1.967e20 0.0 0.0 300. 300. 300. 0.0 0.0 0.0 0.0 1.0
* 0.0 0.0
```

```
*****
* species data file
***** number of species to input taken from problem description
* input -- they MUST be the same
*-----
```

*	ID	Mwt	Mol. mass	Diam.	#Rot.Deg.	Rot.Rot.	Vib.	Rel.	Vib.Temp.	specie wt.	char
*		(kg)		(m)		Freedom	Coll. #	Coll. #	(K)		
---	C1	35.45	0.59e-25	3.831e-10	0.0	0.0	0.0	0.0	0.0	1.0	0.
0	C1+	35.45	0.59e-25	3.831e-10	0.0	0.0	0.0	0.0	0.0	0.01	1.
0	C1-	35.45	0.59e-25	3.831e-10	0.0	0.0	0.0	0.0	0.0	0.01	-
1.0	C12	70.91	1.18e-25	5.405e-10	2.	5.	00.	0000.	0.01	0.0	
0	C12+	70.91	1.18e-25	5.405e-10	2.	5.	00.	0000.	0.01	1	
0	SiC12	98.99	1.647e-25	8.000e-10	2.	5.	0.0	0.0	1.0	0.	

* some of these are based on Chemkin data provided by Ellen Meeks - SNLL
 *

96/10/22
12:13:05

chem

* This input file contains the data characterizing the chemical reactions.
 * If input # reactions = 0, there is no chemistry, and this file is not read.
 * input lines are free format
 * the reaction equation is an input line (a25)

* NOTE: line 1 MUST have 8 integers
 * line 2 for type 0, -1, & -2 MUST have 5 real numbers
 * line 2 for type -3 MUST have 2 integers and 1 real number
 * line 3 for type -3 MUST have 6 real numbers

* first number on line 1 defines reaction type:

0 -- standard Arrhenius collisional chemistry $\kappa = A T^B \exp(-Ea/RT)$
 second line variables
 1 -- number of internal degrees of freedom
 2 -- Ea
 3 -- A
 4 -- B
 5 -- heat of rx (+ for exothermic) - joules

-1 -- Charge Exchange reaction with fixed rate
 second line variables
 1 -- probability
 2 -- sigma CE (m^2)

-2 -- Charge Exchange reaction using model from Rapp & Frances (1962)
 sigma = ($k_1 - k_2 * \log(v_r)$) **2
 second line variables
 1 -- k_1 for elastic collision
 2 -- k_2 for elastic collision
 3 -- k_1 for charge exchange
 4 -- k_2 for charge exchange

-3 -- Electron Impact reactions
 second line variables
 1 -- equation type (if <0, T in K instead of eV)
 2 -- number of products (1 or 2)
 3 -- heat of formation (Frank-Condon) - joules
 third line variables:
 1 - 6 are fit coefficients

* Chlorine chemistry example -- 11 reaction set

* Cl, Cl+, Cl-, Cl2, Cl2+, SiCl2
 * 1 2 3 4 5 6

* Cl+ + Cl -> Cl + Cl+ (charge exchange)
 -1 2 1 1 1 0 2
 * 0.75 120.e-20 0. 0. 0.

* Cl2+ + Cl2 -> Cl2 + Cl2+ (charge exchange)
 -1 5 4 1 1 4 0 5
 * 0.75 120.e-20 0. 0. 0.

* Cl- + Cl -> Cl + Cl- (charge exchange)
 -1 3 1 1 1 0 3
 * 0.90 120.e-20 0. 0. 0.

0

third body probabilities now follow

0

1

```

init2d geo.inp
geo.inp
init2d for DSNC-MP -- version 6.00

starting region 1
starting region connectivity
begin initial processing of region info

starting region 2
starting region connectivity
begin initial processing of region info

starting region 3
starting region connectivity
begin initial processing of region info

starting region 4
starting region connectivity
begin initial processing of region info

starting region 5
starting region connectivity
begin initial processing of region info

starting region 6
starting region connectivity
begin initial processing of region info

starting region 7
starting region connectivity
begin initial processing of region info

starting region 8
starting region connectivity
begin initial processing of region info

starting region 9
starting region connectivity
begin initial processing of region info

opening inlet file, inlet, now
finished reading file--inlet

opening species file, spec, now
finished with file--spec

Opening gas phase chemistry file, chem, now
reading reaction # 1
reading reaction # 2
reading reaction # 3
reading reaction # 4
reading reaction # 5
reading reaction # 6
reading reaction # 7
reading reaction # 8
reading reaction # 9
reading reaction # 10
reading reaction # 11

finished with file--chem

opening surface chemistry file, surf_chem, now
reading surface: material # 1
reading reaction # 1
reading surface: material # 1
reading reaction # 2

```

Prob3: ESA test case: LENS geometry

Prob3: ESA test case (LENS geometry)

- Chemical Species:

O ₂	32.00 gm/gmole	5.31 x 10 ⁻²⁶ kg	3.96 x 10 ⁻¹⁰ m
N ₂	28.016 gm/gmole	4.65 x 10 ⁻²⁶ kg	4.07 x 10 ⁻¹⁰ m
O	16.00 gm/gmole	2.65 x 10 ⁻²⁵ kg	3.00 x 10 ⁻¹⁰ m
N	14.008 gm/gmole	2.325 x 10 ⁻²⁶ kg	3.00 x 10 ⁻¹⁰ m
NO	30.008 gm/gmole	4.98 x 10 ⁻²⁶ kg	4.00 x 10 ⁻¹⁰ m

use a mixture viscosity coefficient of 0.74 @273 K

- Freestream Boundary conditions:

$$V_x = 3053.18 \text{ m/s}$$

$$V_y = 0.0 \text{ m/s}$$

$$\text{number } \rho = 0.895 \times 10^{23} \text{ molecules/m}^3$$

$$T = 218 \text{ K}$$

- Surface Boundary Conditions:

- 100% thermal accommodation
- 100% diffuse surface reaction
- Temperature of all surfaces = 218 K

- Surface Chemistry:

none

- Gas Phase Chemistry:

23 gas phase reactions (refer to Chem file)

- Output:

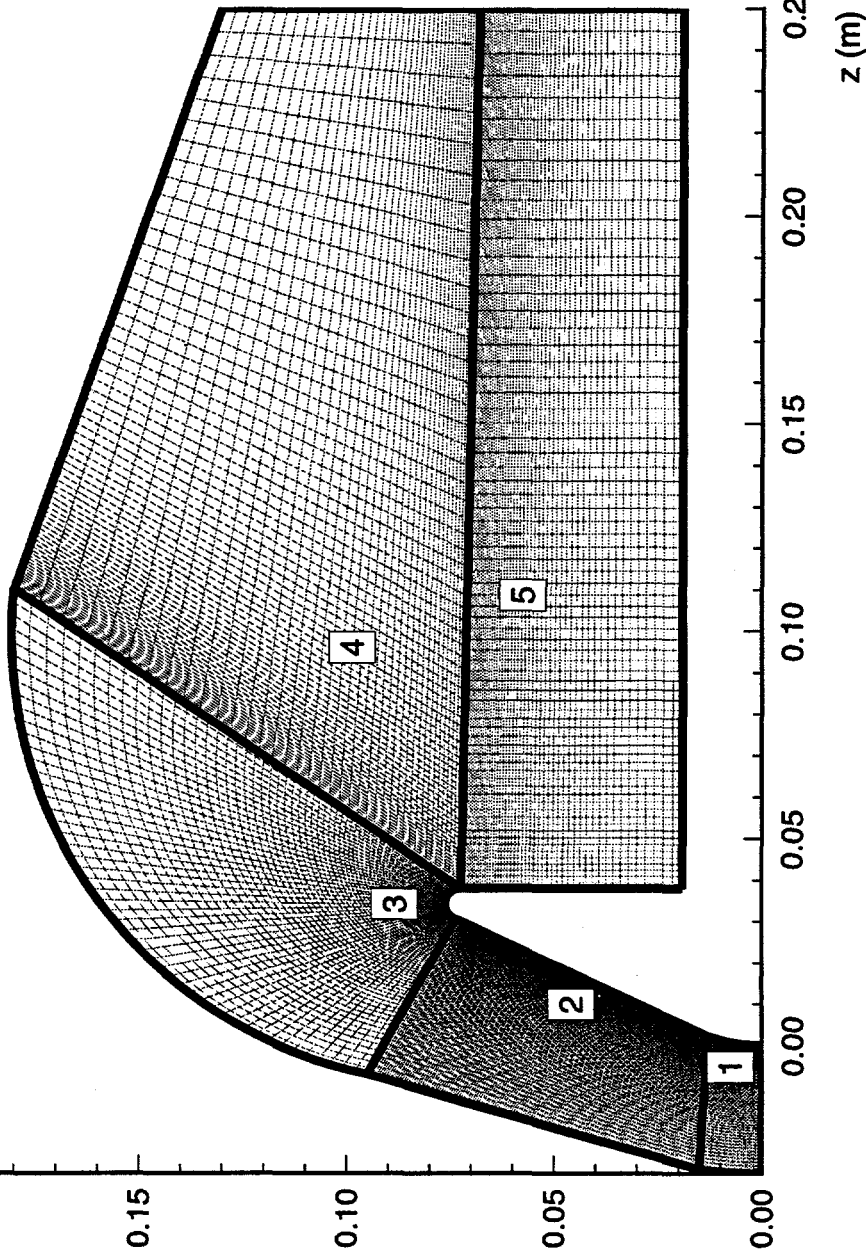
- pressure and species distribution
- angular distribution of incident particles for wafer

- References used to create example:

Marriott, P. M. & Bartel, T. J., "Comparison of DSMC Flowfields Predictions using Different Models for Energy Exchange & Chemical Reaction Probability," **Rarefied Gas Dynamics 19**, Vol. 1, pp. 413-419, Oxford University Press, 1995.

Prob3: ESA test case: LENS geometry

$(\bar{\epsilon})_s$



esa1.inp

```

13      number of global points (must be .le.120)
*      *
*      Global corner pt. coordinates
*      *
*      Pt.      x (m)      y (m)
*      *
*      1      -0.031      0.0
*      2      -0.03      0.015
*      3      -0.007      0.095
*      4      0.03429      0.07239
*      5      0.0      0.0
*      6      0.00229771      0.013031
*      7      0.0307098      0.0736931
*      8      0.11      0.18
*      9      0.0381      0.01905
*      10     0.0381      0.07239
*      11     0.25      0.01905
*      12     0.25      0.06800
*      13     0.25      0.13
*      *
*      Individual Region Definitions Follow
*      *
*      --REGION NUMBERS MUST BE SEQUENTIAL--*
*      *
*      1 <----- Inputs specific to this region follow
*      *
*      6      number of cells along sides 1 and 3
*      30     number of cells along sides 2 and 4
*      100    sides 1 and 3 curvature: 0/1 for line/circ
*      1      sides 1 and 3 cell spacing:
*      0      sides 2 and 4 cell spacing:
*      2      1.0      fmum multiplier
*      5      dbm multiplier
*      1      global points
*      2      2      2
*      6      6
*      30
*      100
*      1
*      0
*      2
*      1.03
*      100
*      5
*      1
*      3
*      7
*      1      number of BC entries
*      *
*      Side    Cell1   Cell2   Spec. refl.   Temp. K   Material#
*      *
*      1      1      100      0.000      300.      0
*      *
*      *
*      Reg. side  reg. sides  Adj. side  Adj. reg.
*      *
*      1      0
*      2      0
*      3      0
*      4      1      2      2
*      *
*      2 <----- Inputs specific to this region follow
*      *
*      1.0      fmum multiplier
*      1.0      dbm multiplier
*      6      global points
*      2

```

esa1.inp

```
1 1 150 0.000 300. 0 0.  
2 1 100 0.000 300. 0 0.  
*-----  
*----- Region interface/matching  
*----- Reg. side reg. sides Adj. side Adj. reg.  
*-----  
*-----  
1 0  
2 0  
3 1 4  
4 0  
*----- END OF EXPERT INPUT FILE  
*-----
```

* This input file contains the data characterizing the chemical reactions.

* If IRA = 0, there is no chemistry, and this file is not read.

* IRA > 0, there are IRA reactions, each characterized by 3 input records

* --note-- the reaction equation is an input line (a25)

*--

* O2 + N --> 2O + N

0 1 4 2 1 3 3 4
1. 1. 8.197E-19 5.993E-12 -1. -8.197E-19

* O2 + NO --> 2O + NO

0 1 5 2 1 3 3 5
1. 1. 8.197E-19 5.993E-12 -1. -8.197E-19

* O2 + N2 --> 2O + N2

0 1 2 2 1 3 3 2
1. 1. 8.197E-19 1.198E-11 -1. -8.197E-19

* 2O2 --> 2O + O2

0 1 1 2 1 3 3 1
1. 1. 8.197E-19 5.193E-11 -1. -8.197E-19

* O2 + O --> 3O

0 1 3 2 1 3 3 1
1. 1. 8.197E-19 1.498E-10 -1. -8.197E-19

* N2 + O --> 2N + O

0 2 3 2 1 4 4 3
0.5 0.5 1.561E-18 3.187E-13 -0.5 -1.561E-18

* N2 + O2 --> 2N + O2

0 2 1 2 1 4 4 1
0.5 0.5 1.561E-18 3.187E-13 -0.5 -1.561E-18

* N2 + NO --> 2N + NO

0 2 5 2 1 4 4 5
0.5 0.5 1.561E-18 3.187E-13 -0.5 -1.561E-18

* 2N2 --> 2N + N2

0 2 2 2 1 4 4 2
1. 1. 1.561E-18 7.968E-13 -0.5 -1.561E-18

* N2 + N --> 3N

0 2 4 2 1 4 4 4
1. 1. 1.561E-18 6.9E-8 -1.5 -1.043E-18

* NO + N2 --> N+O+N2

0 5 2 2 1 4 4 2
1. 1. 1.043E-18 6.59E-10 -1.5 -1.043E-18

* NO + O2 --> N+O+O2

0 0 0 0 0 0 0 0
* 0.0 4.422e-19 1.5e-20 0 9

*--

0 5 1 2 1 4 3 1
1. 1. 1.043E-18 6.59E-10 -1.5 -1.043E-18

* NO + NO --> N+O+NO

0 5 5 2 1 4 3 5
1. 1. 1.043E-18 1.318E-8 -1.5 -1.043E-18

* NO + O --> N + O + O

0 5 3 2 1 4 3 3
1. 1. 1.043E-18 1.318E-8 -1.5 -1.043E-18

* NO + N --> 2N + O

0 5 4 2 1 4 3 4
1. 1. 1.043E-18 1.318E-8 -1.5 -1.043E-18

* NO + O --> 02 + N

0 5 3 1 1 1 0 4
0. 0. 2.719E-19 5.279E-21 1. -2.719E-19

* N2 + O --> NO + N

0 2 3 1 1 1 0 4
0. 0. 5.175E-19 1.120E-16 0. -5.175E-19

* O2 + N --> NO + O

0 1 4 1 1 1 0 3
0. 0. 4.968E-20 1.598E-18 0.5 2.719E-19

* NO + N --> N2 + O

0 5 4 1 1 2 0 3
0. 0. 2.49E-17 0. -5.175E-19

* O+O + M1 --> O2 + M1

0 3 3 1 0 1 0 1
0. 0. 8.297E-45 -0.5 8.197E-19

* N+N + M2 --> N2 + M2

0 4 4 1 0 2 0 -2
0. 0. 3.0051E-44 -0.5 1.561E-18

* N + N + N --> N2 + N

0 4 3 1 0 2 0 -3
0. 0. 6.3962E-40 -1.5 1.5637E-18

* N+O + M3 --> NO + M3

0 4 4 1 0 5 0 -4
0. 0. 2.7846E-40 -1.5 1.043E-18

* N+O --> NO+ + e-

* 4 3 1 1 1 0 9

* 0.0 4.422e-19 1.5e-20 0.5

*--

Screen.out

Screen.out

```

region 3 row - 84 radius = 0.816E-01 center = 0.821E-01 0.724E-01 angle =
0.148E-01
region 3 row - 85 radius = 0.850E-01 center = 0.842E-01 0.724E-01 angle =
0.148E-01
region 3 row - 86 radius = 0.885E-01 center = 0.864E-01 0.724E-01 angle =
0.148E-01
region 3 row - 87 radius = 0.921E-01 center = 0.887E-01 0.724E-01 angle =
0.147E-01
region 3 row - 88 radius = 0.959E-01 center = 0.911E-01 0.724E-01 angle =
0.147E-01
region 3 row - 89 radius = 0.998E-01 center = 0.935E-01 0.724E-01 angle =
0.147E-01
region 3 row - 90 radius = 0.104E+00 center = 0.961E-01 0.724E-01 angle =
0.147E-01
region 3 row - 91 radius = 0.108E+00 center = 0.988E-01 0.724E-01 angle =
0.146E-01

starting region 4
starting region connectivity
begin initial processing of region info

starting region 5
starting region connectivity
begin initial processing of region info

opening species file, spec, now
finished with file--spec

opening gas phase chemistry file, chem, now
reading reaction # 1
reading reaction # 2
reading reaction # 3
reading reaction # 4
reading reaction # 5
reading reaction # 6
reading reaction # 7
reading reaction # 8
reading reaction # 9
reading reaction # 10
reading reaction # 11
reading reaction # 12
reading reaction # 13
reading reaction # 14
reading reaction # 15
reading reaction # 16
reading reaction # 17
reading reaction # 18
reading reaction # 19
reading reaction # 20
reading reaction # 21
reading reaction # 22
reading reaction # 23
finished with file--chem

```

```

total cell volume(m^3) = 2.0047210E-02
8092800 molecules in initial grid
5 regions
28800 computational cells
5 chemical species

```

Prob4: MBF Expansion Chamber

Prob4: Molecular Beam Flurometer

- Input Gases: He & C₃H₆O

- Chemical Species:

	<u>Mwt</u>	<u>Mass</u>	<u>VHS diameter</u>
He	4.004 gm/gmole	6.648×10^{-27} kg	2.19×10^{-10} m
C ₃ H ₆ O	70.91 gm/gmole	9.64×10^{-26} kg	6.67×10^{-10} m

use a mixture viscosity coefficient of 0.658531 @ 273 K

- Boundary conditions:

inlet: sonic choked boundary

Mole fractions:

He= 1.0 C₃H₆O= 0.0

outlet: nonreentrant boundary (perfect vacuum pump)

- Surface Boundary Conditions:

- 100% thermal accommodation
- 100% diffuse surface reaction
- Temperature of all surfaces = 232.31 K

- Surface Chemistry:

no reactions

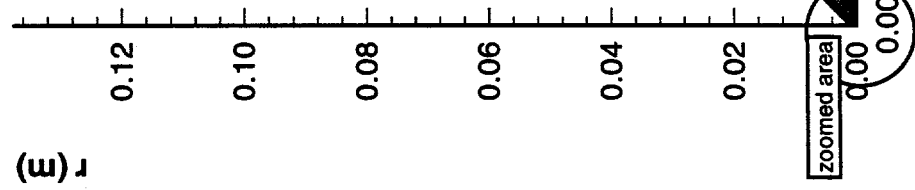
- Output:

- pressure, velocity, temperature and species distribution
- transient flowfield results

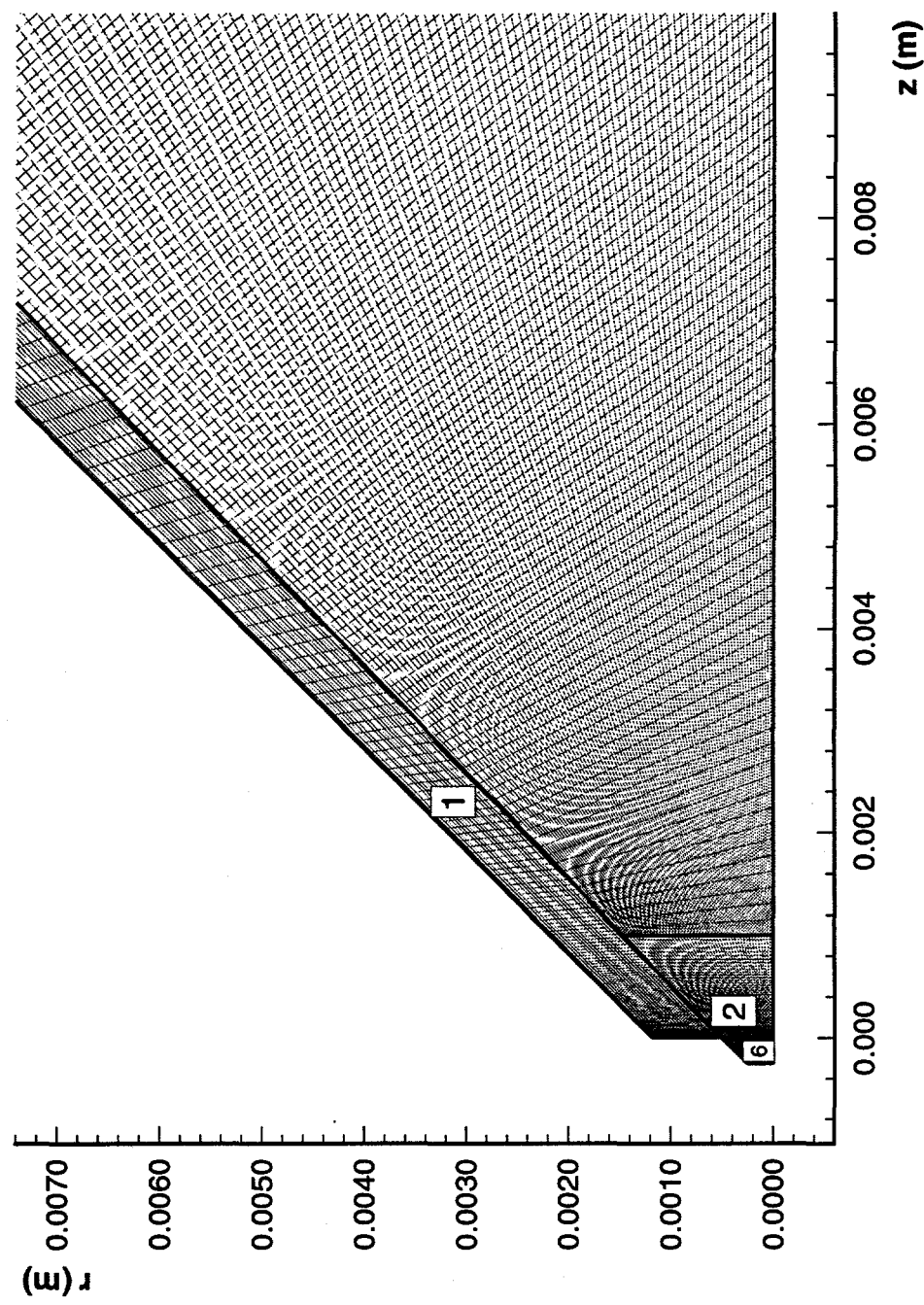
- Reference:

T. J. Bartel et. al., "DSMC Simulation of Nozzle Expansion Flow Fields," AIAA 94-2047, 6th AIAA/ASME Joint Thermophysics & Heat Transfer Conference, Colorado Springs, CO, 1994.

Prob4: Molecular Beam Flurometer



Prob4: Molecular Beam Flurometer (zoomed area)



t1.inp

* Pt. x (m) y (m)

* * asterisk in column 1 indicates comment card

* * MBF - He-Acetone T1

* * control: -1 -- plot grid only;
* * 1 -- initialisation & plot file
* * 0/1 for X-Y or Z-R flow

* * Frestream Conditions

* * 0 0/1 for vacuum/frestream
* * 0.0 x-component of velocity, m/sec (ft/sec x 0.3048)
* * 0.0 Y-component of velocity, m/sec
* * 6.1027e25 number density, molecules/m**3 (mol./ft**3 x 35.315)
* * 232.31 temperature, deg K (deg R/1.8)

* * Specie Information

* * 2 Number of molecular species

* * HE C3-H6-0
* * 1.0 0.0 internal structure of most complex molecule:
* * 3-monatomic, 4-rotation, 5-rotat. + vibrat.
* * # of chem. rx. (from file chem)

* * Weighting Information (particles and time step)

* * 1.e12 base # of real mols. per simulation one
* * base time step, sec
* * -4 cell weighting option

* * Collision Model Input

* * 273.0 ref. temp. for VHS model, deg K
* * 0.658531 temperature exponent of viscosity coeffs.

* * Surface Modelling Information

* * 1.000 thacc: thermal accomodation coefficient

* * Misc Input Section

* * 0 vacuum pump region # (0 - not used in problem)
* * density weighting variable flag in init2dsv
* * extra input 3
* * extra input 4
* * extra input 5
* * 5.08e-4 min radial expansion radius
* * 0 power coefficient
* * 0 extra input 8
* * 0 extra input 9
* * 0 extra input 10

* * Region Definition

* * 6 number of regions (must be 1e. 30)
* * 30 number of global points (must be 1e.120)

* * Global corner pt. Coordinates

* * 1 0.000 0.0
* * 2 1.5875e-2 0.0
* * 3 3.2258e-2 0.0
* * 4 1.905e-1 0.0
* * 5 0.0 5.08e-4
* * 6 1.65215e-2 1.63833e-2
* * 7 0.00 1.1811e-2
* * 8 1.5875e-2 1.7056e-2
* * 9 1.5875e-2 7.62e-2
* * 10 1.905e-1 7.62e-2
* * 11 0.01 0.01
* * 12 0.01 0.0005
* * 13 0.005 0.0005
* * 14 -0.00049 0.0
* * 15 -0.00049 0.0005
* * 16 0.002 0.00
* * 17 0.002 0.002
* * 18 0.015 0.03
* * 19 0.03 0.02
* * 20 0.1 0.0
* * 21 0.001 0.0
* * 22 0.001 1.46892e-2
* * 23 0.01 0.00
* * 24 0.01 1.01207e-2
* * 25 0.01 1.0508e-2
* * 26 0.01 1.1181e-2
* * 27 0.0 0.0
* * 28 -2.54e-4 2.54e-4
* * 29 0.012 0.0
* * 30 0.012 1.31811e-2
* * 1 <----- Inputs specific to this problem
* * 5. fnum multiplier
* * 1.0 dtm multiplier
* * 5 global points
* * 7 sides 1 and 3 curv
* * 8 sides 1 and 3 curv
* * 6 number of cells & boundary type code
* * 200 fnum multiplier
* * 20 number of cells & boundary type code
* * 0 sides 1 and 3 curv
* * 2 sides 2 and 4 cell
* * 40 sides 2 and 4 cell
* * 0 sides 1 and 3 curv
* * 7 sides 1 and 3 curv
* * 5 sides 1 and 3 curv
* * 2 number of BC entries
* * 2 side Cell1 Cell12 Spec. refl
* * 3 1 100 0.000
* * 3 1 200 0.000
* *

0 sides 2 and 4 cell spacing:
1 boundary type code for sides 1 - 4, resp.

7

7

7

0 number of surface bc

* Side Cell1 Cell2 Spec. refl. Temp. K Material# Value

*-----

*-----

*-----

*-----

*-----

*-----

*-----

*-----

*-----

*-----

*-----

*-----

*-----

*-----

*-----

*-----

*-----

*-----

*-----

*-----

*-----

*-----

*-----

*-----

*-----

*-----

*-----

*-----

*-----

*-----

*-----

*-----

*-----

*-----

*-----

*-----

*-----

*-----

*-----

*-----

*-----

*-----

*-----

*-----

*-----

*-----

*-----

*-----

*-----

*-----

*-----

*-----

*-----

*-----

*-----

0 sides 2 and 4 cell spacing:
1 boundary type code for sides 1 - 4, resp.

7

7

7

0 number of surface bc

* Side Cell1 Cell2 Spec. refl. Temp. K Material# Value

*-----

*-----

*-----

*-----

*-----

*-----

*-----

*-----

*-----

*-----

*-----

*-----

*-----

*-----

*-----

*-----

*-----

*-----

*-----

*-----

*-----

*-----

*-----

*-----

*-----

*-----

*-----

*-----

*-----

*-----

*-----

*-----

*-----

*-----

*-----

*-----

*-----

*-----

*-----

*-----

*-----

*-----

*-----

*-----

*-----

*-----

*-----

*-----

*-----

*-----

*-----

*-----

*-----

*-----

*-----

*-----

*-----

96/10/22

12:51:52

1	69	3	table for the MBF nozzle(INCA-M=1.05,plane at 2.53429e-4m)-file:inlet.bc	.001	0.211713E-03	0.605524E+26	948.5890	2.1188 0.2311E+03	0.2311E+03	0.999	
*	table #, # of table entries, BC type			.001	0.214203E-03	0.604427E+26	950.0980	2.6759 0.2308E+03	0.2308E+03	0.999	
*	number density	Vz	Vr	Tt	Tr	Tv	fraction	s			
species 1 2							0.211552E-03	0.603180E+26	951.8240	3.3405 0.2305E+03	
* units are MKS							.001	0.218769E-03	0.601783E+26	953.7870	4.1280 0.2301E+03
0.00000E+00 0.610425E+26 941.7240	0.0000 0.2323E+03 0.2323E+03	0.2323E+03	0.999	0.220861E-03	0.600232E+26	955.0070	5.0556 0.2297E+03	0.2297E+03	0.999		
0.146677E-04 0.610425E+26 941.7240	0.0000 0.2323E+03 0.2323E+03	0.2323E+03	0.999	0.222836E-03	0.598528E+26	958.4950	6.1421 0.2292E+03	0.2292E+03	0.999		
0.284833E-04 0.610423E+26 941.7250	0.0002 0.2323E+03 0.2323E+03	0.2323E+03	0.999	0.224701E-03	0.595664E+26	961.2550	7.4077 0.2287E+03	0.2287E+03	0.999		
0.415138E-04 0.610423E+26 941.7260	0.0004 0.2323E+03 0.2323E+03	0.2323E+03	0.999	0.222462E-03	0.594633E+26	964.2800	8.8731 0.2281E+03	0.2281E+03	0.999		
0.537871E-04 0.610422E+26 941.7270	0.0006 0.2323E+03 0.2323E+03	0.2323E+03	0.999	0.222126E-03	0.592422E+26	967.5460	10.5587 0.2275E+03	0.2275E+03	0.999		
0.653527E-04 0.610422E+26 941.7290	0.0008 0.2323E+03 0.2323E+03	0.2323E+03	0.999	0.222969E-03	0.590004E+26	971.0140	12.4847 0.2268E+03	0.2268E+03	0.999		
0.762515E-04 0.610422E+26 941.7290	0.0009 0.2323E+03 0.2323E+03	0.2323E+03	0.999	0.221185E-03	0.587356E+26	974.6250	14.6690 0.2260E+03	0.2260E+03	0.999		
0.865219E-04 0.610422E+26 941.7280	0.0008 0.2323E+03 0.2323E+03	0.2323E+03	0.999	0.223259E-03	0.584444E+26	978.3060	17.1268 0.2253E+03	0.2253E+03	0.999		
0.962003E-04 0.610423E+26 941.7250	0.0003 0.2323E+03 0.2323E+03	0.2323E+03	0.999	0.223921E-03	0.581242E+26	981.9660	19.8690 0.2245E+03	0.2245E+03	0.999		
0.105321E-03 0.610423E+26 941.7190	-0.0008 0.2323E+03 0.2323E+03	0.2323E+03	0.999	0.223181E-03	0.577728E+26	985.5060	22.8939 0.2237E+03	0.2237E+03	0.999		
0.113916E-03 0.610434E+26 941.7100	-0.0029 0.2323E+03 0.2323E+03	0.2323E+03	0.999	0.223637E-03	0.573890E+26	988.8250	26.1895 0.2230E+03	0.2230E+03	0.999		
0.122016E-03 0.610443E+26 941.6970	-0.0060 0.2323E+03 0.2323E+03	0.2323E+03	0.999	0.221593E-03	0.569716E+26	991.8270	29.7463 0.2224E+03	0.2224E+03	0.999		
0.129639E-03 0.610453E+26 941.6800	-0.0103 0.2323E+03 0.2323E+03	0.2323E+03	0.999	0.223857E-03	0.565195E+26	994.4260	33.5554 0.2218E+03	0.2218E+03	0.999		
0.136833E-03 0.610467E+26 941.6630	-0.0153 0.2323E+03 0.2323E+03	0.2323E+03	0.999	0.223593E-03	0.560317E+26	996.5400	37.6030 0.2213E+03	0.2213E+03	0.999		
0.143622E-03 0.610479E+26 941.6470	-0.0207 0.2323E+03 0.2323E+03	0.2323E+03	0.999	0.2242354E-03	0.543508E+26	999.3340	50.8990 0.2206E+03	0.2206E+03	0.999		
0.161709E-03 0.610485E+26 941.6370	-0.0253 0.2323E+03 0.2323E+03	0.2323E+03	0.999	0.240560E-03	0.555077E+26	998.0970	41.8680 0.2210E+03	0.2210E+03	0.999		
0.156033E-03 0.610486E+26 941.6390	-0.0278 0.2323E+03 0.2323E+03	0.2323E+03	0.999	0.241479E-03	0.549471E+26	999.0400	46.3152 0.2207E+03	0.2207E+03	0.999		
0.143622E-03 0.610479E+26 941.6600	-0.0262 0.2323E+03 0.2323E+03	0.2323E+03	0.999	0.243188E-03	0.537218E+26	998.9510	55.5788 0.2206E+03	0.2206E+03	0.999		
0.161709E-03 0.610483E+26 941.7070	-0.0182 0.2323E+03 0.2323E+03	0.2323E+03	0.999	0.243983E-03	0.530613E+26	997.8610	60.3215 0.2208E+03	0.2208E+03	0.999		
0.167038E-03 0.610443E+26 941.7910	-0.0011 0.2323E+03 0.2323E+03	0.2323E+03	0.999	0.244743E-03	0.523698E+26	998.9740	74.6020 0.2221E+03	0.2221E+03	0.999		
0.172100E-03 0.610387E+26 941.9230	0.0285 0.2323E+03 0.2323E+03	0.2323E+03	0.999	0.2446168E-03	0.501135E+26	985.6220	79.2665 0.2229E+03	0.2229E+03	0.999		
0.176832E-03 0.610299E+26 941.9230	0.2307 0.2321E+03 0.2321E+03	0.2321E+03	0.999	0.248703E-03	0.492995E+26	980.2630	83.8187 0.2238E+03	0.2238E+03	0.999		
0.189555E-03 0.609987E+26 942.3720	0.1400 0.2322E+03 0.2322E+03	0.2322E+03	0.999	0.245471E-03	0.484526E+26	973.7540	88.2192 0.2250E+03	0.2250E+03	0.999		
0.189556E-03 0.609747E+26 942.7140	0.2307 0.2321E+03 0.2321E+03	0.2321E+03	0.999	0.248103E-03	0.475739E+26	965.8640	92.4555 0.2264E+03	0.2264E+03	0.999		
0.193289E-03 0.609437E+26 943.1540	0.3517 0.2320E+03 0.2320E+03	0.2320E+03	0.999	0.249285E-03	0.466583E+26	955.2080	96.5942 0.2281E+03	0.2281E+03	0.999		
0.196827E-03 0.609050E+26 943.7030	0.5090 0.2319E+03 0.2319E+03	0.2319E+03	0.999	0.249508E-03	0.457380E+26	944.3170	100.7240 0.2302E+03	0.2302E+03	0.999		
0.203309E-03 0.607992E+26 945.1890	0.9614 0.2317E+03 0.2317E+03	0.2317E+03	0.999	0.249805E-03	0.424901E-03						
0.206716E-03 0.607298E+26 946.1510	1.2733 0.2315E+03 0.2315E+03	0.2315E+03	0.999	0.249508E-03	0.424901E-03						
0.209074E-03 0.606479E+26 947.2800	1.6554 0.2313E+03 0.2313E+03	0.2313E+03	0.999	0.249850E-03	0.457380E+26	944.3170	100.7240 0.2302E+03	0.2302E+03	0.999		

9/10/2012 12:50:54

0.250400E-03	0.447682E+26	929.7660	104.6890	0.2327E+03	0.2327E+03	0.2327E+03	0.999
0.250938E-03	0.437375E+26	911.8630	107.9540	0.2358E+03	0.2358E+03	0.2358E+03	0.999
.001							
0.251465E-03	0.426346E+26	889.0870	109.7260	0.2395E+03	0.2395E+03	0.2395E+03	0.999
.001							
0.251982E-03	0.414573E+26	858.6020	108.9840	0.2439E+03	0.2439E+03	0.2439E+03	0.999
.001							
0.252493E-03	0.402026E+26	815.4470	103.9530	0.2494E+03	0.2494E+03	0.2494E+03	0.999
.001							
0.252998E-03	0.388550E+26	750.9500	90.3279	0.2560E+03	0.2560E+03	0.2560E+03	0.999
.001							
0.253500E-03	0.374430E+26	649.8740	57.8191	0.2628E+03	0.2628E+03	0.2628E+03	0.999
.001							
0.254000E-03	0.311123E+26	0.0000	0.0000	0.3000E+03	0.3000E+03	0.3000E+03	0.999
.001							

 * species data file
 * *****
 * number of species to input taken from problem description
 * input -- they MUST be the same
 * *****

 * ID ID Mwt. Mol. mass Diam. #Rot.Deg. Rot.Rel. Vib. Rel. Vib.Temp. specie wt. char
 * ge (kg) (m) Freedom Coll. # Coll. # (K)
 * -----
 He 4.004 6.648e-27 2.19e-10 0.0 0.0 0.0 0.0 1.00 0.0
 C2H5O 58.08 9.64e-26 6.67e-10 0.0 0.0 0.0 0.0 0.01 0.
 O 0
 NO 30.008 4.98E-26 4.E-10 2. 1. 50. 2740. 1.0 0.0
 O2 32.00 5.31E-26 3.96E-10 2. 5. 50. 2270. 1.0 0.0
 N2 28.016 4.65E-26 4.07E-10 2. 5. 50. 3390. 1.0 0.0
 O 16.00 2.65E-26 3.E-10 0. 0. 0. 0. 1.0 0.0
 N 14.008 2.325E-26 3.E-10 0. 0. 0. 0. 1.0 0.0
 NO 30.008 4.98E-26 4.E-10 2. 1. 50. 2740. 1.0 0.0
 He 4.004 6.648e-27 2.19e-10 0.0 0.0 0.0 0.0 1.00 0.0
 Ar 39.94 6.63e-26 4.04e-10 0. 0. 0000. 1.0 0.0

96/10/22
12:52:40

screen.out

init2d t1.inp
init2d for DSMC-MP -- version 6.00

starting region 1
starting region connectivity
begin initial processing of region info

starting region 2
starting region connectivity
begin initial processing of region info

starting region 3
starting region connectivity
begin initial processing of region info

starting region 4
starting region connectivity
begin initial processing of region info

opening inlet file, inlet, now
finished reading file--inlet

starting region 5
starting region connectivity
begin initial processing of region info

starting region 6
starting region connectivity
begin initial processing of region info

opening species file, spec, now
finished with file--spec

total cell volume(m^3) = 3.1904490E-03
7136729 molecules in initial grid
6 regions
38800 computational cells
2 chemical species

66 region connections
1022 grid data size
100 boundary elements
420 surface elements
39816 cell corner points
50 inlet table boundary cells

beat%{ ./prob4}

1

Prob5: Sputter Deposition

Prob5: Sputter Deposition

- Input Gases: N₂ & Ar

- Wafer Surface: Stainless Steel (no etching)

- Chemical Species:

	<u>Mwt</u>	<u>Mass</u>	<u>VHS diameter</u>
Ar	39.93 gm/gmole	0.66 x 10 ⁻²⁵ kg	3.555 x 10 ⁻¹⁰ m
N ₂	28.01 gm/gmole	0.47 x 10 ⁻²⁵ kg	3.675 x 10 ⁻¹⁰ m
Ti	47.90 gm/gmole	0.663 x 10 ⁻²⁵ kg	3.60 x 10 ⁻¹⁰ m

use a mixture viscosity coefficient of 0.77 @ 300 K

- Boundary conditions:

inlet: ring radius = 0.15 m

150 sccm

use an inlet temperature of 300 K and a velocity of 200 m/s

outlet: symmetric pump

1150 1/s flow rate

no inlet screen blockage

- Surface Boundary Conditions:

- 100% thermal accommodation

- 100% diffuse surface reaction

- Temperature of all surfaces = 300 K

- Surface Chemistry:

Ar --> Ar rate => 100%

N₂ --> Ar rate => 100%

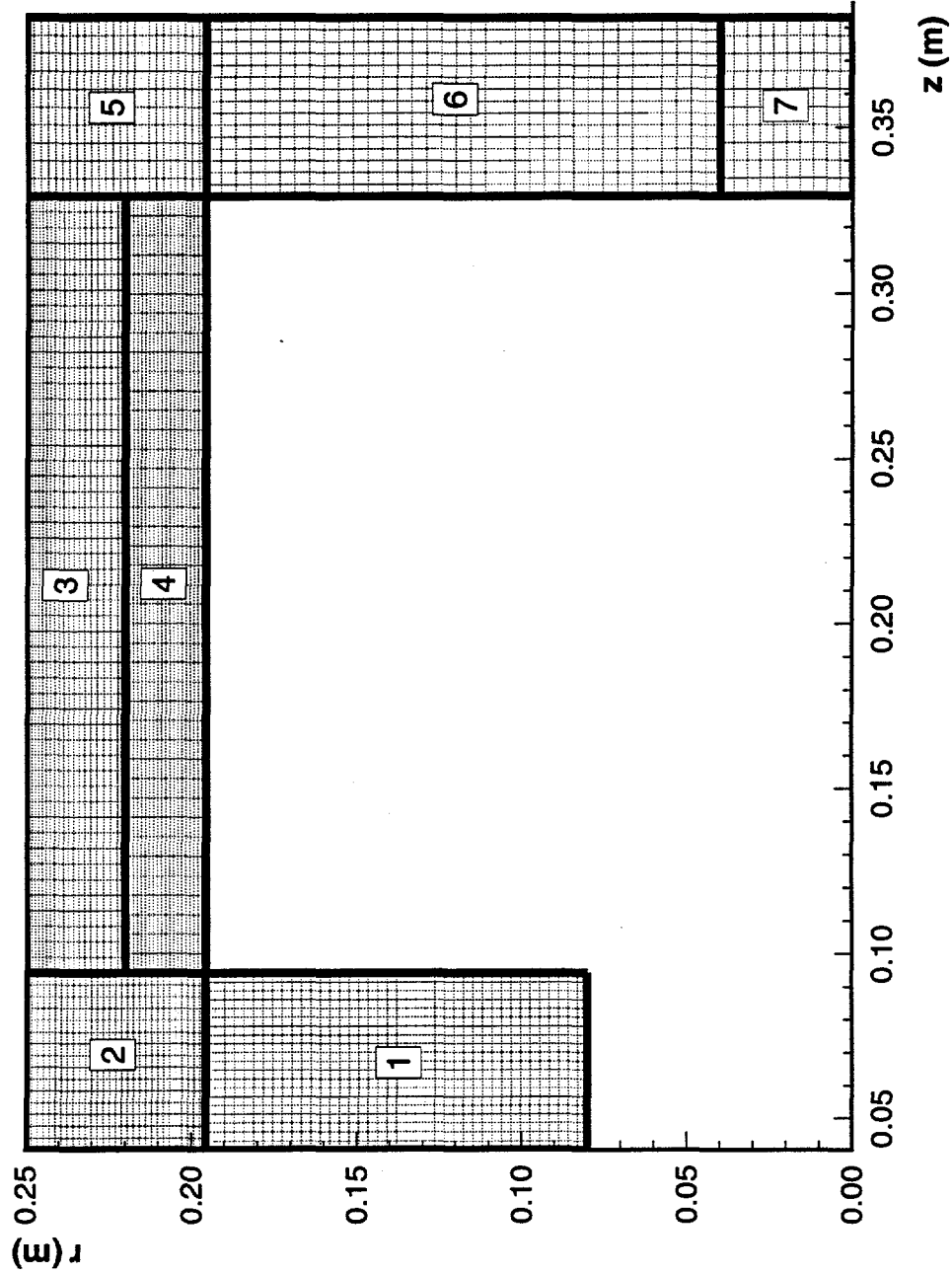
Ti --> Ar rate => 100%

- Output:

- pressure and species distribution

- angular distribution of incident particles for wafer

Prob5: Sputter Deposition



96/10/22
12.53.51

卷之三

calc7.inp

calc7.inp

10 number of cells along sides 1 and 3
 25 number of cells along sides 2 and 4
 0 sides 1 and 3 curvature: 0/1 for line/circular arc
 0 sides 1 and 3 cell spacing:
 0 sides 2 and 4 cell spacing:
 7 boundary type code for sides 1 - 4: resp.

fnm multiplier
dtm multiplier
global points

Side	Cell1	Cell2	Material#	Value
7	10	10	Spec. refl:	Temp. K
5	10	10	number of cells along sides 1 and 3	
5	0	0	number of cells along sides 2 and 4	
2	0	0	sides 1 and 3 curvature: 0/1 for line/circular arc	
			sides 1 and 3 cell spacing:	
			sides 2 and 4 cell spacing:	
			boundary type code for sides 1 - 4, resp.	

		Region interface/matching		Region interface/region		Region matching/region	
3	1	100	0.000	300.00	2	0.	
4	1	100	0.000	300.00	2	0.	

|-> only need $IVN > 0$; then supply IVN pairs of IVR, IVS ,
 Number adj. Adj. side | Adj. reg.
 reg. sides no. (IVS) | no. (IVR)

1	1	3	6	4	4	3
2	2	4	4	4	0	0
3	0	0	0	0	0	0
4	0	0	0	0	0	0

```
6 <----- Inputs specific to this region follow
  1.0          num multiplier
  1.0          dtm multiplier
  20          c1-b1 multiplier
  20          c2-b2 multiplier
```

22	global points
26	
28	
30	number of cells along sides 1 and 3
15	number of cells along sides 2 and 4
35	sides 1 and 3 curvature: 0/1 for line/circular arc
0	sides 1 and 3 cell spacing:
0	sides 2 and 4 cell spacing:
7	boundary rule code for sides 1 - 4 ^{rcen}

Boundary Opt. Code for Sacco + 1/2 DE						
	Side	Cell1	Cell2	Spec. refl.	Temp. K	Material#
5	2	1	100	0.000	300.00	2
7	4	1	100	0.000	300.00	2
5						0.
5						0.
2						

	Region interface/matching		
- - - ->	Only need if IVN > 0; then supply IVN pairs of (IVR, IVS)		
Number adj.			
Reg. side	Adj. side	Adj. reg.	
reg. sides			
(IVN)	(IVS)	no. (IVR)	

1	1	3	7
2	0		
3	1	1	5
4	0		

*	Side	Cell1	Cell2	Spec. refl.	Temp. K	Material #	Value
1.0							
1.0							
31							
29							
30							
32							
10							
10							
0							
0							
0							
0							
5							
5							
5							
5							
7							
3							

*	1	1	100	0.000	300.00	2	0.
1	1	100	0.000	300.00	2	0.	0.
2	1	100	0.000	300.00	2	0.	0.
4	1	100	0.000	300.00	2	0.	0.

- * |-----> Region interface/matching
- * |-----> Only need if IVN > 0; then supply IVN pairs of (IVR, IVS)

Reg. side	Adj. side	Adj. reg.
number adj.	reg. sides	no. (IVR)

END OF EVIDENCE TESTIMONY BY					
1	0	0			
2	0	0			
3		1	1	6	
4	0				

THE PRACTICAL APPROACH TO THE PRACTICAL APPROACH

111

1275351

inlet

* N2 & Ar inlet to Ti sputter reactor

2
1 1 1
0.067 6.73e19 0.00 320. 250. 250. 0.5 0.5 0.0
*used inlet at 300K and 1 torr into system at 3mtorr. 150 sccm inlet

*Ti Sputter target

2 2
0.095 5.0e19 0.00 -9629.0 500. 500. 0.0 0.0 1.0
0.327 5.0e19 0.00 -9629.0 500. 500. -500. 0.0 0.0 1.0
*Assumed Ti coming off surface was at 23ev.

96/0/22
12:53:51

spec

* species data file

* number of species to input taken from problem description
* input --- they MUST be the same
*-----
* ID Mol. mass Diam. #Rot.Deg. Rot.Rel. Vib. Rel. Vib.Temp. specie wt. cha
rge (kg) (m) Freedom Coll. # Coll. # (K)
*-----
*-----
Ar 39.93 0.66e-25 3.555e-10 0.0 0.0 0.0 0.0 1.0 0.0
N2 28.01 0.47e-25 3.675e-10 0.0 0.0 0.0 0.0 1.0 0.0
Ti 47.90 0.663e-25 3.60e-10 0.0 0.0 0.0 0.0 1.0 0.0
*Diameter for Ti has not been looked up, just a random number right now.
*-----

```
/* this file contain surface chemistry information for the
 * Sputter example problem
 * Ar, N2, Ti,
 * 1 2 3
 *
 * variable order for each reaction:
 * (reaction type) (species-i) (species-r1) (species-r2) (create prob1) (create prob2) (degree
 * of specular) (Rx prob)
 *
 * number of material table types
 *
 * material 1 (wafer), number of reactions (sputter of Ti to deposit TiN)
 1. 1 1.0
 1. 3. 0. 0.0 0.0 0.0 1.0
 *
 * material 2 (chamber walls), number of reactions
 2. 1 1.0
 1. 3. 3. 0. 0.0 0.0 0.0 1.0
 *
 * material 3 (Ti target), number of reactions
 3. 1 1.0
 1. 3. 3. 0. 0.0 0.0 0.0 1.0
 *
 *
```

```
bear{./prob5} init2d calc7.inp
calc7.inp
  init2d for DSMC-MP -- version 6.00
```

```
starting region      1
starting region connectivity
begin initial processing of region info
```

```
opening inlet file, inlet, now
finished reading file--inlet
```

```
starting region      2
starting region connectivity
begin initial processing of region info
```

```
starting region      3
starting region connectivity
begin initial processing of region info
```

```
starting region      4
starting region connectivity
begin initial processing of region info
```

```
starting region      5
starting region connectivity
begin initial processing of region info
```

```
starting region      6
starting region connectivity
begin initial processing of region info
```

```
starting region      7
starting region connectivity
begin initial processing of region info
```

```
opening species file, spec, now
finished with file--spec
```

```
opening surface chemistry file, surf_chem, now
reading surface: material #      1 reaction #      1
reading surface: material #      2 reaction #      1
reading surface: material #      3 reaction #      1
finished with file--surf_chem
```

```
total cell volume(m^3) =  3.5339266E-02
832100 molecules in initial grid
  7 regions
  3925 computational cells
  3 chemical species
```

```
  76 region connections
  354 grid data size
  70 boundary elements
  370 surface elements
  4272 cell corner points
  51 inlet table boundary cells
```

```
bear{./prob5}
```

Prob6: Si etch by Chlorine Plasma in UH geometry

Prob6: Si etch by Chlorine Plasma in UH geometry

- Input Gases: Cl₂

- Wafer Surface: Si

- Chemical Species:

	<u>Mwt</u>	<u>Mass</u>	<u>VHS diameter</u>
Cl	35.45 gm/gmole	0.59 x 10 ⁻²⁵ kg	3.831 x 10 ⁻¹⁰ m
Cl ⁺	35.45 gm/gmole	0.59 x 10 ⁻²⁵ kg	3.831 x 10 ⁻¹⁰ m
Cl ⁻	35.45 gm/gmole	0.59 x 10 ⁻²⁵ kg	3.831 x 10 ⁻¹⁰ m
Cl ₂	70.91 gm/gmole	1.18 x 10 ⁻²⁵ kg	5.405 x 10 ⁻¹⁰ m
Cl ₂ ⁺	70.91 gm/gmole	1.18 x 10 ⁻²⁵ kg	5.405 x 10 ⁻¹⁰ m
SiCl ₂	98.99 gm/gmole	1.647 x 10 ⁻²⁵ kg	8.000 x 10 ⁻¹⁰ m

use a mixture viscosity coefficient of 1.00 @ 300 K

- Boundary conditions:

inlet: ring radius = 0.15 m

140 sccm Cl₂

use an inlet temperature of 255.79 K and a velocity of 200 m/s

outlet: symmetric pump

1150 1/s flow rate

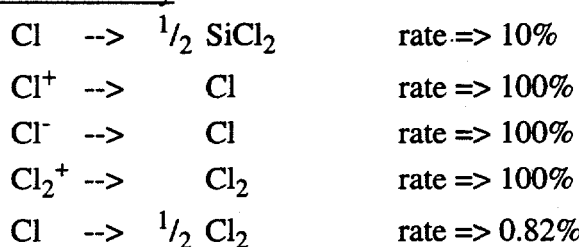
Pressure control to 2 mtorr.

no inlet screen blockage

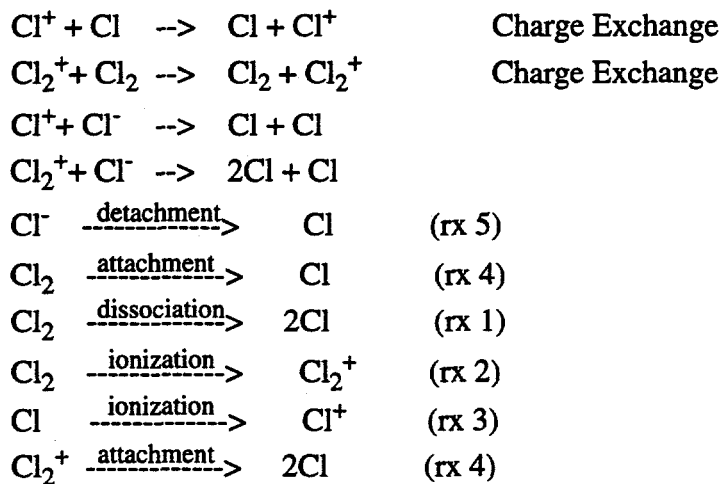
- Surface Boundary Conditions:

- 100% thermal accommodation
- 100% diffuse surface reaction
- Temperature of all surfaces = 300 K

- Surface Chemistry:



- Gas Phase Chemistry:



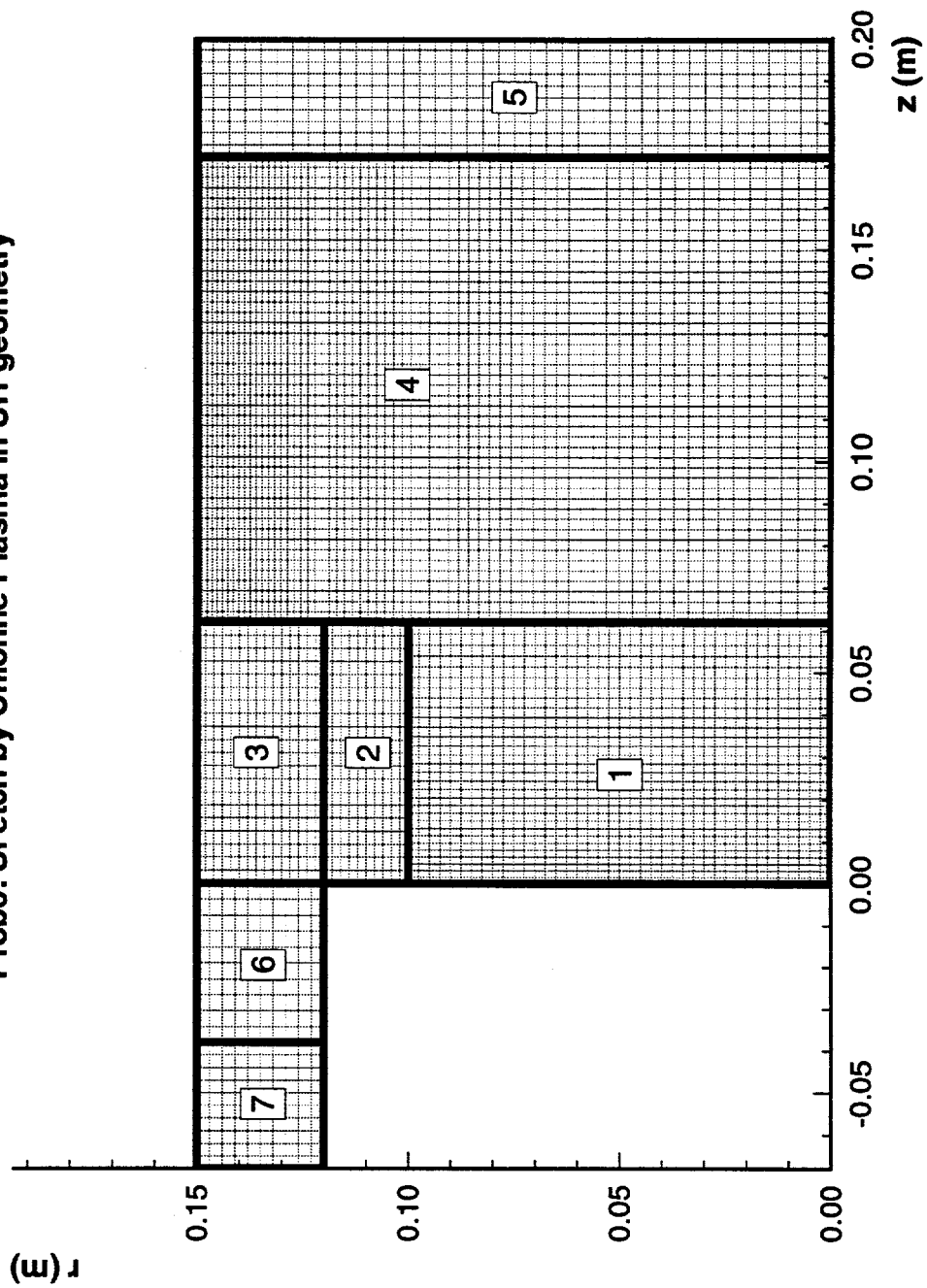
- Output:

- pressure, velocity, temperature and species distribution
- surface etch rate
- angular distribution of incident particles for wafer

- References used to create example:

D. J. Economou et.al., "Two-Dimensional Direct Simulation Monte Carlo (DSMC) of Reactive Neutral and Ion Flow in High Density Plasma Reactor," *IEEE Trans. Plasma Sci.*, Vol.23, #4, pp. 581 - 590, August 1995.

Prob6: Si etch by Chlorine Plasma in UH geometry



17 number of global points (must be .1e.120)

*--> astrick in column 1 indicates comment card

*--> Global corner pt. coordinates

*--> Pt. z (m) r (m)

UH GEOM2 -- run26x

*--> point injection model for inlet

*-->

*--> 1 control: -1 -- plot grid only;
 *--> 1 -- initialization & plot file

*--> 1 0/1 for X-Y or Z-R flow

*-->

*--> 1 Freestream Conditions

*--> 1 0/1 for vacuum/freestream

0. x-component of velocity, m/sec (ft/sec x 0.3048)

0. y-component of velocity, m/sec

3.0e19 number density, molecules/m³ (mol./ft³*3 x 35.315)

300.00 temperature, deg K (deg R/1.8)

*-->

*--> 1 Species Information

*--> 6 Number of molecular species

*--> C1 C1+ C1- C12 C12+ SIC12

*--> 0.8 0.0 0.0 0.2 0.0 0.0

*-->

*--> 3 internal structure of most complex molecule:
 3-monatomic, 4-rotation, 5-rotat. + vibrat.

*--> 10 # of chem. rxn. (from file chem)

*-->

*--> 1 Weighting Information (particles and time step)

*--> 1.0e10 base # of real mols. per simulation one

1.E-06 base time step, sec

4 cell weighting option

*-->

*--> 1 Collision Model Input

*--> 300.0 ref. temp. for VHS model, deg K

1.0 temperature exponent of viscosity coeffs.

*-->

*--> 1.000 thacc: thermal accommodation coefficient

*-->

*--> 1 Misc Input Section

*--> 7 vacuum pump region #

0 ic region distribution

1 wafer material type

17 pressure iteration control pt.

*-->

*--> 0.0005 min radial expansion radius

1 power coeff 8

0 extra input 9

0 use external cross-sections

*-->

*--> 7 number of regions (must be .1e. 30)

*-->

*--> 1 Global corner pt. coordinates

*--> Pt. z (m) r (m)

1 0.0 0.0 0.0

2 0.0619 0.0 0.0

3 0.1719 0.0 0.0

4 0.2 0.0 0.0

5 0.0 0.10 0.10

6 0.0619 0.1 0.1

7 0.0 0.12 0.12

8 0.0619 0.12 0.12

9 0.0 0.15 0.15

10 0.0619 0.15 0.15

11 0.1719 0.15 0.15

12 0.2 0.15 0.15

13 -0.0381 0.12 0.12

14 -0.0381 0.15 0.15

15 -0.0681 0.12 0.12

16 -0.0681 0.15 0.15

17 0.0 0.135 0.135

*--> Individual Region Definitions Follow

*--> -REGION NUMBERS MUST BE SEQUENTIAL--

*--> 1 <---- Inputs specific to this region follow

*--> 1.0 fmum multiplier

*--> 1.0 dtm multiplier

*--> 1.0 global points

*-->

*--> 2 number of cells along sides 1 and 3

*--> 3 number of cells along sides 2 and 4

*--> sides 1 and 3 curvature: 0/1 for line/circular arc

*--> sides 1 and 3 cell spacing:

*--> 5 1.02

*--> 30 sides 2 and 4 cell spacing:

*--> 0 boundary type code for sides 1 - 4, resp.

*--> 1 1

*--> 2 1 50 0.000 375.00 1 0.

*-->

*--> 7 Region interface/matching

*--> 1 Reg. side reg. sides Adj. side Adj. reg.

*--> 1 0 0

*--> 2 1 0

*--> 3 1 1 1 2

*--> 4 1 2 4

*-->

run26x.inp

2 <----- Inputs specific to this region follow

2 ~~-----~~ Inputs specific to this region follow

961022
12:59:12

spec

* species data file *

* number of species to input taken from problem description
* input --- they MUST be the same

	ID	Mol.	mass	Diam.	#Rot.Deg.	Rot.Rel.	Vib.	Rel.	Vib.Temp.	specie	wt.	char
ge		(kg)		(m)		Freedom	Coll. #	Coll. #	(K)			
---	---	---	---	---	---	---	---	---	---	---	---	---
C1	35.45	0.59e-25	3.831e-10	0.0	0.0	0.0	0.0	0.0	1.0	0.		
C1+	35.45	0.59e-25	3.831e-10	0.0	0.0	0.0	0.0	0.0	1.0	1.0		
C1-	35.45	0.59e-25	3.831e-10	0.0	0.0	0.0	0.0	0.0	1.0	-1.		
0	70.91	1.18e-25	5.405e-10	2.	5.	00.	0000.	0000.	1.0	0.		
0	C12+	70.91	1.18e-25	5.405e-10	2.	5.	00.	0000.	1.0	1.		
0	SiC12	98.99	1.647e-25	8.000e-10	2.	5.	0.0	0.0	1.0	0.		
*	*	*	*	*	*	*	*	*	*	*	*	*

some of these are based on Chemkin data provided by Ellen Meeks - SNL
*

chem

This input file contains the data characterizing the chemical reactions.
 If input # reactions = 0, there is no chemistry, and this file is not read.
 input lines are free format
 the reaction equation is an input line (a25)

NOTE: line 1 MUST have 8 integers
 line 2 for type 0, -1, & -2 MUST have 5 real numbers
 line 2 for type -3 MUST have 2 integers and 1 real number
 line 3 for type -3 MUST have 6 real numbers

first number on line 1 defines reaction type:

0 -- Standard Arrhenius collisional chemistry $k = A T^B \exp(-E_a/kT)$
 second line variables:
 1 -- number of internal degrees of freedom
 2 -- Ea
 3 -- A
 4 -- B
 5 -- heat of rx (+ for exothermic) - joules

-1 -- Charge Exchange reaction with fixed rate
 second line variables:
 1 -- probability
 2 -- sigma CE (m^2)

-2 -- Charge Exchange reaction using model from Rapp & Frances (1962)
 sigma = $(k1 - k2 * \log(vr))^{1/2}$
 second line variables:
 1 -- k1 for elastic collision
 2 -- k2 for elastic collision
 3 -- k1 for charge exchange
 4 -- k2 for charge exchange

-3 -- Electron Impact reactions
 second line variables:
 1 -- equation type (if <0, T in K instead of eV)
 2 -- number of products (1 or 2)
 3 -- heat of formation (Frank-Candom) - joules
 third line variables:
 1 - 6 are fit coefficients

Chlorine chemistry example -- 11 reaction set

Cl, Cl+, Cl-, Cl2, Cl2+, SiCl2
 1 2 3 4 5 6

Cl+ + Cl -> Cl + Cl+ (charge exchange)
 -1 2 1 1 0 2
 0.75 120.e-20 0. 0. 0.

Cl2+ + Cl2 -> Cl2 + Cl2+ (charge exchange)
 -1 5 4 1 4 0 5
 0.75 120.e-20 0. 0. 0.

Cl- + Cl -> Cl + Cl- (charge exchange)
 -1 3 1 1 0 3
 0.90 120.e-20 0. 0. 0.

* C1+ + Cl- -> Cl + Cl- (recombination)
 -4 2 3 1 1 0 1
 0.0 0.0 5.e-14 0.0 1.5e-18

* C12+ + Cl- -> 2Cl + Cl- (recombination)
 -4 5 3 2 1 1 0 1
 0.0 0.0 5.e-14 0.0 1.26e-18

* C12 attachment to Cl + Cl- (electron impact)
 -3 4 4 1 1 0 3
 ***** 2 2 3.0e-19 made up number
 ***** 2 2 5.78e-19 Franck-Condon

* C1- detachment to Cl- (electron impact)
 -3 3 3 1 0 1 0 0
 1 1 0.0
 2.94e-14 0.680 3.7994 0.0 0.0 0.0

* C12 dissociation to 2Cl (electron impact)
 -3 4 4 1 1 0 1
 1 2 0.96e-19
 3.99e-14 0.115 4.43 0.0 0.0 0.0

* C12 ionization to Cl2+ (electron impact)
 -3 4 4 1 0 5 0 0
 1 1 0.0
 2.13e-14 0.771 11.7 0.0 0.0 0.0

* Cl2 ionization to Cl+ (electron impact)
 -3 1 1 0 2 0 0
 1 1 0.0
 2.96e-14 0.554 13.1 0.0 0.0 0.0

* C12+ attachment to 2Cl (electron impact)
 -3 5 5 1 1 0 1
 3 2 1.84e-18
 9.0e-13 0.025826 0.61 0.0 0.0 0.

* third body probabilities now follow
 0

96/10/22
12:59:11

1

inlet

```
* new inlet format -- pt. source == #/s now
*          -- 140sccm -- point source -- new grid2
1 1 1
0.1119 6.207e19 0.00 -199.725 255.79 255.79 255.79 0. 0.0 0.0 1.0 0.0 0
.0
* base case calc.
* *
```

```
* this file contain surface chemistry information for the
* UH - GEOM1 Problem C12 chemistry
* Cl, Cl+, Cl-, C12, C12+, SiC12
* 1 2 3 4 5 6
*
* variable order for each reaction:
* (reaction type) (Species-r1) (Species-r2) (create prob1) (create prob2) (degree
* of specular) (Rx prob)
*
* number of material table types
3
* material 1 (water), number of reactions (etch of Si --> SiC12)
1 4 1.0
1. 1. 6. 0. 0.5 0. 0. 0.1
1. 2. 1. 0. 1. 0. 0. 1.0
1. 3. 1. 0. 1. 0. 0. 1.0
1. 5. 4. 0. 1. 0. 0. 1.0
*
* material 2, number of reactions
2 4 1.0
1. 1. 4. 0. 0.5 0. 0. 0.0082
1. 2. 1. 0. 1.0 0. 0. 1.0
1. 3. 1. 0. 1.0 0. 0. 1.0
1. 5. 4. 0. 1.0 0. 0. 1.0
*
* material 3, number of reactions
3 4 1.0
1. 1. 4. 0. 0.5 0. 0. 0.0082
1. 2. 1. 0. 1.0 0. 0. 1.0
1. 3. 1. 0. 1.0 0. 0. 1.0
1. 5. 4. 0. 1.0 0. 0. 1.0
*
```

post2d.vlist

```

*   *   * in col 1 for comment or to comment out a line
*   *   species number fractions are 5x where x is the specie #
*   *   species velocities are in pairs of 10x and 20x for Vz and Vr
*   *   species translational temp (K) are 30x where x is the specie #
*   *   species number fractions are 5x where x is the specie #
*   *   species velocities are in pairs of 10x and 20x for Vz and Vr
*   *   species translational temp (K) are 30x where x is the specie #

*Var. name(10 Char MAX) multi. factor Var. index
R(m) -1. 2
Z(m) 1. 1
#/cell 1. 3
n 1. 4
p(motor) 7.50075 5
*cellwt 1. 6
Vr (m/s) -1. 8
Vz (m/s) 1. 7
rt(k) 1. 9
*tr(k) 1. 10
*rv(k) 1. 11
*tav(k) 1. 12
*kn 1. 13
*cfl 1. 14
c1 1. 51
c1+ 1. 52
c1- 1. 53
c12 1. 54
c12+ 1. 55
sic12 1. 56
vr c1 -1.
vz c1 1.
vr c1+ -1.
vz c1+ 1.
vr c1- -1.
vz c1- 1.
vr c12 -1.
vz c12 1.
vr c12+ -1.
vz c12+ 1.
vr sic12 -1.
vz sic12 1.
c1 t 1.
c1+ t 1.
c1- t 1.
c12 t 1.
c12+ t 1.
sic12 t 1.

END

```

901022
12:59:11

1

Prob7: NO nozzle expansion and data comparison

Prob7: NO nozzle expansion and data comparison

- Input Gases: NO

- Chemical Species:

NO:

Mwt (gm/ gmole)	Mass (kg)	VHS diameter (m)	# Rot. Deg. of Freedom	Rot. Coll. #	Vib. Coll. #	Vib. Temp. (K)
30.008	4.98×10^{-26}	4.00×10^{-10}	2	1	50	2740

use a mixture viscosity coefficient of 0.9 @ 273 K

- Boundary conditions:

inlet: 25 torr pulsed valve (radial inlet)

outlet: vacuum

- Surface Boundary Conditions:

- 100% thermal accommodation
- 100% diffuse surface reaction
- Temperature of all surfaces = 373 K

- Output:

- rotational temperature, density and pressure

- Reference:

Justiz, C. R. & Bartel, T. J., "DSMC Simulation of Ionized Rarified Flows," **AIAA 93-3095**,
AIAA, 24th AIAA Fluids Dynamics Conference, Orlando, FL, 1993.

Prob7: NO Expansion

r (m)

0.035
0.030
0.025
0.020
0.015
0.010
0.005
0.000

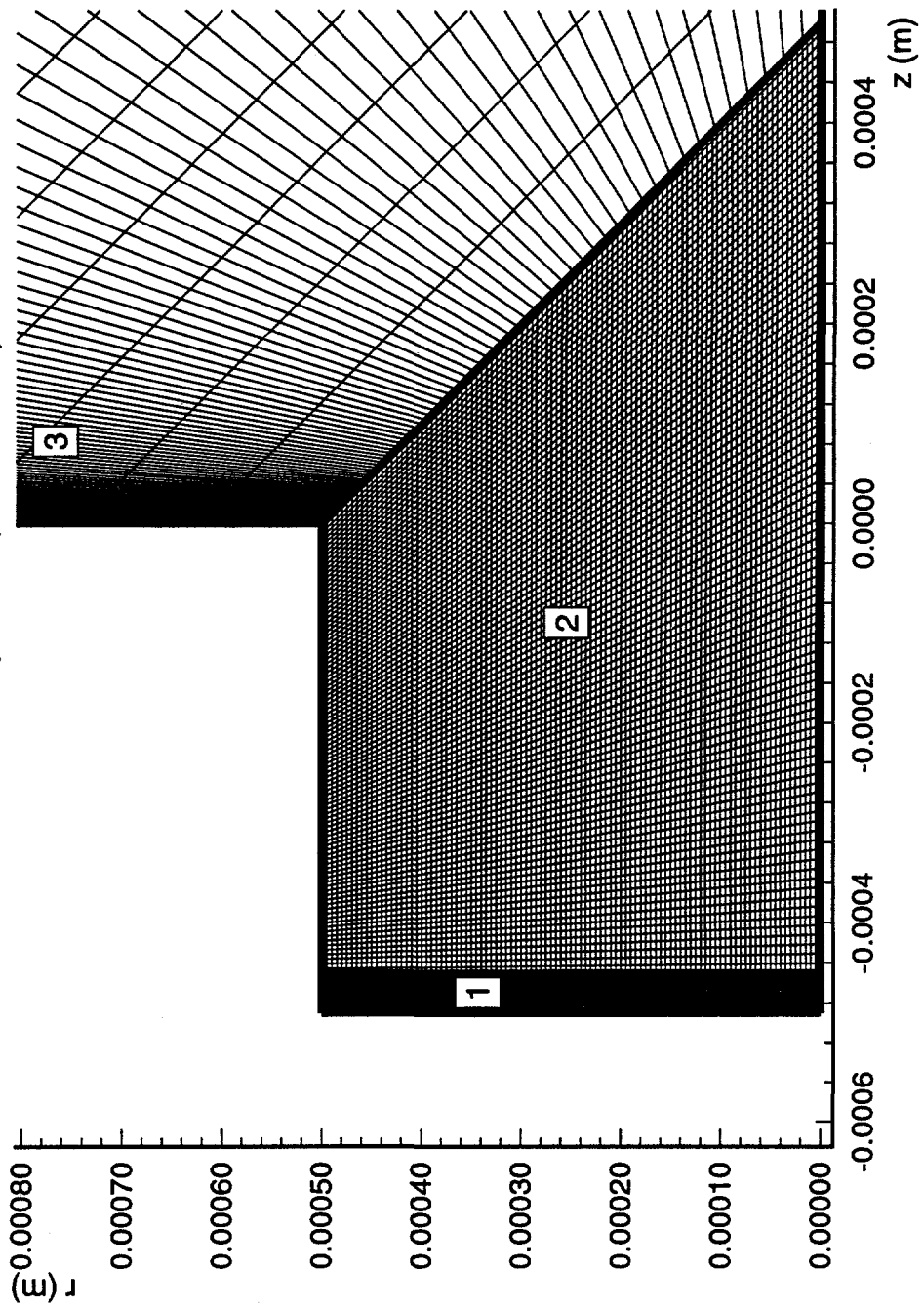
0.040
0.030
0.020
0.010
0.000

zoomed area

4

3

Prob7: NO Expansion (zoomed area)



no_new.inp

```

*      asterisk in column 1 indicates comment card
*      pulsed valve-25T- NO diffuse
*
*      1      control:      -1 -- plot grid only;
*      *      *      1 -- initialization & plot file
*      1      0/1 for X-Y or Z-R flow
*      *      *      Initial Conditions
*
*      0      0/1 for vacuum/freestream
*      0      x-component of velocity, m/sec (ft/sec x 0.3048)
*      -625.  y-component of velocity, m/sec
*      1.24e23 number density, molecules/m^3 (mol./ft^3 x 35.315)
*      300.00  temperature, deg K (deg R/1.8)
*
*      *      *      Species Information
*      1      Number of molecular species
*      *      NO
*      1.0
*      *
*      *      *      internal structure of most complex molecule:
*      5      3-monatomic, 4-rotation, 5-rotat. + vibrat.
*      *      # of chem. rx. (from file chem)
*      0
*
*      *      *      Weighting Information (particles and time step)
*      1.e8  base # of real mols. per simulation one
*      0.1E-06 base time step, sec
*      -4      cell weighting option
*
*      *      *      Collision Model Input
*
*      273.0  ref. temp. for VHS model, deg K
*      0.9  temperature exponent of viscosity coeffs.
*
*      *      *      Surface Modelling Information
*
*      1.000  thacc: thermal accomodation coefficient
*
*      *      *      Misc Input Section
*
*      0      vacuum pump region #
*      0      ic region distribution
*      0      wafer material type
*      0      pressure iteration control pt.
*      0      min radial expansion radius
*      0      ne mult
*      0.0      extra input 8
*      0.0      extra input 9
*      0.0      use external cross-sections
*
*      *      *      Region Definition
*
*      4      number of regions (must be .1e. 30)
*      1.9      number of global points (must be .1e. 120)

```

```

2 <---- Inputs specific to this region follow
=====
* 1.0
  fnum multiplier
  dtm multiplier
  global points
  1
  2
  3
  4
  5
  6
  7
  8
  9
  10
  11
  12
  13
  14
  15
  16
  17
  18
  19
  20
  21
  22
  23
  24
  25
  26
  27
  28
  29
  30
  31
  32
  33
  34
  35
  36
  37
  38
  39
  40
  41
  42
  43
  44
  45
  46
  47
  48
  49
  50
  51
  52
  53
  54
  55
  56
  57
  58
  59
  60
  61
  62
  63
  64
  65
  66
  67
  68
  69
  70
  71
  72
  73
  74
  75
  76
  77
  78
  79
  80
  81
  82
  83
  84
  85
  86
  87
  88
  89
  90
  91
  92
  93
  94
  95
  96
  97
  98
  99
  100
  101
  102
  103
  104
  105
  106
  107
  108
  109
  110
  111
  112
  113
  114
  115
  116
  117
  118
  119
  120
  121
  122
  123
  124
  125
  126
  127
  128
  129
  130
  131
  132
  133
  134
  135
  136
  137
  138
  139
  140
  141
  142
  143
  144
  145
  146
  147
  148
  149
  150
  151
  152
  153
  154
  155
  156
  157
  158
  159
  160
  161
  162
  163
  164
  165
  166
  167
  168
  169
  170
  171
  172
  173
  174
  175
  176
  177
  178
  179
  180
  181
  182
  183
  184
  185
  186
  187
  188
  189
  190
  191
  192
  193
  194
  195
  196
  197
  198
  199
  200
  201
  202
  203
  204
  205
  206
  207
  208
  209
  210
  211
  212
  213
  214
  215
  216
  217
  218
  219
  220
  221
  222
  223
  224
  225
  226
  227
  228
  229
  230
  231
  232
  233
  234
  235
  236
  237
  238
  239
  240
  241
  242
  243
  244
  245
  246
  247
  248
  249
  250
  251
  252
  253
  254
  255
  256
  257
  258
  259
  260
  261
  262
  263
  264
  265
  266
  267
  268
  269
  270
  271
  272
  273
  274
  275
  276
  277
  278
  279
  280
  281
  282
  283
  284
  285
  286
  287
  288
  289
  290
  291
  292
  293
  294
  295
  296
  297
  298
  299
  300
  301
  302
  303
  304
  305
  306
  307
  308
  309
  310
  311
  312
  313
  314
  315
  316
  317
  318
  319
  320
  321
  322
  323
  324
  325
  326
  327
  328
  329
  330
  331
  332
  333
  334
  335
  336
  337
  338
  339
  340
  341
  342
  343
  344
  345
  346
  347
  348
  349
  350
  351
  352
  353
  354
  355
  356
  357
  358
  359
  360
  361
  362
  363
  364
  365
  366
  367
  368
  369
  370
  371
  372
  373
  374
  375
  376
  377
  378
  379
  380
  381
  382
  383
  384
  385
  386
  387
  388
  389
  390
  391
  392
  393
  394
  395
  396
  397
  398
  399
  400
  401
  402
  403
  404
  405
  406
  407
  408
  409
  410
  411
  412
  413
  414
  415
  416
  417
  418
  419
  420
  421
  422
  423
  424
  425
  426
  427
  428
  429
  430
  431
  432
  433
  434
  435
  436
  437
  438
  439
  440
  441
  442
  443
  444
  445
  446
  447
  448
  449
  450
  451
  452
  453
  454
  455
  456
  457
  458
  459
  460
  461
  462
  463
  464
  465
  466
  467
  468
  469
  470
  471
  472
  473
  474
  475
  476
  477
  478
  479
  480
  481
  482
  483
  484
  485
  486
  487
  488
  489
  490
  491
  492
  493
  494
  495
  496
  497
  498
  499
  500
  501
  502
  503
  504
  505
  506
  507
  508
  509
  510
  511
  512
  513
  514
  515
  516
  517
  518
  519
  520
  521
  522
  523
  524
  525
  526
  527
  528
  529
  530
  531
  532
  533
  534
  535
  536
  537
  538
  539
  540
  541
  542
  543
  544
  545
  546
  547
  548
  549
  550
  551
  552
  553
  554
  555
  556
  557
  558
  559
  560
  561
  562
  563
  564
  565
  566
  567
  568
  569
  570
  571
  572
  573
  574
  575
  576
  577
  578
  579
  580
  581
  582
  583
  584
  585
  586
  587
  588
  589
  590
  591
  592
  593
  594
  595
  596
  597
  598
  599
  600
  601
  602
  603
  604
  605
  606
  607
  608
  609
  610
  611
  612
  613
  614
  615
  616
  617
  618
  619
  620
  621
  622
  623
  624
  625
  626
  627
  628
  629
  630
  631
  632
  633
  634
  635
  636
  637
  638
  639
  640
  641
  642
  643
  644
  645
  646
  647
  648
  649
  650
  651
  652
  653
  654
  655
  656
  657
  658
  659
  660
  661
  662
  663
  664
  665
  666
  667
  668
  669
  670
  671
  672
  673
  674
  675
  676
  677
  678
  679
  680
  681
  682
  683
  684
  685
  686
  687
  688
  689
  690
  691
  692
  693
  694
  695
  696
  697
  698
  699
  700
  701
  702
  703
  704
  705
  706
  707
  708
  709
  710
  711
  712
  713
  714
  715
  716
  717
  718
  719
  720
  721
  722
  723
  724
  725
  726
  727
  728
  729
  730
  731
  732
  733
  734
  735
  736
  737
  738
  739
  740
  741
  742
  743
  744
  745
  746
  747
  748
  749
  750
  751
  752
  753
  754
  755
  756
  757
  758
  759
  759
  760
  761
  762
  763
  764
  765
  766
  767
  768
  769
  770
  771
  772
  773
  774
  775
  776
  777
  778
  779
  779
  780
  781
  782
  783
  784
  785
  786
  787
  788
  789
  789
  790
  791
  792
  793
  794
  795
  796
  797
  798
  799
  799
  800
  801
  802
  803
  804
  805
  806
  807
  808
  809
  809
  810
  811
  812
  813
  814
  815
  816
  817
  818
  819
  819
  820
  821
  822
  823
  824
  825
  826
  827
  828
  829
  829
  830
  831
  832
  833
  834
  835
  836
  837
  838
  839
  839
  840
  841
  842
  843
  844
  845
  846
  847
  848
  849
  849
  850
  851
  852
  853
  854
  855
  856
  857
  858
  859
  859
  860
  861
  862
  863
  864
  865
  866
  867
  868
  869
  869
  870
  871
  872
  873
  874
  875
  876
  877
  878
  879
  879
  880
  881
  882
  883
  884
  885
  886
  887
  888
  889
  889
  890
  891
  892
  893
  894
  895
  896
  897
  898
  899
  899
  900
  901
  902
  903
  904
  905
  906
  907
  908
  909
  909
  910
  911
  912
  913
  914
  915
  916
  917
  918
  919
  919
  920
  921
  922
  923
  924
  925
  926
  927
  928
  929
  929
  930
  931
  932
  933
  934
  935
  936
  937
  938
  939
  939
  940
  941
  942
  943
  944
  945
  946
  947
  948
  949
  949
  950
  951
  952
  953
  954
  955
  956
  957
  958
  959
  959
  960
  961
  962
  963
  964
  965
  966
  967
  968
  969
  969
  970
  971
  972
  973
  974
  975
  976
  977
  978
  979
  979
  980
  981
  982
  983
  984
  985
  986
  987
  988
  989
  989
  990
  991
  992
  993
  994
  995
  996
  997
  998
  999
  999
  1000
  1001
  1002
  1003
  1004
  1005
  1006
  1007
  1008
  1009
  1009
  1010
  1011
  1012
  1013
  1014
  1015
  1016
  1017
  1018
  1019
  1019
  1020
  1021
  1022
  1023
  1024
  1025
  1026
  1027
  1028
  1029
  1029
  1030
  1031
  1032
  1033
  1034
  1035
  1036
  1037
  1038
  1039
  1039
  1040
  1041
  1042
  1043
  1044
  1045
  1046
  1047
  1048
  1049
  1049
  1050
  1051
  1052
  1053
  1054
  1055
  1056
  1057
  1058
  1059
  1059
  1060
  1061
  1062
  1063
  1064
  1065
  1066
  1067
  1068
  1069
  1069
  1070
  1071
  1072
  1073
  1074
  1075
  1076
  1077
  1078
  1078
  1079
  1080
  1081
  1082
  1083
  1084
  1085
  1086
  1087
  1088
  1088
  1089
  1090
  1091
  1092
  1093
  1094
  1095
  1095
  1096
  1097
  1098
  1099
  1099
  1100
  1101
  1102
  1103
  1104
  1105
  1106
  1107
  1108
  1109
  1109
  1110
  1111
  1112
  1113
  1114
  1115
  1116
  1117
  1118
  1119
  1119
  1120
  1121
  1122
  1123
  1124
  1125
  1126
  1127
  1128
  1129
  1129
  1130
  1131
  1132
  1133
  1134
  1135
  1136
  1137
  1138
  1139
  1139
  1140
  1141
  1142
  1143
  1144
  1145
  1146
  1147
  1148
  1148
  1149
  1150
  1151
  1152
  1153
  1154
  1155
  1156
  1157
  1158
  1159
  1159
  1160
  1161
  1162
  1163
  1164
  1165
  1166
  1167
  1168
  1168
  1169
  1170
  1171
  1172
  1173
  1174
  1175
  1176
  1177
  1178
  1178
  1179
  1180
  1181
  1182
  1183
  1184
  1185
  1186
  1187
  1188
  1188
  1189
  1190
  1191
  1192
  1193
  1194
  1195
  1195
  1196
  1197
  1198
  1199
  1199
  1200
  1201
  1202
  1203
  1204
  1205
  1206
  1207
  1208
  1209
  1209
  1210
  1211
  1212
  1213
  1214
  1215
  1216
  1217
  1218
  1218
  1219
  1220
  1221
  1222
  1223
  1224
  1225
  1226
  1227
  1228
  1228
  1229
  1230
  1231
  1232
  1233
  1234
  1235
  1236
  1237
  1238
  1238
  1239
  1240
  1241
  1242
  1243
  1244
  1245
  1246
  1247
  1248
  1248
  1249
  1250
  1251
  1252
  1253
  1254
  1255
  1256
  1257
  1258
  1259
  1259
  1260
  1261
  1262
  1263
  1264
  1265
  1266
  1267
  1268
  1268
  1269
  1270
  1271
  1272
  1273
  1274
  1275
  1276
  1277
  1278
  1278
  1279
  1280
  1281
  1282
  1283
  1284
  1285
  1286
  1287
  1288
  1288
  1289
  1290
  1291
  1292
  1293
  1294
  1295
  1295
  1296
  1297
  1298
  1299
  1299
  1300
  1301
  1302
  1303
  1304
  1305
  1306
  1307
  1308
  1309
  1309
  1310
  1311
  1312
  1313
  1314
  1315
  1316
  1317
  1318
  1318
  1319
  1320
  1321
  1322
  1323
  1324
  1325
  1326
  1327
  1328
  1328
  1329
  1330
  1331
  1332
  1333
  1334
  1335
  1336
  1337
  1338
  1338
  1339
  1340
  1341
  1342
  1343
  1344
  1345
  1346
  1347
  1348
  1348
  1349
  1350
  1351
  1352
  1353
  1354
  1355
  1356
  1357
  1358
  1359
  1359
  1360
  1361
  1362
  1363
  1364
  1365
  1366
  1367
  1368
  1368
  1369
  1370
  1371
  1372
  1373
  1374
  1375
  1376
  1377
  1378
  1378
  1379
  1380
  1381
  1382
  1383
  1384
  1385
  1386
  1387
  1388
  1388
  1389
  1390
  1391
  1392
  1393
  1394
  1395
  1395
  1396
  1397
  1398
  1399
  1399
  1400
  1401
  1402
  1403
  1404
  1405
  1406
  1407
  1408
  1409
  1409
  1410
  1411
  1412
  1413
  1414
  1415
  1416
  1417
  1418
  1418
  1419
  1420
  1421
  1422
  1423
  1424
  1425
  1426
  1427
  1428
  1428
  1429
  1430
  1431
  1432
  1433
  1434
  1435
  1436
  1437
  1438
  1438
  1439
  1440
  1441
  1442
  1443
  1444
  1445
  1446
  1447
  1448
  1448
  1449
  1450
  1451
  1452
  1453
  1454
  1455
  1456
  1457
  1458
  1459
  1459
  1460
  1461
  1462
  1463
  1464
  1465
  1466
  1467
  1468
  1468
  1469
  1470
  1471
  1472
  1473
  1474
  1475
  1476
  1477
  1478
  1478
  1479
  1480
  1481
  1482
  1483
  1484
  1485
  1486
  1487
  1488
  1488
  1489
  1490
  1491
  1492
  1493
  1494
  1495
  1495
  1496
  1497
  1498
  1499
  1499
  1500
  1501
  1502
  1503
  1504
  1505
  1506
  1507
  1508
  1509
  1509
  1510
  1511
  1512
  1513
  1514
  1515
  1516
  1517
  1518
  1518
  1519
  1520
  1521
  1522
  1523
  1524
  1525
  1526
  1527
  1528
  1529
  1529
  1530
  1531
  1532
  1533
  1534
  1535
  1536
  1537
  1538
  1538
  1539
  1540
  1541
  1542
  1543
  1544
  1545
  1546
  1547
  1548
  1548
  1549
  1550
  1551
  1552
  1553
  1554
  1555
  1556
  1557
  1558
  1559
  1559
  1560
  1561
  1562
  1563
  1564
  1565
  1566
  1567
  1568
  1568
  1569
  1570
  1571
  1572
  1573
  1574
  1575
  1576
  1577
  1578
  1578
  1579
  1580
  1581
  1582
  1583
  1584
  1585
  1586
  1587
  1588
  1588
  1589
  1590
  1591
  1592
  1593
  1594
  1595
  1595
  1596
  1597
  1598
  1599
  1599
  1600
  1601
  1602
  1603
  1604
  1605
  1606
  1607
  1608
  1609
  1609
  1610
  1611
  1612
  1613
  1614
  1615
  1616
  1617
  1618
  1618
  1619
  1620
  1621
  1622
  1623
  1624
  1625
  1626
  1627
  1628
  1629
  1629
  1630
  1631
  1632
  1633
  1634
  1635
  1636
  1637
  1638
  1638
  1639
  1640
  1641
  1642
  1643
  1644
  1645
  1646
  1647
  1648
  1648
  1649
  1650
  1651
  1652
  1653
  1654
  1655
  1656
  1657
  1658
  1659
  1659
  1660
  1661
  1662
  1663
  1664
  1665
  1666
  1667
  1668
  1668
  1669
  1670
  1671
  1672
  1673
  16
```

03/10/22
13:11:09

inlet

* table for the 25torr pulsed valve -- radial inlet
1 5 3 table#, # of entries, BC type
1 5 3 table#, # of entries, BC type
-0.00049 5.6e23 0.0 -90. 300. 300. 300. 1.
-0.00048 6.2e23 7.0 -240. 270. 270. 270. 1.
-0.00047 6.2e23 18.0 -275. 260. 260. 260. 1.
-0.00046 5.6e23 36.0 -290. 250. 250. 250. 1.
-0.00045 4.6e23 0.0 -170. 280. 280. 280. 1.

100

SPEC

```
***** species data file *****  
***** number of species to input taken from problem description *****  
***** input -- they MUST be the same *****
```

ID	Mol. wt	Mol. mass	Diam.	#Rot.Deg.	Rot.Rel.	Vib.Temp.	specie	wt.	char
re	re	re	(m)	Freedom	Coll. #	Coll. #	(K)		
re	re	re	(kg)						
NO	30.008	4.98E-26	4.E-10	2.	1.	50.	2740.	1.0	0.0
N ₂	32.00	5.31E-26	3.96E-10	2.	5.	50.	2270.	1.0	0.0
O ₂	28.016	4.65E-26	4.07E-10	2.	5.	50.	3390.	1.0	0.0
O	16.00	2.65E-26	3.E-10	0.	0.	0.	0.	1.0	0.0
N	14.008	2.325E-26	3.E-10	0.	0.	0.	0.	1.0	0.0
NO	30.008	4.98E-26	4.E-10	2.	1.	50.	2740.	1.0	0.0
He	4.004	6.648e-27	2.19e-10	0.0	0.0	0.0	0.0	1.00	0.0
Ar	39.94	6.63e-26	4.04e-10	0.	0.	0.	0000.	1.0	0.0

screen.out

bear@{./prob7} init2d no_new.inp
no_new.inp

init2d for DSMC-MP -- version 6.00

starting region 1
starting region connectivity

begin initial processing of region info

opening inlet file, inlet, now

finished reading file--inlet

starting region 2
starting region connectivity

begin initial processing of region info

starting region 3
starting region connectivity

begin initial processing of region info

starting region 4
starting region connectivity

begin initial processing of region info

opening species file, spec, now

finished with file--spec

total cell volume(m^3) = 6.3486761E-05

101849727 molecules in initial grid

4 regions

33900 computational cells

1 chemical species

34 region connections

688 grid data size

170 boundary elements

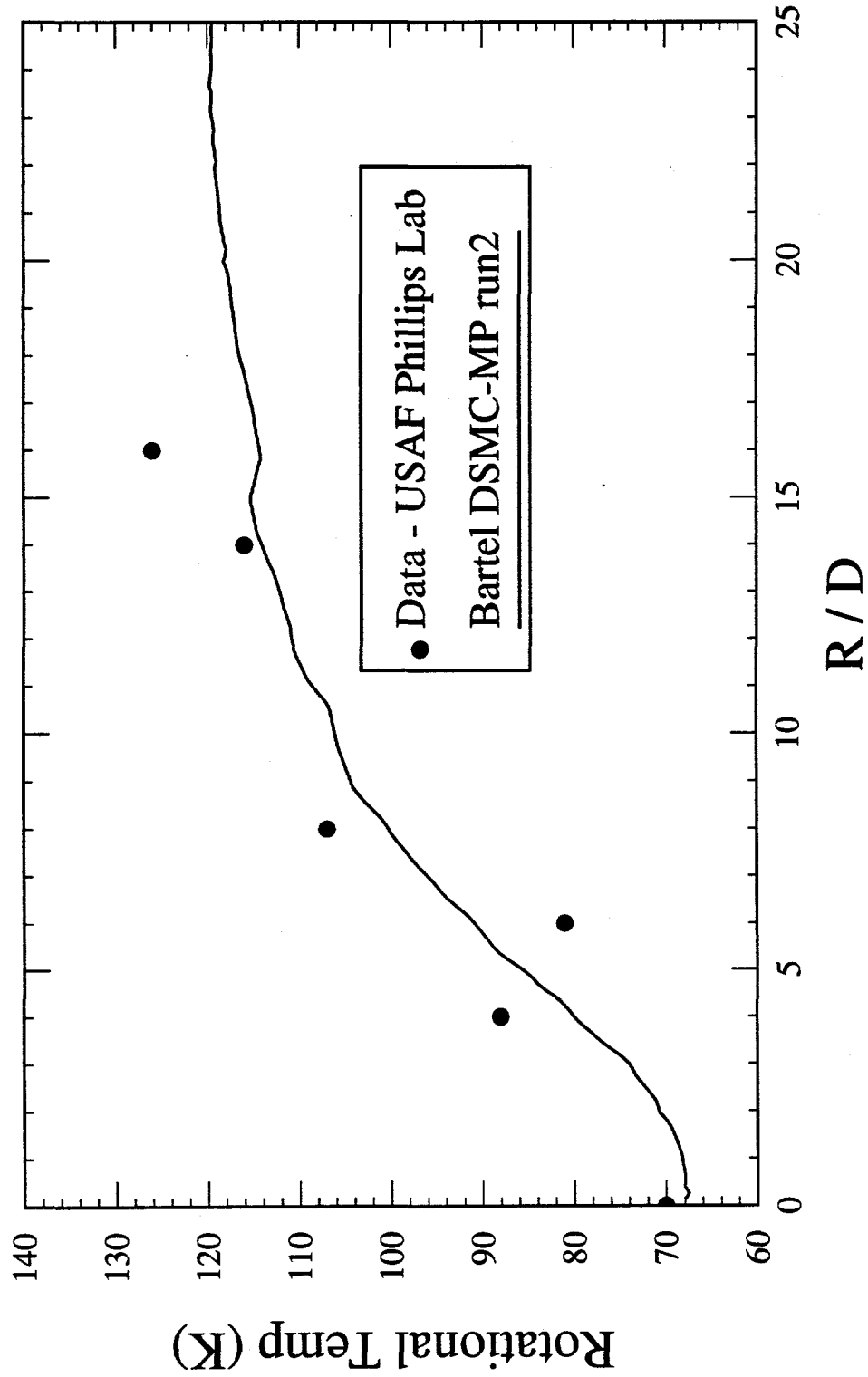
350 surface elements

34584 cell corner points

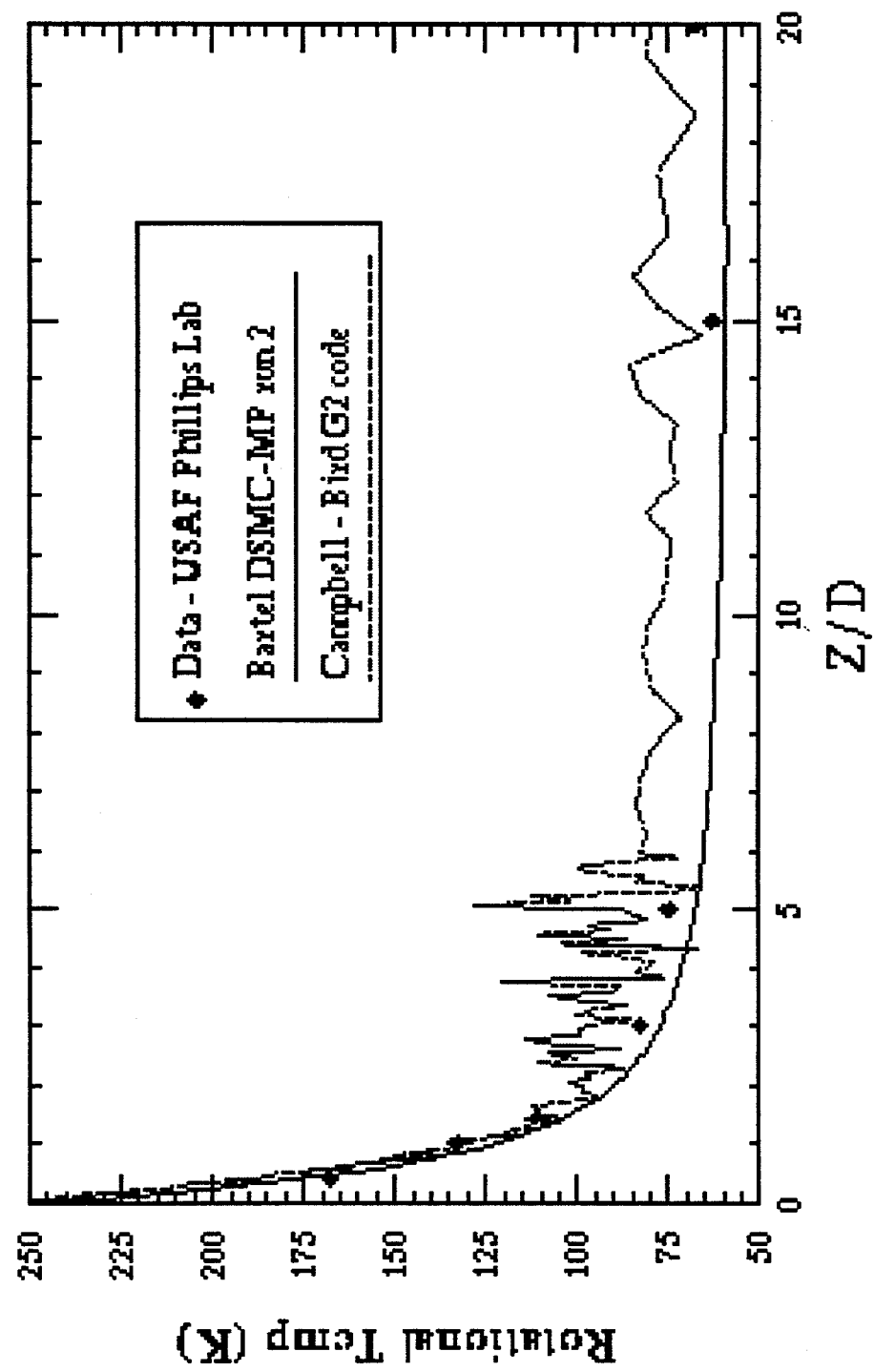
30 inlet table boundary cells

bear@{./prob7}

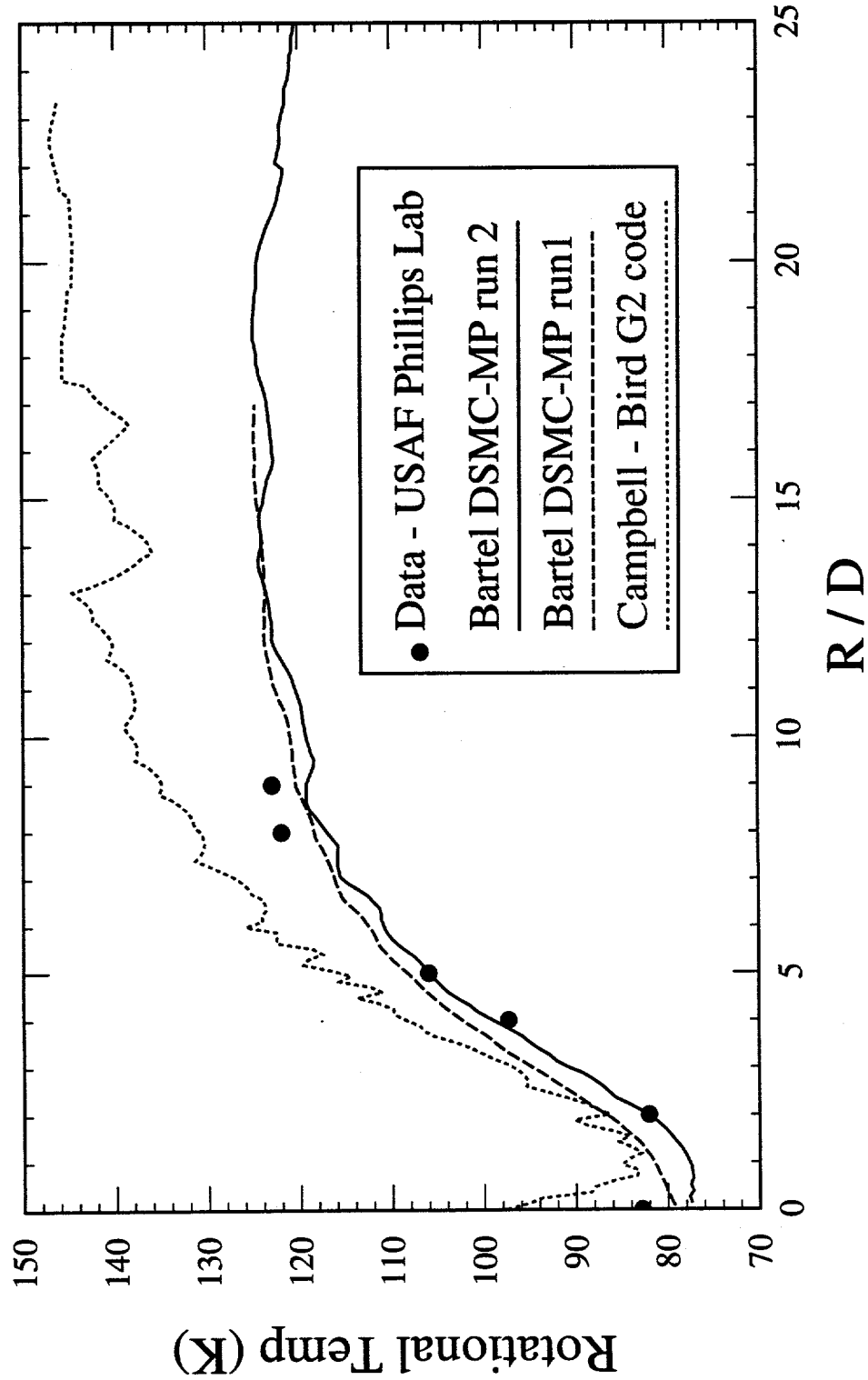
25 Torr Orifice Expansion - NO (Z/D=5)



25 Torr Orifice Expansion - NO (Centerline)



25 Torr Orifice Expansion - NO (Z/D=3)



Prob8: NO vibrational relaxation (time dependent)

Prob8: NO Vibration Relaxation

- Input Gases: NO

- Chemical Species:

	<u>Mwt</u>	<u>Mass</u>	<u>VHS diameter</u>
NO (V_0)	30.0061 gm/gmole	4.98×10^{-26} kg	4.26×10^{-10} m
1 st excited state of NO (V_1)	30.0061 gm/gmole	4.98×10^{-26} kg	4.26×10^{-10} m
2 nd excited state of NO (V_2)	30.0061 gm/gmole	4.98×10^{-26} kg	4.26×10^{-10} m

use a mixture viscosity coefficient of 0.90 @ 300 K

- Surface Boundary Conditions:

- 100% thermal accommodation
- 100% diffuse surface reaction
- Temperature of all surfaces = 300 K

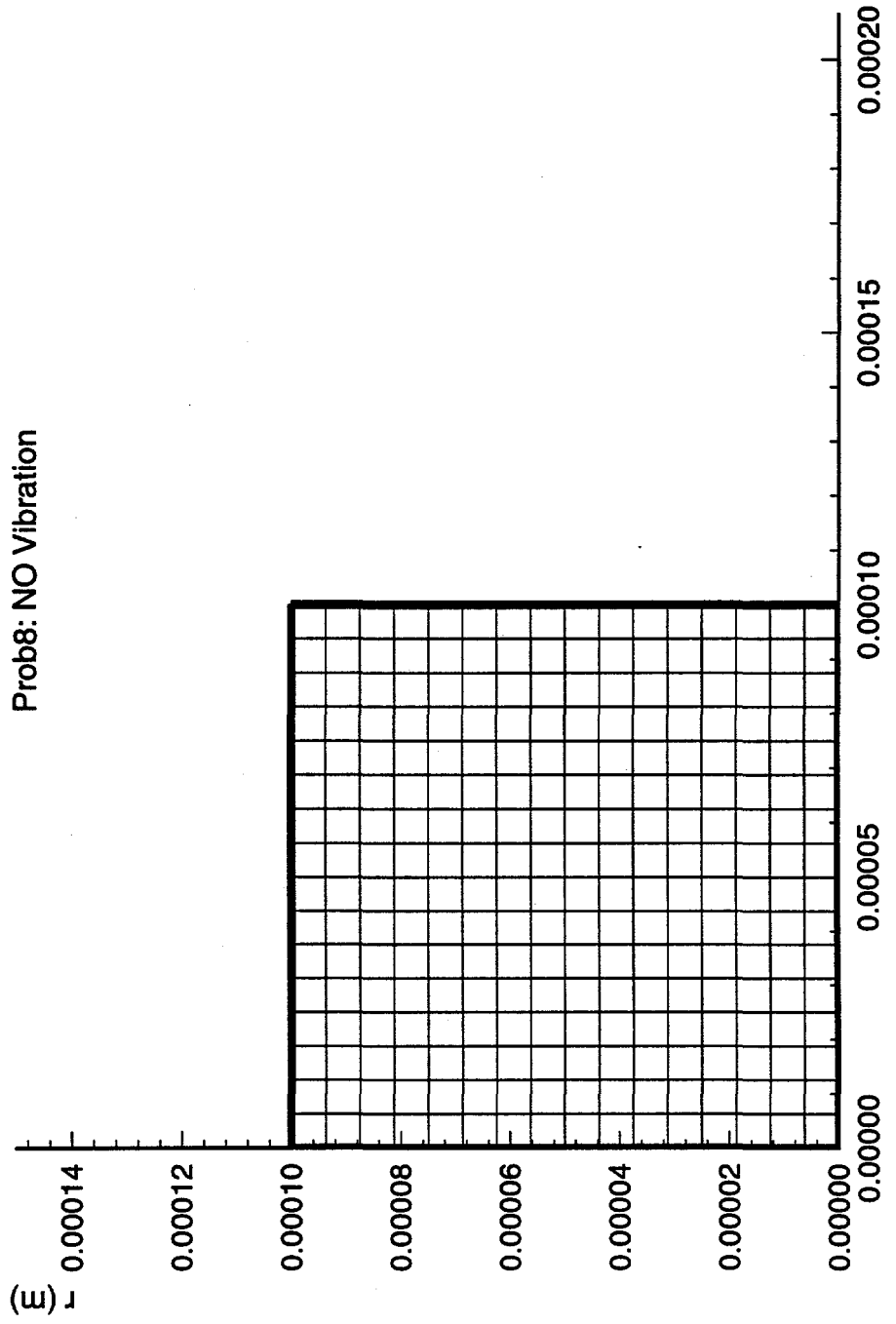
- Gas Phase Chemistry:

6 gas phase reactions (refer to chem file)

- Output:

- pressure, velocity, temperature and species distribution
- portray species weighting model
- time accurate mole fractions

Prob8: NO Vibration



new_inp.inp

```

*----- asterick in column 1 indicates comment card
*----- 1 Region NO vib. relaxation 3 levels
*
*----- 1 control:      -1 -- plot grid only;
*-----          1 -- initialization & plot file
*----- 0          0/1 for X-Y or Z-R flow
*
*----- Freestream Conditions
*----- 1          0/1 for vacuum/freestream
*-----          x-component of velocity, m/sec (ft/sec x 0.3048)
*-----          0.0
*-----          y-component of velocity, m/sec
*-----          0.0
*-----          number density, molecules/m**3 (mol./ft**3 x 35.315)
*-----          3.296e22
*-----          temperature, deg K (deg R/1.8)
*-----          293.0
*
*----- Species Information
*----- 3          Number of molecular species
*-----          NO(0)    NO(1)    NO(2)
*-----          0.9998  0.0001  0.0001
*-----          internal structure of most complex molecule:
*-----          3-monatomic, 4-rotational, 5-rotational, + vibrational
*-----          6          # of chem. rx. (from file chem)
*
*----- Weighting Information (particles and time step)
*----- 2.00E+08  base # of real mols. per simulation one
*-----          base time step, sec
*-----          0.00E-07  cell weighting option
*-----          0.0
*
*----- Collision Model Input
*-----          ref. temp. for VHS model, deg K
*-----          temperature exponent of viscosity coeffs.
*
*----- Surface Modelling Information
*-----          1.000  thacc: thermal accommodation coefficient
*
*----- Misc Input Section
*-----          vacuum pump region #
*-----          0          extra input 2
*-----          0          extra input 3
*-----          0          extra input 4
*-----          0          extra input 5
*-----          0          min radial expansion radius
*-----          0          extra input 7
*-----          0          extra input 8
*-----          0          extra input 9
*-----          0          extra input 10
*
*----- Region Definition
*-----          1          number of regions (must be .1e. 30)
*-----          4          number of global points (must be .1e. 120)
*
*----- Global corner pt. coordinates
*-----          Pt.      x (m)      y (m)
*-----          *          *          *

```

96/10/22
13:14:35

1
13:14:35

chem

* This input file contains the data characterizing the chemical reactions.

* If IRA = 0, there is no chemistry, and this file is not read.

* IRA > 0, there are IRA reactions, each characterized by 3 input records

*

*

--note-- the reaction equation is an input line (a25)

*

* NO vibrational set 3 levels

V2 + V0 --> V1 + V1

*

0. 3 1 1 1 2 0 2 1.706E-19 0.5 -5.559E-22

*

0. 2 1 1 1 3 0 1 8.885E-21 0.5 -3.669E-20

*

0. 1 1 1 2 0 1 4.442E-21 0.5 -3.725E-20

*

0. 3.725E-20 0 1 4.442E-21 0.5 -3.725E-20

*

V0 + V0 --> V1 + V0

*

0. 1 1 1 2 0 1 4.442E-21 0.5 -3.725E-20

*

0. 3.725E-20 0 1 4.442E-21 0.5 -3.725E-20

*

V1 + V1 --> V2 + V0

*

0. 2 2 1 1 3 0 1 1.706E-19 0.5 5.559E-22

*

0. 0.00 0.00 1.706E-19 0.5 5.559E-22

*

V2 + V0 --> V1 + V0

*

0. 3 1 1 1 2 0 1 8.885E-21 0.5 3.669E-20

*

0. 0.00 0.00 8.885E-21 0.5 3.669E-20

*

* third body probabilities now follow

*

0

* species data file
* *****
* number of species to input taken from problem description
* input -- they MUST be the same
*-----
* ID Mwt Mcl. mass Diam. #Rot. Deg. Rot. Rel. Vib. Rel. Vib. Temp. species
* (kg) (kg) (m) Freedom Coll. # Coll. # (K)
*-----
v0 30.0061 4.98E-26 4.26E-10 2. 1. 1. 0. 1.0 0
v1 30.0061 4.98E-26 4.26E-10 2. 1. 1. 0. 0.001 0
v2 30.0061 4.98E-26 4.26E-10 2. 1. 1. 0. 0.001 0

96/10/22
13:15:12

1

screen.out

```
bear{./prob8} init2d new_inp.inp
new_inp.inp
init2d for DSMC-MP -- version 6.00
```

```
starting region          1
starting region connectivity
begin initial processing of region info
opening species file, spec, now
finished with file--spec

opening gas phase chemistry file, chem, now
reading reaction #      1
reading reaction #      2
reading reaction #      3
reading reaction #      4
reading reaction #      5
reading reaction #      6
finished with file--chem
```

```
total cell volume(m^3) = 9.9999822E-09
197832 molecules in initial grid
1 regions
256 computational cells
3 chemical species
6 # of chemical rx
4 region connections
34 grid data size
0 boundary elements
64 surface elements
289 cell corner points
0 inlet table boundary cells
```

```
bear{./prob8}
```

```
# Test file for Vib -- 1000
log file          dsmc.log
output screen      50
zero flag          50
random seed        3847

read def          1.0 dsmc.def
adapt flag
time factor      200000 0.25
                  0.02
output special
run               400
                  1000000 0
```

SNL DSMCMP-2D Simulations

Engineering Sciences Center

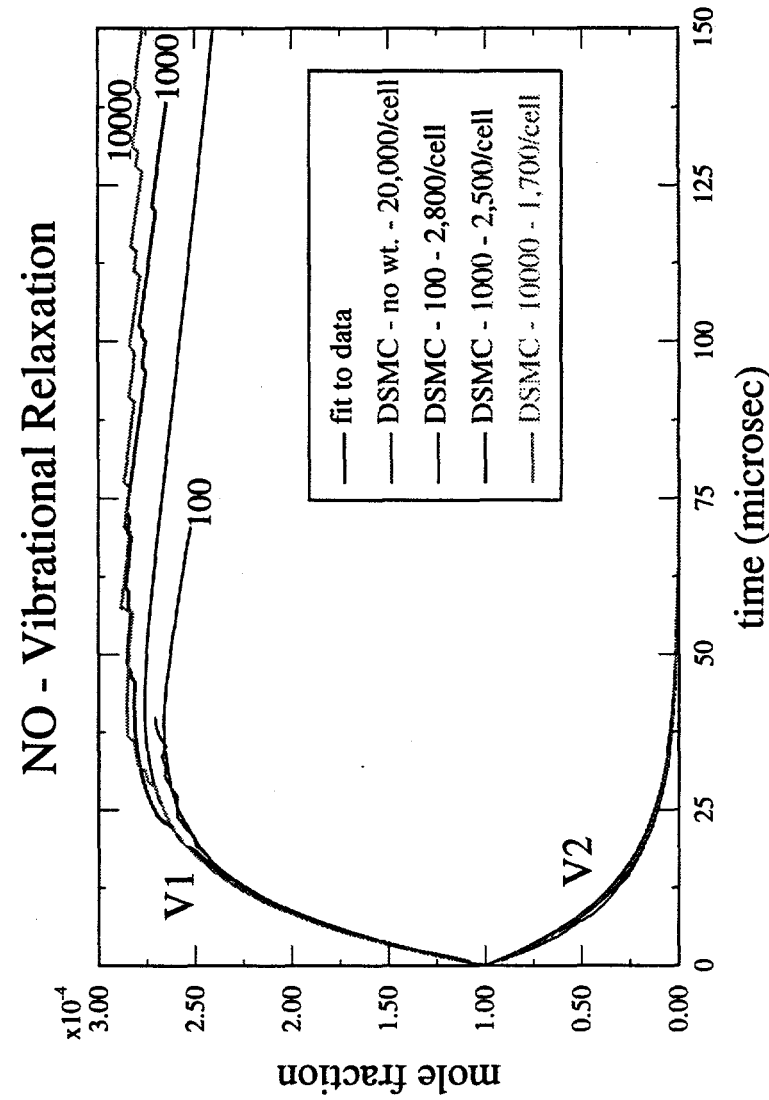
Problem - Accurate simulation of trace concentrations using DSMC

Solution - Develop trace species model for DSMCMP

Verify -
model vibrational relaxation of NO
model V_0 , V_1 , and V_2 as separate accurate solution

USAF Phillips Lab data

6 rate equation model



MS 0367	R. J. Buss, 1812	MS 0899	Technical Library, 4414 (5)
MS 0603	P. Esherick, 1126	MS 0619	Review & Approval Desk, 12630 (2) for DOE/OSTI
MS 0603	W. G. Breiland, 1126	N. Alvi	
MS 0603	M. E. Coltrin, 1126	SEMATECH	
MS 0603	J. R. Creighton, 1126	2706 Montopolis Drive	
MS 0603	P. Ho, 1126	Austin, TX 78741	
MS 0603	H. K. Moffat, 1126		
MS 1423	G. H. Hays, 1128		
MS 1423	M. E. Riley	E. Aydil	
MS 0826	W. Hermina, 9111	Dept. Chemical & Nuclear Engineering	
MS 0827	R. T. McGrath, 9114	University of California at Santa Barbara	
MS 0827	T. J. Bartel, 9114 (25)	Santa Barbara, CA 93106	
MS 0827	S. J. Choi, 9114		
MS 0827	M. L. Hudson, 9114	J. N. Bardsley	
MS 0827	D. J. Rader, 9114	MS L296	
MS 0827	A. J. Russo, 9114	Lawrence Livermore National Laboratory	
MS 0827	C. C. Wong, 9114	P. O. Box 808	
MS 0825	J. Payne, 9115	Livermore, CA 94550	
MS 0841	P. J. Hommert, 9100		
	Attn: R. D. Skocpec, 9102	Vikram Singh	
	J. H. Biffle, 9103	Lam Research Corporation	
	E. D. Gorham, 9104	4650 Cushing Parkway	
	A. C. Ratzel, 9112	Fremont, CA 94538-6401	
	T. Bickel, 9113		
	W. H. Rutledge, 9115	L. A. Berry	
	C. W. Peterson, 9116	Fusion Energy Division	
MS 1077	M. G. Blain, 1326	Oak Ridge National Laboratory	
MS 1078	C. W. Gwyn, 1302	P. O. Box 2009	
MS 1078	J. D. McBrayer, 1302	Oak Ridge, TN 37831-8071	
MS 1079	A. D. Romig, 1300		
	Attn: R. S. Blewer, 1305	T. S. Cale	
	G. V. Herrera, 1308	Dept. Chemical & Materials Engineering	
	J. Y. Tsao, 1311	Arizona State University	
	L. M. Cecchi, 1326	Tempe, AZ 85287	
MS 1111	J. N. Shadid, 9221		
MS 1111	S. Plimpton, 9221 (5)	J. L. Cecchi	
MS 1139	M. F. Young, 6421	Dept. Chemical & Nuclear Engineering	
MS 9042	C. M. Hartwig, 8345	209 Farris Engineering Center	
MS 9042	G. H. Evans, 8345	University of New Mexico	
MS 9042	J. F. Grcar, 8345	Albuquerque, NM 87131-1341	
MS 9042	W. G. Houf, 8345		
MS 9042	R. J. Kee, 8303	D. Economou	
MS 9042	E. Meeks, 8345	Department of Chemical Engineering	
MS 9042	J. W. Shon, 8345	University of Houston	
MS 9042	A. Ting, 8345	Houston, TX 77204-4792	
MS 9018	Central Tech Files, 8523-2		

D. B. Graves
Department of Chemical Engineering
University of California at Berkeley
Berkeley, CA 94720

Y. Ye
Applied Materials
M/S 0225
3050 Bowers Avenue
Santa Clara, CA 95054

M. J. Hartig
Motorola
MD: K-10
3501 Ed Bluestein Boulevard
Austin, TX 78721

M. J. Kushner
Dept. Electrical & Computer Engineering
University of Illinois at Urbana-Champaign
Urbana, IL 61801

A. H. Labun
M/S HL02-3 J09
Digital Equipment Corporation
Hudson, MA 01749

Y. Ra
Watkins-Johnson Company
440 Kings Village Road
Scotts Valley, CA 95066-4081

C. Scott
EG3
NASA Johnson Space Center
Houston, TX 77058

V. Vahedi
Lam Research Corporation
4650 Cushing Parkway
Fremont, CA 94538-6470

P. A. Vitello
Mail Stop L296
Lawrence Livermore National Laboratory
P. O. Box 808
Livermore, CA 94550

R. Walker
Group T-12, M. S. B268
Los Alamos National Laboratory
Los Alamos, NM 87545